The hormone-bound vitamin D receptor regulates turnover of target proteins of the SCF$^{\text{FBW7}}$ E3 ligase

By

Reyhaneh Salehi Tabar

Department of Experimental Medicine

McGill University

Montreal, QC, Canada

April 2016

A thesis submitted to McGill University in partial fulfillment of the requirements

of the degree of Doctor of Philosophy

Table of Contents

Abbreviations

AF2	Activation function 2
AP1	Activating protein 1
ARE	AU-rich elements
ATG3	Autophagy related 3
AUF1	ARE/poly(U)-binding/degradation factor 1
BCL2	B-cell lymphoma 2
BR	Basic region
C/ EBP	CCAAT-enhancer-binding proteins
CBP	CREB binding protein
CDC25A	Cell division cycle 25 homolog A
CDKN2B	Cyclin-Dependent Kinase Inhibitor 2B
CHIP	Carboxy-terminus of Hsc70 interacting protein
CHX	Cycloheximide
CML	Chronic myelogenous leukemia
CNBP	Cellular nucleic acid binding protein
COX2	Cyclooxygenase 2
CRD	Coding Region instability Determinant
CRL	Cullin-RING ligases
CSF-1	Colony-stimulating factor-1
CYP24	24-hydroxylase
CYP2R1	Cytochrome P450 2R1
DD	Dimerization domain
DRIP	Vitamin D Receptor-Interacting Proteins
DUB	Deubiquitinating enzyme
EGR1	Early growth response protein 1
FBP	FUSE binding protein
FBW7	F-box and WD repeat domain-containing 7
FBX	F-box domain
FBXL	F-box E3s containing Leu-rich repeat
FBXO	F-box and other domains
FBXW	F-box E3s containing WD40 domain
FIR	FBP-interacting repressor
FUSE	Far UpStream Element
GABA	GA-binding protein-α chain
GSK	Glycogen synthase kinase 3

HDAC	Histone deacetylases
HDACs	Histone deacetylases
HECT	Homologous to E6-associated protein C-terminus
HIF-1	Hypoxia-inducible factor
HL60	Human promyelocytic leukemia cells
hnRNP	Heterogeneous nuclear ribonucleoprotein
HNSCC	Head and neck squamous cell carcinoma
HPGD	15-hydroxyprostaglandin dehydrogenase
IGF1	Insulin-like growth factor 1
IGF2BP1	Insulin-like growth factor 2 mRNA binding protein 1
IGFBP3	IGF-binding protein 3
IKK	IκB kinase
IOM	Institute of Medicine
LANA	The latency-associated protein
MARRS	Membrane-associated rapid response steroid binding protein
MDSR	Myc dependent serum response
memVDR	Membrane receptor VDR
MIZ1	Myc-interacting zinc finger protein
MMP	Matrix metalloproteinases
MRE	MicroRNA response elements
MXD1	MAX dimerization protein 1
Myc (c-Myc, N-Myc, L-Myc)	V-Myc Avian Myelocytomatosis Viral Oncogene Homolog
NCoA62–SKIP	Nuclear coactivator-62 kDa–Ski-interacting protein
NCOR1	Nuclear Receptor Corepressor 1
NEDD4	Neural precursor cell expressed developmentally down-regulated protein 4
NEMO	NF-kB essential modulator
NHIII	Nuclease hypersensitive element
NPM1	Nucleophosmin
PBAF	Polybromo- and SwI-2-related gene 1 associated factor
PCC	Pheochromocytoma
PEST	Proline, glutamic acid, serine, threonine, and aspartic acid
PP2A	Protein phosphatase 2A
PPP2CA	Protein Phosphatase 2, Catalytic Subunit, Alpha Isozyme
PTM	post-translational modifications
RB	Retinoblastoma
RBP2	Retinoblastoma binding protein 2
RBR	RING in between RING–RING

RING	Really interesting new gene
RSK	P90 ribosomal kinase
RXR	Retinoid X receptor
S6K	Serine/threonine kinase
SID	SIN3 interacting domain
SKP2	S-Phase Kinase-Associated Protein 2, E3 Ubiquitin Protein Ligase
SKP2	SKP1, CUL1 and F-box protein complex
SMRT	Silencing mediator for retinoid and thyroid hormone receptors
SRC	Steroid receptor coactivators
STAT3	Signal transducer and activator of transcription 3
TAD	Terminal transactivation domain
TBP	TATA-box-binding protein
TERT	Telomerase reverse Transcriptase
TFIIB	Transcription factor IIB
TGFβ	Transforming growth factor-β
TPA	Phorbolester12-O-tetradecanoylphorbol-13-acetate
TRIM32	Tripartite Motif Containing 32
TRRAP	Transactivation/transformation Associated Protein
TRUSS	Tumor necrosis factor receptor-associated ubiquitous scaffolding and signaling protein
USP28	Ubiquitin Specific Peptidase 28
VDIR	VDR-interacting repressor
VDR	Vitamin D receptor
VDRE	Vitamin D response elements

Abstract

Cancer is one of the leading causes of death worldwide. Genetic and epigenetic alterations in cells lead to dysregulated expression and activity of two main categories of genes, tumor suppressors and oncogenes, which results in aberrant cell signaling, proliferation and tumor formation. One of the highly expressed oncogenes in many cancer types is the c-Myc transcription factor. c-Myc drives tumor initiation and progression as well as tumor maintenance. MXD1, another transcription factor, antagonizes c-Myc activity. The two arms of c-Myc/MXD1 network are regulated by changes in protein expression and turnover, which determines whether a cell proliferates or remains in quiescent state. Increasing evidence has revealed that vitamin D has anti-proliferative and pro-differentiating effects. Epidemiological data strongly suggest that vitamin D acts as a cancer chemopreventive agent, and its levels are inversely correlated with cancer risk, however the underlying mechanisms have not been fully elucidated.

In this study, we have investigated the effect of hormonal 1,25-dihydroxyvitamin D (1,25D) on the expression and activity of c-Myc and MXD1 transcription factors. This work has uncovered new molecular mechanisms of cancer chemopreventive effects of vitamin D through cooperation with the FBW7 E3 ubiquitin ligase, a key regulator of c-Myc and MXD1 turnover. FBW7 is a tumor suppressor that regulates the turnover over several drivers of cell proliferation and tumorigenesis. We have shown through *in vitro* and *in vivo* studies that the 1,25D-bound vitamin D receptor (VDR) profoundly alters the balance in function of c-Myc and its antagonist MXD1 through multiple mechanisms. 1,25D inhibited transcription of c-Myc-regulated genes *in vitro*, and topical 1,25D application to mouse skin suppressed expression of c-Myc and its target gene Setd8. In contrast, MXD1 levels were elevated *in vitro* and after topical application of 1,25D to mice skin. 1,25D also accelerated c-Myc protein turnover, but enhanced MXD1 expression and

stability, which resulted in a profound alteration in the ratios of recruited c-Myc and MXD1 to the promoters of target genes. In addition, c-Myc expression increased upon *VDR* knockdown. This effect was abolished following knockdown of β-catenin (*CTNNB1*), an activator of *MYC* gene transcription. Consistent with these findings, c-Myc expression was widely elevated in *Vdr-/-* mouse tissues. This included intestinal epithelia, where enhanced proliferation has been reported, and skin epithelia, where phenotypes of VDR-deficient mice are similar to those overexpressing epidermal c-Myc.

Unexpectedly, we found that the E3-ubiquitin ligase FBW7 not only regulates the stability of c-Myc, the oncogenic arm of the c-Myc/MXD1 push-pull network, but also regulates the turnover of the tumor suppressor arm, MXD1. FBW7 ablation attenuated 1,25D regulation of c-Myc and MXD1 turnover. FBW7 interacted with c-Myc, MXD1 and VDR in coimmunoprecipitation assays. The association of FBW7 with c-Myc was enhanced and that of MXD1 was inhibited in the presence of 1,25D, consistent with the effects of 1,25D on their turnover. Furthermore, FBW7 was recruited to the promoter of c-Myc target genes in association with c-Myc, MXD1 and VDR. The recruitment of FBW7 to the promoter of c-Myc target genes was not altered following treatment of the cells with 1,25D, however, its association with c-Myc was enhanced, in agreement with the elevated c-Myc degradation. In contrast, association of FBW7 with DNA-bound MXD1 declined in the presence of 1,25D.

In addition to its effects on c-Myc and MXD1, 1,25D attenuated the protein expression of several other FBW7 substrates implicated in tumorigenesis and cell proliferation. This effect was rescued after FBW7 ablation. Consistent with these results, the antiproliferative effects of 1,25D were attenuated by FBW7 knockdown. To extend these findings, the proteome was screened for "phospho-degron" motifs recognized by FBW7, revealing numerous potential novel target

11

proteins, including approximately the same ratio of identified tumor suppressors and oncogenes. From this list, expression of E2F1 and TCF7L2, products of oncogenes selected for their roles in gene transcription, was attenuated following 1,25D treatment.

Remarkably, the screen also revealed a phospho-degron motif in an unstructured "linker" region in the ligand binding domain of the VDR. Analysis of VDR expression suggested that FBW7 increases the turnover of VDR protein in the presence of 1,25D, without having any effect on its mRNA expression. These results reveal that VDR and FBW7 regulate each other's function. They also provide a novel molecular basis for cancer preventive actions of vitamin D, as well as insights into the mechanisms by which 1,25D signaling regulates cell proliferation.

Résumé

Le cancer est une des principales causes de mortalité à travers le monde. Des modifications génétiques et épigénétiques entrainent des dérégulations d'expression et d'activité de deux grandes catégories de gènes, les gènes suppresseurs de tumeur et les oncogènes, entraînant à leur tour des dérégulations de voie métaboliques allant de la prolifération et la formation de tumeurs. Un des oncogènes le plus exprimé est le facteur de transcription c-Myc qui déclenche l'initiation, la progression et le maintien de la tumeur. MXD1, un autre facteur de transcription, antagonise l'activité c-Myc. Les deux branches du réseau c-Myc/MXD1 sont régulées par des changements du niveau d'expression et le renouvellement de protéines, ce qui détermine si la cellule prolifère ou reste quiescente. Des preuves grandissantes ont révélé que la vitamine D a un effet anti-prolifératif et entraine la differentiation cellulaire. Des données épidémiologiques suggèrent que la vitamine D protège chimiquement du cancer, et que ses niveaux sont inversement corrélés au risque de cancer. Les mécanismes de ce phénomene ne sont toutefois pas élucidés.

Dans cette etude, nous avons étudié l'effet hormonal de 1,25-dihydroxyvitamine D (1,25D) sur l'expression et l'activité des facteurs de transcription c-Myc et de MXD1. Ce travail a révélé de nouveaux mécanismes moléculaires dans la chimioprotection liée a la vitamin D à travers une coopération avec l'ubiquitine ligase FBW7 E3, un régulateur clé du renouvellement de c-Myc et MXD1. FBW7 est un suppresseur de tumeur qui régule le renouvellement de plusieurs agents de la prolifération cellulaire et de la tumorigenèse. Nous avons montré avec des études in vitro et in vivo que le récepteur de la vitamine D (VDR) couplé à 1,25D change profondément l'équilibre et la function de c-Myc et antagonise MXD1 à travers divers mécanismes. 1,25D inhibe la transcription de gènes sous le contrôle de c-Myc. L'application locale de 1,25D sur la peau murine diminue l'expression de c-Myc et de son gène cible Setd8. Par contre, les niveaux de

MXD1 sont élevés in vitro et après application de 1,25D sur la peau murine. 1,25D accélère également le renouvellement de c-Myc alors que MXD1 en augmente l'expression et la stabilité, ce qui entraine un changement majeur du recrutement de c-Myc et de MXD1 au niveau des promoteurs de leurs gènes cibles. De plus, l'expression de c-Myc augmente suite a la diminution d'expression de VDR. Cet effet est bloqué si béta-caténine, un activateur du gène *MYC*, est préalablement inhibée. En accord avec ces découvertes, l'expression de c-Myc était largement augmentée dans les tissus de souris Vdr-/-. Ceci tant au niveau de l'épithelium intestinal, ou une prolifération accrue a été rapportée, qu'au niveau de la peau, ou les phénotypes de souris VDR-déficientes sont similaires a ceux de souris surexprimant c-Myc.

Nous avons été surpris de trouver que E3-ubiquitine ligase FBW7 régule non seulement la stabilité de c-Myc, l'aspect oncogénique de l'équilibre dynamique c-Myc/MXD1, mais également le renouvellement du suppresseur de tumeur MXD1. La perte de FBW7 atténue la régulation de c-Myc par 1,25D ainsi que le renouvellement de MXD1. FBW7 interagit avec c-Myc, MXD1 et VDR dans des expériences de co-immunoprécipitations. L'association de FBW7 avec c-Myc est facilitée et celle avec MXD1 est inhibée en présence de 1,25D, ce qui va de pair avec l'effet de 1,25D sur leur renouvellement. De plus, FBW7 est recruit au niveau des promoteurs des cibles de c-Myc avec c-Myc, MXD1 et VDR. Le recrutement de FBW7 au niveau des promoteurs des gènes en aval de c-Myc n'est pas affecté suite au traitement avec 1,25D, toutesfois l'association avec c-Myc est augmentée, conformément à l'augmentation de la dégradation de c-Myc. Par contre, l'association de FBW7 avec MXD1 lié à l'ADN diminue en présence de 1,25D.

En plus de ses effets sur c-Myc et MXD1, 1,25D atténue l'expression protéique de plusieurs autres substrats de FBW7 impliqués dans la tumorigenèse et la prolifération cellulaire. Ces effets

sont perdus en absence de FBW7. De même, les effets antiprolifératifs de 1,25D sont atténués par une diminution des niveaux de FBW7. En plus de ces observations, le protéôme a été criblé pour un motif "phospho-degron" reconnu par FBW7, ce qui a permis l'identification de nombreuses nouvelles cibles potentielles, incluant autant d'oncogènes que de gènes suppresseurs de tumeurs. Parmi ceux-ci, E2F1 et TCF7L2, produits d'oncogènes selectionnés pour leur rôle dans la transcription, ont vu leurs niveaux d'expression diminuer suite au traitement avec 1,25D.

De façon intéressante, le criblage a égalemennt révélé un motif de "phosphor-degron" dans une région sans structure dite "linker" dans le domaine d'attachement du ligand de VDR. Une analyse d'expression de VDR suggère que FBW7 augmente le taux de nouvellement protéique de VDR en présence de 1,25D sans aucun effet sur les niveaux de transcrits. Ces résultats montrent que VDR et FBW7 régulent leurs fonctions respectives et apportent un nouveau mécanisme moléculaire par lequel la vitamine D prévient du cancer ainsi que des pistes de mécanismes par lesquels 1,25D agit sur la prolifération cellulaire.

Preface

This thesis is written in manuscript format and resulted in one published paper, one paper under preparation for submission and one published review paper in collaboration.

1- **Reyhaneh Salehi Tabar**, Loan Nguyen-Yamamoto, Luz E. Tavera-Mendoza, Thomas Quail, Vassil Dimitrov, Beum-Soo An, Leon Glass, David Goltzman, and John H. White. Vitamin D receptor as a master regulator of the c-MYC/MXD1 network. PNAS. (2012),109 (46): 18827–18832.

2- **Reyhaneh Salehi Tabar**, Babak Memari, Vassil Dimitrov, John White. The hormone-bound vitamin D receptor regulates turnover of target proteins of the E3 ligase FBW7 (Under preparation)

3- Vassil Dimitrov, **Reyhaneh Salehi Tabar**, Beum-Soo An, John H White. Non-classical mechanisms of transcriptional regulation by the vitamin D receptor: insights into calcium homeostasis, immune system regulation and cancer chemoprevention. J Steroid Biochem Mol Biol. (2014) 144:74-80.

Contribution of authors

Chapter 2

I designed and performed all the experiments presented in this chapter, except: the ChIPseq analysis (Fig. 2.5.D) was performed by Dr. Luz E. Tavera-Mendoza. The immunohistochemistry in (Fig. 2.8.B-E, G, H) was performed by Dr. Loan Nguyen-Yamamoto. All the work was performed under the supervision of Dr. John White. I wrote the first draft of the chapter and this was edited by Dr. John White.

Chapter 3

I have conceptualized and generated all the data presented in this chapter, except (Fig. 3.5.B, C) which was performed by Dr. Loan Nguyen-Yamamoto. All the work was performed under the supervision of Dr. John White. I wrote the first draft of the chapter and this was edited by Dr. John White.

Chapter 4

I designed and performed all the experiments presented in this chapter, except (Fig. 4.7.A) which was performed by Vassil Dimitrov. All the work was performed under the supervision of Dr. John White. I wrote the first draft of the chapter and this was edited by Dr. John White.

Chapter 1- Introduction

Literature Review

Chapter 1-Literature review

1.1. General introduction and overview of thesis

Transformation of normal cells into cancer cells is the result of accumulation of alterations at the cellular, genetic, and epigenetic levels, which authorize cells to break free from the tight network of controls that keep the homeostatic balance between the production of new cells and cell death. These alterations lead to aberrant expression and activity of two large categories of genes, tumor suppressors and oncogenes, which eventually reprogram a cell to go through uncontrolled division. Oncogenes promote cell cycle progression and division, whereas tumor suppressors discourage cell growth and normally hold mitosis in check [1]. In fact, any alterations that lead to either gain of function resulting in increased expression and activity of oncogenes or loss of function resulting in the suppression and inactivation of tumor suppressor genes promotes uncontrolled cell cycle progression [2].

Anticancer agents are able to inhibit oncogenes activation and/or reactivate tumor suppressors to some extent. Increasing evidence has proven that vitamin D displays anti-proliferative and pro-differentiating effects in tumor cells *in vitro* and delays tumor growth *in vivo* [3]. Vitamin D deficiency has been linked with the initiation and progression of various diseases including cancer. It has been shown that the lack of VDR (vitamin D receptor) or severe vitamin D deficiency promotes tumorigenesis in animals [4]. Thus, vitamin D sufficiency is hypothesized to prevent tumorigenesis. 1,25D (1,25-dihydroxyvitamin D3) is a potent regulator of cell growth and differentiation, which binds to VDR. VDR is considered a transcription factor that influences central mechanisms of oncogenesis [5]. Although, the molecular mechanism of its anticancer action is poorly understood, it has been revealed that regulation of the expression of oncogenes

and tumor suppressors is one of the main cancer chemopreventive functions of ligand-bound VDR [6].

The genomics and proteomics studies have revealed that cancer cells have a distinct transcriptional pattern compared to normal cells. Transcription factors, which regulate gene expression patterns and signaling pathways, constitute a large fraction of tumor suppressors and oncogenes [2]. One of the main proto-oncogene transcription factors that is overexpressed in numerous cancers is Myc. Myc activity is antagonized by tumor suppressor MXD1 protein. In normal cells, Myc expression induces apoptosis and halts cell cycle progression, whereas in cancer cells Myc is the quintessential oncogene and promotes tumorigenesis [7]. In 1983, Reitsma et al, showed that vitamin D reduces *MYC* mRNA expression in HL-60 leukemia cells [8]. However, further investigation remained to be done to fully elucidate the anticancer effects of vitamin-D on the expression, stability and function of the Myc oncogene and other members of Myc/MAX/MXD1 network.

In chapters 2 and 3 of this thesis, we will address the anticancer function of vitamin D by investigating the effect of 1,25D-bound VDR on the gene expression, protein stability and function of transcription factors c-Myc and its antagonist MXD1 *in vitro* and *in vivo*. We show that hormonal vitamin D alters the stability of c-Myc and MXD1 through ubiquitin E3 ligase FBW7. In chapter 4, we elucidate the effects of 1,25D on c-Myc and MXD1 through the same E3 ligase. In addition, we provide evidence for cooperation of VDR and FBW7 to inhibit cell proliferation. Further, we show the regulatory effect of FBW7 on VDR.

1.2. 1,25D signaling

Vitamin D is the precursor of the secosteroid hormone calcitriol (1,25D), which after binding to VDR regulates the expression of many genes involved in many physiological processes [9], [10].

Vitamin D3 is obtained either from dietary sources or through ultraviolet irradiation of 7-dehydrocholesterol in the skin. Closely related vitamin D2 is of fungal origin. Vitamin D is converted to 25OHD by cytochrome P450 2R1 (CYP2R1) expressed in a variety of tissues[11]–[15], mitochondrial CYP27A1 mostly expressed in the liver and moderately in the lung [10], [11], [15]–[17], and CYP2J3[17], [18]. It has been suggested that enzymes other than CYP2R1 act upon vitamin D only when its concentration is increased to high nano-molar or micro-molar levels [13]. 25OHD subsequently is carried to the other tissues by blood circulation and is converted to hormonal $1,25OH_2D$ (1,25D) by 1α-hydroxylase (CYP27B1), which is expressed in kidney and several peripheral tissues [11], [19], [20]. In the replete state of 1,25D, the expression of 24-hydroxylase (CYP24), which is directly targeted by the VDR, is upregulated and results in 24-hydroxylation of 25OHD and 1,25D and production of $24,25OH_2D$ and $1,24,25OH_3D$, which are subsequently catabolized to calcitroic acid, which is inactive [21], [22]. Another pathway that promotes degradation of hormonal vitamin D is the C23 lactone pathway which converts it to $1,25OH_2D$ 26,23 lactone [315]. It has been shown that CYP3A4 which is a xenobiotic metabolizing enzyme, catalyzes 4β-hydroxylation of 25OHD, and 23R- and 24S-hydroxylation from 1,25D to deactivate it [23]. Some studies have suggested that CYP3A4, expressed mostly in small intestine and moderately in liver, can convert vitamin D3 to 25OHD [11], [17], [18], [24], [25]. Mutual actions of CYP3A4 might depend on the concentration of vitamin D and its metabolites. The definition of the vitamin D deficiency is based on the concentration of circulating 25OHD on the blood. It is a subject of some controversy, as it was determined to be at 50 nmol/L threshold by the Institute of Medicine (IOM), and at 75nmol/L threshold by the Endocrine Society [10].

1,25D regulates many signaling pathways implicated in proliferation, differentiation, apoptosis, metastasis, angiogenesis and inflammation. Consequently 1,25D has the potential to affect cancer formation and growth [10]. It also has been reported that vitamin D regulates microRNA expression [26]. The biological functions of 1,25D are mediated either by the VDR through genomic pathways, or by VDR and other receptors via non-genomic pathways [27].

1.2.1 The vitamin D receptor

The VDR, which is expressed in a variety of tissues [11], [28], belongs to the nuclear receptor superfamily of ligand-regulated transcription factors [29]. The *VDR* locus encompasses 100 kb on chromosome 12q and consists of promoter and regulatory regions (1a–1f),coding region (exons 2–9) and 3' regulatory region [30]. Several SNPs (single-nucleotide polymorphisms) have been found in VDR. The functional impacts of these SNPs are largely unknown, however their association with increased susceptibility to some cancers including squamous cell carcinoma, breast cancer, prostate cancer, and colorectal cancer have been reported [30].

VDR protein contains two main functional domains, the N-terminal zinc finger DNA binding domain and the C-terminal ligand binding domain. Nuclear localization signals at the N-terminus localize the receptor in the nucleus (Fig. 1.1) [30]. The VDR contains 13 α-helices and one β-sheet at the C-terminal domain, which construct a three-layer structure. In 1,25D signaling, helices 3 and 12 of the ligand binding domain play a critical role to form proper conformational change leading to dimerization and binding to coactivators and corepressors [31]. VDR forms heterodimers with RXR mostly via Helices 9, 10 and part of helices 7,8 [27]. VDR Ligand binding domain displays a high functional domain sequence homology. It consists of residues 124 to 427 and includes a loop in S199 to Q223 residues between helices 2 and 3, which is common in all nuclear receptors. In addition, VDR has a specific insertion domain between H2

23

and H3 including 23 residues, which is unique to VDR. Further, Helix 12 contains a short activation function-2 (AF-2) domain, which contributes to signal activation or repression, but not to ligand binding [31].
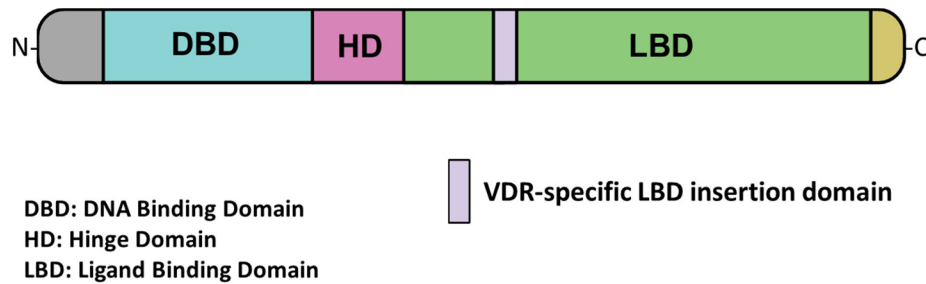
Figure 1.1: Schematic of VDR functional domains.

1.2.2. Non-genomic actions of 1,25D

Non-genomic functions of hormonal vitamin D are rapid and not dependent on its regulation of transcriptional activity. Both a non-classical membrane receptor VDR (memVDR) at the plasma membrane [27] and a MARRS (membrane-associated rapid response steroid binding protein) have been proposed as targets of 1,25D and promote rapid intestinal absorption of Ca^{2+} [30].

1.2.3. Genomic action of 1,25D

1,25D binds to the VDR which results in dimerization of the VDR with RXR (retinoid X receptor). This heterodimer subsequently binds to the vitamin D response elements (VDREs) which consist of 2 consensus hexameric motif (RGKTSA) separated by 3 non-consensus base pairs, in the promoters and distal regulatory sites of target genes and recruits co-regulatory factors [10], [32]. VDREs are mostly in the distal regulatory sites of target genes and the associated VDR makes a regulatory loop with the promoter of target gene and regulates the transcription by recruiting co-modulators [10]. It has been reported that for transcriptional activation, the VDR interacts with the 3′ half-site and RXR occupies the 5′ half-site of VDRE,

whereas for repressing target gene expression, the VDR interacts with the 5′ half-site of the VDRE [30]. Another mechanism for VDR binding is tethering through other DNA-bound transcription factors to the transcriptional machinery [33].

1.2.4. 1,25D-mediated Transcriptional activation

Although VDR DNA-binding is strongly activated by hormone binding, there is some evidence that, in the absence of hormonal vitamin D, the VDR interacts with co-repressor proteins, including NCoR1(nuclear receptor corepressor 1), SMRT (silencing mediator for retinoid and thyroid hormone receptors), hairless and Alien which in turn interact with HDACs (histone deacetylases) inducing chromatin packaging [32]. Binding of hormonal vitamin D and subsequent heterodimerization with RXR result in conformational changes in the VDR which lead to the dissociation of the co-repressors and binding of stimulatory coactivators including SRCs (steroid receptor coactivators), NCoA62–SKIP (nuclear coactivator-62 kDa–Ski-interacting protein) and chromatin modifiers, including CBP (CREB binding protein)–p300 and PBAF (polybromo- and SwI-2-related gene 1 associated factor) which acetylate histones. Opening of the local chromatin promotes DRIPs (vitamin D Receptor-Interacting Proteins; also known as TRAPs or the Mediator) complex formation which binds to the transactivation domain, AF2 (activation function 2) domain, of VDR and interacts with transcriptional machinery proteins such as TFIIB (transcription factor IIB) and RNA polymerase II which in turn, activates the transcription of target genes [30], [32].

1.2.5. 1,25D-mediated Transcriptional repression

The ligand bound-VDR/RXR heterodimer suppresses gene transcription via E-box-type negative VDREs, which is comprised of a CANNTG-like motif in the promoter region of the target genes such as PTH and CYP27B1 [30]. VDIR (VDR-interacting repressor) binds to the E-box-type

negative VDRE and promotes the transcription of target genes. The ligand-bound VDR tends to interact with VDIR and promotes dissociation of HAT (histone acetyltransferase) and recruitment of HDAC co-repressor, which results in transcriptional repression of the target gene [30], [34].

1.2.6. 1,25D signaling in cancer

Multiple observational studies have revealed that low level of circulating of vitamin D, related to geographic latitude, diet and activity, is associated with a higher risk of cancer incidence and mortality [34]. The expression and activity of the VDR is essential for the anticancer effects of hormonal vitamin D. Therefore, lack of VDR, as seen in some malignancies, leads to vitamin D resistance [34]. The VDR expression is different in histologically distinct cancer types and overexpressed in some cancers, while it is repressed in others. VDR is overexpressed in hyperplasia and in the early stages of tumorigenesis, but is repressed in late-stage poorly differentiated tumors and is not expressed in metastases. Tumors of the colon with the highest expression of VDR were most responsive to 1,25D treatment [30].

1.2.7. Anti-proliferative effects of 1,25D

The most well-known anti-cancer activity of 1,25D is its capacity to inhibit cell proliferation. Some cell cycle regulatory genes are direct or indirect targets of VDR [34]. Ligand-bound VDR promotes expression of CDKs inhibitors $p21^{WAF1/CIP1}$ and $p27^{KIP1}$, which in turn, induce G0/G1 cell cycle arrest. In addition, the ligand-bound VDR promotes the expression of growth inhibitors such as transforming growth factor-β (TGFβ), whereas it inhibits the mitogenic signaling through growth factors such as insulin-like growth factor 1 (IGF1) by inducing the IGFBP3 (IGF-binding protein 3) transcription. Furthermore, it modulates the kinase signaling pathways, such as PI3K, p38, MAPK and ERK. Ligand-bound VDR suppress the high

telomerase activity in cancer cells by repressing the expression of TERT (telomerase reverse Transcriptase). In addition, in some cancer cell lines, 1,25D promotes miR-498 expression which leads to downregulation of TERT mRNA [10].

1.2.8. Induction of apoptosis by 1,25D

Vdr-null mice show a delay in apoptosis in mammary epithelia. In addition, it has been shown that 1,25D triggers apoptosis in many cancer cells by cell type-specific mechanisms. The ligand-bound VDR is able to modulate apoptosis mediators by diverse mechanisms. Indeed, it represses the expression of anti-apoptotic genes and induces the expression of the pro-apoptotic genes [10]. Furthermore, 1,25D signaling might promote cell death through alternative pathways, such as decreasing intracellular glutathione, releasing cytochrome c and enhancing the calcium concentration which leads to the production of ROS [34].

1.2.9. 1,25D pro-differentiating effects

1,25D alters the features of some cancer cells to less malignant and more differentiated phenotype. It regulates the expression of more than 60 genes implicated in cell differentiation [34]. For example, it induces terminal differentiation of human myeloid leukemia cells into monocytes and macrophages. Another example of 1,25D pro-differentiating effects is in colon carcinoma, in which it induces differentiation by inhibiting β-catenin signaling and promoting the expression of adhesion proteins such as E-cadherin and vinculin [10].

1.2.10. 1,25D anti-Inflammatory effects

Inflammation leads to the initiation and progression of many types of cancers. 1,25D possesses anti-inflammatory functions in some cancers. Prostaglandins (PGs) are important mediators of inflammation in multiple diseases including cancers. 1,25D suppresses the expression of COX2 (cyclooxygenase 2) which leads to the inhibition of prostaglandin synthesis [35]. Furthermore, it

enhances the expression of the catabolic enzyme HPGD (15-hydroxyprostaglandin dehydrogenase) and represses the expression of prostaglandin receptors which results in inhibition of prostaglandin signaling. 1,25D also enhances the expression of DUSP10 (MAPK phosphatase 5) which in turn, suppresses p38 stress kinase signaling and prevents the pro-inflammatory cytokine production. In addition, 1,25D also inhibits NF-κB signaling [10]. Furthermore, 1,25D regulates innate immunity by promoting the expression of hCAP-18/LL-37 gene which is an antimicrobial peptide [36], [37].

1.2.11. Inhibition of invasion and metastasis by 1,25D

1,25D regulates many genes that are implicated in metastasis, invasion and angiogenesis. For instance, it enhances the expression of E-cadherin which is a tumor suppressor and negatively correlated with tumor metastasis. In addition, it decreases the expression of the proteins involved in metastasis such as β4 integrin and suppresses the activity of the MMPs (matrix metalloproteinases), which are involved in tumor metastasis [10].

1.3. c-Myc Transcription Factor

Most of the oncogenic signaling pathways move toward sets of transcription factors that ultimately control gene expression patterns implicated in tumor initiation and development [38]. One of the first discovered transforming agents in human cells is Myc [39]. It is the cellular homologue of the avian myelocytomatosis virus (MC29) oncogene. Myc is a multifunctional protein that belongs to the Myc family of basic-helix-loop-helix-leucine zipper transcription factors [40], [41]. It is found in all metazoans but not in other multicellular lineages such as fungi and plants [42], [43]. Myc is highly expressed in most proliferating cells and is generally low or absent in quiescent cells [4], [5]. The tissue specific members of Myc , N-Myc and L-Myc, were first identified in neuroblastoma and lung cancer, respectively [44], [45]. Myc is the point of

convergence of various signaling pathways and relays these signals via altering gene expression [46]. enhancing transcription of virtually all genes [47], [48]. Apart from coding, it also regulates non-coding RNA production with rRNA promoters having lower c-Myc affinity compared to its other targets [49]–[51]. The net result is the regulation of genes involved in cell growth, chromatin structure, DNA replication, ribosome biogenesis, metabolic pathways, energy production, cell adhesion, cell size and apoptosis [6], [13]. In cancer , c-Myc expression is independent of growth-factor signaling, which leads to the uncontrolled proliferation [48]. There is evidence that specific tumor cells become addicted to c-Myc overexpression, as blocking its function or knocking it down leads to growth inhibition, differentiation and apoptosis even in tumors driven by other oncoproteins [52], [53].

1.3.1. *MYC* gene

The *MYC* gene is located on chromosome 8 q24 and contains 3 exons and multiple promoters [54]. *MYC* promoters are targeted by several pathways such as RAS/RAF/MAPK, JAK/STAT, TGFβ, NF-κB, and WNT which are often upregulated in tumorigenesis and lead to high level of *MYC* expression. Transcription is initiated mostly at the P1 and P2 promoters accounting for 25% and 75% of mRNA, respectively. GC-rich nuclease hypersensitive element NHIII1 shows strong association with transcriptional initiation [55]. The G-rich strand, under the influence of negative supercoiling conditions, forms intramolecular G-quadruplex structure containing repeated sequences with three or four consecutive guanine bases [55]–[57]. This structure is stabilized by Hoogsteen hydrogen bonds [58]. Some nucleolar proteins such as nucleolin and nucleophosmin can bind with high affinity and selectivity to the *MYC* G-quadruplex motif [59]–[61]. Furthermore, nucleolin induces the formation and stability of the *MYC* G-quadruplex structure [62]. Conversely, in the presence of polyamines, the Pu27 motif can form a double helix

structure which is transcriptionally active [63]. Cellular nucleic acid binding protein (CNBP), heterogeneous nuclear ribonucleoprotein (hnRNP), TATA-box-binding protein (TBP) and RNA polymerase II could attach to active double helix structure and initiate transcription [54], [64]. In fact, the NHE III1 sequence is in an equilibrium between double helix (transcriptionally active form) and G-quadruplex (silenced form) [65]. Sequences with the potential interstrand G-quadruplexes are widely present in all organisms' genome, particularly in the promoter of many oncogenes [62], [66]. Recent studies show that stabilization of G-quadruplexes structure upstream of oncogenes such as *MYC* can silence its transcription [67]. Hence, compounds that can stabilize the G-quadruplex structure in promoter of *MYC* could be used to attenuate its expression and prevent cancer progression [54], [68], [69].

Furthermore, there is another structure that is involved in *MYC* transcription initiation, termed the Far UpStream Element (FUSE), which works as a cruise control element and is located 1.7 kb upstream of the P2 promoter of *MYC*. FUSE is masked by a nucleosome in quiescent cells. FUSE is a stress-induced duplex destabilization sequence, which under negative supercoiling of DNA, tends to become single stranded when *MYC* is being transcribed. Far upstream element (FUSE) binding protein (FBP) binds to FUSE and makes a loop between FUSE and P2 promoter by binding to TFIIH transcription factor. This looping increases transcription of *MYC* by increasing the ability of TFIIH to release paused RNA polymerases under the pressure of the concentrated negative superhelicity [70]. Binding of the (FBP)-interacting repressor (FIR) to the FBP reverses the effect of FBP alone, and brings *MYC* transcription to basal levels [70], [71]. Both of these dynamically induced DNA structures are being considered as targets for molecular therapeutics. Multiple compounds have been found that bind to NHE III1 and stabilize the G-quadruplexes structure [54], [56], [57], [62], [65]–[69], [72], [73] , however just one of them

CX-3543 (Quarfloxin) passed through phase I clinical trial as a drug for neuro-endocrine carcinomas [54].

1.3.2. c-Myc protein

Generally a full length c-Myc protein, 65 kDa, is expressed from the *MYC* gene, however there are several variants of c-Myc protein in the cell that can be generated by alternative start sites (p67 c-Myc and p64 c-Myc [74], [75]), by different translation initiation site on *MYC* mRNA (Myc-S [76]), and by sequence specific proteolytic cleavage of the c-Myc (MYCnick [77]–[79]).

c-Myc contains an N-terminal transactivation domain (TAD) and DNA binding domain at the C-terminus [80], [81]. Alignment across species revealed that it is a highly conserved protein with several homology sequences named Myc box (Myc box I (45-63 a.a.), II (129-143 a.a.), IIIa (188-192 a.a.), IIIb, and IV [82]–[86]). These contain residues which may undergo post-translational modifications leading to alterations in c-Myc stability and activity. Myc box I and II are located in the transactivation domain which is necessary and sufficient for transcriptional activation transforming capacity in most but not all contexts [87]–[89]. Myc box IIIa, IIIb, and IV are located in the central part of the proteinc[84], [86]. Nuclear localization signal is located in Myc box IV (320-328 a.a.) (Fig. 1.2) [90]. Some of the modifications in Myc box I are essential for cellular transformation [91], [92], whilst some are negative regulator of c-Myc protein stability [93]. Myc box II modifications and interactions promote cellular transformation and tumorigenesis [94]. It has been revealed that Myc box III suppresses apoptosis [89]. In addition, Myc box IIIa modifications and interactions promote cellular transformation and tumorigenicity by Myc [89]. L-Myc proteins which possess reduced oncogenic potential compared to other Myc members, lacks MbIIIa motif [95]. Myc box IV is poorly characterized, although it has been demonstrated that it regulates DNA binding, transformation, apoptosis, and G2 arrest [84].

The Myc-S isoform lacks the first 100 N-terminal amino acids, including much of the transactivation domain, but retains MB II [96]–[98]. In addition, cleavage of full length c-Myc by calpains leads to production of MYCnick. It consists of 298 amino acids and lacks nuclear localization signal and DNA binding domain. It alters cytoskeletal architecture and promotes muscle differentiation via the activity of the remaining N-terminal part of c-Myc [77]. Even through it is constrained to the cytoplasm and lacks transcriptional activity, it induces survival, autophagy, and motility by recruiting acetyltransferases that modify cytoplasmic proteins such as ATG3 (autophagy related 3) [79]. In fact, MYCnick is implicated in cell shape and differentiation by promoting α-tubulin acetylation [78], [99]. The ratio of MYCnick to full-length c-Myc increases during hyperactivation of calpains in condition such as muscle cell differentiation [77]. Activation of calpain and increase in the proportion of MYCnick to full length c-Myc protein enhances anchorage independent cell growth and tumorigenicity[79], [100].

1.3.3. c-Myc regulation

The expression of c-Myc set the balance between differentiation and proliferation in mammalian cells. Thus, it is critical for the cell to precisely control the level of c-Myc at multiple steps. Mammalian cells contain a sophisticated network of mechanisms that constantly prevent c-Myc actions. *MYC* RNA and protein undergo stringent controls at every step of Myc expression, including transcription, RNA processing, translation, and protein stability [82].
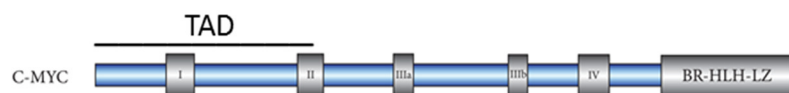
Figure 1.2: Schematic of c-Myc domains.

Modified From: Tansey W.P, New Journal of Science, Volume (2014), Article ID 757534.

1.3.3.1. Regulation of *MYC* transcription

The first stage of Myc regulation is at the transcription level. *MYC* is an immediate early gene and is not transcribed in quiescent cells, however could be induced in the presence of growth factor signaling. *MYC* transcription is regulated at both the initiation and the elongation stage [82]. During transcription, the DNA threads through the RNA polymerase complex, and the movement produces negative supercoiling (under-twisting) behind and positive supercoiling (over-twisting) in front of the transcriptional machinery [70]. Under dynamic stress (negative superhelicity), four-stranded DNA structure (four consecutive guanine bases), named G-quadruplex, is formed in the nuclease hypersensitive element III1 (NHE III1) which is located in upstream of the P1 promoter. This negative supercoil is sufficient to convert the duplex DNA to a G-quadruplex on the G-rich strand and an i-motif on the C-rich strand, which represses *MYC* transcription at the initiation level [67]. Specific proteins have been identified that could promote folding of the G-quadruplex structure and leads to silence *MYC* expression, such as nucleolin [67]. On the other hand, some proteins resolve this structure and activate *MYC* transcription such as NM23-H2 [101]. FUSE which is masked by a nucleosome in quiescent cells is another DNA structure that regulates *MYC* transcription. FBP (FUSE binding protein) binds to FUSE after remodeling of chromatin and makes a loop by interacting to RNA polymerase complex in the p2 promoter to induce transcription. Binding of FIR to FBP, on the other hand, inhibits the initiation thus repressing transcription of *MYC* [70], [102], [103].

It has been reported that there is more than 10-fold reduction in *MYC* mRNA in differentiated HL60 cells (Human promyelocytic leukemia cells). In undifferentiated HL60 there is about 3-fold molar excess of exon 1 RNA over exon 2 whereas in differentiated cells, this ratio increases to an approximately 15 fold. This phenomenon is suggestive of the fact that the major part of

transcriptional down regulation of *MYC* is at the elongation level rather than initiation. The transcriptional blockage has been mapped to the boundary region between the 3' end of exon 1 and intron 1 [104]. *MYC* transcripts which are initiated from the P1 promoter do not terminate at the blockage site whereas those initiated from P2 are either blocked or pass through the blockage signal and complete the transcription. Therefore, it is suggested that overexpression and/or constitutive transcription of the *MYC* gene from P1 promoter may contribute to increased c-Myc level in Burkitt's lymphoma cells[105].

Majority of mature *MYC* mRNAs are within the nucleus compared to cytoplasm. This implies that transport is slower than splicing and the presence of mRNAs in the nuclear fraction is not restricted to high level of gene expression. One of the agents that coordinates the export of *MYC* mRNA is translation initiation factor eIF4E which under direct control of mitogenic signals, binds to *MYC* mRNA during the transcription and coordinates the transport of *MYC* out of the nucleus [69], [124], [125].

1.3.3.2. *MYC* mRNA stability regulation

MYC mRNA turnover is controlled by multiple instability susceptible elements located within both the coding region and the 3'-untranslated region (3'-UTR). It can be decayed by alternative pathways. One involves the Coding Region instability Determinant (CRD) which is located in the last 249 nucleotides of the mRNA coding region and is susceptible to a rapid cleavage by an endonuclease which is associated with mRNA or ribosome. In the presence of a CRD binding protein (CRD-BP), the mRNA is screened from the endonucleases [106]. IGF2BP1 (insulin-like growth factor 2 mRNA binding protein 1) is a CRD-BP protein and associates with CRD, and in complex with at least four other proteins (HNRNPU, SYNCRIP, YBX1, and DHX9) stabilizes the *MYC* mRNA. It is suggested that Complex formation at the CRD inhibits the transfer of *MYC*

mRNA to the polyribosomal fraction and subsequent translation-coupled decay [107]. Long non-coding RNA (lncRNA) gastric carcinoma high expressed transcript 1 (lncRNA-GHET1) which is up-regulated in gastric carcinoma, promotes the interaction between *MYC* mRNA and IGF2BP1 by making a complex with IGF2BP1. lncRNAs are de-regulated in a variety of tumors [108].

The other *MYC* mRNA degradation mechanism involves the 3' untranslated region (UTR), termed 5'-3' decay pathway. It plays a critical role in gene expression by controlling the stability, localization, export, and translation efficiency of the mRNA. It also contains microRNA response elements (MREs), AU-rich elements (AREs), and the poly(A) tail ,which binds miRNAs, ARE binding proteins (ARE-BPs), and poly(A) binding proteins (PABPs) leading to translation repression or mRNA decay. It has been reported that deletion of most of the *MYC* 3'untranslated region (UTR) enhances *MYC* mRNA level. 3' UTR-related decay of *MYC* mRNA involves rapid exoribonucleolytic removal of the poly(A) track, followed by de-capping at 5'and subsequently 5′ to 3′ and/or 3′ to 5′ degradation [109]–[111]. Thus, the 3' UTR is responsible for keeping *MYC* mRNA levels low.

ARE/poly(U)-binding/degradation factor 1 (AUF1), one of the well characterized ARE-BPs, associates with AU-rich elements of *MY*C mRNA and assembles other factors, including translation initiation factor eIF4G, chaperones hsp27 and hsp70, heat-shock cognate protein hsc70, lactate dehydrogenase, poly(A)-binding protein, which are essential to recruit the mRNA degradation machinery. Alteration in the composition of this complex of proteins by numerous signaling pathways changes ARE-dependent *MYC* mRNA degradation rates [111], [112]. However, there is one study which suggests that AUF1 induces *MYC* translation but not mRNA degradation [113].

There are several limiting factors to control and suppress c-Myc translation, including microRNAs (miRNAs) and RNA-binding proteins (RBPs). RNA-binding proteins (RBPs) could play roles in both *MYC* mRNA degradation and translation inhibition such as AUF1 and TIAR, respectively. TIAR is an RNA-binding protein which binds to ARE element in *MYC* mRNA and repress c-Myc translation [113], [114]. Furthermore, set of miRNAs such as MicroRNA-34a and miR-24 bind to *MYC* mRNA and mediate both translation down regulation and degradation of *MYC* mRNA [115] [116].

Some of RBPs prevents c-Myc translation in collaboration with micro RNAs (miRNAs). Examples are ELAVL1/HuR (human antigen R) and let-7b/c miRNA, respectively. let-7b/c miRNA binding to ARE of *MYC* is strongly induced when HuR binds next to a let-7-binding site in 3′ UTR. It has been shown that HuR and let-7 both suppress c-Myc translation through an interdependent process [117], [118].

1.3.3.3. c-Myc Protein stability regulation

c-Myc is under tight control. Its protein is very unstable with a half-life of 20–30 min in cells under normal physiological conditions. It is a subject for multiple post-translational modifications (PTMs), including phosphorylation, ubiquitination, o-glycosylation, SUMOylation, and acetylation [119]. c-Myc interactions also affect both its stability and activity [82]. Regarding function, there are several agents that bind c-Myc or MAX to prevent their interaction and therefore transcriptional activities**.** Most of the c-Myc interactions occur through MBI and II although some have been mapped to other parts.

1.3.3.3.1. c-Myc Modifications

c-Myc can be phosphorylated, ubiquitinated, o-glycosylated, SUMOylated, and acetylated [119]. Thr58, Ser62, Ser71 and Ser81 are four well -characterized phosphorylation residues in c-Myc

transactivation domain, as well as clusters of casein kinase II phosphorylation sites residues 226–270 (including PEST region) and 342–357 a.a. [120], [121] . Phosphorylation at Thr58 by GSK3B or GSK3A (Glycogen synthase kinase 3) leads to protein degradation through the E3 ubiquitin ligase FBW7 [93], [122]. c-MycS, which lacks the first 100 N-terminal amino acids, is unable to interact with GSK3s, suggesting that Thr58 is phosphorylated by GSK3s. Phospho-Ser62 is produced by CDK5, mTOR, ERK2, or JNKs in human and by PPP2CA (Protein Phosphatase 2, Catalytic Subunit, Alpha Isozyme) *in vitro*. Although Ser62 phosphorylation leads to c-Myc stabilization, it also trigger Thr58 phosphorylation which promotes ubiquitination and degradation [123]–[126]. Overexpression of T58A mutant of c-Myc showed enhanced transformation compared to wild type whereas the S62A mutation abolished the ability of c-Myc to promote transformation [127]. Furthermore, the Thr58 mutant demonstrated attenuated cellular apoptotic phenotype compared to wild-type c-Myc [128]. Thr58 has received elevated attention due to the finding that it is a frequent mutation site in Burkitt lymphoma [129].

Phosphorylation at Ser71 and Ser81 and the clusters attenuates c-Myc-induced cellular transformation. Alanine substitutions at these sites show high levels of cellular transformation, but no changes in protein stability [121]. Furthermore, it was reported that stress activated protein kinase PAK2 phosphorylates Thr358, Ser373 and Thr400 which disrupt the interaction of c-Myc with MAX and attenuates DNA binding and transformation [130]. Recently it has been revealed that tyrosine residues at the N-terminus of c-Myc, particularly Tyr-74, are phosphorylated by c-Abl (or Abl). Phosphorylated- Tyr74 form of c-Myc colocalizes to the cytoplasm with either Abl in a subset of mammary carcinomas or Bcr-Abl in chronic myeloid leukemia. The biological function of c-Myc tyrosine residues phosphorylation is to be investigated [131].

O-GlcNAcylation of Myc at Thr58 by O-GlcNAc transferase (OGT) and O-GlcNAcase (OGA) could compete with phosphorylation which would result indirectly in c-Myc stabilization. This modification is the consequence of the enzymatic addition of the N-acetylglucosamine (GlcNAc) moiety to the hydroxyl group of serine or threonine residues [120], [132]–[134].

Acetylation has an important impact on gene expression and metabolism and results in increased c-Myc stability. c-Myc could be acetylated by at least three different histone acetyltransferase (HAT) enzyme (p300/CBP, GCN5, and Tip60) [119]. HECTH9-dependent ubiquitination may stimulate c-Myc acetylation by enhancing CBP/p300 recruitment. It is suggested that ubiquitination and acetylation are coupled in the regulation of c-Myc stability, function and interactions [135], [136]. c-Myc can also be SUMOylated by the SUMO E3 ligase PIAS1. Such modification can trigger ubiquitination and degradation by the proteasome. Addition of multiple monomers of SUMO are sufficient for this effect [137]

1.3.3.3.1.1. Ubiquitination of c-Myc

Although part of Myc is cleaved by Calpain in the cytoplasm, the majority of Myc is degraded by ubiquitin–proteasome system (UPS). c-Myc is mono- or poly-ubiquitinated with several E3 ubiquitin ligases. Ubiquitination promotes several different effects on c-Myc including stabilization, degradation or alteration in the activity of c-Myc.

1.3.3.3.1.1.1. Ubiquitination and c-Myc degradation

1.3.3.3.1.1.1.1. Ubiquitination by FBW7

 The most well-known c-Myc E3 ubiquitin ligase is FBW7 (F-box and WD repeat domain-containing 7). FBW7 activation controls the c-Myc level in the late G1 and early S phases of the cell cycle [138], [139]. To be recognized by E3 ligases c-Myc protein should be marked by phosphorylation. The most important phosphodegron is located in MB I. Ser62 stabilizing

phosphorylation in the phosphodegron allows the association of c-Myc with Axin1. Subsequently, Axin-1 associated GSK3s phosphorylate Threonine 58, recognized by Pin1 resulting in trans to cis proline 63 isomerization, which allows the PP2A (protein phosphatase 2A) to bind and dephosphorylate serine 62. In fact, Axin1 scaffold protein facilitates the association of Pin1, PP2A, and GSK3s with c-Myc [140]. It has been reported that either mutation in *AXIN1* or down regulation of its expression in human cancers such as breast cancer enhances c-Myc stability [140], [141]. Multiple AXIN1 mutations were found in solid tumors [142]. Dephosphorylation of Ser62 stimulates the binding of the FBW7 and ubiquitination of c-Myc by K48-linked chains of ubiquitin. Disassociation of c-Myc from promoters is promoted by conversion of Proline63 from Cis to Trans by Pin1 which unlocks the stability of c-Myc and ultimately results in proteasomal degradation of c-Myc [92]. It is found that Downregulation of FBW7 results in simultaneously accumulation of cellular and active chromatin-bound c-Myc and consequently leads to an accumulation of cells in S-phase and G2/M-phase of the cell cycle [92], [143].

Some deubiquitinating enzymes (Ubiquitin Specific Peptidase) antagonize the effect of E3 ligases. USP28 and USP36, which are ubiquitin-specific proteases, cleave the ubiquitin chains from c-Myc by interacting with FBW7α and FBW7γ respectively. c-Myc stabilization induced by USP28 and USP36, is required for its transcriptional activity and tumor cell proliferation [144], [145]. Recently has been revealed that in fact USP28 deubiquitinates both autoubiquitinated FBW7 and its target proteins. However its preference is deubiquitination of FBW7. In mice with monoallelic loss of USP28, FBW7 remains stable whereas FBW7 substrates are ubiquitinated by FBW7 and subsequently degraded [146]. Another direct regulator of c-Myc stability is NEMO (NF-kB essential modulator). In the nucleus, NEMO binds to the c-Myc

protein and inhibits its ubiquitination through FBW7 [147]. FBW7 expression is required for survival and maintenance of various cancer such as chronic myelogenous leukemia (CML). Fbw7-c-Myc axis is considered as an attractive therapy target in cancer studies [148].

In addition, c-Myc degradation can be triggered by TRUSS (tumor necrosis factor receptor-associated ubiquitous scaffolding and signaling protein) [149], TRIM32 (Tripartite Motif Containing 32) [150], [151], FBXW8 [152], FBXO32 [126], carboxy-terminus of Hsc70 interacting protein (CHIP) [153], and Neural precursor cell expressed developmentally down-regulated protein 4 (NEDD4) [152] E3 ligases.

1.3.3.3.1.1.2. Ubiquitination for stabilization or activation

Ubiquitination of c-Myc through β-TrCP [154], LANA (The latency-associated protein) [128] leads to its stabilization. In addition, c-Myc ubiquitination by HectH9[135], FBXO28[155] SKP2 (S-Phase Kinase-Associated Protein 2, E3 Ubiquitin Protein Ligase) [156] promotes its activity. SKP2 has a dual regulation effect on c-Myc. In contrast to FBW7, which promotes c-Myc degradation and downregulates its activity, SKP2 regulates c-Myc degradation, but induces its transcriptional activity [157], [158].

1.3.4. Transcriptional activation by c-Myc

Myc determines cell fate by heterodimerization with MAX to regulated target genes expression by recruiting co-activator complexes. Myc-dependent transcriptional activation starts by binding of transactivation/transformation Associated Protein (TRRAP) to the N-terminal MB II, which in turn recruits HATs such as GCN5 and TIP60. These acetylates histone 4 , resulting in open chromatin conformation, and K323/K417 on c-Myc increasing its stability [159]. In addition, p300 binds to the residues 1 to 110 of TAD and acetylates c-Myc at several lysine residues, located in between TAD and DBD, which results in transcription of target genes[119].

1.3.5. Transcriptional repression by c-Myc

Although a numerous genes are repressed by c-Myc, the mechanisms are poorly studied. In the case of *CDKN2B* (Cyclin-Dependent Kinase Inhibitor 2B) gene, this is achieved through interaction of c-Myc/Max heterodimer with MIZ1 (Myc-interacting zinc finger protein). In fact, MIZ1 induces gene expression, but binding of c-Myc leads to suppression of this gene [160]. In the absence of TGFβ signaling, c-Myc interacts with MIZ1 and suppress the transcription of CDKN2B [161]. It is shown that the promoter of repressed genes are poorly enriched in consensus E-box sequences and c-Myc commonly attaches to these promoters in complex with other transcription factors [162], [163]. In the presence of TGFβ, c-Myc expression is suppressed, therefore NPM1 (Nucleophosmin) is recruited as a MIZ1 cofactor to induce *CDKN2B* transcription and promote cell-cycle arrest [160], [164].

1.3.6. DNA binding of c-Myc

c-Myc is a DNA binding protein and at physiological concentrations forms an extended coiled coil heterodimer with another member of Myc family, MAX, through bHLHLZ motif [4], [5]. Following heterodimerization, Two Basic region (BR) helixes of c-Myc and Max insert into the major groove of the DNA [165]. Electrophoretic mobility shift assay revealed that c-Myc-Max heterodimer has significant preference to bind to the Enhancer-box (E-box) motif, CAT/CGTG, however this heterodimer displays affinity for any DNA sequence and vast majority of binding sites lack the consensus E-box [166]. The E-box is located in the CpG island where the context of chromatin is active and characterized by specific histone modifications such as histone H3 lysine 4 trimethylation (H3K4me3) or H3K27 acetylation (H3K27ac)[47], [167], [168]. At physiological levels (low expression) c-Myc binds to the accessible promoter that is labeled by H3K4me3 and presence of RNA pol II [167]–[170]. At the overexpression level, more promoters become

occupied and c-Myc starts to bind to the distal regulatory elements which already have active chromatin profile with a high ratio of H3K4me1 /H3K4me3[47], [48], [167], [169]. At the overexpression level, DNA binding is less selective and c-Myc also binds to non-consensus E boxes that have low affinity for c-Myc [27]. Finally at extreme level, c-Myc and MAX heterodimer binds to progressively larger proportions (87-94%) of active promoters and enhancers, a phenomenon termed 'chromatin invasion' [47], [48], [167]. In this case, binding of the c-Myc-MAX to the DNA could be less sequence specific [168], [171]–[173]. ChIP–seq data revealed that The strongest signals related to high-affinity DNA sequences captured in the vast majority of cells, whereas the low signals correspond to low-affinity and non-consensus sequences[167]. c-Myc at the physiological levels does not attach to the low-affinity sequence, hence these genes are not assumed as c-Myc target genes in normal cells. At the overexpressed level, c-Myc binds to all active regulatory elements, however, the relative binding to the high affinity sites is still higher compared to low affinity sequences [167], [169]. Based on chromatin immunoprecipitation followed by high-throughput DNA sequencing (ChIP-Seq) analysis for other enriched motifs in the c-Myc low affinity binding sites, it was suggested that probably c-Myc is tethered to chromatin by tethering factors such as early growth response protein 1 (EGR1), GA-binding protein-α chain (GABPA) and activating protein 1 (AP1) [174].

1.3.7. Functions of c-Myc

c-Myc is critical for normal development. c-Myc has a critical role in the maintenance of normal cells. Germ-line inactivation of c-Myc in mice leads to small embryonic size, multiple abnormalities, and lethality before embryonic day 10.5 [175], [176]. c-Myc plays an essential role in pluripotency, self-renewal and cell size in many tissues during development [177]. The proliferation in the cell is a proportion of c-Myc protein. c-Myc biological activities include

angiogenesis, metabolism, expansion of cellular biomass and blocking differentiation results in high level of cell proliferation [178]. Although c-Myc promotes cell proliferation, it has been revealed that it also contributes to cell apoptosis [179].

c-Myc contributes to cell biological events via both transcriptional activities, in collaboration with RNA polymerase I, II, and III [51], [180], [181], and non-transcriptional activities including regulation of translation and DNA replication [182], [183]. c-Myc promotes transcription of numerous target genes which are involved in different biological processes including cell cycle control, metabolism, apoptosis, protein biosynthesis, and microRNA regulation and with this function contributes to alterations in cell growth, self-renewal, pluripotency, proliferation, cell death, DNA damage responses and senescence [184]–[191]. c-Myc non-transcriptional activities contribute to DNA replication and morphological differentiation [182], [192], [193].

1.3.7.1. Cell cycle regulation by c-Myc

The cell cycle refers to the series of consecutive events consisting of 4 phases, DNA synthesis (S-phase), cell division (M-phase), gap phases to allow cell growth (G1-phase) and the check for the integrity of genomic material (G2-phase). The cell cycle is regulated by a series of CDKs (cyclin-dependent kinases) and become irreversible by the regulated degradation of cyclin subunits. c-Myc plays a crucial role in cell cycle progression. The role of c-Myc in the cell cycle is to promote the G0 to G1 and G1 to S phase transitions. In quiescent cells lacking mitogenic signaling, c-Myc overexpression is sufficient to induce cell cycle entry. c-Myc promotes the expression of positive regulators and suppresses inhibitors of the cell cycle by different mechanisms [194]. In the early G1-phase, the D-cyclins and CDKs 4 and 6 are active. During G1, cells are stimulated by extracellular signaling specially mitogenic signaling such as MAPK [195]. c-Myc expression is promoted by mitogenic pathways and induces cyclin D1-Cdk4 and cyclin

D1-Cdk6 transcription during the G0-to-S transition which is considered as the earliest cell cycle effect of c-Myc [196]. In late G1, cyclin D–CDK4/6 activity diminishes and cyclin E–CDK2 activity increases. In this step, c-Myc activates cyclin E/Cdk2 kinase by stimulating the transcription of cyclin E. Furthermore, c-Myc prevents p27^{Kip1} inhibitor binding to newly formed CycE/Cdk2 and promotes activation of this complex [197]. Cyclin E-Cdk2 kinase mediates E2F transcription [193], but Cyclin A/CDK2 phosphorylates E2F1 and inhibits its DNA binding [194]. During G1 progression, the Rb (retinoblastoma protein) is phosphorylated. This phosphorylation attenuates its inhibition on E2F, subsequently E2F promotes transcription of a number of genes that are important for S-phase entry and progression. E2F proteins play a crucial role during the G1/S transition and induce S-phase entry from a quiescent state. E2Fs regulate transcription of sets of cyclins, CDKs, checkpoint regulators, DNA repair and replication proteins [195]. c-Myc has dramatic impacts on E2Fs activity through several different mechanisms. c-Myc induces the transcription of E2F1-3 genes. It has been revealed that passing a threshold amplitude of E2F accumulation results in cell cycle commitment. c-Myc acts as an amplifier for some active proteins with low expression levels, such as E2Fs, and promotes their expression to high levels.

c-Myc plays a crucial role in regulating the amplitude of E2F. c-Myc controls the level of E2Fs accumulation via interfering with E2Fs auto-regulation [195]. c-Myc is also essential to allow the interaction of the E2F1-3 protein with the E2Fs target gene promoters. Myc interaction with the E-box of the E2F target gene promoters is required for E2Fs binding and subsequent transcription of the genes [198], [199]. In fact, c-Myc establishes a growth-competent state and allows E2F-mediated S phase entry [198]. During early S-phase, cyclin E is degraded and cyclin A and CDK2 make a complex to drive cell from S-phase to G2. Another major effect of c-Myc

on cell cycle is though CDC25A (cell division cycle 25 homolog A) protein phosphatase, which is c-Myc target gene and is expressed in G1 phase. CdC25A is essential for both progression through mitosis and for c-Myc-induced apoptosis. Cdc25A dephosphorylates and activates Cdk2 and Cdk4 kinases which subsequently phosphorylate Rb [200]. RB also is silenced by H19 long non coding RNA (lncRNA) which is expressed by c-Myc protein [201], [202]. In addition, c-Myc regulates miRNAs which target critical cell cycle regulators including CDKs, cyclins and E2Fs. Further, the transcription of p21^{CIP1} and P15 ^{INK4b}, which are cyclin-CDK complexes inhibitors, are repressed by the association of c-Myc-Max heterodimer with MIZ-1 [194], [203], [204].

1.3.7.2. Apoptosis induction by c-Myc

In normal cells high expression of c-Myc promotes apoptosis to avoid tumorigenesis. c-Myc is able to induce apoptosis and cell death through two major pathways. First, c-Myc promotes transcription of ARF tumor suppressor proteins that interact with Mdm2 and leads to the release of tumor protein P53, which subsequently turns on the cell death cascade by inducing activation of pro-apoptotic genes and cell cycle mediators. c-Myc also induces P53 activation by enhancing genomic instability. Second, c-Myc suppresses the transcription of anti-apoptotic genes, e.g. Bcl-2 (B-cell lymphoma 2). In addition, c-Myc upregulates endogenous pro-apoptotic genes such as Bak and Bax [179]. In fact, c-Myc disturbs the equilibrium between pro- and anti-apoptotic agents to induce apoptosis [82].

1.3.8. c-Myc Deregulation in Cancer

In normal cells, the *MYC* gene transcription is induced by multiple of mitogens, and its expression is elevated in proliferating cells. Any alteration in the cell that induces overexpression of c-Myc, independency of c-Myc expression from signaling pathways or inhibition of c-Myc check points, results in c-Myc-driven cancer. Myc is required for tumor initiation and tumor

maintenance[205]. It is revealed that after formation, tumor becomes addicted to c-Myc and reduction in c-Myc expression leads to tumor regression [206].

In most of the human cancers c-Myc is overexpressed including, lymphoma, melanoma, multiple myeloma, and neuroblastoma, as well as breast, colon, and lung cancers. There are two major alterations, intrinsic and extrinsic that result in overexpression of c-Myc in cancer cells. In the intrinsic model, an alteration is occurred in the *MYC* loci including chromosomal translocation, gene amplification, retroviral insertion or mutation in the gene or upstream regulatory motifs, which leads to high level of *MYC* mRNA expression. In the extrinsic fashion, an alteration is occurred out of the *MYC* loci and leads to disarm critical regulatory processes such is mutation in the FBW7 E3 ligase binding site [82]. The first discovered mechanism that resulted in overexpression of c-Myc was retroviral promoter insertion upstream of *MYC* gene [207]. Overexpression of *MYC* is mostly due to gene amplifications including focal amplifications, large amplifications, and double minute chromosomes [208]–[211]. There are some genomic alterations that do not affect *MYC* gene but alters the rate of mRNA transcription. Rs6983267 is a polymorphism on chromosome 8q24 upstream of *MYC* gene, which enhances Wnt signaling by inducing the recruitment of TCF-4 to distal *MYC* enhancer and is associated with increased risk for colorectal and prostate cancer [212], [213].

Burkitt's lymphoma is characterized by dysregulation of the *MYC* gene. Most of Burkitt's lymphoma tumors are characterized by translocation of the *MYC* gene to the regulatory elements of the λ, κ light chains or μ heavy chain genes of immunoglobulin located in chromosomes 14, 22, or 2, respectively [214]. In colorectal cancer, high levels of c-Myc expression are due to inactivation of APC/β-catenin pathway [215]. In 17.1% of patients with breast cancer, high levels of c-Myc expression are detected as a result from receptor tyrosine kinase HER2/neu, a c-Myc

upstream signal transducer, overactivity [216]. Another study showed that patients with a Rapid recurrence of disease or progression (mean disease free survival: 1.4 years) has c-Myc amplifications with 56% frequency, whereas patients with >6.4 years of mean disease free survival have 30% frequency of c-Myc amplifications [216], [217]. It has been revealed that loss of BRCA1 and high level of c-Myc expression results in the development of breast cancer especially basal-like breast cancer [218]. In prostate cancer there are accumulative alterations that lead to high c-Myc transcriptional activity, including c-Myc amplification and MXI1, a c-Myc antagonist, mutations [216], [219], [220]. In Melanoma cancer, high level of c-Myc expression is found in metastatic lesions but not in primary lesions and provides a powerful independent prognostic marker for regional metastatic melanoma. β-catenin, a transcription factor on the *MYC* promoter, is mutated in some melanoma cell lines suggesting that c-Myc expression levels may be deregulated in melanoma via the same mechanism as colorectal cancer [221], [222].

Aberrant activation of Wnt signaling pathway induces release of Transcription factor 4 (TCF-4) which promotes overexpression of *MYC* [223]. Deregulation of Wnt signaling and consequent *MYC* overexpression has been reported in several cancers including Colorectal cancers (CRCs), childhood T-cell acute, non-small-cell lung cancer (NSCLC) and breast cancer [224]–[227]. Another signaling pathway involved in tumorigenesis through c-Myc is the colony-stimulating factor-1 (CSF-1) and its receptor CSF-1R, which physiologically regulates the monocyte/macrophage system and breast development. Aberrant expression of CSF-1R induces several human epithelial tumors, including breast carcinomas by binding to the proto-oncogenes promoter, including c-Myc [228].

Stability of the *MYC* transcript can be increased in cancer cells, mostly by increasing the expression of mRNA binding proteins and long noncoding RNAs such as lncRNA gastric

carcinoma high expressed transcript 1 (lncRNA-GHET1) which is up-regulated in gastric carcinoma. Its expression is correlated with tumor size, tumor invasion and poor survival [108]. In normal cells *MYC* mRNA mostly remain in the nucleus, but in some cancer cells its transportation to cytoplasm and translation are increased by deregulation and overexpression of translation factor eIF4E [229]. The stability of c-Myc oncoprotein is mostly enhanced by viral oncogenes or inactivation of critical regulators such as ubiquitin E3 ligases [156].

1.3.8.1. *MYC* Mutations in Cancer

The contribution of changes in the *MYC* coding sequence in cancer is doubtful. These mutations are found in very small groups of cancer, particularly Burkitt's lymphoma. Mutations in coding sequence of *MYC* are found in approximately 50% of Burkitt's lymphomas. Mutations in *MYC* is associated with other genomic rearrangement and it is suggested that the translocated *MYC* is located within a hypermutable region of the genome and mutations are resulted from these translocations [230]. It is believed that overexpression of c-Myc is sufficient for tumorigenesis which mostly occur through *MYC* gene rearrangements. However most of the mutations are in the transactivation domain principally in Thr58 which is critical for proteasomal degradation of c-Myc and it seems that these mutations have additional impact on tumorigenesis. It has been reported that *MYC*T58A expression (in knock-in mice) increases the density of mammary gland, hyperplastic foci, cellular dysplasia, and mammary carcinoma, and attenuates apoptosis relative to wild type *MYC* [231]. In another study, it was shown that expression of two mutant *MYC* alleles (P57S and T58A), which are frequently observed in Burkitt's lymphoma, retain the ability to stimulate proliferation and are defective at inducing apoptosis [94]. In addition, mutations in residues 243–249, within the central part of c-Myc protein promote phenocopy effects of mutations within Myc box I in terms of stability and tumorigenesis [232]. It is suggested that

most of the point mutations on *MYC* enhance stability and change the activity of c-Myc [135], [158], [233].

1.3.8.2. c-Myc Signaling in Cancer

22% of all genes are direct targets of c-Myc. 300 Myc dependent serum response (MDSR) genes have been identified in fibroblasts. This set contains approximately 6% of c-Myc direct target genes. MDSR genes are dominantly implicated in nucleotide metabolism, ribosome biogenesis, RNA processing, and DNA replication [160], [234]. In addition to its role in regulating RNA Pol II mediated transcription, c-Myc also regulates RNA Pol I, and Pol III-mediated transcription. Therefore, protein biosynthesis is intrinsically linked to c-Myc function. In this regard, many direct c-Myc target genes are ribosomal proteins [160]. In addition, c-Myc is involved in the regulation of chromatin structure which is essential for cancer initiation [235]. c-Myc promotes Bmi-1 and EZH2 expression, which are polycomb proteins and linked to the different forms of cancer [160]. Furthermore, c-Myc directly activates genes that are involved in glycolysis, glutamine metabolism, and mitochondrial biogenesis and by which c-Myc upregulates energy metabolism [160]. The most important role of c-Myc in cancer is driven from direct regulation of genes involved in cell-cycle regulation, such as CDC25A and CDK4. Perhaps the main role of c-Myc in induction of cancer is through regulating cell cycle progression genes [236], [237].

1.4. MAX protein

MAX is a constitutively expressed protein that is a central axis in the c-Myc/MAX/MXD1 network. It has bHLHZ DNA-binding domain, but lacks transactivation domain. Although MAX is required for both the promotion and repression of the transcriptional activity in the E-box containing target genes promoter, c-Myc is able to retain considerable biologic function, at high level of expression, probably by homodimerization in the absence of MAX protein [238]. Loss-

of-function mutations in the MAX gene were found in patients with pheochromocytoma (PCC) a rare neural crest cell tumor in the adrenal medulla, which is rarely metastasizes [239]. Furthermore, MAX is able to homodimerize, however this homodimer is very unstable and its physiological role is unclear [240], [241].

1.4.1. c-Myc/MAX/MXD1 network

c-Myc heterodimerizes with MAX to activate target gene transcription. It was demonstrated that the association between c-Myc and MAX is mediated by van der Waals interactions and hydrogen bonds. Although it has been suggested that c-Myc and MAX are able to form homodimers, the stability of these are very low, in contrast to the heterodimers. MAX is also able to heterodimerize with a range of other bHLHZ proteins including the MXD family of transcription factors, which are antagonists of c-Myc. Thus, competition of c-Myc and MXD proteins for MAX is a way of reaching a complex equilibrium that determines the activation or repression of target genes. In addition to MAX, MAX-like bHLHZ protein (MLX) can also dimerize with a subset of c-Myc antagonists including MXD1, MXD4 and MNT. Other players include members of the Mondo family, which accumulates in the nucleus in response to changes in metabolic flux and are able to antagonize the binding of MXD family members to MLX. In fact, various MAX and MLX interactions establish an extended network through which c-Myc, MXD, and Mondo families stimulate a broad transcriptional response to mitogenic, growth arrest, and metabolic signals [242].

1.5. MXD1 Transcription Factor

MXD1 belongs to the MXD family of bHLHZ proteins which consists of MXD1–MXD4 and MNT. Although in several aspects it antagonizes c-Myc activity, but Similar to c-Myc, MXD1 has a bHLHZ DNA-binding domain, forms heterodimers with MAX protein and binds to E-box

motifs on the promoter of c-Myc target genes. c-Myc protein levels are higher in proliferating cells, whereas MXD1 is more abundant in differentiated cells. A short N-terminal domain in MXD1, called SID (for mSIN3 interacting domain, is responsible for transcriptional repression achieved through recruitment of mSIN3 and its associated HDAC activity [243].

1.5.1. MXD1 cofactors antagonize c-Myc cofactors

All MXD family members contain SID domain [243]. mSIN3 recruits histone deacetylases (HDAC) such as HDAC1 and HDAC2, and therefore suppresses transcription by deacetylating core histones [244], [245]. Furthermore, MXD1 regulates histone methylation through recruitment of demethylases [246]. It was observed that MXD1 recruits the histone demethylase RBP2 (Retinoblastoma binding protein 2) to the telomerase promoter and decreases trimethylation of lysine 4 of histone H3, which in turn modifies the chromatin structure to suppress the active promoter [246]. On the other hand, Myc recruits ASH2-MLL complexes, which are core subunits of KMT2 methyltransferase. It is therefore associated withH3K4 trimethylase activity [247]. Thus, MXD antagonizes c-Myc not only by interacting with MAX and competing for DNA binding , but also by recruiting co-repressors, which antagonize c-Myc effects on chromatin remodeling [248], [249].

1.5.2. Regulation of proliferation and apoptosis by MXD1

The basic regions of c-Myc, MAX, and MXD are highly conserved therefore c-Myc/MAX and MAX/MXD1 bind to identical DNA sequences and regulate common target genes, although there are no high-throughput data sets available for MXD1. The c-Myc to MXD1 ratio is a crucial determinant of heterodimerization with MAX and in turn, transcriptional activation or suppression. Several genes implicated in proliferation (hTERT, CCND2, FOXM1, and eIF4s subunits) [250]–[253] and apoptosis (PTEN) [254] are found to be suppressed by MXD1. In

addition, MXD1 can stimulate differentiation in Friend murine erythroleukemia cells [255], [256], but not in U937 monoblasts [243]. It has been revealed that ablation of MXD1 suppresses the differentiation of granulocytes in mouse [243]. Interestingly, expression of MXD1 in fibroblasts, dominantly suppresses the S phase progression and c-Myc is unable to rescue this effect. However, cyclin E/CDK2, but not other cyclin/CDK are able to induce S phase progression in the presence of MXD1, suggesting they act downstream of MXD1 in cell cycle regulation. In addition, it was suggested that cyclin E/CDK2 could rescue the inhibition of S phase by interfering with the interaction of mSIN3 with MXD1, but the molecular mechanism has not been fully elucidated yet [249].

1.5.3. Regulation of *MXD1* transcription

The expression pattern for *MXD1* is inversely correlated with that of *MYC* [249]. Differentiation inducing factors, such as the phorbolester12-O-tetradecanoylphorbol-13-acetate (TPA), retinoic acid and cytokine granulocyte-colony stimulating factor (G-CSF) in granulocytes, induce *MXD1* expression [257], [258]. The proximal region of the *MXD1* promoter, homology region, is highly conserved in humans and other mammalian species, such as rat and mouse. It is characterized by increased DNaseI hypersensitivity , open chromatin, GpC island enrichment, and lack of a TATA box [257]. In U937 cells, Polymerase II is constitutively bound to *MXD1* transcription start site revealing that the gene promoter is in a pre-active state. The proximal promoter region contains two CCAAT-boxes which are C/ EBPα and β (CCAAT-enhancer-binding proteins) binding sites and SP transcription factors associated to the GC-rich region. Similar to Pol II, C/EBP proteins are constitutively bound to the promoters. The G-CSF cytokine has a crucial role in stimulating the differentiation and maturation of myeloid progenitor cells toward granulocytes. The G-CSF receptor (G-CSFR) activates multiple signaling pathways including JAK/STAT and

the RAS/RAF/MAPK pathways. The STAT3 (Signal transducer and activator of transcription 3) and the RAS/RAF/ERK signaling pathways can also activate *MXD1* transcription. In particular, STAT3 directly upregulates *MXD1* expression by binds to its promoter through C/EBPβ [257].

One of the most important signaling pathways that activates transcription of MXD1 is TGFβ [259]. It activates SMAD2 and SMAD3, which bind to the C/ EBPs on the promoter of *MXD1* to activate its transcription. In addition, IKKα (The IκB kinase), independent of its kinase activity, is recruited to *MXD1* promoter as a cofactor along with SMAD2 and SMAD3. In invasive squamous cell carcinomas that are resistant to TGFβ signaling, IKKα is defective and is not able to enter to the nucleus and stimulate *MXD1* expression [259].

1.5.4. Regulation of MXD1 protein

Similar to c-Myc, MXD1 is an unstable protein compared with the long-lived MAX. MXD1 could be poly-ubiquitinated at multiple sites and subsequently degraded via the proteasome. c-IAP1 is one of the E3 ligases that promotes MXD1 ubiquitination and degradation [260]. c-IAP1 is an oncogene and its expression is elevated in many tumors [261], [262]. Insulin can promote MXD1 phosphorylation at Ser145 by either p70 S6 (S6K) serine/threonine kinase or p90 ribosomal kinase (RSK) [263]. However, Ser145 phosphorylation induces MXD1 degradation independent of c-IAP1. S6K and RSK kinases are important for cell cycle progression[249].

1.6. Protein ubiquitination

Ubiquitination is a protein post translational modification that plays a crucial role in the regulation of various cellular process including protein trafficking, protein degradation, cell-cycle regulation, DNA repair, apoptosis, and signaling. Proteins are ubiquitinated by ubiquitinating complexes which contain a substrate recognizing unit termed ubiquitin E3 ligase. Ubiquitin can be removed by deubiquitinating enzymes belonging to either metalloprotease or

cysteine protease families. It is estimated that around 1000 E3s ligase and 100 deubiquitinating enzymes are working in mammalian cells [264], [265].

1.6.1. Ubiquitin Proteasome System (UPS)

Ubiquitination is mediated by the sequential function of ubiquitin-activating (E1), ubiquitin-conjugating (E2) and ubiquitin-ligating (E3) enzymes that activate and transfer the ubiquitin to the target proteins. In humans there are two E1 enzymes (UBE1L2 and E1-L2), Approximately 40 E2s, and about 600 E3s [266]–[269]. Initially, E1 enzyme activates ubiquitin by adenylating the C-terminal of ubiquitin, which is ATP-dependent, forming an E1-ubiquitin thioester. The thioester bond is between a cysteine residue at the active site of the E1 enzyme and C-terminus of the conjugated ubiquitin. In the second step, E1 catalyzes a trans-thioesterification and transfers the activated ubiquitin to an E2. E3 enzymes transfer the ubiquitin from E2 enzymes to target protein [269]. Ubiquitin is generally transferred to the lysine residues on the target protein, however by less frequency, it can be also transferred to the N-terminus of the substrate [270].

1.6.1.1. Proteasome complex

Proteasome is a protein complex that degrades extra and damaged proteins by proteolysis. Proteasome complexes are located in both nucleus and cytoplasm [271]. Proteasome is a cylindrical structure with a core of four rings that form the central pore. The inner two rings are formed of seven β subunits that contain three to seven catalytic sites. These catalytic domains are located on the interior part of the rings. Each of the two outer rings contains seven α subunits acting as a gate for the complex. These α subunits are under the control of cap structure (regulatory particle) which contains the ATPase ring and recognizes poly-ubiquitin tags on the proteins [272]. The 26S proteasome is composed of a 20S core which is capped by a 19S regulatory at one or both ends [272].

1.6.1.2. Ubiquitin

Ubiquitin (Ub) is a conserved, 76-amino acid peptide which is present in almost all eukaryotic tissues. Ubiquitin is expressed by 4 different genes. UBA52 and RPS27A genes code for a single copy of ubiquitin fused to the ribosomal proteins. UBB and UBC genes code for a polyubiquitin precursor with head to tail repeats. The number of repeats differ between species and strains. It has been shown that proteasome inhibition and oxidative stress upregulate the transcription of UBB and UBC genes [273]. UBB and UBC polyubiquitin precursors mostly are cleaved by UCHL3, USP9X, USP7, USP5 and Otulin/Gumby/FAM105b deubiquitinases to make mature ubiquitin peptides [274]. The carboxyl group of the C-terminal glycine residue of ubiquitin (Gly76) covalently bind to the target proteins via an isopeptide bound. Ubiquitin contains several lysine residues, therefore, is able to binds to other ubiquitins and forms poly-ubiquitin chains [264]. Proteins can be ubiquitinated by a single ubiquitin (monoubiquitination) or several independent ubiquitins (multiple monoubiquitination). Mono ubiquitination and multi-monoubiquitination are implicated in several cell processes such as DNA repair, trafficking, transcription, and degradation. In addition, proteins can be poly-ubiquitinated by a chain of ubiquitins. Ubiquitin chain is composed of multiple ubiquitin which are linked via isopeptide bonds through Met1 and all seven Lys residues (Lys6, Lys11, Lys27, Lys29, Lys33, Lys48, and Lys63) within ubiquitin peptide. Each type of ubiquitination is implicated in different cell processes. It has been revealed that Lys48-linked chain poly-ubiquitination of proteins results in their degradation, whereas Lys63-linked chain poly-ubiquitination involves in a variety of nonproteolytic roles such as DNA repair, trafficking and signaling [270], [275]. DUBs function as editors of poly-ubiquitin and are able to promote the conversion of one type to another type of Ub chain. Another layer of regulation to ubiquitinated proteins is formed by acetylation or

phosphorylation of the ubiquitin peptide on the target proteins. It has been shown that Ub acetylation prevents elongation of poly-Ub chain [275], [276]. There are also various ubiquitin-like protein modifiers including SUMOs, NEDDs, SAMPs, ISG, UFM, APGs, FAT, Hub, and URM which possess distinct enzymatic machineries and are linked to distinct biological processes [269], [277]–[279].

1.6.2. E3 ligases

E3 ligases are the substrate recognizing agents of the ubiquitination complex. There are several different ubiquitination complex, each has one or several specific E3 ligases. E3s are a diverse group of proteins, each of them characterized by a specific defined motif. Each type of E3 ligase, mediates protein ubiquitination with different mechanisms. A number of factors, including substrate post-translational modifications such as phosphorylation or hydroxylation determine the timing and specificity of target protein recognition by the E3 ligase. Other factors such as the respective location of substrate protein and E3 ligase also might play important role in the specificity. Further, many E3 ligases are able to auto-regulate by self-ubiquitination [280].

Three major groups of E3 ligases have been found. They are classified into HECT (homologous to E6-associated protein C-terminus), RING (really interesting new gene) and U-box (a modified RING motif without the full complement of Zn2+-binding ligands) domain containing E3 ligases. Two subclasses of the RING containing E3s have further been defined, CRL (Cullin-RING ligases), multi-protein complex E3 ligases, and RBR (RING in between RING–RING) domain. In addition, several proteins have been identified which lack these identified motifs, but are able to act as an E3 ligase. It has been revealed that some of the DUB (deubiquitinating enzyme) such as UCHL1 (ubiquitin C-terminal hydrolase L1), has dual function and can act as both E3 ubiquitin ligases and deubiquitinating enzyme[270], [280]. There are two different

mechanisms of function for E3s. They act either as a non-catalytic scaffolding protein which mediates direct ubiquitination of the target protein by E2 or as a catalytic intermediates which bind to Ub to transfer it to the substrate [270].

1.6.2.1. HECT domain E3s

Approximately 30 HECT domain E3s exist in mammals. HECT is an approximately 40 kDa catalytic domain containing 350 amino acids which is found at the C-terminus of HECT E3s [281], [282]. The HECT domain consists of two lobes, the N-terminal lobe interacts with E2 and the C-terminal lobe contains the active cysteine which mediates thioester bonds with ubiquitin molecules. These two lobes are linked via flexible hinge allowing them to position at the proper distance from each other during Ub transfer. The N-terminus in different HECT E3s is varied and involved in substrate recognition. HECT E3s have important role in the immune response, protein trafficking, and pathways which regulate Proliferation and cellular growth [281].

1.6.2.2. RING finger E3s

RING fingers are the largest group of E3s; there are hundreds of E3s containing a RING finger domain in mammalian cells. Many RING finger proteins act as E3s *in vitro*, but not *in vivo*. RING finger E3s do not form a catalytic intermediate with ubiquitin, in fact they act as scaffolding partners to bring the E2 and substrate to a proximal distance. A conserved ring finger is a Zn2+-coordinating domain consisting of 40-60 residues with a series of specifically spaced cysteines and histidines. Consensus cysteine and histidine residues coordinate two Zn2+ ions in a "cross-braced" pattern to produce a platform for binding of E2 to a cysteine residue. The RING-like U-box E3s have a similar structure for binding of E2, but without Zn2 + coordination [280], [283]. In ring type E3s, E2 is responsible for both E3 selection and substrate ubiquitination [280], [284]. RING-type E3s mutations are generally associated with human

disease (e.g. The E3 ligase BRCA1 which involved in DNA repair, is mutated in breast and ovarian cancer) [270].

RING finger E3s can act as monomers, dimers or multi-subunit complexes. Dimerization is through RING finger domains and result in either homodimers such as cIAP, RNF4, BIRC7 and SIAH or heterodimers such as BRCA1–BARD1, Mdm2–MdmX, and RING1B–Bmi1. In most of the heterodimer RING finger E3s, one of the RING finger domains lacks the ligase activity and the partner acts as an enhancer of the activity. RING-type E3s dimerize either through the sequences outside the RING, or due to the RING per se which is potent to dimerize. In both types, the ring domains are positioned in a manner that the E2 binding sites face away from each other [270], [282].

1.6.2.2.1. Multi-subunit RING finger E3s

Multi-subunit RING finger E3s consist of several units with different functions [285].

1.6.2.2.1.1. Cullin Ring Ligases (CRLs)

CRLs are largest group of substrate-specific and multi-subunit ring E3 ligases. There are multiple CRL subfamilies. CRLs are characterized by a cullin protein (Cul-1,2, 3, 4a, 4b, 5, or 7) as a scaffold protein which binds to a small RING finger protein, generally Rbx1 [270], [282], [286]. In addition, a cullin-specific adaptor protein that binds interchangeably to the substrate recognition element, is associated with these subfamilies. Receptors can recognize multiple target proteins. The most well-known of this group are the F-box protein ligases containing complexes termed SCF (SKP1, Cullin, F-box), and Anaphase-Promoting Complex, also known as cyclosome or APC/C [270].

SCF has extended substrates involved in extremely regulated cell processes such as cell-cycle regulation and signaling and deregulation of these complexes results in oncogenesis and other diseases. SCF consists of a cullin, Cul1, and an adaptor protein, SKP1, which binds to the substrate recognizing F-box proteins. There are approximately 69 F box proteins in humans [287]. Ubiquitin-like protein, Nedd8 (Neural Precursor Cell Expressed, Developmentally Down-Regulated 8), binds covalently to Cul1 and promotes conformational alteration in Cul1 promoting the activation of the SCF complex by allowing the skp1 and F-box protein binding to the Cul1. In the absence of Nedd8, CAND1 (cullin-associated and neddylation-dissociated 1) binds to the Cul1-Ring box1 leading to inactivation of the complex which lacks Skp1-F box compounds. CAND1 dissociates when Cul1 is neddylated [287], [288].

APC/C is a protein complex that promotes the degradation of the cell cycle proteins time dependently, therefore highly regulates the cell cycle progression. APC/C has great structural complexity with at least thirteen components including a small RING protein (Apc11), a cullin-like protein (Apc2) and two interchangeable substrate recognition subunits (Cdc20 and Cdh1) which recognize distinct substrates in a time dependent manner and are active sequentially during different phases of the cell cycle[270].

1.6.2.2.2. RING-IBR-RING E3s

There are single proteins that contain multiple RINGs. RING-IBR-RING (RBR) E3s are a class of approximately 13 proteins that have two RINGs domain that are linked by a Cys/His-rich region termed IBR (in between RING). The N-terminus RING domain is essential for E2 and substrate binding. This domain is similar to other RING finger containing proteins. The role of IBR domain is unknown and it is suggested that might position the N-RING and C-RING for accurate E2/substrate recognition and binding. The C-RING has a different topology from

canonical RING finger domains. C-RING structure resembles a zinc ribbon motif with a criss-cross form, similar to that of Rbp12 subunit of RNA polymerase II. This group of E3s share features of both RING and HECT E3s, however they catalyze ubiquitination and auto-regulate themselves in a distinct manner [270], [280]. RBR proteins Use a RING–HECT hybrid mechanism to ubiquitinate the target proteins. N-RING is essential for the recognition and binding of E2 (similar to the RING mechanism), however ubiquitin is transferred to a specific Cys within C-RING before being transferred to a recognized substrates in C-RING (similar to the HECT mechanism) [270]. Some RBR E3s, are able to be activated alone and with cullin-containing complexes, such as parkin [289].

1.6.2.3. U-Box proteins

The U-box is similar to the RING finger domain but it lacks the essential residues for metal chelation. The most well-known of the U-box proteins is CHIP which first was known as a co-chaperone of hsp70 or hsp90. It has been revealed that hsp70 or hsp90 have essential role in the substrate recognition by CHIP [289].

1.6.3. Substrate recognition mediator in SCF E3 ligase complex

1.6.3.1. F-Box proteins

SCF complexes use a class of F-box proteins as a substrate recognition mediator to degrade a large number of regulatory proteins implicated in variety of processes. There are three classes of F-Box proteins categorized based on their recognizable domains beyond the F-box. The F-box E3s containing WD40 domain (FBXW) class which is composed of 12 proteins, the F-box E3s containing Leu-rich repeat (FBXL) class which is composed of 21 proteins and the remaining 36 F-box E3s which generally have conserved homology domains either not identified or not present in a large number of F-box E3s, therefore they are named FBXO (F-box and other

domains). At least 21 conserved domains have been characterized in the FBXO class which interact with the target proteins [288]. Both F-box protein–substrate interaction and the F-box protein itself are under tight regulation. In response to various stimuli, the regulation of the SCF activity occurs via substrate recruitment through substrate modification [288]. Activation of F-Box containing E3s through different signaling pathways, results in regulation of multiple cell processes [288].

1.6.3.1.1. FBW7

F-box and WD repeat domain-containing7 (FBW7, CDC4, FBXW7, AGO, SEL10) is a substrate recognition subunit of SCF (SKP1, CUL1 and F-box protein complex) ubiquitin ligase and regulates degradation of a series of proteins that play crucial roles in cell cycle progression, cell growth and differentiation including c-Myc, cyclin E, Notch and c-Jun. Most FBW7 substrates that have been identified, are proteins involved in oncogenesis.

1.6.3.1.1.1. FBW7 gene and isoforms

FBW7 Gene is located on chromosome 4 and transcribed into three different mRNAs (FBW7α, β and γ) by alternative splicing, from different promoters [290]. Recently, a paper has reported seven additional FBW7α splicing isoforms which are transcribed from three newly identified exons upstream of the previously reported first exon [291]. FBW7α is a nuclear protein constantly expressed in various tissues, whereas FBW7β is localized in cytoplasm and restricted to the brain and thymus tissue. FBW7γ is expressed mostly in heart and skeletal muscle and exhibits a nucleolar distribution pattern [290]. It has been shown that FBW7α is responsible for the ubiquitination and consequently degradation of most FBW7 target proteins [292]. FBW7 recruits the target proteins to the SCF in a phosphorylation-dependent manner (Fig. 1.3). WD-40 repeats at the C-terminal form a phosphodegron binding site by adopting a 7-bladed beta-

propeller fold. FBW7 is able to recognize most of its identified substrates via a phosphodegron which contains (T/S-p-X-X-S/T/E) termed CDC4 phosphodegron (CPD). FBW7 is recruited to the SCF complex through direct interaction of F-box with SKP1 [293].
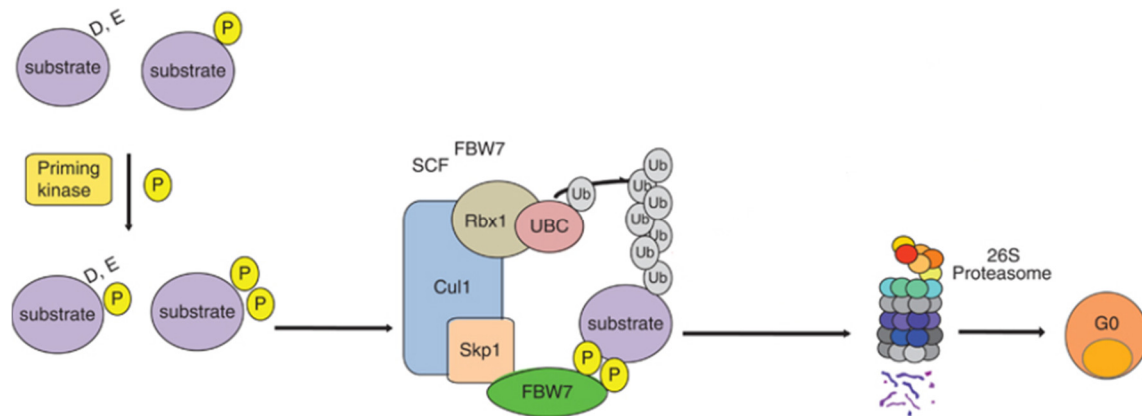
Figure 1.3: FBW7 mediated degradation.

Modified From: Crusio KM, King B, Reavie LB and Aifantis I, oncogene, 2010, 29(35):4865-73

All isoforms contain a dimerization domain (DD), an F-box domain (FBX), seven WD-40 repeats, and an isoform-specific N-terminus that may be implicated in regulation of FBW7 expression and function as well as its subcellular localization. Dimerization via DD domain is crucial for FBW7 to gain multiple geometries, which are essential for substrate recognition and subsequent interaction. It is suggested that the dimeric FBW7 complex might incorporate the binding pocket to which phosphorylated targets interact [294]. However it has been reported that in some cases, such as cyclin E which has two degrons, FBW7 has more affinity to one degron (T_{380}-P-X-X-S) in the monomeric form and in the high FBW7 concentration, it can form a dimer and bind to both degrons, the high affinity degron and the second degron (T_{62}-P-X-X-E) with lower affinity [293]. Therefore, high-affinity degrons can be targeted by monomeric FBW7, but

low-affinity degrons might need to cooperate with other degrons in the presence of high concentration of FBW7 which results in its dimerization [293].

1.6.3.1.1.2. FBW7 and GSK3s

GSK3α and GSK3β are proline-directed serine/threonine kinases that are constitutively active and phosphorylate the central threonine of the phosphodegron in substrates containing a priming phosphorylation, such as cyclin E, c-Myc, c-Jun and SREBP. Most, but not all of the GSK3 substrates need to be pre-phosphorylated (priming) as a binding site for GSK3s. In fact, CPDs are regulated by both GSK3 and FBW7. There are various mitogen signals that negatively regulate the GSK3s activity including (PI3K)–Akt and Wnt pathways [293], [295]. Phosphorylation of certain residues in GSK3s alters their ability to bind to substrate. Phosphorylation of Tyr216 in GSK3s and Tyr-279 in GSK3α promote their activities, whereas phosphorylation at Ser9 in GSK-3s and Ser21 in GSK3α significantly reduce their active site availability [296].

1.6.3.1.1.3. FBW7 as a tumor suppressor

FBW7 locus is frequently deleted in cancers [297]. Most FBW7 targets are essential regulatory proteins involved in diverse cell processes. Cyclin E is implicated in cell cycle regulation. c-Myc and c-Jun are crucial for cell cycle progression. In addition, Notch signaling acts as a regulator of cell differentiation and Mcl-1 is a member of Bcl-2 superfamily which is an anti-apoptotic protein. It has been shown that approximately 6% of tumors contain mutations in *FBW*7, however this rate is variable in different cancers [293]. The highest mutation rate of *FBW7* (30%) has been reported in Cholangiocarcinomas (CCCs) and T-cell acute lymphoblastic leukaemias (T-ALL) [293], [298]. On the other hand, many cancers do not harbor any mutation in *FBW7* gene including leukaemias (other than T-ALL) and pancreatic ductal adenocarcinoma, as well as

liver, lung, breast, ovary, bladder and bone cancers. In addition, different cancer types have different *FBW7* mutational patterns. While mutations in *FBW7* can affect the degradation of FBW7 targets simultaneously, mutation in CPDs of a target protein can disrupt FBW7 binding specifically to that target protein [293].

1.6.3.1.1.4. Regulation of FBW7

Multiple signaling pathways and factors such as p53, C/EBP-δ, EBP2, Pin1, Hes-5 and Numb4 regulate the activity of FBW7. It also can be regulated by microRNAs such as miR-223, miR-27a, miR-25, and miR-129-5p [298], [299]. The tumor suppressor P53 increases the expression of FBW7 directly and any impairment in P53 signaling can reduce the FBW7 expression. By contrast, the transcription factor C/EBPδ inhibits *FBW7* transcription [298]. In some cancers dominant oncogenes can suppress FBW7 activity. In pancreatic ductal adenocarcinoma, KRAS (Kirsten Rat Sarcoma Viral Oncogene Homolog) mutations leads to ERK activation. Activated ERK consequently binds and phosphorylates FBW7 at Thr205, which induces FBW7 ubiquitination and degradation [300]. MiRNAs mostly are upregulated in various cancers and suppress the expression of FBW7. In T-cell acute lymphoblastic leukemia, Notch and NF-kB cooperatively promote the miR-223 transcription which consequently suppress the expression of FBW7 [299], [301].

Chapter 2

1,25D signaling regulates c-Myc expression and function by repressing its transcription and inducing its turnover through FBW7.

2.1. Preface

Vitamin D has attracted widespread interest because of the growing evidence that it has multiple "non-classical" actions, independent of its calcium homeostatic functions, consistent with the ubiquitous expression of the vitamin D receptor (VDR). One of these actions is its roles in regulating cellular proliferation and differentiation in a variety of tissues and its potential as a cancer chemopreventive agent. Previously it was shown that 1,25D bound VDR, down regulates the transcription of multiple oncogenes including c-Myc, a key regulator of cell cycle progression. We investigated the effect of this down regulation on c-Myc protein levels. Unexpectedly, we observed a profound reduction on c-Myc protein levels, suggesting that 1,25D not only affects *MYC* transcription, but it also down regulates c-Myc at the protein levels. We became curious to know the mechanism by which 1,25D regulates c-Myc at the protein level.

2.2. Abstract

Epidemiological data have shown links between vitamin D insufficiency, and the prevalence of multiple cancers. Vitamin D sufficiency reduces total cancer incidence and mortality, especially in digestive cancers. Hormonal 1,25D possesses cancer chemopreventive effects through multiple mechanisms. Transcriptome analyses have revealed that vitamin D signaling suppresses expression of numerous genes implicated in cell cycle progression including genes regulated by c-Myc, a transcription factor whose expression is frequently elevated in cancer. Here, we provide evidence for a novel mechanism by which 1,25D-bound VDR reduces c-Myc levels. In this study, we have shown that 1,25D suppressed the transcription of *MYC* and its target genes. Coincidently c-Myc was dissociated from the E-box motif of its target genes. 1,25D signaling reduced c-Myc protein levels by promoting its turnover. Multiple pathways induce c-Myc turnover. We revealed that 1,25D signaling enhanced c-Myc turnover through SCF^{FBW7} E3 ubiquitin ligase complex which is major regulator of c-Myc stability. In addition, VDR associated with c-Myc and this association increased in the presence of 1,25D. VDR is recruited to the E-box region of c-Myc target genes, which is 1,25D-dependant. Analyzing the ChIPseq for potential associations between VDR and c-Myc binding sites on the genome demonstrated an overlap between one half of the VDR binding sites detected in the absence of 1,25D, and almost one quarter of those in the presence of 1,25D, with high fidelity c-Myc sites. Further, we showed that c-Myc levels are elevated in the VDR-ablated cells. This observed increase was the result of increased transcription, not enhanced protein stability. The association of β-catenin, as an activator of *MYC* transcription, with the promoter of *MYC* gene increased in the VDR-deficient cells, while 1,25D induced its dissociation in VDR-replete cells. Furthermore, *in vivo* studies revealed that c-Myc protein levels were substantially elevated in skin, colon, heart, muscle and

brain of *Vdr*-null mice. Topical application of 1,25D to wild-type mouse skin repressed c-Myc and its target gene, Setd8, levels. These results suggest that 1,25D signaling inhibits c-Myc expression by reducing its transcription and inducing its turnover through SCF[FBW7]E3 ligase.

2.3. Introduction

Vitamin D is obtained naturally from limited dietary sources. It is also generated by cutaneous conversion of 7-dehydrocholesterol in the presence of adequate surface solar ultraviolet B radiation, which varies with latitude and time of year [302]. Vitamin D has attracted broad clinical interest because insufficiency or deficiency is widespread in several populations worldwide [303]–[305]. Although initially identified as a regulator of calcium homeostasis, vitamin D is now known to have a broad spectrum of actions, driven by the virtually ubiquitous expression of the vitamin D receptor (VDR), a nuclear receptor and hormone-regulated transcription factor. It acts as a chemopreventive agent in several animal models of cancer, and induces cell cycle arrest and non-malignant and malignant cell differentiation [306], [307]. Epidemiological data have provided associations between lack of UVB exposure, vitamin D insufficiency, and the prevalence of certain cancers [30]. A large prospective study associated vitamin D sufficiency with reduced total cancer incidence and mortality, particularly in digestive cancers [head and neck squamous cell carcinoma (HNSCC), esophageal, pancreatic, stomach and colorectal cancers] and leukemias [308]. VDR gene polymorphisms also correlate with protection against different malignancies, including HNSCC [30], [309]. However, results of epidemiological studies on the protective effects of vitamin D are not unanimous, and uncertainties as to the potential benefits persist [310], [311], underlining the need for not only more clinical studies, but also a better understanding of potential molecular mechanisms of the protective effects of vitamin D. The VDR is bound by hormonal 1,25-dihydroxyvitamin D

(1,25D), which is produced from vitamin D by largely hepatic 25-hydroxylation, followed by 1α-hydroxylation by widely expressed CYP27B1 [312], [313]. Cancer preventive actions of 1,25D signaling through VDR can be explained in part by regulating the gene expression. Recent studies have shown that 1,25D gradually reduces *MYC* mRNA levels in cancer cells [314], [315]. Elevated or deregulated expression of transcription factor c-Myc is widespread in cancer [316], [317]. c-Myc is a critical regulator of cell cycle progression and, like the VDR [318], controls epidermal differentiation [319]. Inducible epidermal expression of c-Myc rapidly induced actinic keratosis, a squamous cell carcinoma precursor [320]. Heterodimers of c-Myc and its cofactor MAX bind E-box motifs (CACGTG) to induce expression of cell cycle regulatory genes such as CDC25A mitosis [200], CCND2 and CDK4[321].

c-Myc is part of c-Myc/MAX/MXD1 network, which in the absence of its antagonist, MXD1, or in the case of overexpression, makes a heterodimer with its partner, MAX, and activates the transcription of target genes [174]. Since c-Myc is implicated in cell growth, proliferation, and metabolic signaling, it is crucial to keep c-Myc activity in check, to avoid undesired oncogenic alterations. Cells have adapted several paths to modulate c-Myc levels, which can be disrupted in cancer cells[138]. c-Myc is highly regulated post-translationally and rapidly turned over by proteasomal degradation controlled by multiple E3 ligases[138]. Ubiquitination promotes c-Myc degradation and also modulates its transcriptional activities. One of the most important regulator of c-Myc stability is the SCF ubiquitin ligase complex containing F-box protein Fbw7 [322]. FBW7 is a tumor suppressor that regulates the stability of multiple drivers of cell proliferation and tumorigenesis. FBW7 regulates the c-Myc levels in the late G1 and early S phases of the cell cycle[138], [139]. c-Myc protein becomes phosphorylated to be recognized by FBW7 . The c-Myc phosphodegron is located in Myc Box I which is recognized by the FBW7. Phosphorylation

of Ser62 residue of the phosphodegron induces the association of c-Myc with Axin1. Pin1 recognizes phosphorylated Ser62 and converts proline 63 from trans to cis. Subsequently the Axin-1 associated GSK3 phosphorylates threonine 58. Pin1 recognizes the Thr58 phosphorylation and returns the proline 63 from cis to trans form, which leads to the PP2A binding. PP2A dephosphorylates Ser62. In fact, Axin1 scaffold protein helps the association of Pin1, PP2A, and GSK3 with c-Myc [140]. Dephosphorylation of S62 leads to the binding of the FBW7, which ubiquitinates c-Myc by K48-linked chains of ubiquitin. Disassociation of c-Myc from promoters is induced via isomerization of P63 from cis to trans, which eventually leads to c-Myc proteasomal degradation [140].

We investigated potential mechanisms of crosstalk between c-Myc and VDR signaling. We found that signaling through VDR controls expression and FBW7-dependent turnover of c-Myc. These findings provide a compelling mechanism for the cancer chemopreventive actions of vitamin D and implicate VDR-dependent regulation of c-Myc in control of epidermal differentiation. Moreover, c-Myc is critical for normal epidermal differentiation and its deregulated expression in skin depletes epidermal stem cells [319], [323], [324], disrupting hair follicle development and increasing sebaceous activity, very similar to *Vdr* knockout mice [318]. Our results are thus consistent with c-Myc overexpression contributing to the alopecia observed in *Vdr*-/- mice.

2.4. Results

2.4.1. 1,25D signaling suppresses c-Myc target gene expression.

c-Myc activates transcription of multiple genes involved in cell cycle progression, including cell division cycle 25 homolog A (CDC25A), Cyclin D2 (CCND2) and Cyclin-dependent kinase 4 (CDK4) [196], [236], [237]. CDC25A is a protein phosphatase expressed in G1 phase and is

essential for progression through mitosis [200]. CCND2 is the regulatory component of the cyclin D2-CDK4 and cyclin D2-CDK6 complexes required for cell cycle G1/S transition [325]. To determine whether the expression of these genes are 1,25D-dependent, the expression of these genes in SCC25 cells were tested upon treating with 1,25D for the times indicated in Fig.1A. RT-qPCR assays revealed that 1,25D inhibited expression of *CDC25A, CCND2* and *CDK4* (Fig. 1A). In addition, the expression of *CDC25A, CCND2* and *CDK4* were measured in primary cultures of keratinocytes, as a model of normal cells, following treatment with 1,25D. A similar decline in the expression of c-Myc target genes was observed in primary cultures of keratinocytes (Fig. 1B).

To clarify whether reduction in the expression of *CDC25A, CCND2* and *CDK4* after 1,25D treatment is due to attenuated c-Myc function, the recruitment of c-Myc to the E-box motif of the promoter of target genes was tested. For this purpose, the SCC25 cells were treated with 1,25D for the times indicated in Fig.1C and the recruitment of c-Myc to the promoter of target genes were measured by chromatin immunoprecipitation assays. The results show that c-Myc binding to E-box regions of the corresponding promoters declined, coincided with the reduction in the transcription of these genes (Fig. 1C). These data suggest that 1,25D attenuates c-Myc function, which consequently results in transcriptional repression of c-Myc target genes in cancerous SCC25 cells and normal primary human keratinocytes.

2.4.2. 1,25D signaling suppresses c-Myc transcription and protein expression.

Previous studies have shown that transcription of *MYC* gene is down regulated by 1,25D signaling [314], [315]. In addition our results show that c-Myc function declines in the presence of 1,25D. To determine whether the attenuated actions of c-Myc is due to its reduced expression, the transcription of *MYC* gene was measured by RT-qPCR assays. *MYC* gene is amplified in

HL60 cells [326], therefore the expression of *MYC* was measured in this cell line along with SCC25 cells and primary human keratinocytes following treatment with 1,25D. In agreement with other studies [14], [15], we observed a gradual diminution of *MYC* mRNA over 24hours in these three cell lines (Fig. 2A).

To investigate the effect of 1,25D on c-Myc protein expression, SCC25, primary human keratinocytes, and HL60 cells were treated with 1,25D for the times indicated in Fig.2 and c-Myc protein expression were measured by western blot assay. A dramatic loss of c-Myc protein was observed in these cell lines upon treatment with 1,25D (Fig. 2B).

Together these results suggest that 1,25D signaling not only attenuates the *MYC* gene transcription, but it also suppress the expression of c-Myc protein expression through an unknown mechanism, in different cell lines. Suppression of c-Myc expression in HL60 indicated that the effect of 1,25D on c-Myc expression is not limited to epithelial cells.

2.4.3. The 1,25D-bound VDR promotes c-Myc turnover.

To find the mechanism by which 1,25D suppresses c-Myc protein levels, the effect of 1,25D on the c-Myc turnover was examined. Stability assays were performed following treatment of the cells with 1,25D. Cycloheximide (CHX) was applied for the times indicated in Fig. 3A. c-Myc protein levels were measured by western blot assay. The results revealed that when protein synthesis was blocked with CHX, c-Myc turnover was accelerated in 1,25D-treated cells (Fig. 3A).

The effect of 1,25D on the c-Myc turnover was verified by knocking down the *VDR* in SCC25 cells. SCC25 cells were transfected with VDR or scrambled siRNA and treated with 1,25D for times indicated in Fig. 3C and c-Myc protein level were analyzed by western blot assay. The

results showed that 1,25D-induced turnover was abolished or largely attenuated by ablation of expression of the VDR (Fig. 3B). These results suggest that 1,25D-bound VDR induces c-Myc turnover through an unknown mechanism.

2.4.4. 1,25D-bound VDR affects c-Myc turnover through FBW7.

To determine the mechanism through which VDR induces c-Myc turnover, several pathways were investigated. ELAVL1 (HuR) is an RNA binding protein that binds to the 3′-untranslated region of *MYC* mRNA and represses its translation [117]. To test whether 1,25D-bound VDR reduces c-Myc levels in the cells, SCC25 cells were transfected with *ELAVL1* or scrambled siRNA and treated with 1,25D. The expression of c-Myc protein were analyzed by western blot assay. The result showed that ELAVL1 ablation does not rescue the attenuated c-Myc levels upon 1,25D treatment (Fig. 4A).

c-Myc protein stability is regulated through multiple pathways[138]. One of these pathways is SCF^{Skp2}, which has been shown to possess dual regulatory effects on c-Myc protein. Skp2 is a transcriptional coactivator of c-Myc and also can promote its degradation [157]. To clarify whether 1,25D-bound VDR attenuates c-Myc levels in the cells through SKP2, SCC25 cells were transfected with *SKP2* or scrambled siRNA and treated with 1,25D. The expression of c-Myc protein were assessed by western blot assay. Ablation of SKP2 had no substantial effect on c-Myc expression in the absence or presence of 1,25D (Fig. 4B).

One of the major regulator of c-Myc turnover is SCF^{FBW7}[327]. To determine whether the effect of 1,25D-bound VDR on c-Myc stability is through SCF^{FBW7}, the F-box component of the SCF^{Fbw7} E3 ubiquitin ligase that recognizes c-Myc was knocked down in SCC25 cells. Subsequently cells were treated with 1,25D for the times indicated in the Fig. 4C. The expression of c-Myc protein were assessed by western blot assays (Fig. 4C). Interestingly, ablation of

FBW7 largely rescued the 1,25D induced turnover of c-Myc protein. Taken together these results suggests that 1,25D-bound VDR accelerates the c-Myc turnover through SCF^{FBW7} complex.

2.4.5. The 1,25D-bound VDR interacts with c-Myc on the promoter of its target genes.

The interaction between VDR and c-Myc was investigated in SCC25 cells following treatment of the cells with 1,25D for indicated times in Fig.5A.-Co-Immunoprecipitation (Co-IP) assays were performed to assess the association of VDR with c-Myc. Coimmunoprecipitation assays showed that 1,25D treatment induced a rapid association (<4h) of the VDR with c-Myc. A peak of increased interaction was observed immediately after applying 1,25D to the cells, followed by slight reduction over 24 hours (Fig.5A). This reduction is due to the attenuated c-Myc levels in the cells. After 24 hours of 1,25D treatment c-Myc expression is profoundly decreased in the cells, while Co-IP assays showed that the association of VDR with c-Myc is slightly reduced. This suggests that association of VDR with c-Myc is enhanced in the presence of 1,25D and the slight reduction after a primary peak of increased interaction, is due to the loss of c-Myc protein in the cells (Fig.5A). The rapid association of c-Myc with the VDR in the presence of 1,25D strongly suggests that regulation of its function contributes to, rather than is a consequence of, cell cycle arrest by 1,25D.

To determine whether VDR is recruited to the promoter of c-Myc target genes, chromatin immunoprecipitation assays were performed for the E-box region of *CDC25A* and *CDK4* following treatment of the SCC25 cells with 1,25D for the times indicated in Fig.5B. The results show 1,25D-dependant recruitment of VDR to E-box regions of the corresponding promoters. Recruitment of VDR to the promoter of c-Myc target genes increased rapidly in the presence of 1,25D and is attenuated gradually after a primary peak of increased association (Fig. 5B). These

data together with Co-IP results suggests that VDR interacts with c-Myc on the promoter of target genes.

To further verify the co-recruitment of VDR and c-Myc on the E-box regions, Re-ChIP assays were performed using anti-VDR for ChIP and anti-c-Myc for Re-ChIP following treatment of SCC25 cells with 1,25D for 24 hours. The results suggest that VDR interacts with c-Myc on the promoter of c-Myc target gene, *CDC25A*, and this association is attenuated after 24 hours of 1,25D treatment (Fig. 5C). Since profound loss of c-Myc is observed following 24 hours of 1,25D treatment (Fig. 2B), the reduction in the co-recruitment of VDR and c-Myc to the E-box region of *CDC25A* is partially due to this lost.

To gain a broader insight into the potential association between the VDR and c-Myc binding sites on the genome, we reanalyzed with equally stringent parameters VDR and c-Myc peaks identified by ChIPseq from related lymphoblastoid cell lines [328], [329]. This revealed an overlap between approximately one half of the VDR binding sites detected in the absence of 1,25D (269/532), and almost one quarter of those (952/4,015) in the presence of 1,25D, with high fidelity c-Myc sites (Fig. 5D).

2.4.6. *MYC* gene transcription is elevated in VDR-deficient cells.

In addition to the effects of 1,25D on c-Myc expression and function, we sought to determine whether VDR ablation affects c-Myc expression. SCC25 cells were transfected with *VDR* or scrambled siRNA and c-Myc protein expression was assessed by western blot assay. c-Myc protein levels were elevated in VDR-deficient cells (Fig. 6A). In addition, to verify that this effect is not limited to SCC25 cells, *VDR* was knocked down in human LNCaP prostate carcinoma cells. Western blot analyses showed that, similar to SCC25 cells, c-Myc protein expression were elevated in VDR-deficient LNCaP cells (Fig. 6B). To test whether 1,25D can

affect *MYC* expression and function in VDR-deficient cells, the SCC25 cells were treated with 1,25D following knockdown of VDR gene. The expression of *MYC* and its target genes were assessed by RT-qPCR assays. The results show that transcription of *MYC* and its target gene *CDC25A* was enhanced in VDR-deficient cells, suggesting that VDR is essential for 1,25D signaling to affect the *MYC* expression and function (Fig. 6C).

To verify whether 1,25D could affect c-Myc turnover in the absence of VDR, stability assays were performed in SCC25 cells following knockdown of VDR. In contrast to *MYC* transcription, Ablation of VDR expression had little effect on c-Myc turnover (Fig. 6D), suggesting that higher *MYC* gene expression rather than increased protein stability led to elevated c-Myc levels and function in the absence of the VDR.

2.4.7. Association of β-catenin with the *MYC* promoter is higher in VDR-deficient cells.

The canonical Wnt signaling pathway stimulates *MYC* transcription through β-catenin [330], and the vitamin D signaling suppresses β-catenin function [331], [332]. To investigate the recruitment of β-catenin to *MYC* promoter, ChIP assays performed in SCC25 cells following knockdown of VDR. Notably, association of β-catenin with the *MYC* promoter was higher in VDR-deficient cells (Fig. 7A). To further investigate the role of 1,25D signaling in *MYC* transcription, we simultaneously ablated β-catenin (*CTNNB1*) and VDR expression, and performed RT-qPCR assays to assess the expression of *MYC* and its target gene *CDC25A*. Ablation of β-catenin and VDR reduced *MYC* and *CDC25A* transcript levels to those seen in VDR-replete cells treated with 1,25D (Figs. 7B, 7C). Furthermore, we determined the recruitment of β-catenin to the *MYC* promoter in SCC25 cells following 1,25D treatment. ChIP assays revealed that, consistent with previous results (Figs. 7A, 7B, 7C), association of β-catenin with the *MYC* promoter in VDR-replete cells was reduced by 1,25D treatment (Fig. 7D).

2.4.8. 1,25D and the VDR control c-Myc expression *in vivo*.

Vdr -/- mice display a hyperproliferative phenotype in colonic epithelia [318]. Therefore, we compared c-Myc levels by western blotting and immunohistochemistry in skin, colonic epithelia, and other tissues including heart, muscle and brain of wild-type and *vdr*-null mice. Normal and malignant breast tissue were used as a control for respectively negative and positive c-Myc overexpression (Fig. 8D). Western blot assays and immunohistochemistry analyses revealed that c-Myc protein levels elevated in skin of null mice to a great extent (Figs. 8A, 8B). In addition, immunohistochemistry analyses revealed that c-Myc protein levels substantially elevated with colonic overexpression visible in epithelial crypt cells (arrowheads; Fig. 8C), as well as in other tissues including heart, muscle and brain (Fig. 8E).

Consistent with observed effects on c-Myc in human cells, topical application of 1,25D to wild-type and *Vdr*-null mice skin suppressed c-Myc levels in wild type but not in *Vdr*-null mice as assessed by Western blot assays and immunohistochemistry analyses (Figs. 4F, 4G). Since c-Myc expression was modest in wild-type skin, we also analyzed the product of one of its epidermal target genes, setd8 [333], whose expression was suppressed by 1,25D (Fig. 4H).

2.5. Discussion

In this study, we identified a novel mechanism of 1,24D signaling by which affects c-Myc levels in the cells. Since, c-Myc overexpression has been implicated in the development of HNSCC [334], and inducible overexpression of c-Myc induces actinic keratosis, an SCC precursor [320]. In this study, we used human SCC25 HNSCC cells as a model to investigate mechanisms of 1,25D-induced cell cycle arrest [335], [336].

Here we showed that, 1,25D reduced the recruitment of c-Myc to the promoter of target genes and attenuated their transcription in SCC25 cells and primary human keratinocytes. The reduced

recruitment of c-Myc to the E-box region can be explained by the loss of c-Myc protein and/or its dissociation from DNA. In addition, 1,25D induced reduction of *MYC* gene transcription and c-Myc protein levels in three different cell lines including SCC25 cells, primary human keratinocytes and HL60 to show that the effect of 1,25D on c-Myc is not limited to one cell line. 24 hours of 1,25D treatment abolished or profoundly reduced the c-Myc levels, a result not justified by gradual reduction in *MYC* transcription. We found that 1,25D induced c-Myc turnover which was rescued by VDR knockdown. We investigated several pathways involved in c-Myc regulation to find the mechanism by which 1,25D signaling affect c-Myc protein levels. We found that 1,25D induced c-Myc degradation through SCF^{FBW7}, which is an E3 ligase that recognizes and ubiquitinates multiple oncoproteins including c-Myc (Fig. 3.6). This finding openes a new window in the mechanisms by which 1,25D can regulates the expression of oncogenes.

Co-IP assays revealed that the association of VDR and c-Myc increased rapidly upon 1,24D treatment followed by slight reduction due to the loss of c-Myc. The recruitment of VDR to the E-box region of c-Myc target genes also showed a primary peak of increased association. Re-ChIP assays clarified the co-recruitment of VDR and c-Myc on E-box motif of c-Myc target genes. This co-recruitment was attenuated after 24 hours of treatment with 1,25D. Comparing the result of Co-IP and Re-ChIP assays reveals that in both experiment association of VDR and c-Myc attenuated after 24 hours of 1,25D treatment which is due to the profound reduction in the c-Myc protein levels. However in the Re-ChIP bigger reduction in the association of VDR and c-Myc on the promoter of *CDC25A* was observed compared to the Co-IP assays which regardless of the place of the association, showed less reduction in the interaction of VDR and c-myc. This suggests that 1,25D induces the interaction of VDR with c-Myc and induce dissociation of c-

Myc from the DNA. Analyzing VDR and c-Myc peaks identified by ChIPseq from related lymphoblastoid cell lines revealed an overlap between approximately one half of the VDR binding sites detected in the absence of 1,25D, and almost one quarter of those in the presence of 1,25D with high fidelity c-Myc sites. This is another evidence that shows VDR associates with c-Myc on the promoter of target genes.

VDR deficient cells showed increased c-Myc levels in SCC25 and LNCap cells. In addition, *MYC* transcription was increased in this cells. In addition protein stability assays revealed that ablation of VDR did not affect c-Myc stability, therefore that enhanced c-Myc levels is due to the increased transcription of its gene, but not due to elevated c-Myc stability. These results together with the results of (Fig. 3B) suggest that 1,25D signaling needs VDR to affect the *MYC* transcription and c-Myc stability.

It has been shown that the canonical Wnt signaling pathway promotes *MYC* transcription [330] We showed that association of β-catenin with the *MYC* promoter was higher in VDR-deficient cells and consequently the transcription of *MYC* and its target gene CDC25A increased. This increased *MYC* transcription rescued by ablation of β-catenin and VDR, to the levels seen in VDR-replete cells treated with 1,25D. In agreement with previous studies, ChIP assays demonstrated that association of β-catenin with the *MYC* promoter in VDR-replete cells was reduced by 1,25D treatment. These observations are striking as *vdr* null mice or patients with vitamin D-resistant rickets due to inactivating mutations in the VDR gene [318], [337] develop alopecia because of dysregulated epidermal differentiation, and studies of vdr null mice have revealed that loss of the VDR in skin leads to elevated β-catenin signaling [318].

Western blot assays and immunohistochemistry analyses of multiple tissues of wild-type and *Vdr* null mice revealed that c-Myc was over expressed in tissues of null mice. This evidence

confirms previous studies which have reported a hyperproliferative phenotype in *Vdr*-null mice [318]. In agreement with our in vitro results, topical application of 1,25D to wild-type and *Vdr*-null mice skin suppressed c-Myc and its epidermal target genes, setd8 in wild-type, but not in *Vdr*-null mice. These results suggests that 1,25D signaling attenuates c-Myc levels not only *in vitro* but also *in vivo* and probably use the same mechanism to suppress the c-Myc.

In conclusion, our results present evidence for the mechanisms by which 1,25D signaling suppresses the c-Myc. We showed here that 1,25D signaling affect both *MYC* expression and c-Myc protein stability. We provided evidence for a novel mechanism by which 1,25D accelerates the c-Myc turnover through FBW7 (Fig. 3.6). However, the molecular basis for this mechanism remains unclear and further studies are needed to elucidate it.
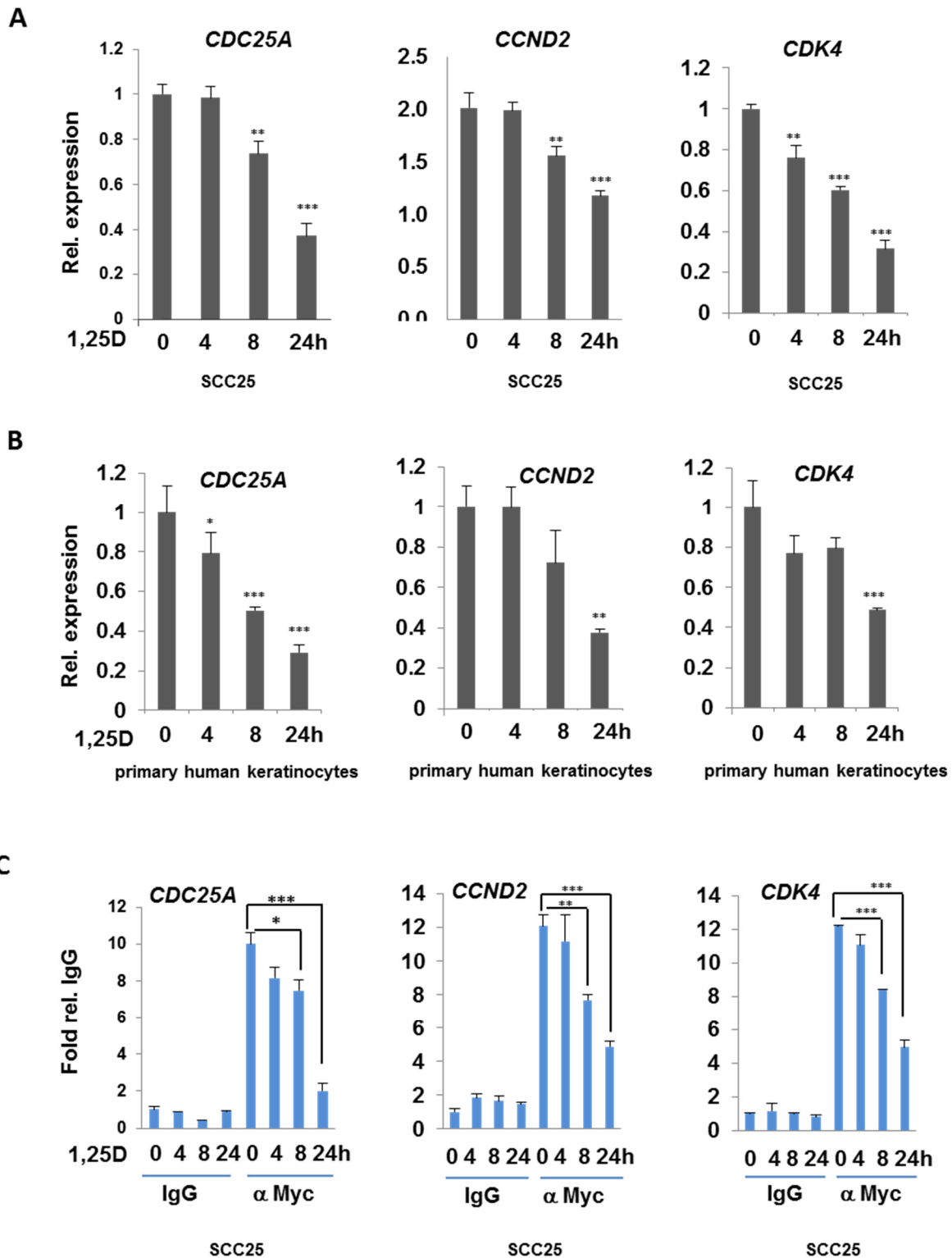
2.1. 1,25D signaling suppresses c-Myc target gene expression.

Figure legend on the next page.

2.1. 1,25D signaling suppresses c-Myc target gene expression.

A) RT-qPCR analysis of c-Myc target genes, *CDC25A*, *CCND2* and *CDK4* transcription in SCC25 cells following treatment with 100 nM of 1,25D for 4, 8, and 24 hours. **B)** RT-qPCR analysis of c-Myc target genes, *CDC25A*, *CCND2* and *CDK4* transcription in primary human keratinocytes following treatment with 100 nM of 1,25D for 4, 8, and 24 hours. **C)** Analysis of the c-Myc recruitment to the E-box motif of promoter of its target genes, *CDC25A*, *CCND2* and *CDK4* by chromatin immunoprecipitation (ChIP) assays followed by qPCR, in SCC25 cells treated with 100 nM of 1,25D for 4, 8, and 24 hours. $*P \leq 0.05$, $**P \leq 0.01$, $***P \leq 0.001$ as determined by One-way ANOVAs followed by Tukey's post hoc test for multiple comparisons.
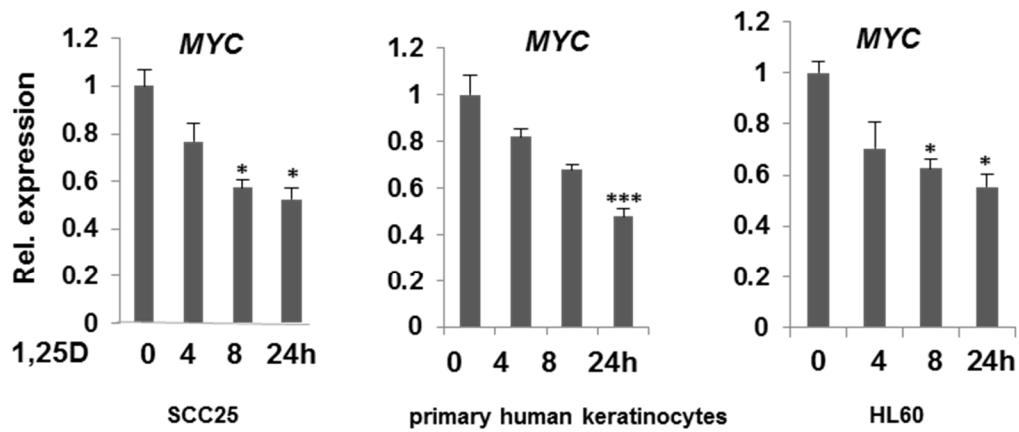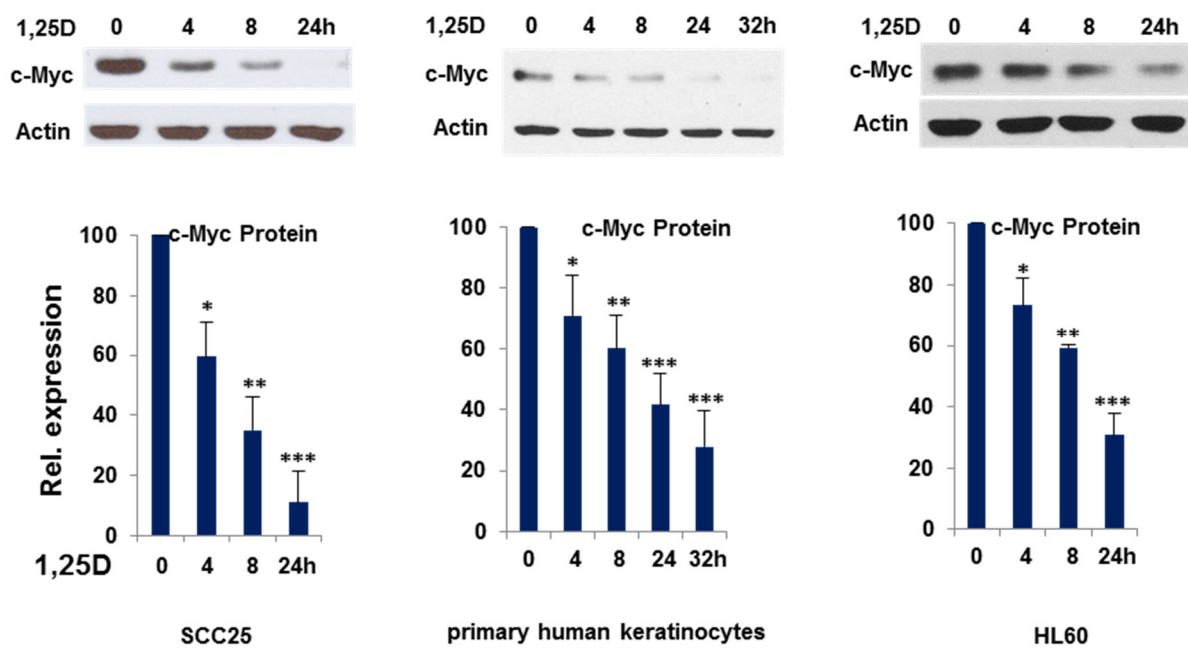
2.2. 1,25D signaling suppresses c-Myc transcription and protein expression.

Figure legend on the next page.

2.2. 1,25D signaling suppresses c-Myc transcription and protein expression.

A) RT-qPCR analysis of *MYC* gene transcription in SCC25 cells, primary human keratinocytes, and HL60 cells following treatment with 100 nM of 1,25D for 4, 8, and 24 hours. **B**, top panel) Western blot analysis of c-Myc levels in SCC25 cells, primary human keratinocytes, and HL60 cells following treatment with 100 nM of 1,25D for 4, 8, and 24 hours (and also 32 hours in primary human keratinocytes). **B**, bottom panel) Quantification of Western blot analyses of c-Myc levels represented in top panel, from four different experiments. *P≤0.05, **P≤0.01, ***P≤0.001 as determined by One-way ANOVAs followed by Tukey's post hoc test for multiple comparisons.
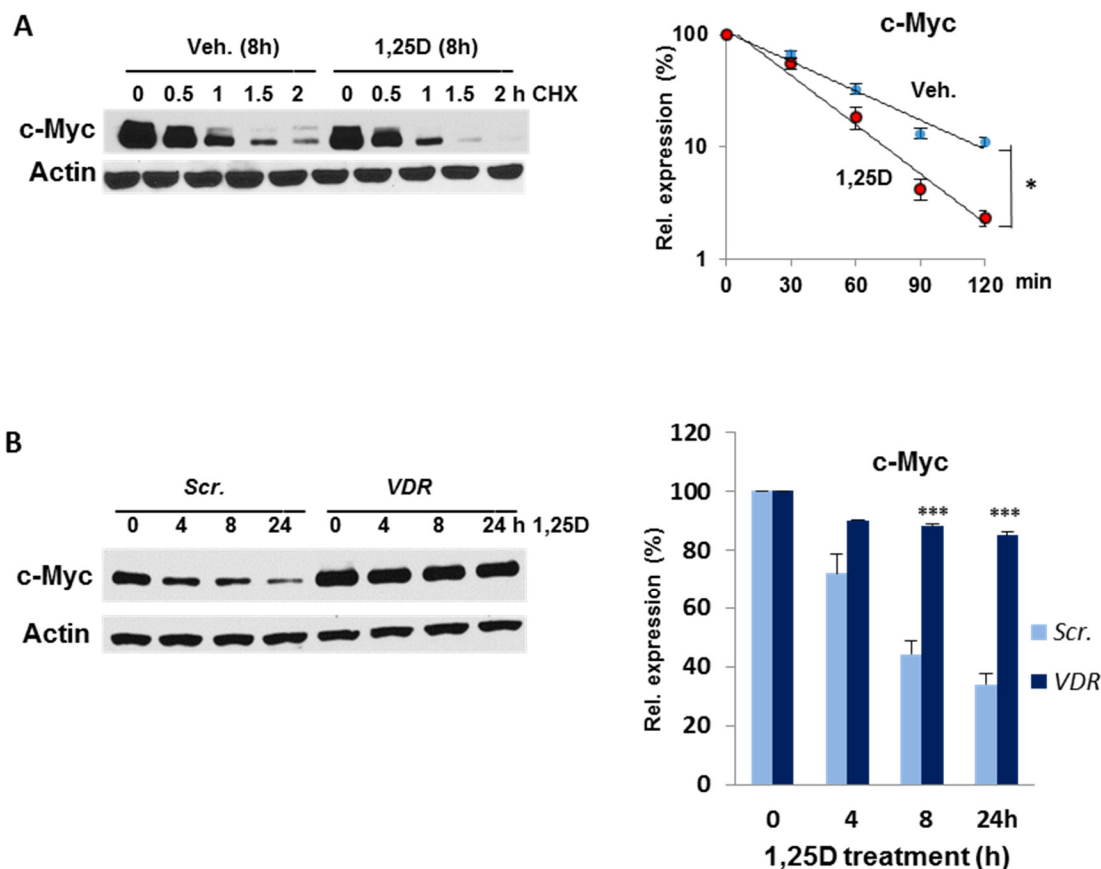
2.3. 1,25D bound VDR promotes c-Myc turnover.

A, left panel) Western blot analysis of c-Myc in protein stability assay. SCC25 cells were treated with 100 nM 1,25D for 8 hours. 4 µg/ml of protein synthesis inhibitor cycloheximide (CHX) was added for 0, 0.5, 1, 1.5 and 2 hours. **A,** right panel) Quantification of Western blot analyses of three independent experiments. **B,** left panel) Western blot analysis of c-Myc levels in VDR-deficient cells. SCC25 cells were transfected with *VDR* or scrambled siRNA and treated with 100 nM of 1,25D for 4, 8, and 24 hours. **B**, right panel) Quantification of Western blot analyses of three independent experiments. * P=0.05 as determined by One-way ANOVAs followed by Tukey's post hoc test for multiple comparisons.

A

ELAVL1

B

SKP2

C
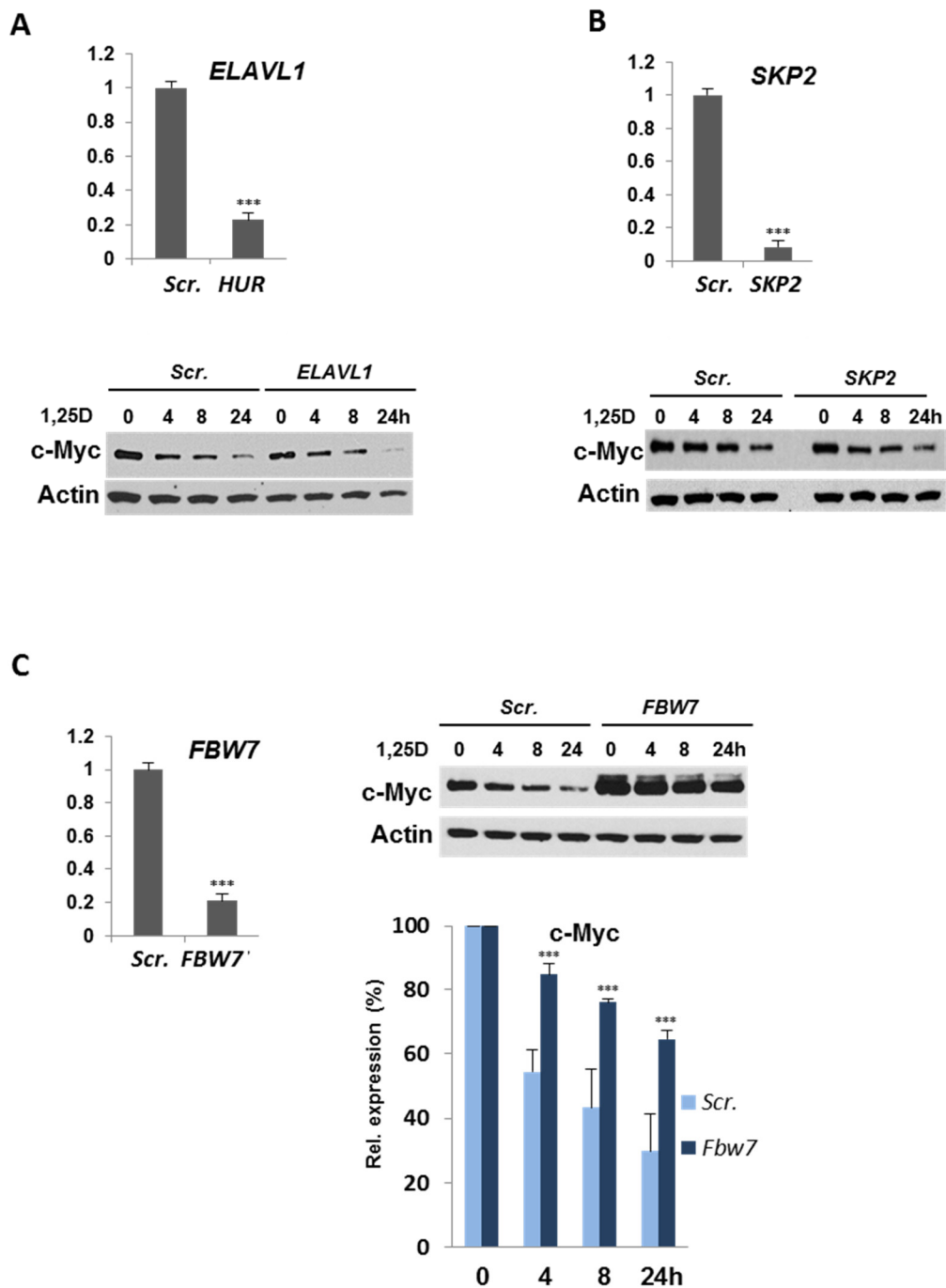
FBW7

c-Myc

2.4. The 1,25D-bound VDR affects c-Myc turnover through FBW7.

Figure legend on the next page.

2.4. The 1,25D-bound VDR affects c-Myc turnover through FBW7.

A, top panel) RT-qPCR analysis of *ELAVL1* gene transcription in SCC25 cells transfected with scrambled or *ELAVL1* siRNA. **A**, bottom panel) Western blot analysis of c-Myc expression in SCC25 cells transfected with scrambled or *ELAVL1* siRNA and treated with 100 nM of 1,25D for 4, 8, and 24 hours. **B,** top panel) RT-qPCR analysis of *SKP2* gene transcription in SCC25 cells transfected with scrambled or *SKP2* siRNA. **B**, bottom panel) Western blot analysis of c-Myc expression in SCC25 cells transfected with scrambled or *SKP2* siRNA and treated with 100 nM of 1,25D for 4, 8, and 24 hours. **C,** left panel) RT-qPCR analysis of *FBW7* gene transcription in SCC25 cells transfected with scrambled or *FBW7* siRNA and treated with 100 nM of 1,25D for 4, 8, and 24 hours. **C**, right, top panel) Western blot analysis of c-Myc expression in SCC25 cells transfected with scrambled or *FBW7* siRNA. **C**, right, bottom panel) Quantification of Western blot analyses of three independent experiments. ***$P \leq 0.001$ as determined by One-way ANOVAs followed by Tukey's post hoc test for multiple comparisons.
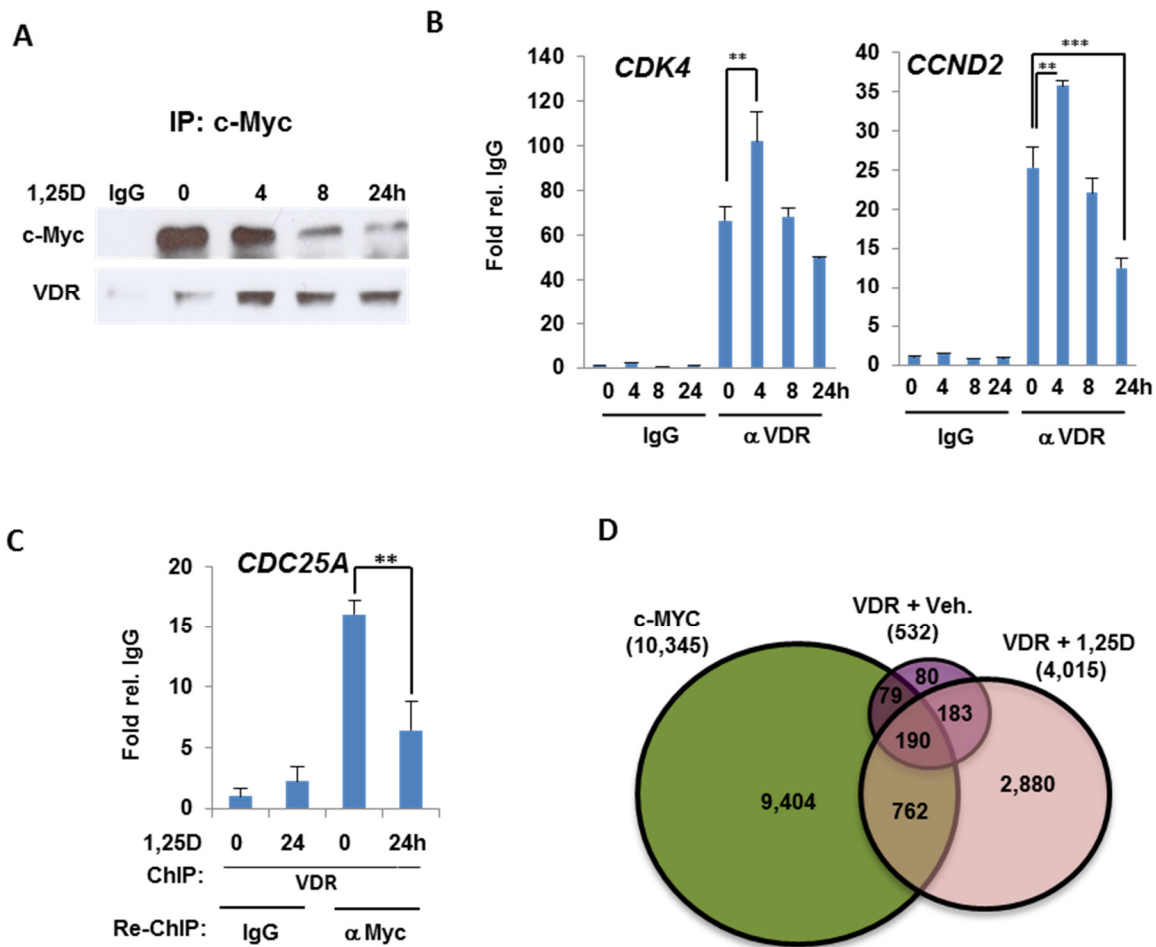
2.5. The 1,25D-bound VDR interacts with c-Myc on the promoter of target genes.

Figure legend on the next page.

2.5. The 1,25D-bound VDR interacts with c-Myc on the promoter of target genes.

A) Western blot analysis of VDR co-immunoprecipitated with IgG or c-Myc, following treatment of SCC25 cells with 100 nM of 1,25D for 4, 8, and 24 hours. **B**) Analysis of the VDR recruitment to the E-box motif of promoter of c-Myc target genes *CCND2* and *CDK4* by ChIP assays followed by qPCR, in SCC25 cells treated with 100 nM of 1,25D for 4, 8, and 24 hours. **C**) Analysis of the VDR and c-Myc co-recruitment to the E-box motif of promoter of c-Myc target gene *CDC25A* by Re-chromatin immunoprecipitation (Re-ChIP) assay, in SCC25 cells following treatment with 100 nM 1,25D for 24 hours. The first round of ChIP for VDR followed by second round of immunoprecipitation for c-Myc. **D**) Results of a comparative analysis of overlap of genomic binding sites from ChIPseq studies of c-Myc and the VDR [from cells treated with vehicle (Veh) or 100 nM 1,25D for 36h] performed in related lymphoblastoid cell lines [338], [339]. **P$\leq$0.01, ***P$\leq$0.001 as determined by One-way ANOVAs followed by Tukey's post hoc test for multiple comparisons.
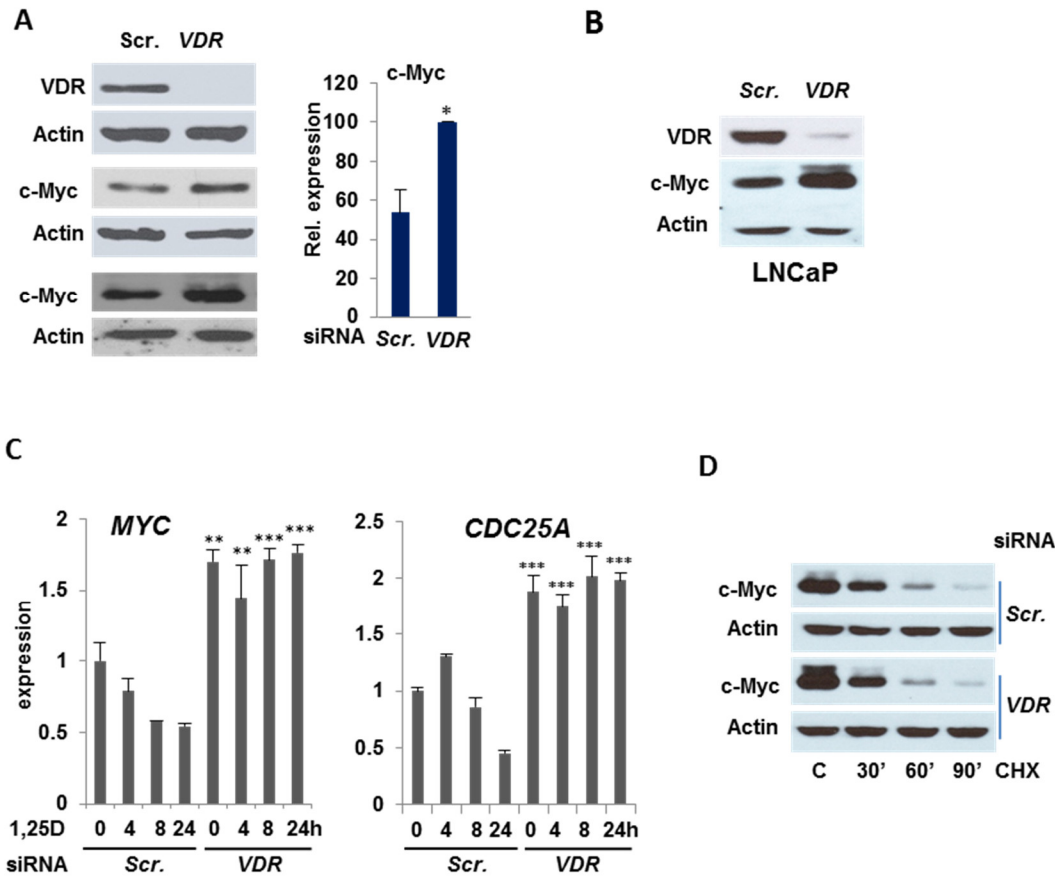
2.6. *MYC* gene transcription is elevated in VDR-ablated cells.

A, left panel) Western blot analyses of c-Myc levels in SCC25 cells transfected with scrambled or *VDR* siRNA. **A,** right panel) Quantification of Western blot analyses represented in left panel.

B) Western blot analysis of c-Myc levels in LNCaP cells transfected with scrambled or *VDR* siRNA. **C**) RT-qPCR analysis of *MYC* and its target gene *CDC25A* transcription in SCC25 cells were transfected with scrambled or *VDR* siRNA and treated with 100 nM of 1,25D for 4, 8, and 24 hours. **D**) Western blot analysis of c-Myc in protein stability assay. SCC25 cells were transfected with scrambled or *VDR* siRNA. 4 µg/ml of CHX was added for 0, 0.5, 1, and 1.5 hours. $*P \leq 0.05$, $**P \leq 0.01$, $***P \leq 0.001$ as determined by One-way ANOVAs followed by Tukey's post hoc test for multiple comparisons.
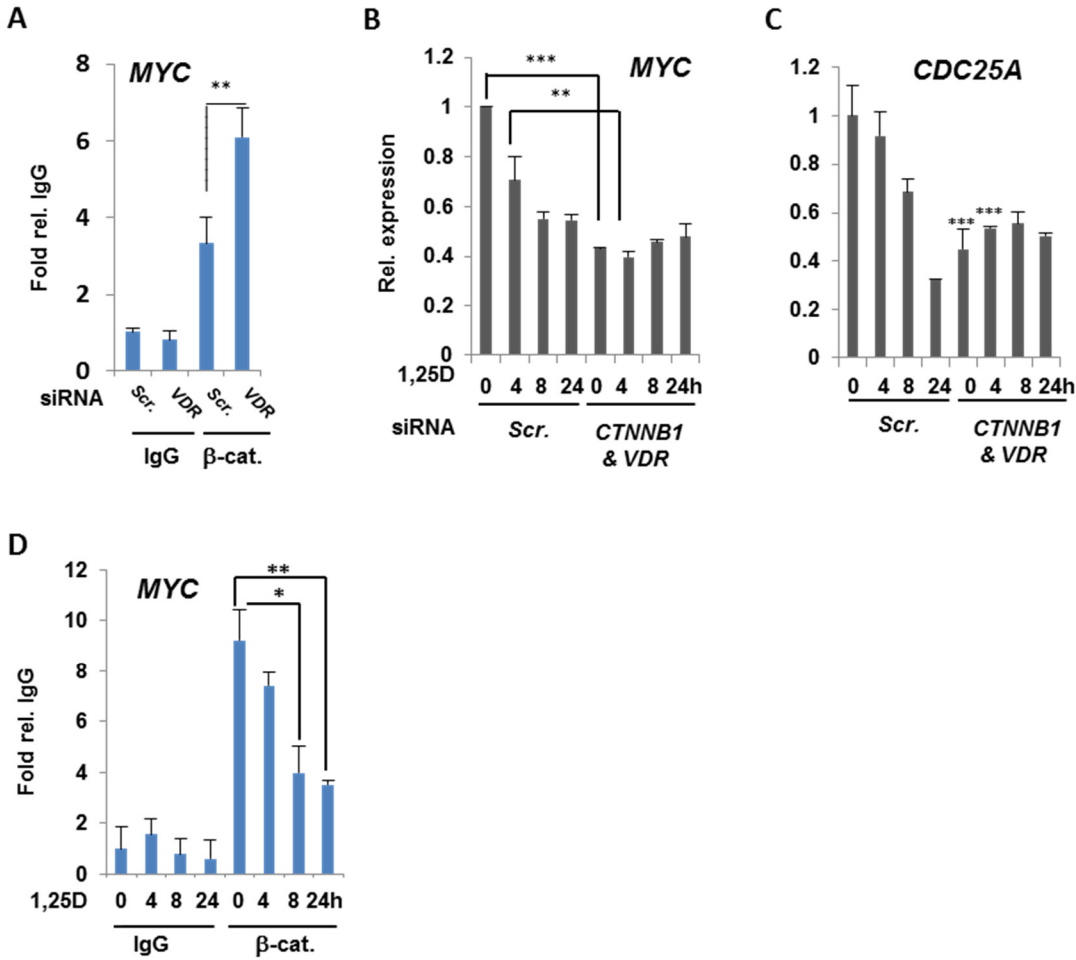
2.7. Association of β-catenin with the *MYC* promoter is higher in VDR-deficient cells.

A) Analysis of the β- catenin recruitment to the promoter of *MYC* by ChIP assays followed by qPCR, in SCC25 cells transfected with scrambled or *VDR* siRNA. **B,C)** RT-qPCR analysis of *MYC* and its target gene *CDC25A* transcription in SCC25 cells transfected with scrambled or *VDR* /*CTNNB1* siRNAs and treated with 100 nM of 1,25D for 4, 8 and 24 hours. **D)** Analysis of the β-catenin recruitment to the promoter of *MYC* by ChIP assays followed by qPCR, in SCC25 cells treated with 100 nM of 1,25D for 4, 8 and 24 hours. *P≤0.05, **P≤0.01, ***P≤0.001 as determined by One-way ANOVAs followed by Tukey's post hoc test for multiple comparisons.
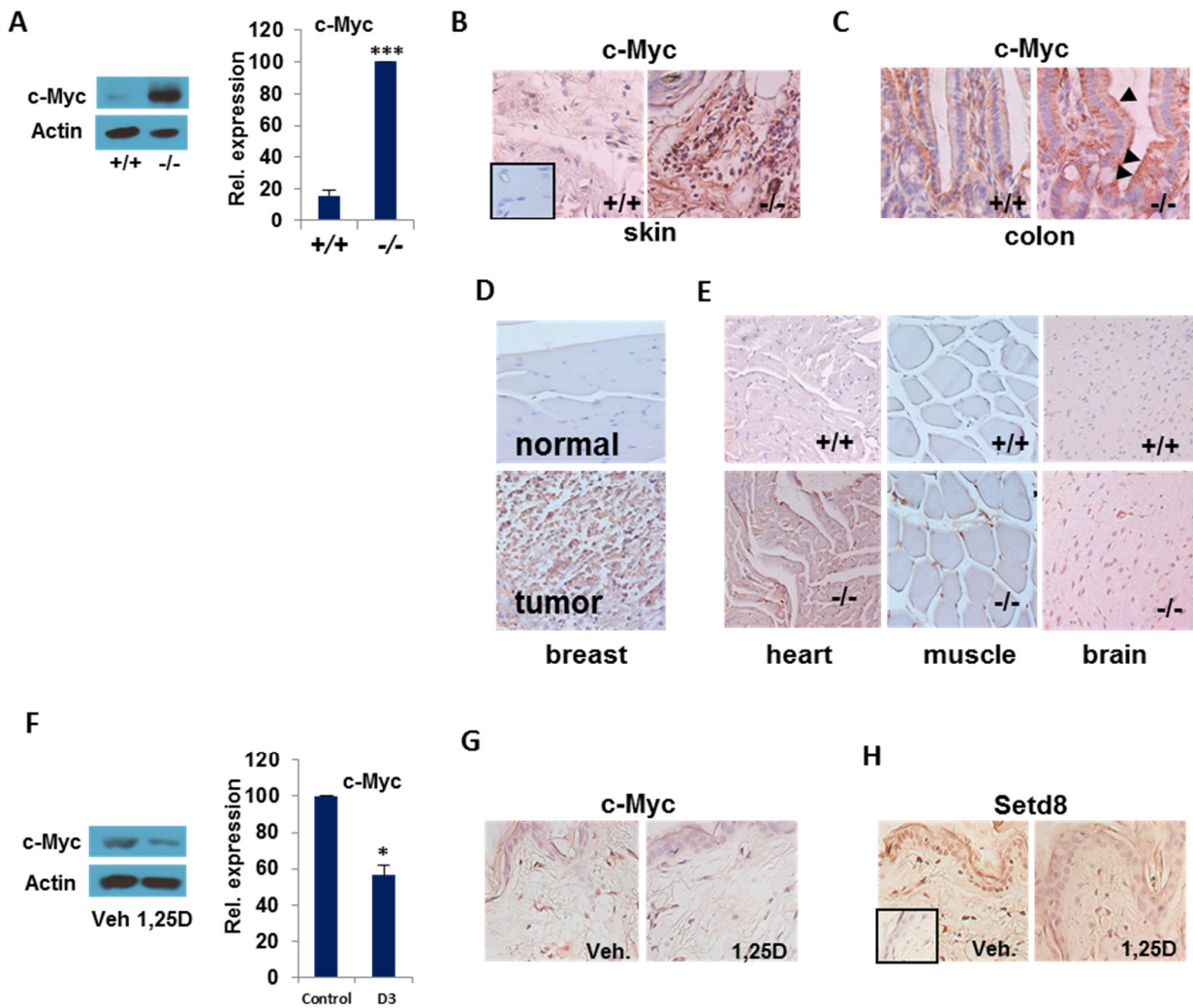
2.8.1,25D and the VDR control c-Myc expression in vivo.

Figure legend on the next page.

2.8.1,25D and the VDR control c-Myc expression in vivo.

A, left panel) Western blot analysis of c-Myc expression in extracts of skin from wild-type (+/+) or *Vdr* null (-/-) mice. **A**, right panel) Quantification of Western blot analyses of c-Myc expression in extracts of skin from wild-type (+/+) or *Vdr* null (-/-) mice. **B**) Immunocytochemistry assay of c-Myc expression in the skin of *Vdr* wild-type (+/+) and null (-/-) mice. **C**) Immunocytochemistry assay of c-Myc expression in the colon of *Vdr* wild-type (+/+) and null (-/-) mice. Arrowheads point to elevated c-Myc expression in enterocytes of null animals. **D**) Immunocytochemistry assay of c-Myc expression in normal and malignant breast tissue, as a positive control for c-Myc overexpression. **E**) Immunohistochemical analysis of c-Myc expression in heart, muscle and brain of *Vdr* wild-type (+/+) and knockout (-/-) mice. **F**, left panel) Western blot analysis of c-Myc expression in extracts of skin from wild-type mice treated topically with vehicle (Veh) or 1,25D (15ng/100μl/cm2) for 24h. **F**, right panel) Quantification of Western blot analyses of c-Myc expression in extracts of skin from wild-type mice treated topically with vehicle or 1,25D (15ng/100μl/cm2) for 24h. **G**) Immunohistochemical analysis of c-Myc expression in extracts of skin from wild-type mice treated topically with vehicle or 1,25D (15ng/100μl/cm2) for 24h. **H**) Immunocytochemistry assay of the product of epidermal c-Myc target gene setd8 in extracts of skin from wild-type mice treated topically with vehicle or 1,25D (15ng/100μl/cm2) for 24h.

2.6. Material and Methods

2.6.1. Cell Culture

SCC25 cells were obtained from the American Type Culture Collection (ATCC) and cultured in DMEM/F12 (319-085-CL, Multicell) supplemented with 10% FBS. LNCaP cells were obtained from the American Type Culture Collection (ATCC) and cultured in RPMI-1640 (30-2001, ATCC) supplemented with 10% FBS. HL60 cells were obtained from ATCC and cultured in RPMI-1640-1X (350-000-CL; Multicell) supplemented with 10% FBS. Primary Human keratinocytes (HEK-a) were obtained from ScienCell and cultured in EpiLife® Medium (M-EPI-500-CA, Invitrogen) supplemented with Supplement S7 (S-017-5, Invitrogen).

2.6.2. Knockdowns

SCC25 cells were transfected with siRNAs for 24 h using Lipofectamine™ 2000 reagent (Invitrogen), and treated with 1,25D. siRNAs were purchased from Qiagen. The sequences of siRNAs are listed in section 2.6.12.

2.6.3. RT-qPCR

Quantitative RT-PCR was performed with SsoFast-EvaGreen real-time PCR kit (Bio-Rad). Expression was normalized to the expression of GAPDH. Primer pairs used for RT-PCR are listed in section 2.6.13.

2.6.4. Immunoprecipitation and Western blot analysis

Cells were lysed with a lysis buffer (20 mM Tris, pH 7.5, 100 Mm NaCl, 0.5% Nonidet P-40, 0.5mM EDTA, 0.5 mM phenylmethylsulfonyl fluoride). 4 ug anti-VDR (D-6; Santa Cruz) Antibody was pre-bound for 2 h to protein A agarose beads, then was washed with PBS plus 5% BSA and added to the lysate, followed by immunoprecipitation overnight. Protein A agarose beads were then washed five times with washing buffer (20 mM Tris, pH 7.5, 200 Mm NaCl, 1%

Nonidet P-40, 0.5mM EDTA, 0.5 mM phenylmethylsulfonyl fluoride) and processed for Western blotting, performed with standard protocols. The following antibodies were used: VDR (H-81), c-Myc (9E10), VDR (D-6), all from Santa Cruz, and c-Myc (D84C12; Cell Signaling). For western blot of mouse skin, 50 mg of skin were ground under liquid nitrogen and homogenized in 1ml of lysis buffer. Lipids were removed by centrifugation at 10,000 RPM for 10min at 2°C. Western blots were quantified using ImageJ 1.45 software.

2.6.5. ChIP assays

Cells were cross-linked with 4% paraformaldehyde for 25 min and were lysed with 500 ul lysis buffer (150 mM NaCl, 0.5% NP-40, 1% Triton X-100,5mM EDTA and 50 mM Tris-HCl, pH 7.5) containing 1x protease inhibitor cocktail. Chromatin was sheared to an average length of 300–500 bp by sonication and supernatants were collected after centrifugation. 4 ug of Antibody was added to chromatin for immunoprecipitation overnight. then protein A agarose beads, ssDNA and BSA was added to the antibody chromatin complexes for 4 h. Protein A Agarose bead–chromatin complexes were then washed three times in TSE I (20 mM Tris-HCl, pH 8.1, 2 mM EDTA, 0.1% SDS, 1% Triton X-100 and 150 mM NaCl) followed by one wash with TSE II buffer (20 mM Tris-HCL, pH 8.1, 2 mM EDTA, 0.1% SDS, 1% Triton X-100 and 500 mM NaCl) and one wash with buffer III (0.25 M LiCl, 1% NP-40, 1% deoxychlolate, 1mM EDTA, 10mM Tris-Hcl, pH 8.1). Immunoprecipitated chromatin was then extracted with extraction buffer (1% SDS and 0.1 M NaHCO3) and was heated at 65 °C for overnight for reversal of the paraformaldehyde crosslinking. DNA fragments were purified with a PCR purification kit (Qiagen) and were analyzed by SsoFast-EvaGreen real-time PCR. The following antibodies were used for ChIP: anti-c-Myc (N-262), anti- VDR (D-6), from Santa Cruz and anti-βcatenin (9562L) and anti-c-Myc (9402) from Cell Signaling. Primer pairs used for ChIP assays are listed in

section 2.6.13. CCND2, *MYC* and *CDK4* primers [172]) and *MYC* primers for βcatenin ChIP assay [328] have been described. For re-ChIP assays, VDR immunocomplexes were eluted by adding 40µl 10 mM DTT for 30 min at 37 C. Supernatants were diluted 1:20 in dilution buffer (150 mM NaCl, 1% Triton X-100,2mM EDTA and 50 mM Tris-HCl, pH 8), and re-ChIP was performed using anti-c-Myc antibody, as indicated in the figures.

2.6.6. Comparative analysis of ChIPseq data sets for the VDR and c-Myc

A *de novo* analysis of VDR ChIPseq data sets generated in the human lymphoblastoid cell line (LCL) GM10855 (GEO accession number GSM558634; [340]) were compared to a c-Myc ChIPSeq data set generated in LCL GM12878 (GEO accession number GSM754334; [329]). Peaks in all data sets were called using model-based analysis for ChIP-Seq (MACS) [341] run using default parameters (p-value cut-off 1×10^{-5}). The Venn diagram was generated on the data intersections using cistrome integrative analysis toolbox [342].

2.6.7. Animal Experiments

All animal experiments were carried out in compliance with and approval by the Institutional Animal Care and Use Committee. *vdr+/-* animals (The Jackson Laboratory, Bar harbor, ME) were mated to generate homozygous for *vdr$^{-/-}$* mice. At 21 days of age, control *vdr$^{+/+}$* and *vdr$^{-/-}$* mice were weaned and maintained until sacrifice on high calcium (rescue) diets containing 1.5% calcium in the drinking water and autoclaved regular chow.

2.6.8. Genotyping of Mice

Genomic DNA was isolated from tail fragments by standard phenol/chloroform extraction and isopropyl alcohol precipitation. To determine the genotype at VDR loci, 2 PCRs were conducted for each animal. The wild type VDR allele was detected using forward primer 5′-CTGCCCTGCTCCACAGTCCTT-3′ and reverse primer 5′-CGAGACTCTCCAATGTGAAGC-

3′. The disrupted VDR allele was assayed using the neo forward primer 5′-GCTGCTCTGATGCCGCCGTGTTC-3′ and a neo reverse primer 5′-GCACTTCGCCCAATAGCAGCCAG-3′. PCR conditions were 30 cycles for all VDR and disrupted VDR allele, 94 °C for 1 min, 65 °C for 1 min, and 72 °C for 1 min; and neomycin, 94 °C for 1 min, 60 °C for 1 min, and 72 °C for 1 min.

2.6.9. Topical treatment with 1,25D

Mice (5-6) at 3 months of age were treated topically on the dorsal surface with vehicle or 1,25D for 18 h. The vehicle was a base lotion containing ethanol: propylene-glycol: water (2:1:1). The 1,25D (Sigma) was dissolved in ethanol and diluted with vehicle. Each mouse was treated with vehicle ($100 \Box l/cm^2$) on the highest part of the back (neck) and with 1,25D ($15ng/100\mu l/cm^2$) on the lowest part of the back (hip) to avoid the contact between 2 treatments. After 18 h of treatment the treated region of skin were immediately removed and fixed in PLP fixative (2% paraformaldehyde containing 0.075 m lysine and 0.01 m sodium periodate) overnight at 4 °C, washed and processed immunohistochemistry (IHC) study.

2.6.10. Immunohistochemistry

c-Myc and Setd8 expression were determined by IHC using the avidin-biotin-peroxidase complex (ABC) technique. Anti-c-Myc (9E10; Santa Cruz) or anti-SET8 (C18B7; Cell Signalling) were applied to dewaxed paraffin sections overnight. After washing with high salt buffer, slides were incubated with secondary antibody, washed and processed using the Vectastain ABC-AP kit (Vector Laboratories) and mounted with Permount (Fisher Scientific). Images from sections were processed using Bioquant image analysis software.

2.6.11. Statistical Analyses

All experiments are representative of 3-5 biological replicates. Unless otherwise indicated in the figures, statistical analysis was conducted using the program SYSTAT13 by performing one-way analysis of variance (ANOVA) followed by the Tukey test for multiple comparisons as indicated: $*P \leq 0.05$, $**P \leq 0.01$, $***P \leq 0.001$.

2.6.12. siRNAs

VDR   5'-TCAGACTCCATTTGTATTATA-3'
FBXW7   5'-CCCTAAAGAGTTGGCACTCTA-3'
MYC   5'-CTCGGTGCAGCCGTATTTCTA-3'
βcatenin   5'-CTCGGGATGTTCACAACCGAA-3'
SKP2   5'-AAGTGATAGTGTCATGCTAAA-3'
ELAVL1   5'-AAGTAGCAGGACACAGCTTGG-3'
Control   5'-CAGGGTATCGACGATTACAAA-3'

2.6.13. Primers

Primers for gene expression:

CCND2-FORWARD   5'-GAGAAGCTGTCTCTGATCCGCA-3'
CCND2-REVERSE   5'-CTTCCAGTTGCGATCATCGACG-3'
CDK4-FORWARD   5'-CCATCAGCACAGTTCGTGAGGT-3'
CDK4-REVERSE   5'-TCAGTTCGGGATGTGGCACAGA-3'
CDC25A-FORWARD   5'-TCTGGACAGCTCCTCTCGTCAT-3'
CDC25A-REVERSE   5'-ACTTCCAGGTGGAGACTCCTCT-3'
MYC-FORWARD   5'-CCTGGTGCTCCATGAGGAGAC-3'
MYC-REVERSE   5'-CAGACTCTGACCTTTTGCCAGG-3'
MXD1-FORWARD   5'-ACCTGAAGAGGCAGCTGGAGAA-3'
MXD1-REVERSE   5'-AGATAGTCCGTGCTCTCCACGT-3'
ELAVL-1-FORWARD   5'-CCGTCACCAATGTGAAAGTG-3'
ELAVL-1-REVERSE   5'-TCGCGGCTTCTTCATAGTTT-3'

SKP2-FORWARD	5'-CTCCACGGCATACTGTCTCA-3'
SKP2-REVERSE	5'-GGGCAAATTCAGAGAATCCA-3'
FBW7-FORWARD	5'-CAGCAGTCACAGGCAAATGT-3'
FBW7-REVERSE	5'-GCATCTCGAGAACCGCTAAC-3'
CTNNB1-Forward	5'-CACAAGCAGAGTGCTGAAGGTG-3'
CTNNB1-Reverse	5'-GATTCCTGAGAGTCCAAAGACAG-3'

Primers for ChIP:

CDC25A-FORWARD	5'-GAGAGATCAGGCCAGGAAAC-3'
CDC25A-REVERSE	5'-CTCTCCCGCCCAACATTC-3'
CDK4-FORWARD	5'-GAGCGACCCTTCCATAACCA-3'
CDK4-REVERSE	5'-GGGCTGGCGTGAGGTAAGT-3'
MYC-FORWARD	5'-TGGGCGGCTGGATACCTT-3'
MYC-REVERSE	5'-GATGGGAGGAAACGCTAAAGC-3'
CCND2-FORWARD	5'-TCAGTAAATGGCCACACATGTG-3'
CCND2-REVERSE	5'-GGAGCTCTCGACGTGGTCAA-3'
MYC-FORWARD	5'-AGGCAACCTCCCTCTCGCCCTA-3'
MYC-REVERSE	5'- AGCAGCAGATACCGCCCTCCT-3'

Chapter 3

1,25D signaling regulates MXD1 expression and function by promoting its transcription and inhibiting its turnover through FBW7.

3.1. Preface

MXD1 is a component of the tumor suppressor arm of the c-Myc/MAX/MXD1 pathway. It antagonizes c-Myc through heterodimer formation with MAX. MXD1 expression is crucial to prevent uncontrolled cell proliferation mediated by Myc. Previously it was shown that 1,25D promotes the expression of multiple tumor suppressors in the cell. In addition, we revealed that 1,25D-bound VDR represses c-Myc expression at the mRNA and protein levels. Further, we showed that it promotes c-Myc degradation through FBW7 E3 ligase. We wanted to know, whether 1,25D affects the expression of c-Myc antagonist. Thus, in this study we investigated the effect of 1,25D-bound VDR on the expression of the MXD1 at the mRNA and protein levels. We also determined the possible effect of FBW7 on MXD1.

3.2. Abstract

1,25D signaling regulates the transcription and protein stability of c-Myc, resulting in a decline in c-Myc expression and function. c-Myc functions in a push-pull network with its antagonists, the major one being MXD1. MXD1 and c-Myc in the c-Myc/MAX/MAD network function as a molecular switch to regulate gene transcription. MXD1 is the transcriptional repressor in this network which inhibits cell cycle progression through multiple target genes. Here, we provide evidence that 1,25D signaling regulates MXD1 through a novel mechanism. We showed that 1,25D enhanced the *MXD1* transcription gradually, while increasing MXD1 protein levels substantially. Protein stability assays revealed that 1,25D enhanced MXD1 protein levels by decelerating its turnover. In addition, MXD1 stability was elevated in FBW7-deficient cells and 1,25D did not alter MXD1 stability in these cells. Increased recruitment of MXD1 and its cofactor to the E-box region of target genes upon 1,25D treatment was verified by chromatin immunoprecipitation assay. Further, the association of MXD1 and VDR were investigated by coimmunoprecipitation assay. The association of MXD1 and VDR gradually increased over 24 hours of 1,25D treatment, which may be the result of increased levels of MXD1. In agreement with our *in vitro* studies, application of 1,25D to the skin of wild type mice increased MXD1 proteins levels, whereas in *Vdr* null mice, similar to SCC4 and SCC9, we did not observe changes in MXD1 expression before and after treatment with 1,25D. Altogether, our results show that 1,25D plays a crucial role in the regulation of MXD1.

3.3. Introduction

1,25D controls several signaling pathways implicated in proliferation, differentiation, invasion, and metastasis. In 1981 for the first time it was showed that 1,25D inhibits cell cycle progression in malignant melanoma cells[343]. Since then, multiple *in vitro* and *in vivo* studies have revealed that 1,25D inhibits proliferation and slows down cancer progression [10]. It has been reported that low levels of circulating 1,25D are linked to increased risk of cancer development and high intake of vitamin D reduces it[5]. The vast majority of identified biological actions of 1,25D-bound VDR are through its genomic functions.1,25D binds to the VDR which triggers its dimerization with RXR and binding to VDR elements on the distal regions and promoters of target genes to regulate their transcription. In addition, multiple non-genomic actions of VDR have been reported including calcium and bone homeostasis [10].

Recently it has been reported that 1,25D can regulate *MYC* expression [314], [315]. c-Myc is acting in a network with multiple antagonist to regulate the transcription of its target genes which are mostly implicated in cell cycle progression. MXD1 is one of the most important antagonists of c-Myc, which competes with c-Myc to make heterodimers with MAX and bind to the E-box promoter regions. It is a bHLHZip transcription factor mostly found in differentiating cells[344]. MXD1 acts as a transcriptional repressor and is an efficient inhibitor of cell cycle progression[249]. It contains a b/HLHZip DNA binding domain and a short N-terminal region termed SID which corepressors including SIN3a interact with MXD1 through this domain[345]. While c-Myc and MXD1differ in the cofactor-binding domain, their DNA binding domains are comparable. c-Myc/MAX and MXD1/MAX complexes have equal affinity to E boxes [249].

MXD1 plays a crucial role in inhibiting cell proliferation and apoptosis induced by c-Myc. It has been shown that overexpression of MXD1 in resting fibroblasts, stimulated by serum, efficiently

suppresses S phase progression [249]. Interestingly, overexpression of c-Myc cannot rescue cell cycle progression and only the co-expression of cyclin E/CDK2 can help to stimulate S phase and cell cycle progression [249].

The mechanisms of MXD1 regulation is not well-understood, but might be due to the fact that MXD1 is generally difficult to detect [249]. It has been shown that some signaling pathways including TGFβ stimulate its transcription [161]. Similar to c-Myc, MXD1 turnover is rapid. Proteasomal inhibitors increased its stability suggesting that MXD1 is degraded by the proteasome [346]. Ablation of c-IAP1 E3 ligase enhances the steady state levels of MXD1 [260]. However the mechanism by which c-IAP1 induces MXD1 turnover is unclear. In addition, turnover of MXD1 can be induced through unknown E3 ligases following stimulation of cells with serum[263]. This stimuli induces MXD1 phosphorylation at Ser145 residue by S6Ks which are oncogenic kinases and needed for cell cycle progression. This phosphorylation trigger MXD1 turnover independent of c-IAP1 [249].

In this study, we investigated the effects of 1,25D signaling on the repressor arm of the MXD1/c-Myc network. We found that similar to c-Myc, 1,25D affects MXD1 expression, but in opposite direction increasing it. In addition, we showed a novel mechanism for regulation of the MXD1 degradation through FBW7 E3 ligase. Furthermore topical application of 1,25D on the wildtype and *Vdr* null mice, showed elevated levels of MXD1 in the skin of wild type mice, which confirms our *in vitro* findings.

3.4. Results

3.4.1. 1,25D signaling promotes *MXD1* transcription and protein expression.

MXD1, as a c-Myc antagonist, has a critical role in suppressing the transcription of c-Myc target genes [249]. MXD1 levels correlate with epithelial differentiation (43, 44), and its expression in

SCCs is associated with the capacity of cells to differentiate (45, 46). In chapter 2, we showed that 1,25D signaling attenuated Myc transcription and protein levels in SCC25 cells. To investigate the effect of 1,25D signaling on *MXD1* transcription, the mRNA levels of *MXD1* were assessed by RT-qPCR assays in SCC25 cells, primary human keratinocytes and HL60 cells, following treatment with 1,25D for indicated times (Fig.1A). Interestingly, the change in *MXD1* mRNA in 1,25D-treated cells was the reverse of that for *MYC* transcripts, increasing modestly over 24h (Fig. 1A).

To determine the effect of 1,25D on MXD1 protein expression, SCC25 cells were treated with 1,25D for the times indicated in Fig.1B. MXD1 protein expression were assessed by western blot assays. Remarkably, a substantial increase was observed in MXD1 protein levels in SCC25 cells upon treatment with 1,25D (Fig. 1B). In fact, there was almost no MXD1 in untreated cells (Fig. 1B). In the western blot assays for MXD1, two bands were observed (Figs. 1B, 1E, 1F). To help ensure which band is representative of MXD1, the *MXD1* gene was knocked down in SCC25 cells. Due to the absence of MXD1 in untreated cells, we treated cells with 1,25D, to have a visible band for MXD1. The result showed that, siRNA-mediated knockdown of *MXD1* expression eliminated the upper band, but had no effect on the lower MW protein (Fig. 1F). This upper band is nuclear, whereas the lower nonspecific band is cytoplasmic (Fig. 1B).

In addition, Treatment of primary human keratinocytes with 1,25D led to changes in MXD1 protein parallel to those seen in SCC25 cells (Fig. 1C). Note that in primary human keratinocytes, MXD1 was visible in untreated cells compared to SCC25 cells and HL60 cells (Fig. 1C). Similar to SCC25 cells, MXD1 expression was strongly enhanced by 1,25D treatment of HL60 cells over 24 hours (Fig. 1D).

SCC9 and SCC4 cells as models resistant to 1,25D signaling [336] were tested for the expression of MXD1 following treatment with 1,25D for the times indicted in Fig.1E. SCC25 cells were used in this experiment as a control. The western blot assays demonstrated that only SCC25 cells expressed MXD1 upon 1,25D treatment, but neither SCC4 nor SCC9 cells (Fig. 1E).

In the c-Myc/MAX/MXD1 network, c-Myc and MXD1 compete to make a heterodimer with MAX protein [249]. The expression of MAX was assessed in the SCC25 cells following 1,24D treatment. Since, in contrast to c-Myc and MXD1, MAX is a highly stable protein [347] 1,25D treatment was extended to 48 hours. The results did not show any significant changes in the MAX protein levels over 48 hours of 1,25D treatment (Fig. 1G).

3.4.2. 1,25D-bound VDR inhibits MXD1 turnover.

Investigating the mechanism by which 1,25D enhanced MXD1 protein levels, we analyzed the effect of 1,25D on the MXD1 turnover. Stability assays were performed following treatment with 1,25D. Cycloheximide (CHX) was applied for the times indicated in Fig. 2A. MXD1 protein levels were assessed by western blot assays from nuclear extracts. Following protein synthesis blockage with CHX, MXD1 turnover was decelerated in 1,25D-treated cells (Fig. 2A). Fig.2B shows the quantification of the western blot analyses from the protein stability assays, confirming that increased MXD1 stability in the presence of 1,25D is significant (Fig. 2A). This result suggests that, in contrast to c-Myc, 1,25D stabilizes MXD1 through an unknown mechanism.

3.4.3. 1,25D-bound VDR inhibits MXD1 turnover through FBW7.

While control of c-Myc turnover has been extensively studied, little is known about regulation of MXD1[138]. Investigating several pathways, we revealed that 1,25D-bound VDR affects the stability of c-Myc through FBW7. To investigate whether, similar to VDR, FBW7 affects both

arms of c-Myc/MXD1 network, SCC25 cells were transfected for scrambled or *FBW7* siRNA and the MXD1 protein levels were assessed by western blot analyses. Remarkably, ablation of FBW7 expression led to increased MXD1 protein levels (Fig. 3A), similar to 1,25D treatment.

FBW7 was knocked down in SCC25 cells to clarify the effect of FBW7 on the MXD1 protein stability. Subsequently cells were treated with CHX for the times indicated in Fig.3B. The expression of MXD1 protein were assessed by western blot assays (Fig. 3B). Interestingly, MXD1 turnover was also reduced, although not abolished, in FBW7-deficient cells (Fig. 3B), similar to c-Myc (Fig. 4C in Chapter 2), revealing that FBW7 regulates both the activator and repressor arms of the c-MYC/MXD1/MAX network.

Notably, 1,25D-treatment had no substantial effect on MXD1 turnover in FBW7-deficient cells (Fig. 3C), consistent with the hormone-bound VDR protecting MXD1 from FBW7-mediated turnover. Regulation of MXD1 turnover by FBW7 was unexpected as it lacks a CDC4 phospho-degron recognized by FBW7, present in c-Myc and in other targets such as cyclin E, characterized by a TPxxS/E core [293]. The control of MXD1 stability by FBW7 may thus be indirect; i.e. by regulating turnover or function of another unknown protein critical for direct regulation of MXD1 degradation. In addition, it is possible that FBW7 can recognize a non-canonical phosphodegron in MXD1, similar to p63 and several other proteins [348].

3.4.4. VDR interacts with MXD1 on the promoter of its target genes.

We showed that the association of c-Myc with the promoter of its target genes declined in the presence of 1,25D. In addition, a coincident repression in the transcription of target genes was observed. Together these findings suggest that MXD1 recruitment to the promoter of c-Myc target genes might be increased in the absence of c-Myc on the E-box region of its target genes. To verify the effect of 1,25D signaling on the recruitment of MXD1 to the promoter of target

genes, chromatin immunoprecipitation (ChIP) assays were performed at the E-box region of *CDC25A, CDK4* and *CCND2* genes following treatment of SCC25 cells with 1,25D for the times indicated in Fig.4A. The results show that, in contrast to c-Myc, recruitment of MXD1 to E-box regions of the corresponding promoters increased over 24 hours with 1,25D treatment (Fig. 4A). This, together with the results from Fig. 1C in chapter 2, shows the substitution of c-Myc with MXD1 on the promoter of target genes.

To further investigate the transcriptional suppression of c-Myc target genes in the presence of 1,25D, ChIP assays were performed using MXD1-associated corepressors HDAC2 and SIN3A antibodies. Similar to MXD1, 1,25D-induced binding of MXD1-associated corepressors HDAC2 and SIN3A to E-box regions of *CDC25A* promoter were observed (Fig. 4B).

The recruitment of VDR to the promoter of *CDC25A* were assessed by ChIP assays following 1,25D treatment. ChIP assays revealed a rapid 1,25D-dependent increase in the association of VDR with the promoter of *CDC25A* followed by a gradual decrease over 24 hours of 1,25D treatment (Fig. 4C),similar to the recruitment of VDR to the *CDK4* and *CCND2* promoters (Fig. 5B in chapter 2),

In chapter 2, we showed that 1,25D signaling rapidly induced interaction of VDR with c-Myc. Here, the interaction between VDR and MXD1 was investigated in SCC25 cells following treatment with 1,25D by Coimmunoprecipitation assay. A gradual increase in the association of VDR and MXD1 was observed (Fig. 4D). Since the MXD1 increased substantially following 1,25D treatment, this observed increase in VDR /MXD1 binding might be due to the large increase in the MXD1 protein levels in the cell (Fig. 4D).

The co-recruitment of the VDR with MXD1 on the *CDC25A* promoter were confirmed by re-ChIP analyses (Fig. 4E). The degree of co-recruitment of the VDR with MXD1 following 24 hours of 1,25D treatment was very consistent with the effects of 1,25D signaling on MXD1 DNA binding. Again, this may be the result of substantial increases in the MXD1 protein levels after 24 hours 1,25D treatment.

Altogether these results suggest that 1,25D signaling increases MXD1 protein levels, which leads to association of the latter with promoters of c-Myc target genes liberated due to 1,25D-mediated c-Myc reduction. The Increase in MXD1 recruitment of to the promoter of c-Myc target genes is coincident with the increase in the recruitment of MXD1-associated corepressors HDAC2 and mSIN3A to the promoter of c-Myc target genes leading to transcriptional suppression.

3.4.5. 1,25D induces MXD1 expression in vivo.

We revealed that $Vdr^{-/-}$ mice tissues express high levels of c-Myc proteins and topical application of 1,25D on their skin modestly declined the c-Myc expression (Figs. 8F, 8G in Chapter 2). Immunohistochemistry assays and western blot analysis performed to investigate the levels of MXD1 protein expression in wild type and *Vdr* null mice after applying topical 1,25D on their skin. The results revealed that in agreement with the induction of MXD1 expression observed in vitro, topical 1,25D application increased MXD1 levels in the skin of wild-type mice (Figs. 5A,5B) but not $Vdr^{-/-}$ mice (Fig. 5C). These results provide evidence for the effect of 1,25D signaling on the MXD1 expression *in vivo*.

3.5. Discussion

The c-Myc/MAX/MAD network plays a crucial role for regulating cell proliferation. MXD1 is the antagonist of c-Myc and competes with c-Myc to bind to the E-box region of promoter of c-Myc target genes. Numerous studies have described regulation of c-Myc, whereas the regulation

of MXD1 is poorly studied [138], [249]. In chapter 2, we revealed that 1,25D signaling attenuates c-Myc levels by affecting its transcription and protein stability. To further investigate the effects of 1,25D signaling on the c-Myc/MAX/MAD network, the expression of MXD1 was examined in the presence of 1,25D. A gradual increase in the *MXD1* transcription and a substantial increase in its protein levels was observed in the presence of 1,25D. In SCC4 and SCC9 cells which are resistant to the 1,25D signaling, we did not observed MXD1 expression. These results demonstrate that 1,25D affects c-Myc and MXD1 with a similar pattern but in opposite direction. This, together with the fact that 1,25D signaling accelerates c-Myc turnover through SCF^{FBW7} E3 ligase, suggests that 1,25D may affect the MXD1 turnover through SCF^{FBW7}. Interestingly we found that MXD1 was turned over through FBW7. Cycloheximide assays confirmed that MXD1 stability was enhanced in FBW7 ablated cells. FBW7 is considered as a tumor suppressor and many of its identified target proteins are oncogenes involved in cell cycle progression [349]. Of note, MXD1 lacks the canonical phosphodegron motif that is recognizable by FBW7. Thus there are two possibility for the MXD1 degradation through FBW7. One possibility is that FBW7 affects MXD1 stability by controlling turnover or function of an unknown protein critical for direct regulation of MXD1 degradation. Another possibility is that FBW7 can recognize a non-canonical phosphodegron in MXD1, similar to some other proteins including p63, MCL1 and KLF4 [348], [350], [351]. In many identified FBW7 target proteins, GSK3s phosphorylate and mark them to be recognized by FBW7 [122]; and MXD1 lacks a favorable site for phosphorylation by GSK3s which is a proline directed kinase [352].

Further investigation of the mechanism that promotes the MXD1 stability in 1,25D signaling revealed that in FBW7 ablated cells, 1,25D did not affect MXD1 stability. This phenomenon can be explained by the fact that in the absence of FBW7, the stability of MXD1 has already been

increased, and 1,25D treatment results in no further increase. Strictly speaking, 1,25D increases the MXD1 stability by inhibiting its FBW7-induced degradation, therefore when FBW7 is ablated 1,25D loses its means to affect MXD1 stability.

Furthermore, the results revealed that the recruitment of MXD1 to the promoter of c-Myc target genes, *CDC25A, CDK4*, and *CCDND2* was increased in the presence of 1,25D. Coincidently, the recruitment of MXD1 cofactors to the promoter of *CDC25* gene increased upon 1,25D treatment. These results suggest that in the reducing levels of c-Myc and increasing levels of MXD1 induced by 1,25D signaling, MXD1 and its cofactors associate with the E-box motifs of c-Myc target genes and suppress their transcription. The Co-IP assays revealed that VDR and MXD1 association increased gradually over 24 hours of 1,25D treatment. In addition, the increased co-recruitment of MXD1 and VDR were observed over 24 hours of 1,25D treatment. This association might be due in part to the increased MXD1 protein levels, rather than increased absolute interaction between MXD1 and 1,25D-bound VDR. Our *in vivo* studies revealed that topical application of 1,25D increased the expression of MXD1 in the skin of wild type mice but not *Vdr* null mice, in agreement with our in vitro studies.

In conclusion, this study revealed that 1,25D signaling regulates MXD1 transcription and protein stability. In addition, we provide evidence that MXD1 stability is affected by FBW7 E3 ligase and 1,25D decelerates MXD1 turnover through FBW7 E3 ligase (Fig. 3.6). 1,25D treatment has opposing effects on MYC and MXD1 mRNA expression and FBW7-dependent turnover of the corresponding proteins. This ultimately leads to elevated DNA binding of MXD1 and its associated corepressors, and inhibition of the transcription of oncogenes involved in cell cycle progression.
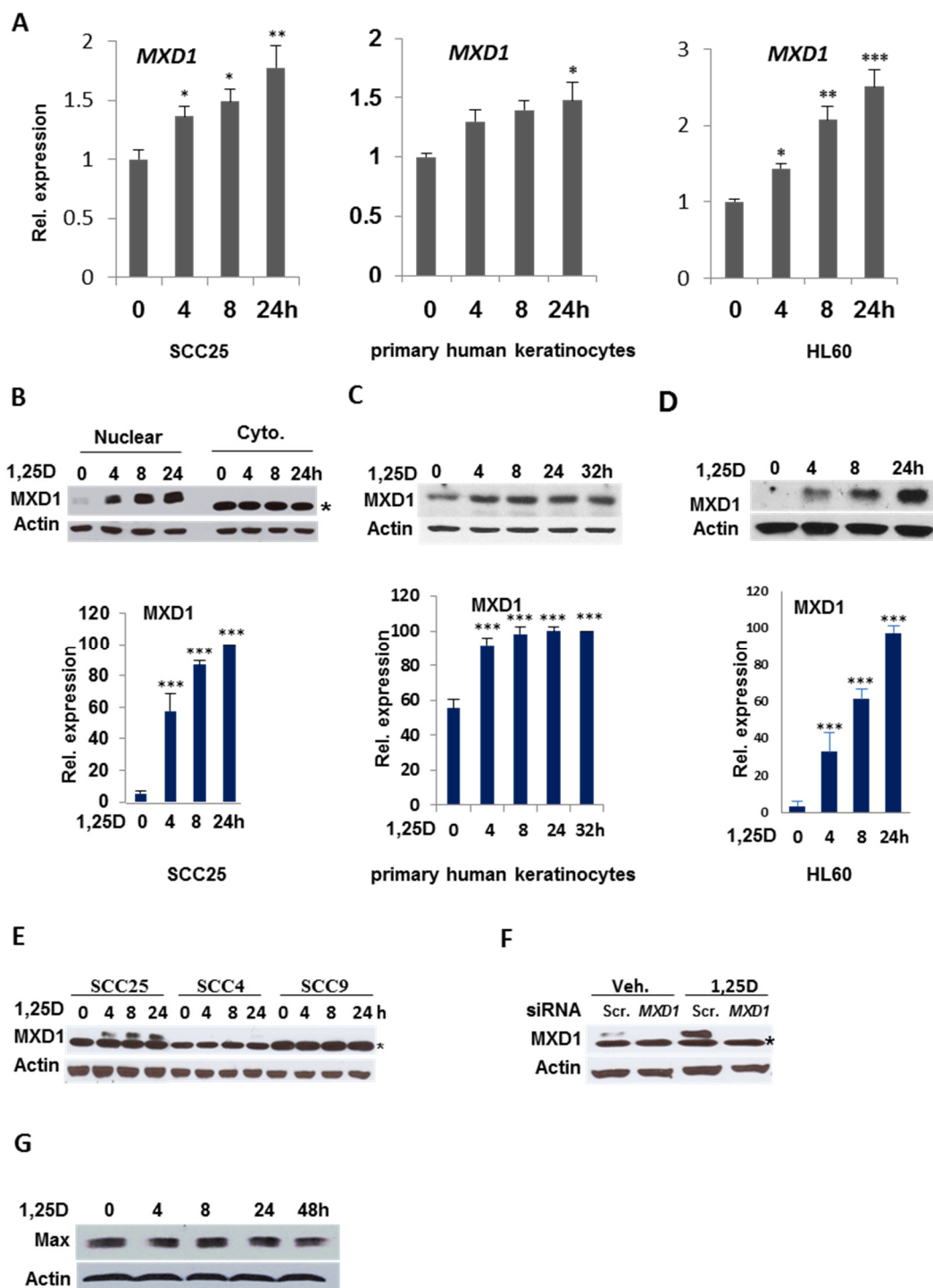
3.1. 1,25D signaling promotes MXD1 transcription and protein expression.

3.1. 1,25D signaling promotes MXD1 transcription and protein expression.

A) RT-qPCR analysis of *MXD1* gene transcription in SCC25 cells, primary human keratinocytes, and HL60 cells following treatment with 100 nM of 1,25D for 4, 8, and 24 hours. **B**, top panel) Western blot analysis of MXD1 levels in SCC25 cells following treatment with 100 nM of 1,25D for 4, 8, and 24 hours. MXD1 is in the nuclear extracts. **B**, bottom panel) Quantification of Western blot analyses of c-Myc levels represented in top panel, from four different experiments. **C**, Top panel) Western blot analysis of MXD1 levels in primary human keratinocytes following treatment with 100 nM of 1,25D for 4, 8, 24 and 32 hours. **C**, Bottom panel) Quantification of Western blot analyses of c-Myc levels represented in top panel, from four different experiments. **D**, top panel) Western blot analysis of MXD1 protein levels in HL60 cells following treatment with 100 nM of 1,25D for 4, 8, and 24 hours. **D**, bottom panel) Quantification of Western blot analyses of c-Myc levels represented in top panel, from four different experiments. **E)** Western blot analysis of MXD1 levels in SCC25, SCC4 and SCC9 cells following treatment with 100 nM of 1,25D for 4, 8, and 24 hours. The upper band corresponds for MXD1. **F)** Western blot analysis of MXD1 levels in SCC25 transfected with scrambled or MXD1 siRNA and treated with 100 nM of 1,25D. **G)** Western blot analysis of MAX protein levels in SCC25 cells following treatment with 100 nM of 1,25D for 4, 8, 24, and 48 hours. In western blot assays actin was presented as an internal control. The band marked by an asterisk in the western blots is a non-specific cytoplasmic protein. *P≤0.05, **P≤0.01, ***P≤0.001 as determined by One-way ANOVAs followed by Tukey's post hoc test for multiple comparisons.
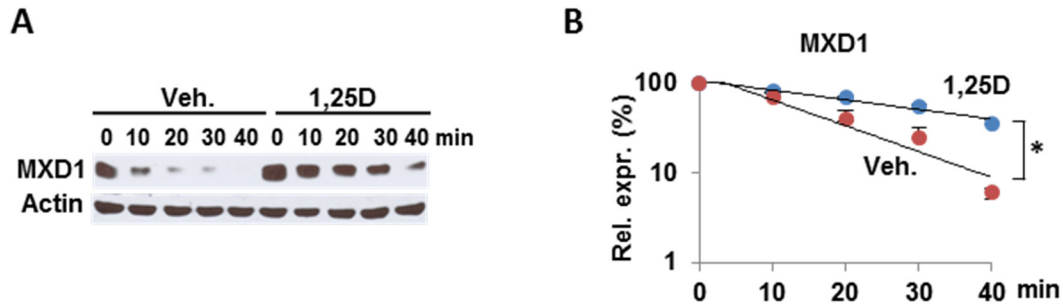
A) Western blot analysis of MXD1 in protein stability assay. SCC25 cells were treated with 100 nM 1,25D for 8 hours. 4 μg/ml of protein synthesis inhibitor cycloheximide (CHX) was added for 0, 10, 20, 30 and 40 mins. Nuclear extracts were analyzed by Western blot assays. Actin was presented as an internal control. **B)** Quantification of Western blot analyses of three independent experiments represented in **A**. *P≤0.05 as determined by One-way ANOVAs followed by Tukey's post hoc test for multiple comparisons.

3.2. 1,25D-bound VDR inhibits MXD1 turnover.

A

siRNA   Scr.   *FBW7*

MXD1   [blot]   *

Actin   [blot]

B

	Scr.					*FBW7*				
	0	10	20	30	40	0	10	20	30	40 min CHX

MXD1   [blot]

Actin   [blot]

[graph: Rel. expr. (%) vs CHX (min); curves labeled *FBW7* and *Scr.*; * significance]

C

	Veh					1,25D				
	0	10	20	30	40	0	10	20	30	40 min CHX

MXD1   [blot]

Actin   [blot]

FBW7 siRNA

[graph: Rel. expr. (%) vs CHX (min); curves labeled 1,25D and Veh.]

Fbw7 deficient cells
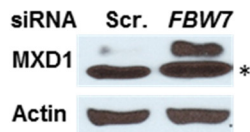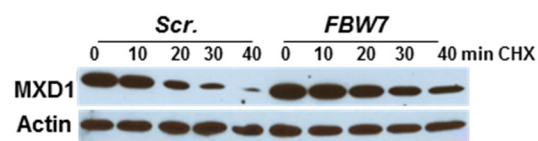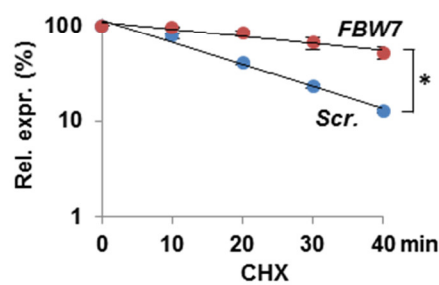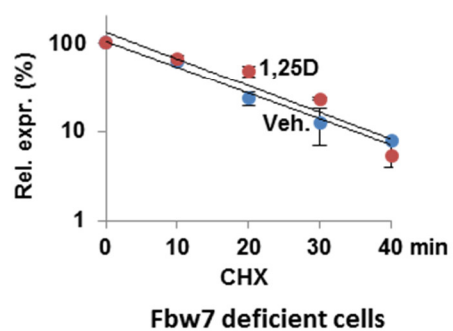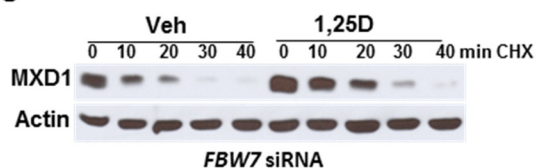
3.3. 1,25D-bound VDR inhibits MXD1 turnover through FBW7.

Figure legend on the next page.

3.3. 1,25D-bound VDR inhibits MXD1 turnover through FBW7.

A) Western blot analysis of MXD1 expression in SCC25 cells transfected with scrambled or *FBW7* siRNA. The band marked by an asterisk is a non-specific cytoplasmic protein. **B**, top panel) Western blot analysis of MXD1 in protein stability assay. SCC25 cells were transfected for scrambled or *FBW7* siRNA. 4 µg/ml of CHX was added for 0, 10, 20, 30 and 40 mins. Nuclear extracts were analyzed by Western blot. **B**, bottom panel) Quantification of Western blot analyses of three independent experiments represented in top panel. **C**, top panel) Western blot analysis of MXD1 in protein stability assay. SCC25 cells were transfected for *FBW7* siRNA and treated with vehicle or 1,25D for 6 hours. 4 µg/ml of CHX was added for 0, 10, 20, 30 and 40 mins. Nuclear extracts were analyzed by Western blot. **C**, bottom panel) Quantification of Western blot analyses of three independent experiments represented in top panel. In western blot analyses actin was presented as an internal control. *$P \leq 0.05$ as determined by One-way ANOVAs followed by Tukey's post hoc test for multiple comparisons.
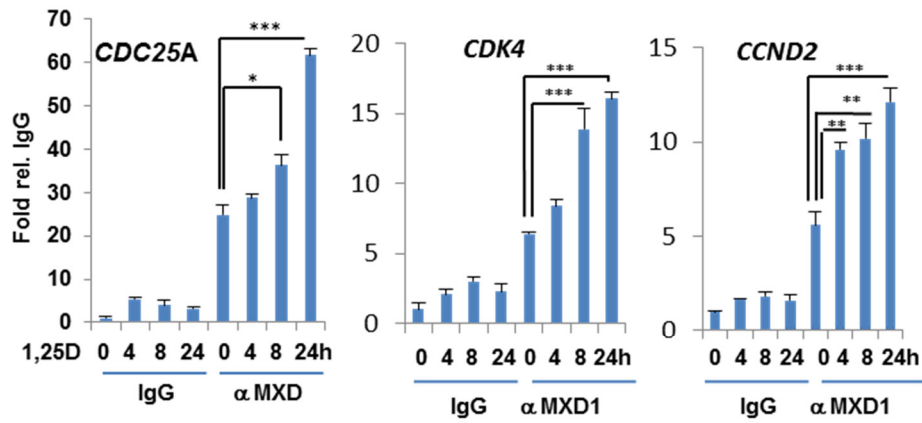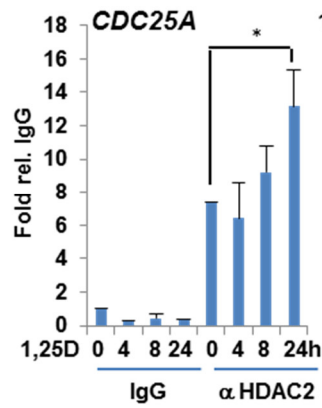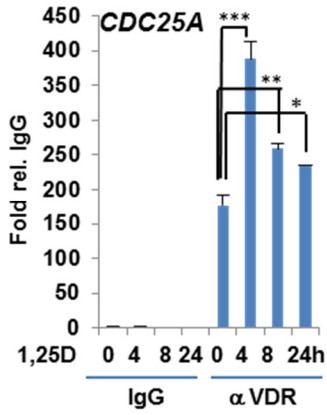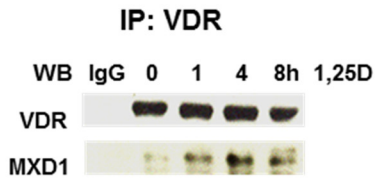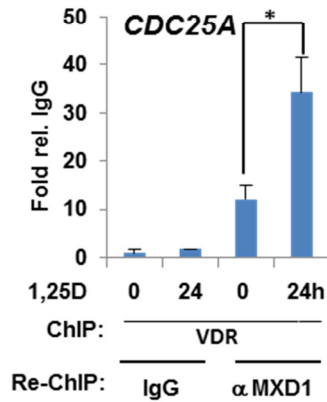
3.4. VDR interacts with MXD1 on the promoter of its target genes.

Figure legend on the next page.

3.4. VDR interacts with MXD1 on the promoter of its target genes.

A) Analysis of the MXD1 recruitment to the E-box motif of promoter of c-Myc target gene *CDC25A* by ChIP assays followed by qPCR, in SCC25 cells treated with 100 nM of 1,25D for 4, 8, and 24 hours. **B)** Analysis of the MXD1 cofactors HDAC2 and SIN3A recruitment to the E-box motif of promoter of c-Myc target gene *CDC25A* by ChIP assays followed by qPCR, in SCC25 cells treated with 100 nM of 1,25D for 4, 8, and 24 hours. **C)** Analysis of the VDR recruitment to the E-box motif of promoter of c-Myc target gene *CDC25A* by ChIP assays followed by qPCR, in SCC25 cells treated with 100 nM of 1,25D for 4, 8, and 24 hours. **D)** Western blot analysis of MXD1 co-immunoprecipitated with IgG or VDR, following treatment of SCC25 cells with 100 nM of 1,25D for 1, 4, and 8 hours. **E)** Analysis of the VDR and MXD1 co-recruitment to the E-box motif of promoter of c-Myc target gene *CDC25A* by Re-chromatin immunoprecipitation (Re-ChIP) assay, in SCC25 cells following treatment with 100 nM 1,25D for 24 hours. The first round of ChIP for VDR was followed by second round of immunoprecipitation for MXD1. *$P \leq 0.05$, **$P \leq 0.01$, ***$P \leq 0.001$ as determined by One-way ANOVAs followed by Tukey's post hoc test for multiple comparisons.

A

+/+

MXD1
Actin

Veh 1,25D

+/+
MXD1 **

120
100
80
60
40
20
0

Rel. expression

Veh. 1,25D

B

MXD1

+/+Veh.   +/+1,25D

C

MXD1

-/- Veh.   -/-1,25D
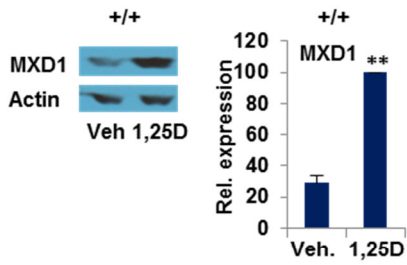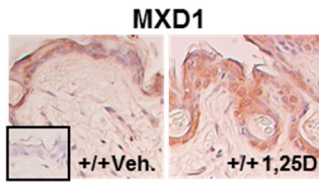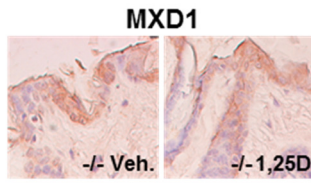
3.5. 1,25D induces MXD1 expression in vivo.

A, left panel) Western blot analysis of MXD1 expression in extracts of skin from wild-type *Vdr* mice treated topically with vehicle (veh.) or 1,25D (15ng/100µl/cm2) for 24h. **A**, right panel) Quantification of Western blot analyses of MXD1 expression in extracts of skin from wild-type mice treated topically with vehicle or 1,25D (15ng/100µl/cm2) for 24h. **B**) Immunohistochemical analysis of c-Myc expression in extracts of skin from wild-type mice treated topically with vehicle or 1,25D (15ng/100µl/cm2) for 24h. **C**) Immunohistochemical analysis of c-Myc expression in extracts of skin from *Vdr* null mice treated topically with vehicle or 1,25D (15ng/100µl/cm2) for 24h. **P≤0.01 as determined by One-way ANOVAs followed by Tukey's post hoc test for multiple comparisons.
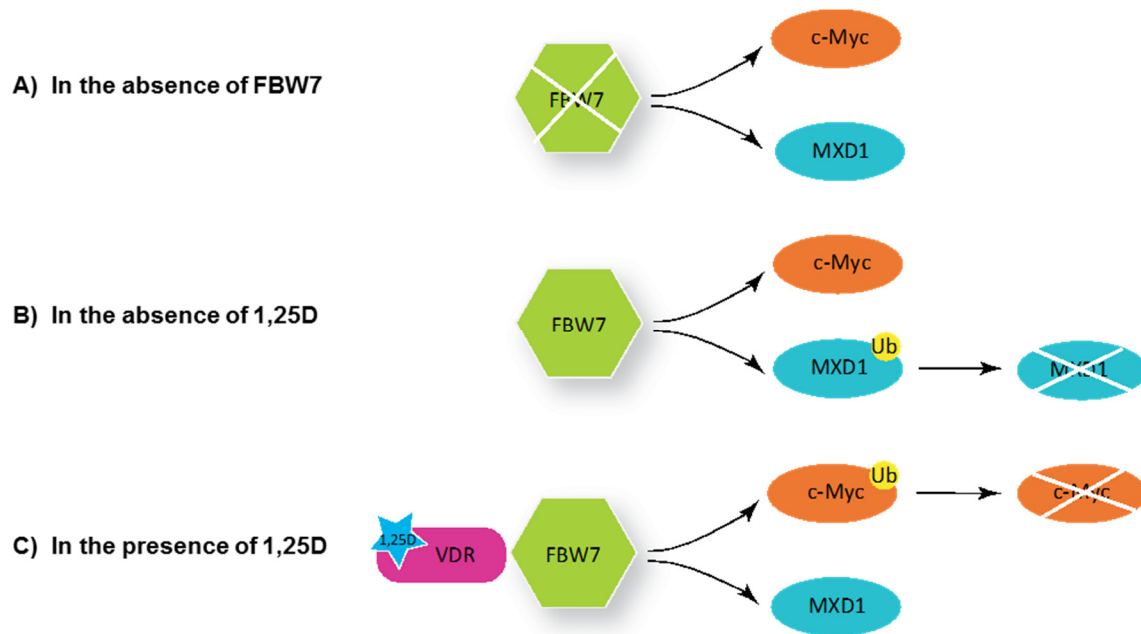
3.6. 1,25D-bound VDR regulates the stability of both arms of MXD1/MAX/c-Myc pull push network through SCF^FBW7.

A) In the absence of FBW7, the levels of both c-Myc and MXD1 are increased. **B)** In the absence of 1,25D, there is high levels of c-Myc protein, whereas MXD1 is mostly degraded. **C)** In contrast, in the presence of 1,25D, c-Myc turnover is accelerated by FBW7 and 1,25D, whereas MXD1 is protected from degradation.

3.6. Material and Methods

3.6.1. Cell Culture

SCC25 cells were obtained from the American Type Culture Collection (ATCC) and cultured in DMEM/F12 (319-085-CL, Multicell) supplemented with 10% FBS. LNCaP cells were obtained from the American Type Culture Collection (ATCC) and cultured in RPMI-1640 (30-2001, ATCC) supplemented with 10% FBS. HL60 cells were obtained from ATCC and cultured in RPMI-1640-1X (350-000-CL; Multicell) supplemented with 10% FBS. Primary Human keratinocytes (HEK-a) were obtained from ScienCell and cultured in EpiLife® Medium (M-EPI-500-CA, Invitrogen) supplemented with Supplement S7 (S-017-5, Invitrogen).

3.6.2. Knockdown

SCC25 cells were transfected with siRNAs for 24 h using LipofectamineTM 2000 reagent (Invitrogen), and treated with 1,25D. siRNAs were purchased from Qiagen. The sequences of siRNAs are listed in section 3.6.11.

3.6.3. RT-qPCR

Quantitative RT-PCR was performed with SsoFast-EvaGreen real-time PCR kit (Bio-Rad). Expression was normalized to the expression of GAPDH. Primer pairs used for RT-PCR are listed in section 3.6.12.

3.6.4. Immunoprecipitation and Western blot analysis

Cells were lysed with a lysis buffer (20 mM Tris, pH 7.5, 100 Mm NaCl, 0.5% Nonidet P-40, 0.5mM EDTA, 0.5 mM phenylmethylsulfonyl fluoride). 4 ug anti-VDR (D-6; Santa Cruz) Antibody was pre-bound for 2 h to protein A agarose beads, then was washed with PBS plus 5% BSA and added to the lysate, followed by immunoprecipitation overnight. Protein A agarose beads were then washed five times with washing buffer (20 mM Tris, pH 7.5, 200 Mm NaCl, 1%

Nonidet P-40, 0.5mM EDTA, 0.5 mM phenylmethylsulfonyl fluoride) and processed for Western blotting, performed with standard protocols. The following antibodies were used: VDR (H-81), VDR (D-6), and MXD1(c-19), all from Santa Cruz. For western blot of mouse skin, 50 mg of skin were ground under liquid nitrogen and homogenized in 1ml of lysis buffer. Lipids were removed by centrifugation at 10,000 RPM for 10min at 2oC. Western blots were quantified using ImageJ 1.45 software.

3.6.5. ChIP assays

Cells were cross-linked with 4% paraformaldehyde for 25 min and were lysed with 500 □l lysis buffer (150 mM NaCl, 0.5% NP-40, 1% Triton X-100,5mM EDTA and 50 mM Tris-HCl, pH 7.5) containing 1x protease inhibitor cocktail. Chromatin was sheared to an average length of 300–500 bp by sonication and supernatants were collected after centrifugation. 4 ug of Antibody was added to chromatin for immunoprecipitation overnight. then protein A agarose beads, ssDNA and BSA was added to the antibody chromatin complexes for 4 h. Protein A Agarose bead–chromatin complexes were then washed three times in TSE I (20 mM Tris-HCl, pH 8.1, 2 mM EDTA, 0.1% SDS, 1% Triton X-100 and 150 mM NaCl) followed by one wash with TSE II buffer (20 mM Tris-HCL, pH 8.1, 2 mM EDTA, 0.1% SDS, 1% Triton X-100 and 500 mM NaCl) and one wash with buffer III (0.25 M LiCl, 1% NP-40, 1% deoxychlolate, 1mM EDTA, 10mM Tris-Hcl, pH 8.1). Immunoprecipitated chromatin was then extracted with extraction buffer (1% SDS and 0.1 M NaHCO3) and was heated at 65 °C for overnight for reversal of the paraformaldehyde crosslinking. DNA fragments were purified with a PCR purification kit (Qiagen) and were analyzed by SsoFast-EvaGreen real-time PCR. The following antibodies were used for ChIP: anti-Sin3a (K-20), anti-HDAC2 (H-54), anti-Mad1 (c-19), and anti- VDR (D-6), from Santa Cruz. Primer pairs used for ChIP assays are listed in section 3.6.12. CCND2, and

CDK4 primers [172] have been described. For re-ChIP assays, VDR immunocomplexes were eluted by adding 40μl 10mM DTT for 30 min at 37 C. Supernatants were diluted 1:20 in dilution buffer (150 mM NaCl, 1% Triton X-100,2mM EDTA and 50 mM Tris-HCl, pH 8), and re-ChIP was performed using anti-MXD1 antibody, as indicated in the figures.

3.6.6. Animal Experiments

All animal experiments were carried out in compliance with and approval by the Institutional Animal Care and Use Committee. *Vdr*+/- animals (The Jackson Laboratory, Bar harbor, ME) were mated to generate homozygous for *Vdr*-/- mice. At 21 days of age, control *Vdr*+/+ and *Vdr*-/- mice were weaned and maintained until sacrifice on high calcium (rescue) diets containing 1.5% calcium in the drinking water and autoclaved regular chow.

3.6.7. Genotyping of Mice

Genomic DNA was isolated from tail fragments by standard phenol/chloroform extraction and isopropyl alcohol precipitation. To determine the genotype at VDR loci, 2 PCRs were conducted for each animal. The wild type VDR allele was detected using forward primer 5′-CTGCCCTGCTCCACAGTCCTT-3′ and reverse primer 5′-CGAGACTCTCCAATGTGAAGC-3′. The disrupted VDR allele was assayed using the neo forward primer 5′-GCTGCTCTGATGCCGCCGTGTTC-3′ and a neo reverse primer 5′-GCACTTCGCCCAATAGCAGCCAG-3′. PCR conditions were 30 cycles for all VDR and disrupted VDR allele, 94 °C for 1 min, 65 °C for 1 min, and 72 °C for 1 min; and neomycin, 94 °C for 1 min, 60 °C for 1 min, and 72 °C for 1 min.

3.6.8. Topical treatment with 1,25D

Mice (5-6) at 3 months of age were treated topically on the dorsal surface with vehicle or 1,25D for 18 h. The vehicle was a base lotion containing ethanol: propylene-glycol: water (2:1:1). The

1,25D (Sigma) was dissolved in ethanol and diluted with vehicle. Each mouse was treated with vehicle (100ul/cm2) on the highest part of the back (neck) and with 1,25D (15ng/100μl/cm2) on the lowest part of the back (hip) to avoid the contact between 2 treatments. After 18 h of treatment the treated region of skin were immediately removed and fixed in PLP fixative (2% paraformaldehyde containing 0.075 m lysine and 0.01 m sodium periodate) overnight at 4 °C, washed and processed immunohistochemistry (IHC) study.

3.6.9. Immunohistochemistry

MXD1 expression was determined by IHC using the avidin-biotin-peroxidase complex (ABC) technique. Anti-MXD1 (SAB2105310; Sigma-Aldrich) was applied to dewaxed paraffin sections overnight. After washing with high salt buffer, slides were incubated with secondary antibody, washed and processed using the Vectastain ABC-AP kit (Vector Laboratories) and mounted with Permount (Fisher Scientific). Images from sections were processed using Bioquant image analysis software.

3.6.10. Statistical Analysis

All experiments are representative of 3-5 biological replicates. Unless otherwise indicated in the figures, statistical analysis was conducted using the program SYSTAT13 by performing one-way analysis of variance (ANOVA) followed by the Tukey test for multiple comparisons as indicated: *$P \leq 0.05$, **$P \leq 0.01$, ***$P \leq 0.001$.

3.6.11. siRNAs

FBXW7   5'-CCCTAAAGAGTTGGCACTCTA-3'
MXD1   5'-CAGTAGCAGATCAACTCACAA-3'
Control   5'-CAGGGTATCGACGATTACAAA-3'

3.6.12. Primers

Primers for gene expression:

CCND2-FORWARD	5'-GAGAAGCTGTCTCTGATCCGCA-3'
CCND2-REVERSE	5'-CTTCCAGTTGCGATCATCGACG-3'
CDK4-FORWARD	5'-CCATCAGCACAGTTCGTGAGGT-3'
CDK4-REVERSE	5'-TCAGTTCGGGATGTGGCACAGA-3'
CDC25A-FORWARD	5'-TCTGGACAGCTCCTCTCGTCAT-3'
CDC25A-REVERSE	5'-ACTTCCAGGTGGAGACTCCTCT-3'
MYC-FORWARD	5'-CCTGGTGCTCCATGAGGAGAC-3'
MYC-REVERSE	5'-CAGACTCTGACCTTTTGCCAGG-3'
MXD1-FORWARD	5'-ACCTGAAGAGGCAGCTGGAGAA-3'
MXD1-REVERSE	5'-AGATAGTCCGTGCTCTCCACGT-3'
ELAVL-1-FORWARD	5'-CCGTCACCAATGTGAAAGTG-3'
ELAVL-1-REVERSE	5'-TCGCGGCTTCTTCATAGTTT-3'
SKP2-FORWARD	5'-CTCCACGGCATACTGTCTCA-3'
SKP2-REVERSE	5'-GGGCAAATTCAGAGAATCCA-3'
FBW7-FORWARD	5'-CAGCAGTCACAGGCAAATGT-3'
FBW7-REVERSE	5'-GCATCTCGAGAACCGCTAAC-3'
CTNNB1-Forward	5'-CACAAGCAGAGTGCTGAAGGTG-3'
CTNNB1-Reverse	5'-GATTCCTGAGAGTCCAAAGACAG-3'

Primers for ChIP assays.

CDC25A-FORWARD	5'-GAGAGATCAGGCCAGGAAAC-3'
CDC25A-REVERSE	5'-CTCTCCCGCCCAACATTC-3'
CDK4-FORWARD	5'-GAGCGACCCTTCCATAACCA-3'
CDK4-REVERSE	5'-GGGCTGGCGTGAGGTAAGT-3'
MYC-FORWARD	5'-TGGGCGGCTGGATACCTT-3'
MYC-REVERSE	5'-GATGGGAGGAAACGCTAAAGC-3'
CCND2-FORWARD	5'-TCAGTAAATGGCCACACATGTG-3'

CCND2-REVERSE   5'-GGAGCTCTCGACGTGGTCAA-3'

MYC-FORWARD   5'-AGGCAACCTCCCTCTCGCCCTA-3'

MYC-REVERSE   5'- AGCAGCAGATACCGCCCCTCCT-3'

Chapter 4

The 1,25D-bound VDR cooperates with FBW7 to inhibit proliferation.

4.1. Preface

The molecular mechanisms of the cancer chemopreventive effects of 1,25D have not been extensive elucidated. Previously, we tested the effect of 1,25D on c-Myc a key regulator of cell cycle progression, and found that this effect is not only through repression of c-Myc transcription, but also by affecting c-Myc protein stability. Therefore, we began searching for mechanisms that may affect c-Myc stability. This led us to the E3 ligase FBW7. Our finding that MXD1, the antagonist of c-Myc, is also degraded by FBW7 opened a new window to determine how VDR regulates the c-Myc/MAX/MXD1 network. We found the VDR regulates the degradation of transcription factors c-Myc and MXD1, which are two arms of a tumor suppressor/oncogenic network, through FBW7. As FBW7 is a tumor suppressor, this provides insights into the cancer-preventive actions of vitamin D. It is therefore important to determine how 1,25D-bound VDR can regulate FBW7 function. To further clarify the cooperative function of 1,25D-bound VDR and FBW7, we studied the interactions of 1,25D-bound VDR and FBW7 with MXD1 and c-Myc. In addition, we analyzed the regulation by 1,25D of other known and putative novel substrates identified in a screen for novel FBW7 target proteins.

4.2. Abstract

The FBW7 E3 ligase degrades both arms of the c-Myc/MAX/MXD1 network. c-Myc is a key regulator of cell cycle progression, and MXD1 antagonizes its effect and represses the transcription of genes that play a crucial role in cell proliferation. It has been shown that Gsk3 kinases are needed to phosphorylate FBW7 substrates to trigger the binding of FBW7. In previous chapters, we demonstrated that the 1,25D-bound VDR influences c-Myc and MXD1 expression through FBW7. FBW7 function needs to be regulated to select the right substrate of this network. Here, by inhibiting GSK3 kinases, we provide evidence that MXD1 is not phosphorylated by GSK3s, but by another kinase. We also provide evidence that FBW7 interactions with c-Myc and MXD1 are 1,25D-dependent and follow the same pattern as VDR interactions with c-Myc and MXD1; FBW7 and c-Myc interaction increases whereas the interaction of FBW7 with MXD1 is attenuated in the presence of 1,25D. Re-ChIP assays revealed that these interactions can occur on the promoters of c-Myc target genes. Determining the effect of 1,25D on the expression of multiple FBW7 oncogenic target proteins revealed that 1,25D reduced their protein levels. This reduction could be rescued by ablation of FBW7. Further, the screening of the proteome for potential targets of FBW7 revealed several oncogenes and tumor suppressors. Investigating, the effects of 1,25D on E2F1 and TCF7L2, chosen for their roles in cell cycle regulation, showed that 1,25D suppressed their expression. In proliferation assays, treating cells with 1,25D strongly suppressed proliferation. This reduction in proliferation was attenuated following FBW7 ablation. Furthermore, screening of the proteome for phosphodegron motifs revealed a canonical phosphodegron in the VDR in a "linker" region of its binding domain. Ablation of FBW7 increased VDR levels and function in the absence of 1,25D, whereas it decreased the stability of VDR in the presence of 1,25D. Collectively, these results

suggest that FBW7 and VDR cooperate to suppress cell proliferation and regulate each other's function.

4.3. Introduction

Ubiquitin-mediated degradation is stimulated by binding of ubiquitin or poly-ubiquitin to a target protein, which serves as a recognition signal by the proteasome system [353]. It is the responsibility of E3 ubiquitin ligases to recognize a substrate and facilitate its ubiquitination. SCFs (Skp1, Cullin-1, F box protein) are a class of E3 ligases, in which Cullin-1 is a scaffold and F box protein is substrate recognition subunit. Multiple F-box proteins can play the substrate recognition role in SCF complex [354]. Fbw7 F-box protein targets a network of substrates including some key oncoproteins for ubiquitination and subsequent degradation. Fbw7 is one of the most commonly dysregulated UPS protein in multiple cancer types [354]. Many of its target proteins are transcription factors enabling FBW7 to modulate multiple oncogenic pathways. Cancer genomics studies have revealed that Fbw7 is among the most mutated cancer genes and its mutations play a central role in tumorigenesis [355]. Various studies have shown that FBW7 recognizes substrates through phosphodegron motifs consisting of T/S-P-X-X-S/T/E. Phosphorylation of substrates at T/S residue, which is essential for being recognized by FBW7, is commonly performed by GSK3β[122], [356], [357].

Multiple FBW7 target proteins are well-known oncogenes that play an effective role in cell cycle progression including Cyclin E, AIB1 (Amplified in breast cancer 1), c-Jun and MCL1 (Myeloid Cell Leukemia 1) [358]. Cyclin E-Cdk2 phosphorylates and inactivates Rb (retinoblastoma protein) and p27Kip1(Cyclin-dependent kinase inhibitor 1B) proteins which inhibit G1 progression [359]. AIB1 is highly expressed in many cancers. It acts as an coactivator for E2F1, nuclear receptors, and the AR (androgen receptor) to induce cancer progression[360]. c-Jun in

combination with c-Fos activates transcription of genes that are crucial for cell cycle progression, such as cyclin D1. In addition, it activates transcription of genes that are involved in tumor progression including matrix metalloproteinases (MMPs) that facilitate growth, and metastasis of cancer cells [361]. Other proteins are essential for cell cycle progression such as E2F, MLL1 and TCF7L2, and are probably targeted by FBW7. However, this remains to be investigated.

One of the well-known FBW7 substrates is c-Myc, which promotes cell proliferation and is a key regulator of cell cycle progression. Myc belongs to the basic helix-loop-helix leucine zipper (bHLHZ) transcription factors family. Transactivation domain of Myc at the N-terminus is highly conserved and contains multiple Myc homology boxes (MB I, II, II, IV), which have variable transforming activity. The phospho-degron recognized by FBW7 is located in MB I. Various mutations in MB I enhance the oncogenic activity of Myc in multiple tumor model [362]. FBW7 recognizes c-Myc phosphorylated by GSK3s at Thr 58 and promotes its ubiquitination. Thr58 is the most frequently mutated residues in lymphoma cells [82]. It has been found that down-regulation of FBW7 result in accumulation of cellular and chromatin-bound MYC[143].

Myc activity is antagonized by another member of bHLHZ transcription factors family, MXD1. Myc is highly expressed in proliferating cells, whereas MXD1 is found mostly in differentiated cells [276], [349]. In contrast to Myc, the N-terminus of MXD1 is short and lacks the homology boxes[249]. Similar to Myc, MXD1 is an unstable protein. It has been revealed that MXD1 is poly-ubiquitinated at multiple residues and applying proteasomal inhibitors enhances the MXD1 stability, suggesting that MXD1 is turned over by proteasome system [249], [346]. Stimulation of cells with insulin or serum induces phosphorylation of MXD1 at Ser145 residue by p90 and p70 ribosomal S6 kinases resulting in MXD1 ubiquitination and degradation[263]. These kinases

promote cell cycle entry and proliferation in response to growth factors[249]. We have shown that similar to c-Myc, MXD1 can be targeted for degradation by FBW7 E3 ligase and that vitamin D receptor (VDR) is able to regulate the stability of c-Myc and MXD1 through FBW7 [363].

The VDR is a ligand-activated transcription factor from the steroid/thyroid hormone receptor superfamily [29]. VDR protein consists of two main functional domains, the N-terminus zinc finger DNA binding domain and the C-terminus ligand binding domain. Nuclear localization signals at the N-terminus localize the receptor to the nucleus[30]. VDR contains 13 α-helices and one β-sheet structure at the C-terminal domain. Helices 3 and 12 form proper conformational change after binding of 1,25D, to interface with RXR and other interacting proteins. VDR contains a specific unstructured and flexible "insertion" domain between H2 and H3 including 23 residues which is unique to VDR [31]. It has been shown that proteasome inhibitors enhance VDR protein levels without affecting VDR mRNA expression. Furthermore, 1,25D inhibits VDR ubiquitination [364]. Thus, 1,25D simultaneously displays dual positive effect on VDR in the cell, by promoting VDR transactivation and inhibiting VDR degradation[364], [365].

In this study, we show that 1,25D bound VDR inhibits cell proliferation through FBW7. In addition, we predicted a list of proteins which contain potential phosphodegron motif, T/S-P-X-X-T/S/E. We studied the direct interaction of FBW7 with MXD1 and VDR by GST pull-down assay and found that presence of hormonal vitamin D enhances the interaction of FBW7 and VDR to c-Myc and decreases their interaction with MXD1. In addition, we found that, in contrast to c-Myc, MXD1 does not appear to be phosphorylated by GSK3. Rather, it appears that one of the PKCs would be responsible for MXD1 phosphorylation and subsequent ubiquitination. We examined VDR stability and found that FBW7 ablation enhances VDR

turnover in the presence of 1,25D. These results suggest that in cooperation with ligand bound VDR can act as a tumor suppressor and inhibit cell cycle progression by controlling protein degradation.

4.4. Results

4.4.1. MXD1 and c-Myc directly interact with FBW7 and VDR in a 1,25D-dependent manner.

c-Myc was an identified FBW7 substrate [93], and we found that MXD1, the other arm of c-Myc/MAX/MXD1 network, also is degraded through FBW7 [363]. To determine whether the binding of FBW7 to c-Myc and MXD1 is 1,25D dependent, we investigated the binding of FBW7-c-Myc and FBW7-MXD1 upon applying 1,25D to SCC25 cells. In the absence of proper antibody for FBW7, SCC25 cells were transfected with Flag-FBW7 and treated with 1,25D. Co-Immunoprecipitation (Co-IP) assays were performed to assess the association of FBW7 with c-Myc and MXD1. Interestingly, the Co-IP results revealed that association of FBW7 with c-Myc and MXD1 are 1,25D dependent. 1,25D enhanced the binding of FBW7 and Myc (Fig. 1A), whereas it reduced the association of FBW7 and MXD1 (Fig. 1B). Since the expression of *FBW7* is not changed significantly upon applying 1,25D (data not shown), the increased interaction of FBW7 with c-Myc does not appear to be due to increased expression of FBW7.

We observed an increased interaction of VDR with c-Myc and MXD1 upon applying 1,25D, which was attenuated following a primary peak of increased interaction in SCC25 cells [363]. To investigate whether this increased association is due to the increased expression of VDR following treatment with 1,25D, or is due to greater direct interaction of ligand bound VDR with c-Myc or MXD1, GST-pull down assays were performed using GST or GST-VDR and in vitro translated c-Myc and MXD1. 1,25D or vehicle were applied to the reaction. The amount of

pulled-down c-Myc and MXD1 was assessed by western blot. Our results show that association of c-Myc and VDR increase in the presence of 1,25D (Fig. 1C), whereas the interaction of VDR with MXD1 reduced upon applying 1,25D (Fig. 1D).

Remarkably, these data demonstrate that interaction of FBW7 with c-Myc and MXD1, and interaction of VDR with c-Myc and MXD1, follow the same pattern after applying 1,25D which provides additional evidence for cooperative function of VDR and FBW7.

4.4.2. FBW7 interacts with MXD1.

We showed that, similar to c-Myc, MXD1 is degraded through FBW7 [353], however it lacks the canonical phosphodegron motif to be recognized with FBW7. In previous study, it was shown that multiple proteins can be recognized and signed by FBW7 through non-canonical degrons [Fig. 2B (a)] [348], [350], [366]. To determine whether FBW7 directly interacts with MXD1, GST-pull down assays were performed, using GST or GST-MXD1 and in vitro translated Flag-FBW7. The result revealed that FBW7 interacts directly with MXD1 (Fig.2A). To investigate the most prevalent phosphorylation sites, we used the DISPHOS 1.3 program that predicted different serine and threonine rsidues for phosphorylation in MXD1 [Fig. 2B (b)].

4.4.3. MXD1 phosphorylation for subsequent ubiquitination, in the absence of 1,25D, is through a kinase other than GSK3.

Our previous results determined that both the c-Myc and MXD1 arms of c-Myc/MAX/MXD1 network are degraded through FBW7, however, the patterns of their degradation are different after addition of 1,25D, which suggests that different pathways trigger their recognition by FBW7. In addition, the GSK3 kinases that phosphorylate c-Myc and mark it for degradation, are tumor suppressors [93]. They are upregulated through pathways which help the cell to eliminate

oncogenes, but not tumor suppressors such as MXD1. This raises the possibility that MXD1 might be phosphorylated and marked for FBW7 recognition through kinases other than GSK3s.

To investigate the possibility of phosphorylation of MXD1 with GSK3s, SCC25 cells were treated with CHIR (a GSK3s inhibitor) and 1,25D. Western blot analysis of MXD1 expression revealed that GSK3 inhibitor does not inhibit MXD1 degradation, and even reduces its elevated expression in the presence of 1,25D (Fig. 3A). To further verify the reduced MXD1 expression in CHIR treated cells, RT-qPCR assays were performed to measure the level of *MXD1* mRNA expression following treatment of cells with CHIR. The data showed that the reduction of MXD1 expression after applying CHIR is through its effect on *MXD1* transcription (Fig. 3B).

As a potential inhibitor of several kinases, including oncogenic, staurosporine was used to treat the cells, to investigate the possible kinases that phosphorylate and mark the MXD1 to be recognized by FBW7 following treatment of SCC25 cells with 1,25D. Surprisingly, the expression of MXD1 in non-treated cells was rescued to the same level of 1,25D treated cells after applying staurosporine (Fig. 3C). To ensure that the effect of staurosporine on MXD1 protein was not due to enhanced transcription of *MXD1*, RT-qPCR assay were performed to measure the levels of *MXD1* expression following treatment of cells with staurosporine. The result demonstrated that *MXD1* expression was not altered after treating the cells with staurosporine (Fig. 3D), therefore the increased levels of MXD1 protein is due to inhibition of the kinase that phosphorylates MXD1 and triggers its ubiquitination by FBW7. We investigated multiple potential kinases, which are inhibited by staurosporine including AKT, PKCZ, PKCI, S6K, PKA, PKG and PKCA, using siRNA or specific inhibitors, none of which trigger degradation of MXD1 protein (data not shown). Together, these result suggest that in contrast to

c-Myc, phosphorylation of MXD1 for degradation is not through GSKs, rather it is through a potential kinase that is an inhibitory target of staurosporine.

4.4.4. FBW7 binds to MXD1 and c-Myc on the promoter of target genes, in 125D dependent manner.

We determined that FBW7 binding to the c-Myc and MXD1 is 1,25D dependent and its interactions follow the same pattern as VDR. In addition, in chapters 2 and 3 we showed that VDR is in a complex with the c-MYC or MXD1 on the promoter of c-Myc target genes, in a 1,25D dependent manner. Thus, we investigated whether, similar to VDR, FBW7 is recruited to the promoter region of c-Myc target genes and whether this recruitment is 1,25D dependent. In the absence of proper antibody, a lentiviral vector was made to create a stably expressing SCC25 cell line. To this end, the HA-FBW7 cDNA was inserted into LeGO-iG2 lentiviral vector. SCC25 cells were stably transfected with LeGO-iG2-HA-FBW7 and treated with 1,25D for 6 hours. Chromatin immunoprecipitation (ChIP) assays showed that FBW7 is recruited to the E-Box motif of c-Myc target gene promoters (*CDK4* and *CDC25A*) and these interactions are not 1,25D dependent (Fig. 4A).

To further investigate the FBW7 interaction with c-Myc and MXD1 on the promoter of c-Myc target genes, and to further verify whether these possible interactions are 1,25D dependent, Re-ChIP assays were performed using an anti-HA antibody for ChIP and c-Myc and MXD1 antibodies for Re-ChIP, following treatment of SCC25 cells with vehicle or 1,25D for 6 hours. The results strongly suggest that FBW7 interacts with c-Myc and MXD1 on the promoter of c-Myc target gene, *CDC25A* and these interactions are 1,25D dependent (Fig. 4B, 4C). The interaction of FBW7 with MXD1 dramatically decreased (Fig. 4B), whereas the interaction of FBW7 with c-Myc enhanced after 6 hours of treatment with 1,25D (Fig. 4C). Together these

results suggest that FBW7 interacts, 1,25D dependently, with c-Myc and MXD1 and trigger their degradation on the promoter of c-Myc target genes.

4.4.5. FBW7 binds to VDR on the promoter of target genes, in 125D dependent manner.

In previous chapters we determined that VDR is recruited to the promoter of c-Myc target genes, in a 1,25D dependent manner. Here, we have shown that FBW7 also is recruited to the promoter of c-Myc target genes. Thus, we investigated whether FBW7 associates with the VDR on the promoter of c-Myc target genes. To this end, SCC25 cells were treated with vehicle or 1,25D for 6 hours and Re-ChIP assays were performed. The result suggests that the VDR is recruited to E-box motifs of promoters of c-Myc target genes CDK4 and CDC25A in association with FBW7. This association is decreased upon treatment with 1,25D (Fig. 5A).

To verify the direct interaction of FBW7 with VDR, GST-pull down assays were performed using GST or GST-VDR protein and the in vitro translated conserved part of FBW7 tagged with Flag. The result suggests a direct interaction between conserved part of FBW7 and VDR (Fig. 5B). To further investigate whether direct interaction of VDR and FBW7 is 1,25D dependent, GST-pull down assays were performed using GST or GST-VDR protein and in vitro translated WD40 domain of FBW7. Vehicle or 1,25D were added to the reaction. In agreement with Re-ChIP results, we observed a slight reduction in the association of FBW7 with VDR upon applying 1,25D (Fig. 5C). These results suggest that 1,25D might inhibit FBW7 binding to the VDR. Altogether, these results confirm that FBW7 interacts directly with VDR and this interaction can occur on the promoter of target genes of FBW7 substrates.

4.4.6. Expression of multiple FBW7 target genes involved in cell cycle regulation is controlled by 1,25D.

In previous studies we concluded that the ligand bound VDR induces its anti-proliferative effects in cooperation with FBW7 [363]. We have studied in detail c-Myc and MXD1 as model FBW7 target proteins. However, there are several other known FBW7 substrates implicated in cell cycle control, suggesting that 1,25D signaling might also control their turnover. Therefore, we analyzed some previously characterized FBW7 target proteins (AIB1, Cyclin E, c-Jun, and MCL1) to examine the effect of 1,25D on their expression. For this purpose, SCC25 cells were treated with 1,25D for the times indicated in Fig.6A and AIB1, Cyclin E, c-Jun, and MCL1 protein expression was measured by western blot assays. In agreement with our previous results, we observed reduction in the levels of all these oncoproteins (Fig. 6A). HaCaT cells, a skin cell line, were also were treated for 24 hours with 1,25D, and AIB1 protein expression was measured. Similar to SCC25 cells, treatment of HaCaT cells with 1,25D suppressed AIB1 protein expression (Fig. 6B), indicating that the effect of 1,25D on AIB1 expression is not limited to SCC25 cell line.

To determine whether the effects observed upon applying 1,25D (Fig. 6A) are through FBW7, *FBW7* expression was knocked down in SCC25 cells by siRNA, treated with 1,25D for 24 hours, after which AIB1 and Cyclin E expression were assessed by western blot. Our results demonstrate that *FBW7* knockdown rescued the reduced AIB1 and Cyclin E expression after treatment with 1,25D (Fig. 6C), which confirms that 1,25D-bound VDR anti-proliferative effects are through FBW7.

Taken together, these data suggest that depletion of FBW7 should inhibit the capacity of 1,25D to arrest cell proliferation. To test this hypothesis, *FBW7* expression was knocked down in

SCC25 cells and cells were treated with 1,25D. Cell proliferation was measured by the EdU proliferation assay, which revealed that 1,25D reduces proliferation up to 80% in SCC25 cells. Interestingly, the ablation of *FBW7* reduced the anti-proliferative effect of VDR up to four fold (Fig. 6D). Altogether, these data confirm that ligand-bound VDR induces its anti-proliferative effects in cooperation with FBW7.

4.4.7. Phosphodegron screen for potential novel FBW7 target protein.

To identify other potential FBW7 substrates and potential targets of 1,25D-regulated turnover, the proteome was screened for proteins containing the canonical phosphodegron sequence recognized by FBW7, T/S-P-X-X-T/S/E, using the ScanSite program [368] (Table S4.1). This list may contain several false positives. Therefore, to narrow the list, we selected known oncogenes and tumor suppressors, which revealed approximately the same ratio of identified oncogenes and tumor suppressors as potential FBW7 substrates (Table S4.2, S4.3). We further narrowed the list by focusing on nuclear proteins implicated in transcriptional regulation. This included transcription factor E2F1, a key regulator of cell cycle progression, and TCF4L2, which promotes Wnt signaling. Notably, their expression was greatly reduced by 1,25D treatment, consistent with their turnover being regulated by the hormone-bound VDR (Fig. 7A). This effect was observed in the absence of any effects of 1,25D on their mRNA levels (Fig. 7B).

4.4.8. The VDR is a target protein of FBW7.

Remarkably, screening of the proteome for potential consensus phospho-degrons (Table S4.1) revealed a motif in a linker region of the VDR ligand binding domain, which is conserved from old world monkeys to humans (Fig. 8A). The VDR/RXR tertiary structure was generated by Dr. Natacha Rochel at the IGBMC in Illkirch, France (Fig. 8B). The tertiary structure showed that degron motif is located in the unstructured part of VDR ligand binding domain between helices 2

and 3 (Fig. 8B). This finding and the results that showed the 1,25D-dependent association of the VDR and FBW7 suggest that FBW7 may regulate VDR stability and function. To address this, SCC25 cells were transfected with scrambled or *FBW7*-specific siRNAs and the expression of VDR was assessed by western blot assays. The results showed an increased level of VDR following FBW7 ablation (Fig. 8C). To ensure that the effect of FBW7 ablation on VDR protein was not due to enhanced transcription of the gene, RT-qPCR assays were performed to measure the levels of VDR mRNA expression following the knockdown of *FBW7* in SCC25 cells, revealing that FBW7 ablation did not affect VDR mRNA (Fig. 8C). Interestingly, expression of 1,25D-bound VDR direct target gene *CYP24* was increased upon knock down of *FBW7* (Fig. 8C).

To further investigate whether the VDR canonical phosphodegron is phosphorylated by GSK3s, SCC25 cells were treated with vehicle or GSK3s inhibitor (CHIR) and the expression level of VDR and its target gene, *CYP24*, were assessed by RT-qPCR. Similar to ablation of FBW7, CHIR increased the expression of VDR target gene, while it did not alter the expression of VDR mRNA, suggesting that GSK3s inhibitor and ablation of FBW7 increased the function of VDR through stabilizing VDR protein (Fig. 8D).

To determine the effect of FBW7 ablation in the presence of 1,25D, The SCC25 cells were transfected with *FBW7* or scrambled siRNA and treated with 1,25D. The expression of VDR was assessed by western blot. The ablation of FBW7 led to a slight reduction in total VDR levels in the presence of 1,25D (Fig. 8E). To further investigate potential effects of FBW7 ablation on the stability and function of VDR, SCC25 cells were transfected with *FBW7* or scrambled siRNA and treated with 1,25D. The expression level of VDR target gene *CYP24* was assessed by RT-qPCR. These assay showed that in the presence of 1,25D, FBW7 ablation does not increase,

rather reduces VDR function (Fig. 8F). To confirm the effect of 1,25D to prevent degradation of VDR through its phosphodegron, SCC25 cells were treated with CHIR and 1,25D. In agreement with previous results we observed that CHIR does not increase VDR function in the presence of 1,25D (Fig. 8F).

To determine the effect of FBW7 depletion on the VDR turnover in the presence of 1,25D, we measured the stability of the VDR by treating cells with cycloheximide. SCC25 cells were transfected with *FBW7* or scrambled siRNA and treated with 1,25D. Cycloheximide was applied for the times indicated in Fig. 8G. The results revealed that FBW7 stabilizes VDR in the presence of 1,25D (Fig. 8G). Altogether these results suggest that FBW7 regulates the turnover of the VDR in the presence of 1,25D, increasing its stability.

4.5. Discussion

In previous studies we concluded that VDR might induce its anti-proliferative effects by preventing MXD1 degradation and inducing c-Myc turnover through FBW7. Here, we observed that upon applying 1,25D to cells, FBW7 interaction with c-Myc increased whereas its interaction with MXD1 decreased. GST pull down assays showed the same pattern of interactions for VDR with c-Myc and MXD1. Since the GST pull-down assay is in vitro and an equal amount of protein is used in this assay, direct interaction could be measured compared to an in vivo system. In addition, this in vitro assay eliminates the probability of various modifications through different pathways induced by 1,25D. This data suggest that increased interaction between VDR and MXD1 in SCC25 cells treated with 1,25D may be due to the increased expression of VDR, but not to the increased interaction of ligand bound VDR with MXD1.

Although MXD1 lacks a canonical phosphodegron motif, FBW7 can interact with it and control its stability. Collectively, our results suggest that MXD1 and c-Myc might be phosphorylated through different signaling pathways to trigger FBW7 binding. We showed that a GSK3 inhibitor cannot stabilize MXD1. In contrast, a potential inhibitory target of staurosporine, can increase the levels of MXD1 protein to the same extent as 1,25D. Although we have not identified a potential kinase which can trigger MXD1 recognition by FBW7, these data provide evidence that regulation of c-Myc and MXD1 degradation occurs through different pathways. Further investigation is needed to determine the pathways that might trigger MXD1 degradation.

The expression of *FBW7* mRNA is not altered in the presence of 1,25D. However, the interaction of FBW7 protein with its substrates c-Myc and MXD1 is 1,25D dependent, as is the association of c-Myc and MXD1 with DNA. We demonstrated that FBW7 is recruited to the promoters of c-Myc target genes. Total FBW7 levels associated with promoter of these genes did not appear to be dependent on 1,25D. However, this did not reflect the underlying dynamics of its association with DNA-bound c-Myc and MXD1. Notably, ReChIP assays revealed that FBW7 associated with DNA-bound c-Myc and MXD1 decreased and increased, respectively, in the presence of 1,25D, consistent with the underlying patterns of c-Myc and MXD1 DNA binding.

The results demonstrate that besides c-Myc and MXD1, 1,25D attenuates the expression of multiple previously identified FBW7 oncogenic substrates including Cyclin E, c-Jun, AIB1 and MCL1, all important for tumorigenesis [359]–[361]. This effect of 1,25D could be rescued by ablation of *FBW7*. These results suggest the VDR and FBW7 might have numerous common target proteins. Therefore, we screened the proteome for FBW7 phosphodegron motifs to identify potential novel substrates. The screen identified approximately the same ratio of identified oncogenes and tumor suppressors. The effect of 1,25D on two of these FBW7 potential

target proteins, E2F1 and TCF7L2, revealed that treatment reduced their protein expression, providing another piece for our hypothesized cooperation of FBW7 and VDR. Furthermore, the result of proliferation assays revealed that 1,25D inhibits the proliferation of SCC25 cells up to 80%, and that this effect can be diminished up to four fold following the ablation of FBW7. This confirms our hypothesis that 1,25D-bound VDR possesses anti-proliferative effects by cooperation with FBW7.

The binding of the FBW7 to the VDR was shown to be 1,25D-dependent and VDR levels are reduced in the presence of 1,25D. Screening the sequence of the VDR revealed that there is a phosphodegron motif in the ligand binding domain in an unstructured region between helices 2 and 3. In addition, the VDR turnover in the presence of 1,25D is reduced by ablation of FBW7 expression. We suggested that this phosphodegron might mediate the interaction of VDR and FBW7. GST pull-down assays suggest that the VDR-FBW7 interaction is slightly reduced following application of 1,25D. Our data suggest that, unexpectedly the association of FBW7 with the VDR in the presence of 1,25D protects the VDR from degradation by an unknown mechanism.

In summary, we identified a new regulatory mechanism for FBW7 function through the 1,25D-bound VDR. We showed that 1,25D can regulate the interaction of FBW7 with substrate proteins. Furthermore, we showed that the anti-proliferative effect of 1,25D is attenuated in the absence of FBW7. Furthermore, we showed that FBW7 also affects VDR expression and function. These experiments provide several novel insights into the potential cancer-preventive actions of 1,25D.
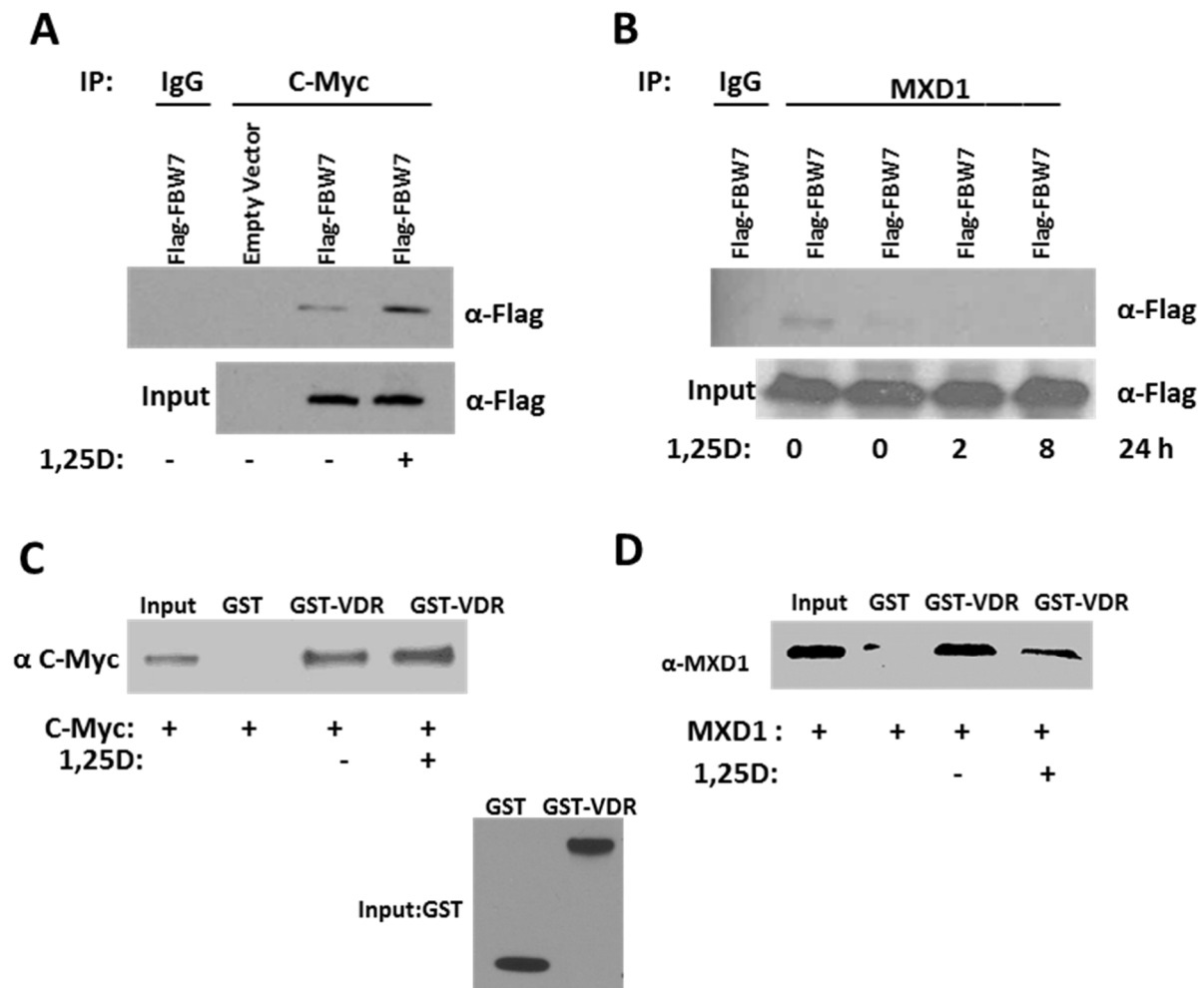
Figure 4.1. MXD1 and c-Myc directly interact with FBW7 and VDR, in 1,25D dependent manner.

Figure legend on the next page.

Figure 4.1. MXD1 and c-Myc directly interact with FBW7 and VDR, in 1,25D dependent manner.

A) Western blot analysis of Flag-FBW7 co-immunoprecipitated with IgG or c-Myc, following treatment of SCC25 cells with 1,25D. SCC25 cells were transfected with empty vector or Flage-*FBW7* and treated with 100 nM of 1,25D for 8 hours. c-Myc was immunoprecipitated from SCC25 cells lysate. The total lysate as "input" and immunoprecipitates were probed for Flag. **B)** Western blot analysis of Flag-FBW7 co-immunoprecipitated with IgG or MXD1, following treatment of SCC25 cells with 1,25D. SCC25 cells were transfected with empty vector or Flage-*FBW7* and treated with 100 nM of 1,25D for 2, 8, and 24 hours. MXD1 was immunoprecipitated from SCC25 cell lysate. The total lysate as "input" and immunoprecipitates were probed for Flag. The MXD1 bands in this experiment were weak, as the expression of MXD1 in non-treated cells is very low. **C)** Western blot analysis of c-Myc pulled down by GST or GST-VDR in the presence of vehicle or 1,25D; and in vitro translated c-Myc as input. BL21 bacteria were transformed with pGEX4T3 or pGEX-4T3-*VDR* and induced to express GST or GST fussed VDR. c-Myc protein was translated in vitro from pCDNA3.1-*c-Myc*. The bacterial lysates were used to pull down the in vitro translated c-Myc. **D)** Western blot analysis of MXD1 pulled down by GST or GST-VDR, in the presence of vehicle or 1,25D; and in vitro translated MXD1 as input. BL21 bacteria were transformed with pGEX4T3 or pGEX-4T3-*VDR* and induced to express GST or GST fussed VDR. MXD1 protein was translated in vitro from pCDNA3.1-*MXD1*. The bacterial lysates were used to pull down the in vitro translated MXD1. GST probed as a loading control.

A
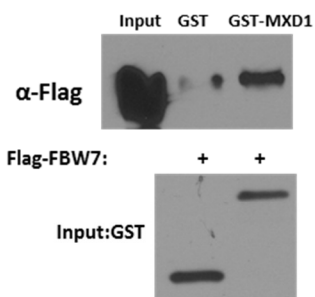
B

a: MCL1: **S**LPS**T**   P63: **S**VSQ**L**   KLF5: **TPDL**D**M**

b:

MAAAVRMNIQMLLEAAD**Y**LERREREAEHGY**A**SMLP**Y**NNKDRDALKRRNK**S**KKNN**SSS**R**S**T
HNEMEKNRRAHLRLCLEKLKGLVPLGPE**SS**RH**TTL**SLL**T**KAKLHIKKLEDCDRKAVHQIDQL
QREQRHLKRQLEKLGIERIRMD**S**IG**S**T**V**SSE**RS**D**S**DREIDVDVE**S**T**D**Y**L**TGDLDW**SSSS**VS
D**S**DERG**S**MQ**S**LG**S**DEG**Y**SS**T**SIKRIKLQD**S**HKAC

http://www.dabi.temple.edu/disphos/
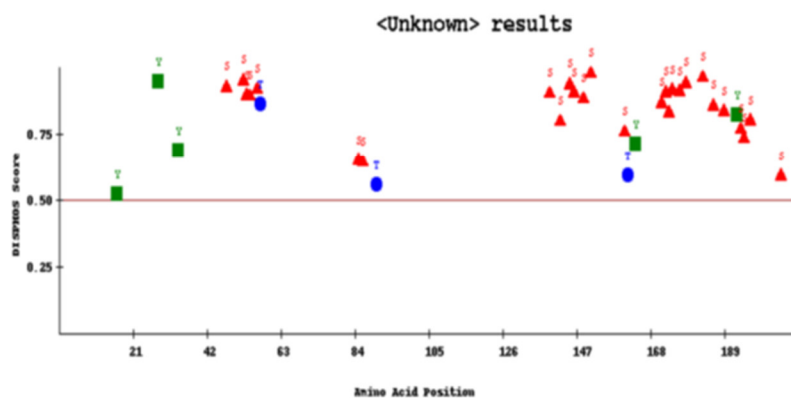
Figure 4.2. FBW7 interacts with MXD1.

Figure legend on the next page

Figure 4.2. FBW7 interacts with MXD1.

A) Western blot analysis of Flag-FBW7 pulled down by GST or GST-MXD1. BL21 bacteria were transformed with pGEX4T3 or pGEX-4T3-*MXD1* and induced to express GST or GST fussed MXD1. Flag-FBW7 protein was translated in vitro from pCDNA3.1-*Flag-FBW7*. The bacterial lysates were used to pull down the in vitro translated Flag-FBW7. GST probed as a loading control. **B**) a: non-canonical phosphodegrons, b: prediction of the phosphorylation probability of MXD1 residues by using http://www.dabi.temple.edu/disphos/
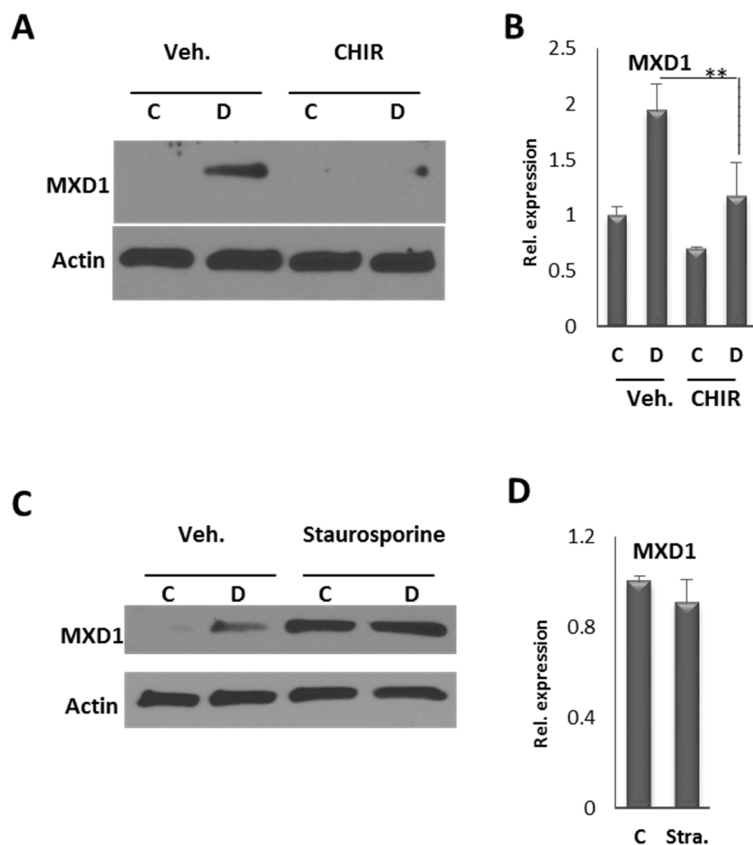
Figure 4.3. MXD1 phosphorylation for subsequent ubiquitination, in the absence of 1,25D, is through a kinase other than GSK3.

A) Western blot analysis of MXD1 in SCC25 cells following treatment with 1uM of CHIR (GSK3 inhibitor) and 100 nM of 1,25D for 24 hours. **B)** RT-qPCR analysis of MXD1 transcription in SCC25 cells following treatment with 1uM of CHIR and 100 nM of 1,25D for 24 hours. **C)** Western blot analysis of MXD1 in SCC25 cells following treatment with 2nM of staurosporine (potential PKC and some other kinases inhibitor) and 100 nM of 1,25D for 24 hours. **D)** RT-qPCR analysis of MXD1 transcription in SCC25 cells following treatment with 2nM of staurosporine and 100 nM of 1,25D for 24 hours. C: control, D: 1,25D treatment. **P≤0.01 as determined by one-way ANOVAs followed by Tukey's post hoc test for multiple comparisons.
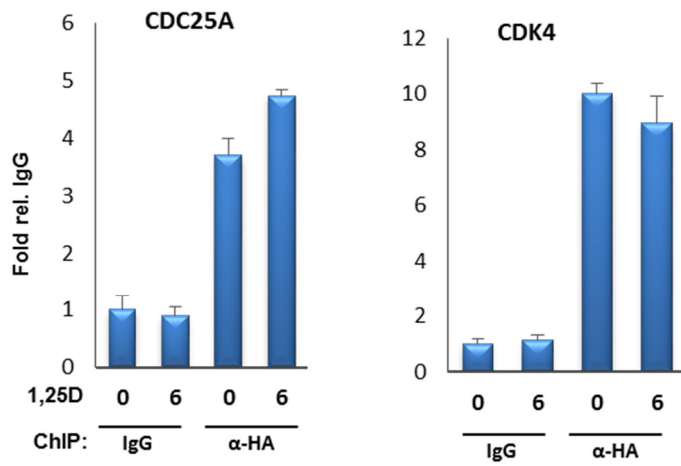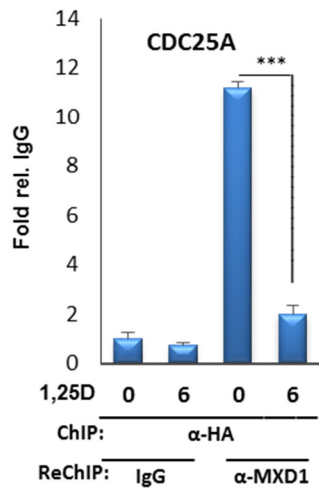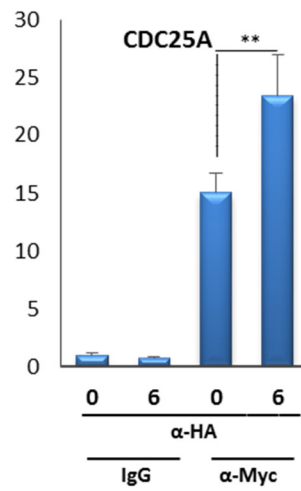
Figure 4.4. FBW7 binds to MXD1 and c-Myc on the promoter of target genes, in 125D dependent manner.

Figure legend on the next page.

Figure 4.4. FBW7 binds to MXD1 and c-Myc on the promoter of target genes, in 125D dependent manner.

A) Analysis of the HA-FBW7 recruitment to the E-box motif of promoter of c-Myc target genes, *CDC25A* and *CDK4*, by chromatin immunoprecipitation (ChIP) assay, in SCC25 cells following treatment with 100 nM of 1,25D. In the absence of proper antibody, a lentiviral vector was made to create stably expressing SCC25 cell line. For this purpose, the HA-*FBW7* cDNA was inserted into LeGO-iG2 lentiviral vector. **B**) Analysis of the HA-FBW7 and MXD1 co-recruitment to the E-box motif of promoter of c-Myc target genes, *CDC25A*, by Re-chromatin immunoprecipitation (Re-ChIP) assay, in SCC25 cells following treatment with 100 nM 1,25D. The first round of ChIP for HA-FBW7 was followed by second round of immunoprecipitation for MXD1. **C**) Analysis of the HA-FBW7 and c-Myc co-recruitment to the E-box motif of promoter of c-Myc target genes, *CDC25A*, by Re-chromatin immunoprecipitation (Re-ChIP) assay, in SCC25 cells following treatment with 100 nM 1,25D. The first round of ChIP for HA-FBW7 followed by second round of immunoprecipitation for c-Myc. ***$P \leq 0.001$, **$P \leq 0.01$ as determined by One-way ANOVAs followed by Tukey's post hoc test for multiple comparisons.

A

CDC25A

CDK4

Fold rel. IgG

1,25D   0   6   0   6   0   6   0   6
ChIP: α-HA   α-HA
ReChIP: IgG   α-VDR   IgG   α-VDR

B

	Input	GST	GST-VDR
α-Flag			
Flag-Con-FBW7:	+	+	+

C

	Input	GST	GST	GST-VDR	GST-VDR
α-Flag					
Flag-WD40:	+	+	+	+	+
1,25D:		-	+	-	+

Input: GST   GST   GST-VDR

D

Conserved Domain

N-(DD | FB | WD40)-C

DD: Dimerization Domain, FB: F-Box

Figure 4.5. FBW7 binds to VDR on the promoter of target genes, in 125D dependent manner.

Figure legend on the next page.

151
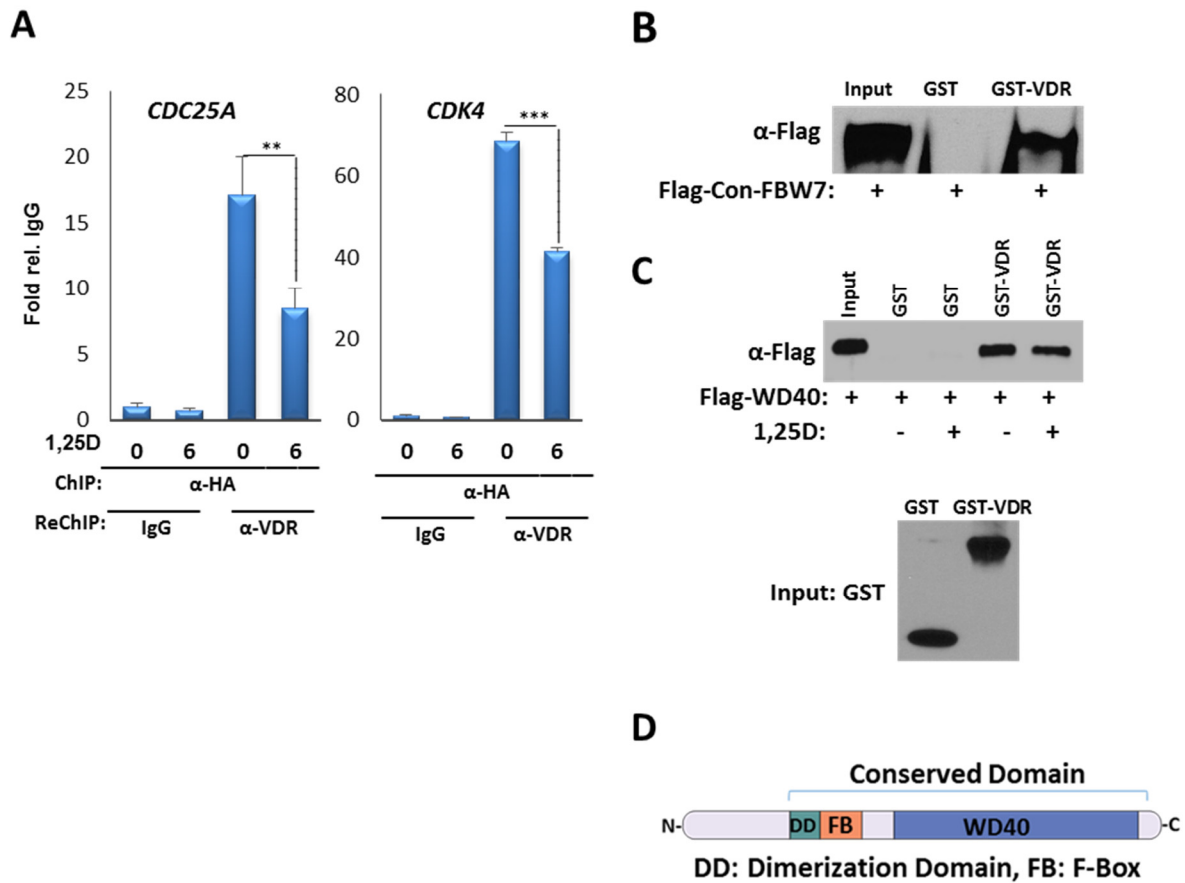
Figure 4.5. FBW7 binds to VDR on the promoter of target genes, in 125D dependent manner.

A) Analysis of the HA-FBW7 and VDR co-recruitment to the E-box motif of promoter of c-Myc target genes, *CDC25A* and *CDK4*, by Re-Chromatin Immunoprecipitation (Re-ChIP) assay, in SCC25 cells following treatment with 100 nM 1,25D. The first round of ChIP for HA-FBW7 was followed by second round of immunoprecipitation by VDR antibody. **B**) Western blot analysis of Flag-conserved sequence of FBW7 (FLAG-Con-FBW7) pulled down by GST or GST-VDR; in vitro translated FLAG-Con-FBW7 was used as input. BL21 bacteria were transformed with pGEX4T3 or pGEX-4T3-VDR and induced to express GST or GST fussed VDR. FLAG-Con-FBW7 protein was translated in vitro from pCDNA3.1-Flag-Con-FBW7. The bacterial lysates were used to pull down the in vitro translated Flag-Con-FBW7. *In vitro* translated FLAG-Con-FBW7 was probed as input. **C**) Western blot analysis of Flag-WD40 domain of FBW7 (FLAG-WD40-FBW7) pulled down by GST or GST-VDR in the presence of vehicle or 1,25D; *in vitro* translated FLAG-WD40-FBW7 was probed as input. **D)** The schematic representation of FBW7 domains. ***P≤0.001, **P≤0.01 as determined by One-way ANOVAs followed by Tukey's post hoc test for multiple comparisons.
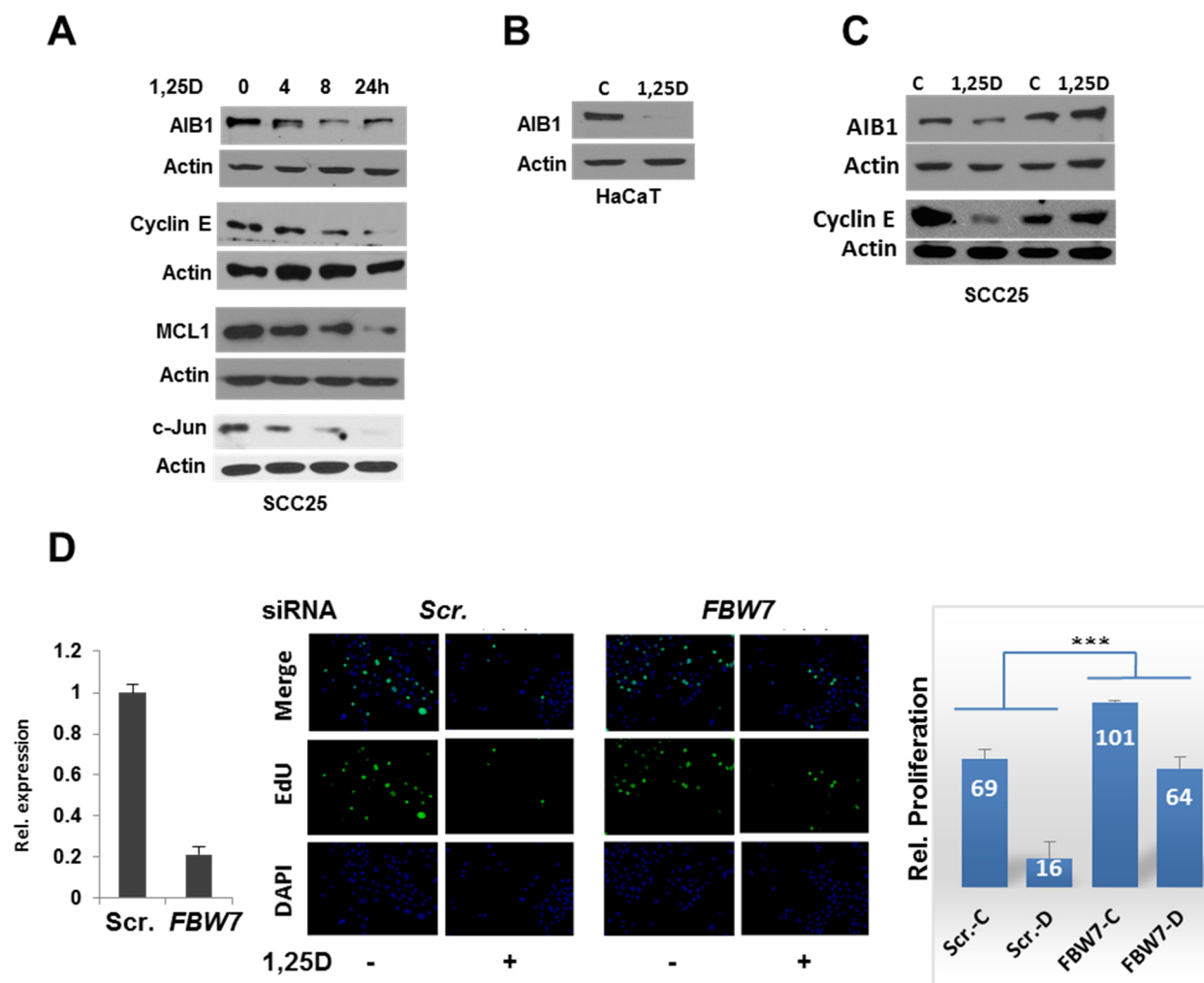
Figure 4.6. Multiple FBW7 target genes involved in cell cycle, are regulated by 1,25D.

Figure legend on the next page.

Figure 4.6. Multiple FBW7 target genes involved in cell cycle, are regulated by 1,25D.

A) Western blot analysis of AIB1, cyclin E, MCL1 and c-Jun levels in SCC25 cells following treatment with 100 nM of 1,25D for 4, 8, and 24 hours. **B)** Western blot analysis of AIB1 in HaCaT cells following treatment with 100 nM of 1,25D for 24 hours. **C)** Western blot analysis of AIB1 and cyclin E levels in SCC25 cells transfected with scrambled or *FBW7* siRNA and treated with vehicle or 100 nM of 1,25D. **D**, Left) RT-qPCR assay of *FBW7* mRNA expression after knockdown of its gene. **D,** middle panel) EdU cell proliferation assay in SCC25 cells transfected with scrambled or *FBW7* siRNA and treated with vehicle or 100 nM of 1,25D. **D**, right panel) the quantification of EdU cell proliferation assays. ***$P \leq 0.001$ as determined by One-way ANOVAs followed by Tukey's post hoc test for multiple comparisons.
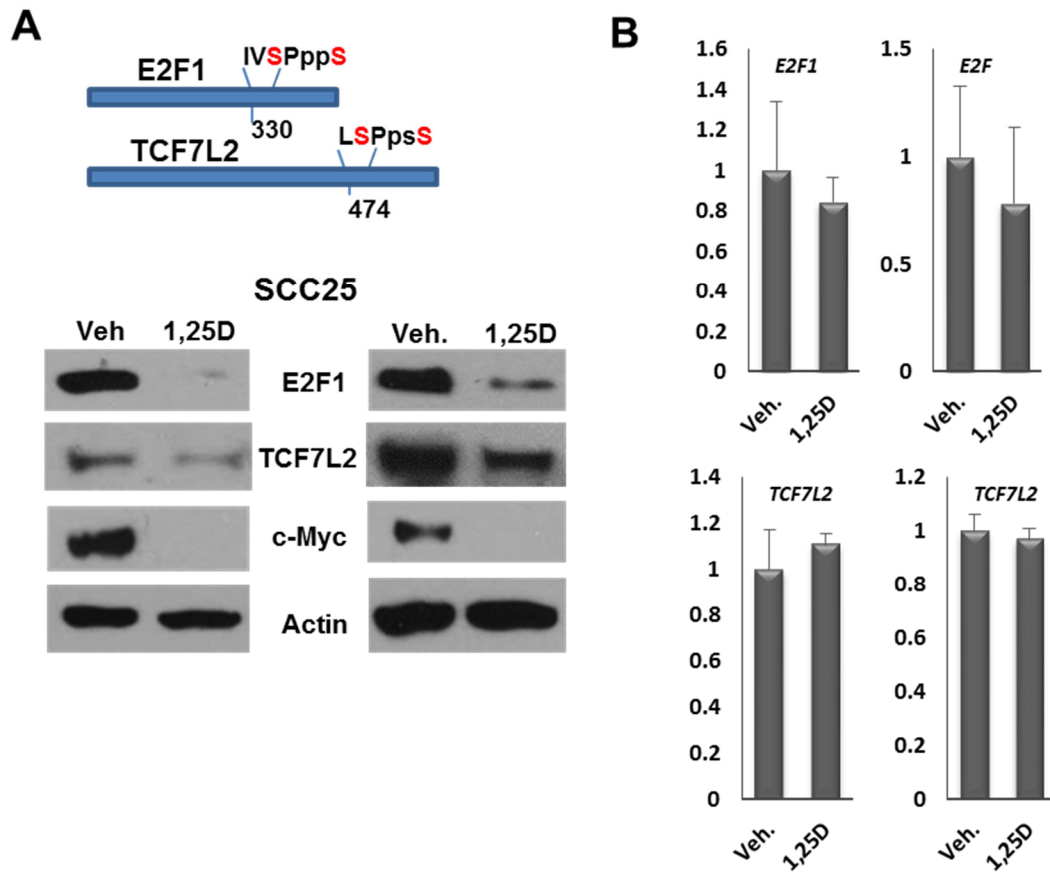
Figure 4.7. Effect of 1,25D on the potential novel FBW7 target proteins.

A, top panel) The schematic representation of the phosphodegron location on the E2F1 and TCF7L2. **A**, bottom panel) Western blot analysis of the E2F1 and TCF7L2 levels in SCC25 cells treated with vehicle or 100 nM of 1,25D. c-Myc and Actin were probed as controls. **B**) RT-qPCR analysis of the *E2F1* and *TCF7L2* transcription levels in SCC25 cells treated with vehicle or 100 nM of 1,25D.
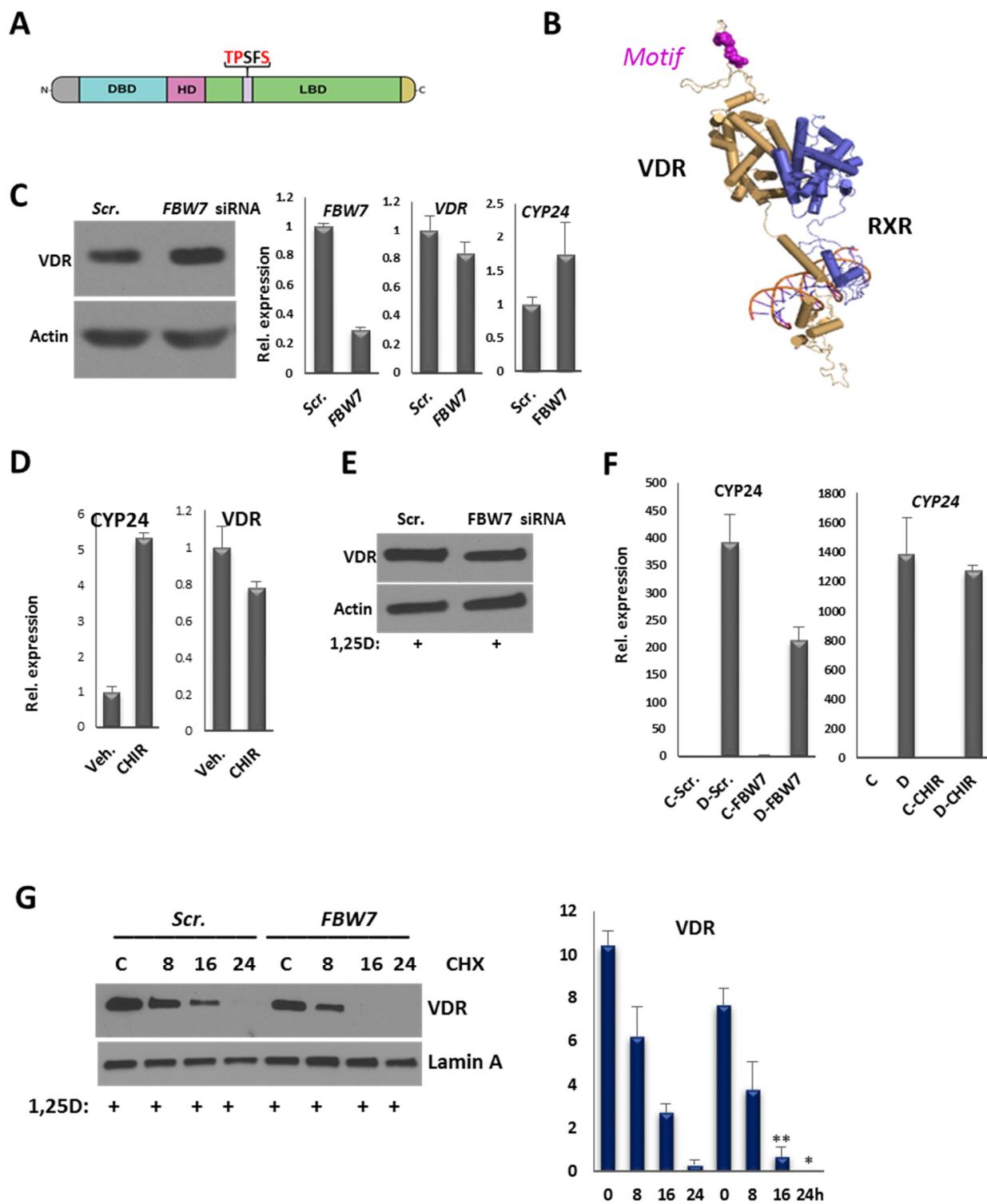
Figure 4.8. VDR is a target protein of FBW7 in the absence of 1,25D.

Figure legend on the next page.

Figure 4.8. VDR is a target protein of FBW7 in the absence of 1,25D.

A) The schematic representation of the phosphodegron location on the VDR. **B)** Tertiary structure of VDR:RXR showing the phosphodegron location on the VDR structure. The VDR/RXR tertiary structure was generated by Dr. Natacha Rochel at the IGBMC in Illkirch, France. **C,** left panel) Western blot analysis of VDR from SCC25 cells transfected with scrambled or *FBW7* siRNA, **C,** right panel) RT-qPCR analysis of *FBW7*, *VDR* and *CYP24* transcription from SCC25 cells transfected with scrambled or *FBW7* siRNA. **D)** RT-qPCR analysis of *CYP24* and *VDR* transcription from SCC25 cells following treatment with 1 uM CHIR. **E)** Western blot analysis of VDR from SCC25 cells transfected with scrambled or *FBW7* siRNA and treated with 100 nM 1,25D for 24 hours. **F)** RT-qPCR analysis of *CYP24* transcription from SCC25 cells following knockdown of *FBW7* or treatment with 1 uM CHIR and treatment with 100 nM 1,25D. C stand for vehicle and D stand for 1,25D. **G,** left panel) Western blot analysis of VDR in protein stability assay. SCC25 cells were transfected for *FBW7* or scrambled siRNA and treated with 100 nM 1,25D. 4 µg/ml of Cycloheximide were added for 8, 16 and 24 hours. Lamin-A was used as an internal control. **G**, right panel) The quantification of western blot analyses presented in left panel.

$**P \leq 0.01$, $*P \leq 0.05$ as determined by One-way ANOVAs followed by Tukey's post hoc test for multiple comparisons.

4.6. Materials and Methods

4.6.1. Cell Culture

SCC25 cells were obtained from the American Type Culture Collection (ATCC) and cultured in DMEM/F12 (319-085-CL, Multicell) supplemented with 10% FBS. HaCaT cells (gift from Dr. Lebrun's lab) were cultured in DMEM (319-005-CL, Multicell) supplemented with 10% FBS. SCC25 cells with stable expression for HA-FBW7 were generated using LeGO-iG2-HA-*FBW7*. HEK 293-T17 (gift from Dr. Pelletier's Lab) were cultured in DMEM (319-005-CL, Multicell) supplemented with 10% FBS.

4.6.2. Reagents

1α,25-Dihydroxyvitamin D3 (BML-DM200) was purchased from enzolifesciences, Staurosporine (S5921) and cycloheximide (C7698) were purchased from Sigma and CHIR 99021(4423) was purchased from Tocris.

4.6.3. Plasmid

In this study following constructs were generated: pcDNA 3.1-*MXD1*, pcDNA 3.1-*MYC*, pcDNA 3.1-Flag-*FBW7*, pcDNA 3.1-Flag-Con-*FBW7* (containing conserved part of FBW7, dimerization domain and WD40 domain), pcDNA 3.1-Flag-WD40-*FBW7*(containing WD40 domain of FBW7), pGEX-4T3-*MXD1*, pGEX-4T3-*VDR*, and LeGO-iG2-HA-*FBW7*.

4.6.4. FBW7 knockdown

SCC25 cells were transfected with SMARTpool: ON-TARGETplus FBXW7 siRNA L-004264-00-0005 or scrambled siRNA (Dharmacon) for 24 hours, using Pepmute transfection reagent (SL100566) from signagen.

4.6.5. RT-qPCR

Quantitative RT-PCR was performed with SsoFast-EvaGreen real-time PCR kit (Bio-Rad). Expression was normalized to the expression of GAPDH. Primer pairs used for RT-PCR are listed in section 4.6.12.

4.6.6. Immunoprecipitation and Western blot analysis

Cells were lysed with a lysis buffer (20 mM Tris, pH 7.5, 100 Mm NaCl, 0.5% Nonidet P-40, 0.5mM EDTA, 0.5 mM phenylmethylsulfonyl fluoride). 4 ng anti-c-Myc (D84C12, cell signaling) or MXD1(c-19, Santa Cruz) Antibodies were pre-bound for 2 hours to protein A agarose beads, then was washed with PBS plus 5% BSA and added to the lysate, followed by immunoprecipitation overnight. Protein A agarose beads were then washed five times with washing buffer (20 mM Tris, pH 7.5, 200 Mm NaCl, 1% Nonidet P-40, 0.5mM EDTA, 0.5 mM phenylmethylsulfonyl fluoride) and processed for Western blotting, performed with standard protocols. The following antibodies were used for western blot analysis: VDR (H-81), c-Myc (9E10), VDR (D-6), MXD1(c-19), HA (Y-11), c-Jun (H-79), Cyclin E (M-20), TCF4L2 (H-125) from Santa Cruz, AIB1 (5E11), E2F1 (3742), and c-Myc (D84C12) from cell signaling, Flag (M2) from sigma, and Lamin-A (Gift from Dr. Stochaj's lab).

4.6.7. GST pull down assay

GST pull down assays were performed using the MagneGST Pull-Down System (Promega) according supplier's instruction. BL21 bacteria were transformed with appropriate pGEX4T3 constructs and induced to express GST or GST fussed proteins. The total lysates of bacteria were used to pull-down in vitro translated proteins. The Pulled-Down proteins were analyzed by western blot assay.

4.6.8. ChIP and Re-ChIP assays

ChIP assays were performed as described previously[363] . DNA fragments were purified with a PCR purification kit (Qiagen) and were analyzed by SsoFast-EvaGreen real-time PCR. Anti-HA (Y-11) from Santa Cruz was used for ChIP. For re-ChIP assays, HA-FBW7 immunocomplexes were eluted by adding 40µl 10mM DTT for 30 min at 37 C. Supernatants were diluted 1:20 in dilution buffer (150 mM NaCl, 1% Triton X-100,2mM EDTA and 50 mM Tris-HCl, pH 8), and re-ChIPs were performed using anti-c-Myc (9402-Cell signaling), anti-MXD1(c-19- Santa Cruz) or anti- VDR (D-6- Santa Cruz) antibodies. Primer pairs used for ChIP assays are listed in section 4.6.12.

4.6.9. Proliferation assays

Proliferation assay were performed by using Click-iT EdU Alexa Fluor 647 high-throughput imaging assay kit (Invitrogen) according to the manufacturer's protocol. SCC25 cells were transfected with FBW7 or scrambled siRNAs and treated with 1,25D for 24 hours. Cells were incubated with Alexa-EdU for 1 hour and fixed with 3.7% formaldehyde. DAPI was used to stain the nucleus. Images were captured by High-content screening (HCS) microscope using ImageXpressMicro program and analyzed with MetaXpress.

4.6.10. Statistical Analysis

All experiments are representative of 3-5 biological replicates. Unless otherwise indicated in the figures, statistical analysis was conducted using the program SYSTAT13 by performing one-way analysis of variance (ANOVA) followed by the Tukey test for multiple comparisons as indicated: $*P{\leq}0.05$, $**P{\leq}0.01$, $***P{\leq}0.001$.

4.6.11. Tertiary structure generation

The VDR/RXR tertiary structure was generated by Dr. Natacha Rochel at the IGBMC in Illkirch, France.

4.6.12. Primers
Primers for qPCR:

MXD1-FORWARD	5'-ACCTGAAGAGGCAGCTGGAGAA-3'
MXD1-REVERSE	5'-AGATAGTCCGTGCTCTCCACGT-3'
FBW7-FORWARD	5'-CAGCAGTCACAGGCAAATGT-3'
FBW7-REVERSE	5'-GCATCTCGAGAACCGCTAAC-3'
VDR-FORWARD	5'-CGCATCATTGCCATACTGCTGG-3'
VDR-REVERSE	5'-CCACCATCATTCACACGAACTGG-3'
CYP24A1-FORWARD	5'-GCTTCTCCAGAAGAATGCAGGG-3'
CYP24A1-REVERSE	5'-CAGACCTTGGTGTTGAGGCTCT-3'

Primers for ChIP:

CDC25A-FORWARD	5'-GAGAGATCAGGCCAGGAAAC-3'
CDC25A-REVERSE	5'-CTCTCCCGCCCAACATTC-3'
CDK4-FORWARD	5'-GAGCGACCCTTCCATAACCA-3'
CDK4-REVERSE	5'-GGGCTGGCGTGAGGTAAGT-3'

Chapter 5

Discussion

5.1. Major findings

This study has revealed a novel mechanism of regulation of the c-Myc/MXD1 network by 1,25D signaling, which clarifies the molecular basis for at least a part of its antiproliferative effects. We demonstrated that 1,25D regulates both arms of c-Myc/MXD1 signaling to suppress cell cycle progression. We showed that 1,25D suppresses c-Myc expression, whereas it promotes that of MXD1. In addition, our results reveal that 1,25D affects the turnover of c-Myc and MXD1 through FBW7. Interestingly, in FBW7-ablated cells, high levels of MXD1 protein were observed, which suggests that FBW7 turns over both arms of c-Myc/MXD1 network. In addition, we showed that 1,25D-bound VDR induces the degradation of multiple FBW7 target proteins. Our results demonstrate that 1,25D-mediated reduction in cell proliferation can be rescued by ablation of FBW7. Screening the proteome for phosphodegron motifs revealed that VDR contains a canonical one in a "linker" region of its binding domain. In addition, our results demonstrated that FBW7 triggers VDR degradation in the absence of 1,25D, but not in its presence. Altogether, our data suggest that VDR and FBW7 cooperate to repress cell cycle progression and regulate each other's function.

5.2. 1,25D signaling regulates c-Myc expression and function by repressing its transcription and inducing its turnover through FBW7.

To investigate the anti-proliferative effects of 1,25D, we examined its effect on the expression and function of c-Myc, one of the main regulator of cell cycle progression. Since c-Myc overexpression has been involved in the development of HNSCC [334], we used human SCC25 HNSCC cells as a model to investigate mechanisms of 1,25D anti-proliferative effects [335], [336].

First, we determined the effect of 1,25D on c-Myc function by assessing the expression of *CCND2*, *CDK4*, and *CDC25A*, which are implicated in regulating cell cycle [200], [321], in SCC25 cells and primary human keratinocytes. 1,25D signaling repressed the expression of these genes. Coincidentally, the recruitment of c-Myc to the E-region of the corresponding promoters declined in SCC25 cells. This confirms that reduction observed in the expression of c-Myc target genes are due to the decline in c-Myc activity on their promoters. To investigate the reason of the declined c-Myc association with those E-regions, we assessed *MYC* transcription and protein expression. In agreement with previous studies [309], [310], we observed a gradual reduction in its transcription over 24 hours of 1,25D treatment, in SCC25 cells, primary human keratinocytes and HL60 cells, which were quite relevant for the project as the *MYC* gene is amplified [326].

The reduction in the c-Myc protein levels were substantial in these three cell lines and it almost disappeared in the SCC25 cells, which suggested that 1,25D might affect the c-Myc protein stability. Protein stability assays revealed that 1,25D signaling affects c-Myc turnover through an unknown mechanism. In addition, we observed that in VDR-ablated cells, c-Myc is stabilized and 1,25D cannot affect its turnover, which shows that the presence of VDR is essential in 1,25D signaling for affecting the c-Myc stability. Since c-Myc plays a crucial role in cell cycle progression, following transcription it is under intense control at the mRNA and protein levels. c-Myc is subject to a variety of post translational modifications and its half-life is short [119] [138], [369]. Several different mechanisms control its mRNA and translation as well as protein stability [117], [138]. We chose three of these pathways to examine whether they are implicated in the effects of 1,25D signaling converging on c-Myc. One of them was ELAVL1 (HuR) which is an mRNA binding protein. It binds to the 3′-untranslated region of *MYC* mRNA and induces recruitment of let-7/RISC which is an miRNA system to suppress its translation [117]. Ablation

of HuR in SCC25 cell, did not rescue the effect of 1,25D on c-Myc. Further, we knocked down SKP2, which could trigger c-Myc degradation. In fact, SKP2 has a dual effect on c-Myc, it also can act as an activator for c-Myc [157]. SKP2 ablation also did not affect the reduced c-Myc stability induced by 1,25D. In addition, We knocked down the *FBW7*, which is one of the main inducers of c-Myc degradation [327]. Interestingly, we observed that the effect of 1,25D on the c-Myc stability were mediated by FBW7 and its ablation rescued the 1,25D-induced diminished c-Myc stability, which suggests a cooperation between 1,25D signaling and FBW7 to induce c-Myc turnover.

We observed a primary peak of increased association of c-Myc and VDR upon treatment of cells with 1,25D, which followed by a gradual decrease over 24 hours, which could be the result of reduced c-Myc levels. Comparing to input, the result showed that the direct interaction of c-Myc with 1,25D was increased in the presence of 1,25D. In addition, co-recruitment of c-Myc and VDR to E-box region of c-Myc target genes declined after 24 hours of 1,25D exposure, which might be due to the profound loss of c-Myc and/or dissociation of c-Myc from DNA. In addition, previous studies have shown that following phosphorylation of Thr58, FBW7 triggers c-Myc degradation. On the other hand, Pin1 isomerase also recognize the Tre58 and switches the Proline 63 from cis to trans. This leads to dissociation of c-Myc from DNA [92]. Interestingly, here we observed that degradation of c-Myc is coincided with its DNA dissociation, which is in accordance with previous findings.

VDR as a transcription factor, generally forms a heterodimer with RXR to bind VDREs in the promoter or distal regions of target genes. However, recent studies have shown multiple mechanisms through which VDR associates with other classes of transcription factors to regulate transcription [328], [370]–[372]. For example, it can be tethered to other transcription factors

[33]. Our data showed that VDR recruitment to the E-box motif of c-Myc target genes increased rapidly following treatment with 1,25D which followed by a gradual decline. Reanalyzing the VDR and c-Myc peaks identified by ChIPseq from related lymphoblastoid cell lines [328], [329] revealed an overlap between approximately one half of the VDR binding sites identified in the absence of 1,25D (269/532), and approximately one quarter of those (952/4,015) in the presence of 1,25D, with high fidelity c-Myc sites. While this type of comparison is not as definitive as ChIPseq studies performed in parallel in the same cell line, it nonetheless supports our experimental findings that DNA-bound c-Myc and the VDR do associate *in vivo*. Altogether, these results suggest that VDR associates with c-Myc and induces its turnover on the promoter of target genes.

Antiproliferative effects of 1,25D have been shown in LNCaP cells (human prostate cancer cell line) [373]. We found that c-Myc protein levels are elevated in VDR-ablated LNCaP and SCC25 cells. This increase was due to the increased *MYC* transcription, rather than increased stability, which suggests that the presence of VDR in 1,25D signaling is essential for regulating the c-Myc turnover. It has been shown that β-catenin, a transcription factor downstream of oncogenic Wnt signaling pathway, upregulates the c-Myc transcription [374], [375]. In addition, 1,25D is a multilevel regulator of β-catenin [376], [377]. 1,25D-bound VDR interacts with β-catenin and inhibits its interaction with TCF transcription factor on the promoter of target genes while promoting CDH1 expression. The latter codes for E-cadherin, which binds to β-catenin and inhibits its function. Of note, 1,25-bound VDR down-regulates the β-catenin induced transcription, which results in cell cycle arrest in keratinocytes [378]. In agreement with previous studies[377], [378], our results showed that VDR ablation increased the recruitment of β-catenin to the c-Myc promoter and increased c-Myc transcription, regardless of the presence of 1,25D.

Further, simultaneous ablation of both VDR and β-catenin repress the c-Myc transcription, regardless of the presence of 1,25D. This shows that β-catenin induces c-Myc transcription, while 1,25D-bound VDR inhibits its activity.

We examined the effects of 1,25D signaling on c-Myc expression in wild type and *Vdr* null mice, to confirm our *in vitro* findings. *Vdr* null mice phenotypically resemble patient with hereditary vitamin D-dependent rickets type II [379]. The skin of these mice is hyper-proliferative and displays disruption of hair follicles [380]. As a control for this experiment we used basal-like subtype of breast cancer, in which c-Myc is overexpressed [218]. We observed that c-Myc is overexpressed in multiple *Vdr* null mice tissues, including skin, colon, heart, muscle, and brain. Furthermore, topical 1,25D application on wild type mice skin downregulated c-Myc at the site of application. In addition, we investigated for the expression of c-Myc target gene (Setd8) after application of 1,25D. Setd8 is a histone methyltransferase which is required for mitosis in cultured cells *in vitro*, but its role in tissues is uncovered [333]. Immunohistochemistry assays revealed a reduction in the expression of Setd8 in the skin of wild type mice after 1,25D application. Altogether, we found that 1,25D signaling suppresses *MYC* transcription, by suppressing β-catenin function. In addition, we revealed that 1,25D signaling induces c-Myc turnover through SCF^{FBW7} E3 ligase.

5.3. 1,25D signaling regulates MXD1 expression and function by promoting its transcription and inhibiting its turnover through FBW7.

In chapter 2, we investigated the effect of 1,25D signaling on the oncogenic arm of c-Myc/MXD1 network. As a c-Myc antagonist, MXD1 plays an essential role in suppressing proliferation. Recently it has been shown that in gastric cancer cells, miRNA-19a/b induced invasion and metastasis by targeting the MXD1[381].This study demonstrated that over

expression of MXD1 resulted in declined c-Myc and miRNA-19a/b levels, which rescued the malignant phenotype in mice [381]. We observed that 1,25D signaling represses *MYC* expression, which led us to examine its effects on *MXD1*. It has been shown that *MXD1* is expressed in a reverse fashion to *MYC* [345]. In agreement with this finding, we observed an enhanced *MXD1* transcription in the presence of 1,25D signaling and lower *MYC* expression. In addition, MXD1 protein levels substantially increased upon 1,25D treatment. Generally in proliferating cells, c-Myc is highly expressed, whereas MXD1 is poorly or not at all expressed [249]. Of note, the basal expression of MXD1 in primary human keratinocytes was higher compared to HL60 or SCC25 cells, reflective of their higher differentiation status. In SCC4 and SCC9 which are resistant to 1,25D signaling [336], we did not observe any MXD1 protein expression. In brief, our data showed that MXD1 levels in cancerous cells and 1,25D signaling can substantially increase its expression. In protein stability assays, we observed that 1,25D signaling enhanced the MXD1 stability. Since 1,25D-bound VDR affects c-Myc stability through FBW7, we investigated the possibility of FBW7 effect on MXD1. Interestingly, we observed that in the FBW7 ablated cells, MXD1 protein levels were enhanced and its stability increased. Since FBW have been known as a tumor suppressor and its identified substrates mostly are oncogenes [293], it was unexpected to observe these results. The other reason that these results were unanticipated is that MXD1 lacks the FBW7 recognition phosphodegron which is composed of T/S-P-X-X-T/S/E [351]. However, some of its identified substrates are tumor suppressors such as p63 [348] and KLF2 [382] or hold both oncogenic and tumor suppressor effects such as KLF5 [383]. Thus, we hypothesized that FBW7 regulates the MXD1 stability through another intermediate factor, or FBW7 could recognize MXD1 through an unknown phosphodegron. We examined these hypotheses in the chapter 4. Further, we observed that in the FBW7-ablated

cells, 1,25D signaling has no effects on the stability of the MXD1. In fact, in the absence of FBW7, MXD1 is stabilized with no further increase by 1,25D. This suggests that the total effect of 1,25D signaling on MXD1 stability is only through FBW7.

Several c-Myc target genes, main regulator of cell cycle progression (e.g. ND2) or important for cell proliferation (TERT), have been shown to be suppressed by MXD1 [250], [251] suggesting that its expression can result in a proliferative block. Our results revealed that, in contrast to c-Myc, recruitment of MXD1 and its cofactors to the promoter of c-Myc target genes was enhanced over 24 hours of 1,25D treatment. We investigated the binding of MXD1 for the exact E-box motif that we tested for c-Myc recruitment at the same target genes: *CDC25*, *CDK4*, and *CCND2*. The observed increase shows that 1,25D signaling replaces the c-Myc/MAX with MXD1/MAX. In addition, it has been demonstrated that overexpression of MXD1 can arrest the cells in S phase, which cannot be rescued by c-Myc overexpression[384]. This phenomenon suggests that the affinity of MXD1 to the MAX might be greater than that of c-Myc. Thus, 1,25D-induced MXD1 expression can be even more effective in cell cycle arrest, than the 1,25D-dependent reduction of c-Myc. In addition, co-immunoprecipitation assays revealed that co-recruitment of MXD1 and VDR was augmented over 24 hours of treatment. We also observed a gradual increase in the association of VDR and MXD1 over 8 hours in the same conditions. Of note, MXD1 protein levels are higher following treatment with 1,25D, therefore, increased association between VDR and MXD1 could be due to this increased MXD1 protein levels. In addition, after 24 hours of treatment, we have a substantial amount of DNA-bound MXD1, which can enhance the observed co-recruitment of VDR-MXD1 to the DNA. Next we decided to confirm our *in vitro* results in an *in vivo* system. It has been shown that disruption of *MXD1* in mice lead to defects in cell-cycle withdrawal during the late stage of myeloid differentiation

[385] suggesting that it is essential for differentiation. We observed that topical application of 1,25D on the mice skin, increased the MXD1 expression in wild type mice but not *Vdr* null mice.

Altogether, our results showed that in contrast to c-Myc, 1,25D upregulates MXD1 expression and stability, which triggers the replacement of c-Myc/MAX activator to MXD1/MAX suppressor in the promoters of genes implicated in cell cycle progression. This switch from activator to suppressor leads to cell cycle exit. In addition, we demonstrated that FBW7 participates in the turn-over of both arms of this network.

5.4. The 1,25D-bound VDR cooperates with FBW7 to inhibit proliferation.

In previous chapters we revealed that 1,25D signaling affects c-Myc and MXD1 stability through SCF^{FBW7} E3 ligase. We demonstrated that 1,25D induces the turnover of c-Myc through FBW7, whereas it inhibits the FBW7-induced degradation of MXD1. These results suggest that 1,25D-bound VDR in cooperation with FBW7, affects the c-Myc and MXD1 stability. Strictly speaking, it regulates the function of FBW7 to select the right substrate, in order to suppress the cell cycle progression. To verify this hypothesis, we performed co-immunoprecipitation assays in order to show the alterations in binding preferences of FBW7 to c-Myc and MXD1. Interestingly, we discovered that 1,25D signaling induced interaction between Flag-FBW7 and c-Myc, whereas it attenuates that between Flag-FBW7 and MXD1, suggestive of the regulatory role of 1,25D signaling on FBW7. Since the basal expression of MXD1 extremely low in the cells [249], western blot analyses for these assays showed a very faint western blot band in untreated cells. Further investigation revealed that in GST-pull down assays, VDR shows the same pattern of interactions with c-Myc and MXD1 as FBW7. In previous chapters we showed that there was a substantial increase in MXD1 protein levels upon 1,25D treatment. We also showed that association between VDR and MXD1 increased slightly after 1,25D treatment. Here

we investigated the effects of 1,25D on the interaction of VDR with c-Myc and MXD1 by adding vehicle or 1,25D to the GST-pulldown assays. These assays showed that in fact the interaction between MXD1 and VDR decreased after 1,25D treatment.

We identified MXD1 as a new substrate for FBW7. Previous studies have shown that it can be ubiquitinated through an unknown E3 ligase [263] and degraded by the proteasome machinery [346]. For example, c-IAP1 triggers MXD1degradation [260] and interferes with its anti-proliferative actions [249]. A previous study showed that phosphorylation of Ser145 residue trigger MXD1 degradation [263]. In our study, GST-Pull down assays revealed that FBW7 interacts with MXD1. Since, in GST-Pull down assay we did not used whole cell lysate and used the *in vitro* translated FBW7 and bacterial expressed GST-MXD1, we might conclude that interaction between FBW7 and MXD1 is direct and degradation of MXD1 is not through an intermediate factor. We are performing further studies to identify the exact motif within MXD1 recognized by FBW7.

We also searched for potential kinases that phosphorylate MXD1 and trigger its degradation. Various studies showed that FBW7 generally recognizes the residues which are phosphorylated by GSK3s [93], [349], [386]. GSK3s are proline-directed kinases, which can also phosphorylate Thr or Ser residues in close proximity to another phosphorylated residue termed "primed" site [352], [387]. Despite lack of a proper phosphorylation site for GSK3s. we still investigated such a possibility by treating SCC25 cells with a GSK3s inhibitor (CHIR 99021). As expected, we found that GSK3s do not trigger MXD1 degradation. CHIR 99021 decreased the levels of MXD1 protein, which might be due to the decreased MXD1 transcription as assessed by RT-qPCR. Next, we searched for a kinase inhibitor that acts as an antagonizer for MXD1 function. MXD1 is a transcription repressor which acts as an anti-proliferative and anti-apoptotic factor

[249]. We found the staurosporine, which is an apoptotic inducer and also inhibits several kinases which act in favor of certain oncogenic pathways [388], [389]. Interestingly, we discovered that it enhances the basal MXD1 protein levels to the same levels seen in 1,25D- treated cells, without affecting its transcription, which suggests that it inactivates the kinase that triggers MXD1 degradation. Staurosporine inhibits a series of kinases of which we tested AKT, PKCZ, PKCI, S6K, PKA, PKG and PKCA, using siRNA or specific inhibitors. We found that none of these kinases trigger the MXD1 degradation (data not shown). We are currently performing further research to investigate other kinases, which might phosphorylate MXD1 and trigger its degradation.

We observed that recruitment of FBW7 to the promoters of c-Myc target genes is not 1,25D-dependent. Its association with c-Myc on these promoters increased, however, but decreased with MXD1 following 6 hours of 1,25D treatment, which is in accordance with our Co-IP results. This together with the fact that FBW7 expression is not altered in the presence of 1,25D (data not shown), suggests that the function of FBW7, rather than its expression, is regulated by 1,25D. We revealed that besides c-Myc and MXD1, multiple identified FBW7 target proteins involved in cell cycle progression, such as cycline E, c-Jun, MCL1 and AIB1, are regulated by 1,25D signaling, which provides another evidence for our hypothesis that VDR and FBW7 acts cooperatively to inhibit the cell cycle progression. Various studies have shown the anti-proliferative effects of 1,25D [373], [390]–[393]. We investigated the effect of 1,25D signaling in FBW7-deficient cells, where it reduced cell proliferation up to 80%. Interestingly, we found that the anti-proliferative effect of 1,25D was attenuated in FBW7 ablated cells. We screened the proteome to find candidates containing phosphodegron motifs and identify potential FBW7 substrates. We discovered numerous oncogenes and tumor suppressors possess the canonical

phosphodegron, from which We selected TCF7L2 (a transcription factor which acts together with β-catenin in metabolic pathways [394], [395]) and E2F1 (a transcription factor which promotes cell proliferation [396]) and investigated the effect of 1,25D on them. Interestingly, we found that 1,25D signaling attenuated their expression at the protein level, but not at the mRNA level.

In GST-pull down assays, we showed that VDR interacts with FBW7. Searching the VDR sequence for FBW7 recognition sites, we found a canonical phosphodegron motif which is located in the "linker" region of its LBD binding domain. It has been shown this region is not involved in ligand binding, dimerization and transactivation by VDR [397]. We observed that VDR interacts with FBW7 WD40 domain which does not contain dimerization sequence. Suggesting that VDR can interact with monomeric FBW7. It has been reported that dimerization for FBW7 is required when the substrate possesses only one negative charge in its phosphodegron, therefore dimerization of FBW7 is needed for stable association. Having another phosphorylated residue (pT or pS) or a negative charge (E/D) at the +4 position of the main phosphorylated residue in the phosphodegron provides a high affinity binding site for FBW7. In this case, FBW7 dimerization is not essential for interaction [398]. This implies that both Ser residues in VDR phosphodegron are phosphorylated. Since the VDR phosphodegron is located in an unstructured motif, it is possible to be phosphorylated in both Ser residues. Interestingly, we observed attenuated VDR and FBW7 interaction in the presence of 1,25D in GST-pulldown assays. We also showed that the association of VDR and FBW7 on the promoter of c-Myc target genes declined following 6 hours 1,25D treatment. Our results demonstrate that in the absence of 1,25D, VDR protein levels increased in FBW7-deficient cells, without affecting VDR transcription. However, in the presence of 1,25D, ablation of FBW7 not only does not stabilize

VDR protein, but it reduces VDR stability through an unknown pathway. These results together with the fact that VDR transcription is not altered (data not shown, and [399]) but its protein levels substantially increased after treatment with 1,25D, suggest that FBW7 probably interacts with VDR through its phosphodegron which is located in the linker region of LBD. In addition, binding of 1,25D to the LBD of VDR probably disturbs FBW7 binding to the phosphodegron motif. We are performing further studies to address the FBW7 regulatory effects on VDR. Together, these observations showed that FBW7 and VDR have mutual overlapping regulatory effects on each other.

5.5. General Conclusions

Our work defines a new regulatory pathway of 1,25D and VDR on transcription and protein stability of c-Myc and MXD1 to induce cell cycle arrest. We have demonstrated a novel regulatory role of 1,25D and VDR in cooperation with FBW7, on protein stability, which could be considered as a new non-genomic function of 1,25D-bound VDR. However, the molecular basis of this cooperation remains to be characterized. In addition, we have provided evidence for the regulatory effects of FBW7 on VDR protein stability. Further investigations are required to fully understand the mutual regulatory network of FBW7 and VDR. Answers to questions like: how does VDR regulate the FBW7 function and prompts recognition of the right substrate and how does FBW7 induce VDR degradation in the absence of 1,25D but not in its presence, will clarify the mechanism of this interplay. We will combine bioinformatics, proteomics, and functional validation to investigate the 1,25D-dependent interactome of FBW7. This will provide important insights into 1,25D-induced antiproliferative effects and its role in cancer prevention.

In addition, we identified MXD1 as a new FBW7 substrate. Further investigations are required to elucidate the FBW7 binding site within MXD1 and the protein kinase, which phosphorylates a residue in this degron. This may contribute to the discovery of a novel class of FBW7 substrates.

References

[1]   Z. Herceg and P. Hainaut, "Genetic and epigenetic alterations as biomarkers for cancer detection, diagnosis and prognosis," *Mol. Oncol.*, vol. 1, no. 1, pp. 26–41, Jun. 2007.

[2]   L. F. Zerbini, "Oncogenic Transcription Factors: Target Genes," in *eLS*, John Wiley & Sons, Ltd, 2001.

[3]   M. Giammanco, D. Di Majo, M. La Guardia, S. Aiello, M. Crescimannno, C. Flandina, F. M. Tumminello, and G. Leto, "Vitamin D in cancer chemoprevention," *Pharm. Biol.*, vol. 53, no. 10, pp. 1399–1434, 2015.

[4]   L. Hargrove, T. Francis, and H. Francis, "Vitamin D and GI cancers: shedding some light on dark diseases," *Ann. Transl. Med.*, vol. 2, no. 1, Jan. 2014.

[5]   L. Vuolo, C. Di Somma, A. Faggiano, and A. Colao, "Vitamin D and Cancer," *Front. Endocrinol.*, vol. 3, Apr. 2012.

[6]   C. K. Chakraborti, "Vitamin D as a promising anticancer agent," *Indian J. Pharmacol.*, vol. 43, no. 2, pp. 113–120, Apr. 2011.

[7]   J. A. Nilsson and J. L. Cleveland, "Myc pathways provoking cell suicide and cancer," *Oncogene*, vol. 22, no. 56, pp. 9007–9021, Dec. 2003.

[8]   P. H. Reitsma, P. G. Rothberg, S. M. Astrin, J. Trial, Z. Bar-Shavit, A. Hall, S. L. Teitelbaum, and A. J. Kahn, "Regulation of myc gene expression in HL-60 leukaemia cells by a vitamin D metabolite," *Nature*, vol. 306, no. 5942, pp. 492–494, Dec. 1983.

[9]   M. Di Rosa, M. Malaguarnera, F. Nicoletti, and L. Malaguarnera, "Vitamin D3: a helpful immuno-modulator," *Immunology*, vol. 134, no. 2, pp. 123–139, Oct. 2011.

[10]   D. Feldman, A. V. Krishnan, S. Swami, E. Giovannucci, and B. J. Feldman, "The role of vitamin D in reducing cancer risk and progression," *Nat. Rev. Cancer*, vol. 14, no. 5, pp. 342–357, May 2014.

[11]   A. I. Su, T. Wiltshire, S. Batalov, H. Lapp, K. A. Ching, D. Block, J. Zhang, R. Soden, M. Hayakawa, G. Kreiman, M. P. Cooke, J. R. Walker, and J. B. Hogenesch, "A gene atlas of the mouse and human protein-encoding transcriptomes," *Proc. Natl. Acad. Sci. U. S. A.*, vol. 101, no. 16, pp. 6062–6067, Apr. 2004.

[12]   "CYP2R1 (cytochrome P450 family 2 subfamily R member 1) | Gene Report | BioGPS." [Online]. Available: http://biogps.org/#goto=genereport&id=120227. [Accessed: 26-Mar-2016].

[13]   G. Jones, "Metabolism and biomarkers of vitamin D," *Scand. J. Clin. Lab. Investig. Suppl.*, vol. 243, pp. 7–13, 2012.

[14]   S. Christakos, P. Dhawan, A. Verstuyf, L. Verlinden, and G. Carmeliet, "Vitamin D: Metabolism, Molecular Mechanism of Action, and Pleiotropic Effects," *Physiol. Rev.*, vol. 96, no. 1, pp. 365–408, Jan. 2016.

[15]   D. D. Bikle, "Vitamin D Metabolism, Mechanism of Action, and Clinical Applications," *Chem. Biol.*, vol. 21, no. 3, pp. 319–329, Mar. 2014.

[16]   "CYP27A1 (cytochrome P450 family 27 subfamily A member 1) | Gene Report | BioGPS." [Online]. Available: http://biogps.org/#goto=genereport&id=1593. [Accessed: 25-Mar-2016].

[17]   J. Lundqvist, "Vitamin D as a regulator of steroidogenic enzymes," *F1000Research*, Jul. 2014.

[18]   S. Jovičić, S. Ignjatović, and N. Majkić-Singh, "Biochemistry and metabolism of vitamin D / Biohemija i metabolizam vitamina D," *J. Med. Biochem.*, vol. 31, no. 4, pp. 309–315, 2012.

[19]   "CYP27B1 (cytochrome P450 family 27 subfamily B member 1) | Gene Report | BioGPS." [Online]. Available: http://biogps.org/#goto=genereport&id=1594. [Accessed: 25-Mar-2016].

[20]   "Cyp27b1 (cytochrome P450, family 27, subfamily b, polypeptide 1) | Gene Report | BioGPS." [Online]. Available: http://biogps.org/#goto=genereport&id=13115. [Accessed: 25-Mar-2016].

[21]   H. F. DeLuca, "History of the discovery of vitamin D and its active metabolites," *BoneKEy Rep.*, vol. 3, p. 479, Jan. 2014.

[22] W. Luo, P. A. Hershberger, D. L. Trump, and C. S. Johnson, "24-Hydroxylase in cancer: Impact on vitamin D-based anticancer therapeutics," *J. Steroid Biochem. Mol. Biol.*, vol. 136, pp. 252–257, Jul. 2013.

[23] Z. Wang, E. G. Schuetz, Y. Xu, and K. E. Thummel, "Interplay between Vitamin D and the Drug Metabolizing Enzyme CYP3A4," *J. Steroid Biochem. Mol. Biol.*, vol. 136, pp. 54–58, Jul. 2013.

[24] "CYP3A4 (cytochrome P450 family 3 subfamily A member 4) | Gene Report | BioGPS." [Online]. Available: http://biogps.org/#goto=genereport&id=1576. [Accessed: 26-Mar-2016].

[25] D. E. Prosser and G. Jones, "Enzymes involved in the activation and inactivation of vitamin D," *Trends Biochem. Sci.*, vol. 29, no. 12, pp. 664–673, Dec. 2004.

[26] R. Jorde, J. Svartberg, R. M. Joakimsen, and D. H. Coucheron, "Plasma profile of microRNA after supplementation with high doses of vitamin D3 for 12 months," *BMC Res. Notes*, vol. 5, p. 245, 2012.

[27] M. R. Haussler, P. W. Jurutka, M. Mizwicki, and A. W. Norman, "Vitamin D receptor (VDR)-mediated actions of 1α,25(OH)2vitamin D3: Genomic and non-genomic mechanisms," *Best Pract. Res. Clin. Endocrinol. Metab.*, vol. 25, no. 4, pp. 543–559, Aug. 2011.

[28] "VDR (vitamin D (1,25- dihydroxyvitamin D3) receptor) | Gene Report | BioGPS." [Online]. Available: http://biogps.org/#goto=genereport&id=7421. [Accessed: 26-Mar-2016].

[29] *Vitamins and Hormones: Steroids*. Academic Press, 1994.

[30] K. K. Deeb, D. L. Trump, and C. S. Johnson, "Vitamin D signalling pathways in cancer: potential for anticancer therapeutics," *Nat. Rev. Cancer*, vol. 7, no. 9, pp. 684–700, Sep. 2007.

[31] L.-Y. Wan, Y.-Q. Zhang, M.-D. Chen, Y.-Q. Du, C.-B. Liu, and J.-F. Wu, "Relationship between Structure and Conformational Change of the Vitamin D Receptor Ligand Binding Domain in 1α,25-Dihydroxyvitamin D3 Signaling," *Mol. Basel Switz.*, vol. 20, no. 11, pp. 20473–20486, 2015.

[32] C. Carlberg and S. Seuter, "A Genomic Perspective on Vitamin D Signaling," *Anticancer Res.*, vol. 29, no. 9, pp. 3485–3493, Sep. 2009.

[33] V. Dimitrov, R. Salehi-Tabar, B.-S. An, and J. H. White, "Non-classical mechanisms of transcriptional regulation by the vitamin D receptor: insights into calcium homeostasis, immune system regulation and cancer chemoprevention," *J. Steroid Biochem. Mol. Biol.*, vol. 144 Pt A, pp. 74–80, Oct. 2014.

[34] L. Díaz, M. Díaz-Muñoz, A. C. García-Gaytán, and I. Méndez, "Mechanistic Effects of Calcitriol in Cancer Biology," *Nutrients*, vol. 7, no. 6, pp. 5020–5050, Jun. 2015.

[35] Q. Wang, Y. He, Y. Shen, Q. Zhang, D. Chen, C. Zuo, J. Qin, H. Wang, J. Wang, and Y. Yu, "Vitamin D inhibits COX-2 expression and inflammatory response by targeting thioesterase superfamily member 4," *J. Biol. Chem.*, vol. 289, no. 17, pp. 11681–11694, Apr. 2014.

[36] D. Svensson, D. Nebel, and B.-O. Nilsson, "Vitamin D3 modulates the innate immune response through regulation of the hCAP-18/LL-37 gene expression and cytokine production," *Inflamm. Res. Off. J. Eur. Histamine Res. Soc. Al*, vol. 65, no. 1, pp. 25–32, Jan. 2016.

[37] T.-T. Wang, F. P. Nestel, V. Bourdeau, Y. Nagai, Q. Wang, J. Liao, L. Tavera-Mendoza, R. Lin, J. W. Hanrahan, S. Mader, J. H. White, and J. H. Hanrahan, "Cutting edge: 1,25-dihydroxyvitamin D3 is a direct inducer of antimicrobial peptide gene expression," *J. Immunol. Baltim. Md 1950*, vol. 173, no. 5, pp. 2909–2912, Sep. 2004.

[38] J. E. Yeh, P. A. Toniolo, and D. A. Frank, "Targeting transcription factors: promising new strategies for cancer therapy," *Curr. Opin. Oncol.*, vol. 25, no. 6, pp. 652–658, Nov. 2013.

[39] P. J. Enrietto, M. J. Hayman, G. M. Ramsay, J. A. Wyke, and L. N. Paynet, "Altered pathogenicity of avian myelocytomatosis (MC29) viruses with mutations in the v-myc gene," *Virology*, vol. 124, no. 1, pp. 164–172, Jan. 1983.

[40] J.-M. Blanchard, M. Piechaczyk, C. Dani, J.-C. Chambard, A. Franchi, J. Pouyssegur, and P. Jeanteur, "c-myc gene is transcribed at high rate in G0-arrested fibroblasts and is post-transcriptionally regulated in response to growth factors," *Nature*, vol. 317, no. 6036, pp. 443–445, Oct. 1985.

[41]   M. D. Cole, "The myc oncogene: its role in transformation and differentiation," *Annu. Rev. Genet.*, vol. 20, pp. 361–384, 1986.

[42]   A. Mahani, J. Henriksson, and A. P. H. Wright, "Origins of Myc Proteins – Using Intrinsic Protein Disorder to Trace Distant Relatives," *PLoS ONE*, vol. 8, no. 9, p. e75057, Sep. 2013.

[43]   S. L. Young, D. Diolaiti, M. Conacci-Sorrell, I. Ruiz-Trillo, R. N. Eisenman, and N. King, "Premetazoan Ancestry of the Myc–Max Network," *Mol. Biol. Evol.*, vol. 28, no. 10, pp. 2961–2971, Oct. 2011.

[44]   M. M. Nau, B. J. Brooks, J. Battey, E. Sausville, A. F. Gazdar, I. R. Kirsch, O. W. McBride, V. Bertness, G. F. Hollis, and J. D. Minna, "L-myc, a new myc-related gene amplified and expressed in human small cell lung cancer," *Nature*, vol. 318, no. 6041, pp. 69–73, 1985.

[45]   N. E. Kohl, N. Kanda, R. R. Schreck, G. Bruns, S. A. Latt, F. Gilbert, and F. W. Alt, "Transposition and amplification of oncogene-related sequences in human neuroblastomas," *Cell*, vol. 35, no. 2, Part 1, pp. 359–367, Dec. 1983.

[46]   A. R. Wasylishen and L. Z. Penn, "Myc: The beauty and the beast," *Genes Cancer*, vol. 1, no. 6, pp. 532–541, 2010.

[47]   Z. Nie, G. Hu, G. Wei, K. Cui, A. Yamane, W. Resch, R. Wang, D. R. Green, L. Tessarollo, R. Casellas, K. Zhao, and D. Levens, "c-Myc Is a Universal Amplifier of Expressed Genes in Lymphocytes and Embryonic Stem Cells," *Cell*, vol. 151, no. 1, pp. 68–79, Sep. 2012.

[48]   C. Y. Lin, J. Lovén, P. B. Rahl, R. M. Paranal, C. B. Burge, J. E. Bradner, T. I. Lee, and R. A. Young, "Transcriptional amplification in tumor cells with elevated c-Myc," *Cell*, vol. 151, no. 1, pp. 56–67, Sep. 2012.

[49]   N. Gomez-Roman, Z. A. Felton-Edkins, N. S. Kenneth, S. J. Goodfellow, D. Athineos, J. Zhang, B. A. Ramsbottom, F. Innes, T. Kantidakis, E. R. Kerr, J. Brodie, C. Grandori, and R. J. White, "Activation by c-Myc of transcription by RNA polymerases I, II and III," *Biochem. Soc. Symp.*, no. 73, pp. 141–154, 2006.

[50]   C. Grandori, N. Gomez-Roman, Z. A. Felton-Edkins, C. Ngouenet, D. A. Galloway, R. N. Eisenman, and R. J. White, "c-Myc binds to human ribosomal DNA and stimulates transcription of rRNA genes by RNA polymerase I," *Nat. Cell Biol.*, vol. 7, no. 3, pp. 311–318, Mar. 2005.

[51]   N. Gomez-Roman, C. Grandori, R. N. Eisenman, and R. J. White, "Direct activation of RNA polymerase III transcription by c-Myc," *Nature*, vol. 421, no. 6920, pp. 290–294, Jan. 2003.

[52]   C. Arvanitis and D. W. Felsher, "Conditional transgenic models define how MYC initiates and maintains tumorigenesis," *Semin. Cancer Biol.*, vol. 16, no. 4, pp. 313–317, Aug. 2006.

[53]   T. R. Kress, A. Sabò, and B. Amati, "MYC: connecting selective transcriptional control to global RNA production," *Nat. Rev. Cancer*, vol. 15, no. 10, pp. 593–607, Oct. 2015.

[54]   B.-J. Chen, Y.-L. Wu, Y. Tanaka, and W. Zhang, "Small Molecules Targeting c-Myc Oncogene: Promising Anti-Cancer Therapeutics," *Int. J. Biol. Sci.*, vol. 10, no. 10, pp. 1084–1096, Sep. 2014.

[55]   A. S. Kudlicki, "G-Quadruplexes Involving Both Strands of Genomic DNA Are Highly Abundant and Colocalize with Functional Sites in the Human Genome," *PLoS ONE*, vol. 11, no. 1, p. e0146174, Jan. 2016.

[56]   A. Siddiqui-Jain, C. L. Grand, D. J. Bearss, and L. H. Hurley, "Direct evidence for a G-quadruplex in a promoter region and its targeting with a small molecule to repress c-MYC transcription," *Proc. Natl. Acad. Sci.*, vol. 99, no. 18, pp. 11593–11598, Sep. 2002.

[57]   M. A. Keniry and E. A. Owen, "The flanking sequence contributes to the immobilisation of spermine at the G-quadruplex in the NHE (nuclease hypersensitivity element) III1 of the c-Myc promoter," *FEBS Lett.*, vol. 588, no. 10, pp. 1949–1954, May 2014.

[58]   D.-L. Ma, M. Wang, S. Lin, Q.-B. Han, and C.-H. Leung, "Recent Development of G-Quadruplex Probes for Cellular Imaging," *Curr. Top. Med. Chem.*, vol. 15, no. 19, pp. 1957–1963, 2015.

[59]   V. González, K. Guo, L. Hurley, and D. Sun, "Identification and characterization of nucleolin as a c-myc G-quadruplex-binding protein," *J. Biol. Chem.*, vol. 284, no. 35, pp. 23622–23635, Aug. 2009.

[60] P. L. Scognamiglio, C. Di Natale, M. Leone, M. Poletto, L. Vitagliano, G. Tell, and D. Marasco, "G-quadruplex DNA recognition by nucleophosmin: New insights from protein dissection," *Biochim. Biophys. Acta BBA - Gen. Subj.*, vol. 1840, no. 6, pp. 2050–2059, Jun. 2014.

[61] A. Gallo, C. Lo Sterzo, M. Mori, A. Di Matteo, I. Bertini, L. Banci, M. Brunori, and L. Federici, "Structure of nucleophosmin DNA-binding domain and analysis of its complex with a G-quadruplex sequence from the c-MYC promoter," *J. Biol. Chem.*, vol. 287, no. 32, pp. 26539–26548, Aug. 2012.

[62] V. Brázda, L. Hároníková, J. C. C. Liao, and M. Fojta, "DNA and RNA quadruplex-binding proteins," *Int. J. Mol. Sci.*, vol. 15, no. 10, pp. 17493–17517, 2014.

[63] N. Kumar, R. Basundra, and S. Maiti, "Elevated polyamines induce c-MYC overexpression by perturbing quadruplex–WC duplex equilibrium," *Nucleic Acids Res.*, vol. 37, no. 10, pp. 3321–3331, Jun. 2009.

[64] S. Chen, L. Su, J. Qiu, N. Xiao, J. Lin, J.-H. Tan, T.-M. Ou, L.-Q. Gu, Z.-S. Huang, and D. Li, "Mechanistic studies for the role of cellular nucleic-acid-binding protein (CNBP) in regulation of c-myc transcription," *Biochim. Biophys. Acta*, vol. 1830, no. 10, pp. 4769–4777, Oct. 2013.

[65] D. Panda, "A Nucleus-Imaging Probe That Selectively Stabilizes a Minor Conformation of c-MYC G-quadruplex and Down-regulates c-MYC Transcription in Human Cancer Cells," *Sci. Rep.*, vol. 5, p. 13183, 2015.

[66] D. Rhodes and H. J. Lipps, "G-quadruplexes and their regulatory roles in biology," *Nucleic Acids Res.*, p. gkv862, Sep. 2015.

[67] T. A. Brooks and L. H. Hurley, "Targeting MYC Expression through G-Quadruplexes," *Genes Cancer*, vol. 1, no. 6, pp. 641–649, Jun. 2010.

[68] K. V. Diveshkumar, S. Sakrikar, S. Harikrishna, V. Dhamodharan, and P. I. Pradeepkumar, "Targeting promoter G-quadruplex DNAs by indenopyrimidine-based ligands," *ChemMedChem*, vol. 9, no. 12, pp. 2754–2765, Dec. 2014.

[69] H. R. Nasiri, N. M. Bell, K. I. E. McLuckie, J. Husby, C. Abell, S. Neidle, and S. Balasubramanian, "Targeting a c-MYC G-quadruplex DNA with a fragment library," *Chem. Commun.*, vol. 50, no. 14, pp. 1704–1707, Jan. 2014.

[70] T. A. Brooks and L. H. Hurley, "The role of supercoiling in transcriptional control of MYC and its importance in molecular therapeutics," *Nat. Rev. Cancer*, vol. 9, no. 12, pp. 849–861, Dec. 2009.

[71] C. D. Cukier, D. Hollingworth, S. R. Martin, G. Kelly, I. Díaz-Moreno, and A. Ramos, "Molecular basis of FIR-mediated c-myc transcriptional control," *Nat. Struct. Mol. Biol.*, vol. 17, no. 99, pp. 1058–1064, Sep. 2010.

[72] J. Dai, M. Carver, L. H. Hurley, and D. Yang, "Solution structure of a 2:1 quindoline-c-MYC G-quadruplex: insights into G-quadruplex-interactive small molecule drug design," *J. Am. Chem. Soc.*, vol. 133, no. 44, pp. 17673–17680, Nov. 2011.

[73] H. You, J. Wu, F. Shao, and J. Yan, "Stability and Kinetics of c-MYC Promoter G-Quadruplexes Studied by Single-Molecule Manipulation," *J. Am. Chem. Soc.*, vol. 137, no. 7, pp. 2424–2427, Feb. 2015.

[74] M. H. Ji, S.-K. Kim, C.-Y. Kim, J. H. Phi, H. J. Jun, S. W. Blume, and H. S. Choi, "Physiological Expression and Accumulation of the Products of Two Upstream Open Reading Frames mrtl and MycHex1 Along With p64 and p67 Myc From the Human c-myc Locus," *J. Cell. Biochem.*, p. n/a-n/a, Dec. 2015.

[75] S. R. Hann and R. N. Eisenman, "Proteins encoded by the human c-myc oncogene: differential expression in neoplastic cells.," *Mol. Cell. Biol.*, vol. 4, no. 11, pp. 2486–2497, Nov. 1984.

[76] G. D. Spotts, S. V. Patel, Q. Xiao, and S. R. Hann, "Identification of downstream-initiated c-Myc proteins which are dominant-negative inhibitors of transactivation by full-length c-Myc proteins.," *Mol. Cell. Biol.*, vol. 17, no. 3, pp. 1459–1468, Mar. 1997.

[77] M. Conacci-Sorrell and R. N. Eisenman, "Post-translational control of Myc function during differentiation," *Cell Cycle*, vol. 10, no. 4, pp. 604–610, Feb. 2011.

[78]   C. Janke and J. Chloë Bulinski, "Post-translational regulation of the microtubule cytoskeleton: mechanisms and functions," *Nat. Rev. Mol. Cell Biol.*, vol. 12, no. 12, pp. 773–786, Dec. 2011.

[79]   M. Conacci-Sorrell, C. Ngouenet, S. Anderson, T. Brabletz, and R. N. Eisenman, "Stress-induced cleavage of Myc promotes cancer cell survival," *Genes Dev.*, vol. 28, no. 7, pp. 689–707, Apr. 2014.

[80]   J. Barrett, M. J. Birrer, G. J. Kato, H. Dosaka-Akita, and C. V. Dang, "Activation domains of L-Myc and c-Myc determine their transforming potencies in rat embryo cells," *Mol. Cell. Biol.*, vol. 12, no. 7, pp. 3130–3137, Jul. 1992.

[81]   K. Bhatia, K. Huppi, G. Spangler, D. Siwarski, R. Iyer, and I. Magrath, "Point mutations in the c-Myc transactivation domain are common in Burkitt's lymphoma and mouse plasmacytomas," *Nat. Genet.*, vol. 5, no. 1, pp. 56–61, Sep. 1993.

[82]   W. P. Tansey and W. P. Tansey, "Mammalian MYC Proteins and Cancer, Mammalian MYC Proteins and Cancer," *New J. Sci. New J. Sci.*, vol. 2014, 2014, p. e757534, Feb. 2014.

[83]   S. F. Farina, J. L. Huff, and J. T. Parsons, "Mutations within the 5' half of the avian retrovirus MC29 v-myc gene alter or abolish transformation of chicken embryo fibroblasts and macrophages.," *J. Virol.*, vol. 66, no. 5, pp. 2698–2708, May 1992.

[84]   V. H. Cowling, S. Chandriani, M. L. Whitfield, and M. D. Cole, "A conserved Myc protein domain, MBIV, regulates DNA binding, apoptosis, transformation, and G2 arrest," *Mol. Cell. Biol.*, vol. 26, no. 11, pp. 4226–4239, Jun. 2006.

[85]   D. Schwinkendorf and P. Gallant, "The conserved Myc box 2 and Myc box 3 regions are important, but not essential, for Myc function in vivo," *Gene*, vol. 436, no. 1–2, pp. 90–100, May 2009.

[86]   N. Meyer and L. Z. Penn, "Reflecting on 25 years with MYC," *Nat. Rev. Cancer*, vol. 8, no. 12, pp. 976–990, Dec. 2008.

[87]   G. J. Kato, J. Barrett, M. Villa-Garcia, and C. V. Dang, "An amino-terminal c-myc domain required for neoplastic transformation activates transcription," *Mol. Cell. Biol.*, vol. 10, no. 11, pp. 5914–5920, Nov. 1990.

[88]   J. Stone, T. de Lange, G. Ramsay, E. Jakobovits, J. M. Bishop, H. Varmus, and W. Lee, "Definition of regions in human c-myc that are involved in transformation and nuclear localization," *Mol. Cell. Biol.*, vol. 7, no. 5, pp. 1697–1709, May 1987.

[89]   A. Herbst, M. T. Hemann, K. A. Tworkowski, S. E. Salghetti, S. W. Lowe, and W. P. Tansey, "A conserved element in Myc that negatively regulates its proapoptotic activity," *EMBO Rep.*, vol. 6, no. 2, pp. 177–183, Feb. 2005.

[90]   C. V. Dang and W. M. Lee, "Identification of the human c-myc protein nuclear translocation signal.," *Mol. Cell. Biol.*, vol. 8, no. 10, pp. 4048–4054, Oct. 1988.

[91]   K. Myant, X. Qiao, T. Halonen, C. Come, A. Laine, M. Janghorban, J. I. Partanen, J. Cassidy, E.-L. Ogg, P. Cammareri, T. Laiterä, J. Okkeri, J. Klefström, R. C. Sears, O. J. Sansom, and J. Westermarck, "Serine 62-Phosphorylated MYC Associates with Nuclear Lamins and Its Regulation by CIP2A Is Essential for Regenerative Proliferation," *Cell Rep.*, vol. 12, no. 6, pp. 1019–1031, Aug. 2015.

[92]   A. S. Farrell, C. Pelz, X. Wang, C. J. Daniel, Z. Wang, Y. Su, M. Janghorban, X. Zhang, C. Morgan, S. Impey, and R. C. Sears, "Pin1 regulates the dynamics of c-Myc DNA binding to facilitate target gene regulation and oncogenesis," *Mol. Cell. Biol.*, vol. 33, no. 15, pp. 2930–2949, Aug. 2013.

[93]   M. Welcker, A. Orian, J. Jin, J. E. Grim, J. A. Grim, J. W. Harper, R. N. Eisenman, and B. E. Clurman, "The Fbw7 tumor suppressor regulates glycogen synthase kinase 3 phosphorylation-dependent c-Myc protein degradation," *Proc. Natl. Acad. Sci. U. S. A.*, vol. 101, no. 24, pp. 9085–9090, Jun. 2004.

[94]   M. T. Hemann, A. Bric, J. Teruya-Feldstein, A. Herbst, J. A. Nilsson, C. Cordon-Cardo, J. L. Cleveland, W. P. Tansey, and S. W. Lowe, "Evasion of the p53 tumour surveillance network by tumour-derived MYC mutants," *Nature*, vol. 436, no. 7052, pp. 807–811, Aug. 2005.

[95] C. E. Nesbit, L. E. Grove, X. Yin, and E. V. Prochownik, "Differential apoptotic behaviors of c-myc, N-myc, and L-myc oncoproteins," *Cell Growth Differ. Mol. Biol. J. Am. Assoc. Cancer Res.*, vol. 9, no. 9, pp. 731–741, Sep. 1998.

[96] Q. Xiao, G. Claassen, J. Shi, S. Adachi, J. Sedivy, and S. R. Hann, "Transactivation-defective c-MycS retains the ability to regulate proliferation and apoptosis," *Genes Dev.*, vol. 12, no. 24, pp. 3803–3808, Dec. 1998.

[97] V. H. Cowling and M. D. Cole, "An N-Myc truncation analogous to c-Myc-S induces cell proliferation independently of transactivation but dependent on Myc homology box II," *Oncogene*, vol. 27, no. 9, pp. 1327–1332, Aug. 2007.

[98] C. Benassayag, L. Montero, N. Colombié, P. Gallant, D. Cribbs, and D. Morello, "Human c-Myc Isoforms Differentially Regulate Cell Growth and Apoptosis in Drosophila melanogaster," *Mol. Cell. Biol.*, vol. 25, no. 22, pp. 9897–9909, Nov. 2005.

[99] M. Conacci-Sorrell, C. Ngouenet, and R. N. Eisenman, "Myc-nick: A cytoplasmic cleavage product of Myc that promotes α-tubulin acetylation and cell differentiation," *Cell*, vol. 142, no. 3, pp. 480–493, Aug. 2010.

[100] M. Niapour, Y. Yu, and S. A. Berger, "Regulation of Calpain Activity by c-Myc through Calpastatin and Promotion of Transformation in c-Myc-negative Cells by Calpastatin Suppression," *J. Biol. Chem.*, vol. 283, no. 31, pp. 21371–21381, Aug. 2008.

[101] T. S. Dexheimer, S. S. Carey, S. Zuohe, V. M. Gokhale, X. Hu, L. B. Murata, E. M. Maes, A. Weichsel, D. Sun, E. J. Meuillet, W. R. Montfort, and L. H. Hurley, "NM23-H2 may play an indirect role in transcriptional activation of c-myc gene expression but does not cleave the nuclease hypersensitive element III(1)," *Mol. Cancer Ther.*, vol. 8, no. 5, pp. 1363–1377, May 2009.

[102] J. Liu, F. Kouzine, Z. Nie, H.-J. Chung, Z. Elisha-Feil, A. Weber, K. Zhao, and D. Levens, "The FUSE/FBP/FIR/TFIIH system is a molecular machine programming a pulse of c-myc expression," *EMBO J.*, vol. 25, no. 10, pp. 2119–2130, May 2006.

[103] D. Levens, "How the c-myc Promoter Works and Why It Sometimes Does Not," *J. Natl. Cancer Inst. Monogr.*, no. 39, pp. 41–43, 2008.

[104] D. L. Bentley and M. Groudine, "A block to elongation is largely responsible for decreased transcription of c-myc in differentiated HL60 cells," *Nature*, vol. 321, no. 6071, pp. 702–706, Jun. 1986.

[105] C. A. Spencer, R. C. LeStrange, U. Novak, W. S. Hayward, and M. Groudine, "The block to transcription elongation is promoter dependent in normal and Burkitt's lymphoma c-myc alleles.," *Genes Dev.*, vol. 4, no. 1, pp. 75–88, Jan. 1990.

[106] J. Ross, P. Bernstein, R. D. Prokipcak, and D. J. Herrick, "Regulation of c-myc mRNA Half-Life by an RNA-Binding Protein," in *Tumor Biology*, A. S. Tsiftsoglou, A. C. Sartorelli, D. E. Housman, and T. M. Dexter, Eds. Springer Berlin Heidelberg, 1996, pp. 257–272.

[107] D. Weidensdorfer, N. Stöhr, A. Baude, M. Lederer, M. Köhn, A. Schierhorn, S. Buchmeier, E. Wahle, and S. Hüttelmaier, "Control of c-myc mRNA stability by IGF2BP1-associated cytoplasmic RNPs," *RNA*, vol. 15, no. 1, pp. 104–115, Jan. 2009.

[108] F. Yang, X. Xue, L. Zheng, J. Bi, Y. Zhou, K. Zhi, Y. Gu, and G. Fang, "Long non-coding RNA GHET1 promotes gastric carcinoma cell proliferation by increasing c-Myc mRNA stability," *FEBS J.*, vol. 281, no. 3, pp. 802–813, Feb. 2014.

[109] G. Brewer, "Characterization of c-myc 3' to 5' mRNA decay activities in an in vitro system," *J. Biol. Chem.*, vol. 273, no. 52, pp. 34770–34774, Dec. 1998.

[110] G. Brewer, "Evidence for a 3'-5' decay pathway for c-myc mRNA in mammalian cells," *J. Biol. Chem.*, vol. 274, no. 23, pp. 16174–16179, Jun. 1999.

[111] F. M. Gratacós and G. Brewer, "The role of AUF1 in regulated mRNA decay," *Wiley Interdiscip. Rev. RNA*, vol. 1, no. 3, pp. 457–473, Dec. 2010.

[112] C. T. DeMaria and G. Brewer, "AUF1 Binding Affinity to A+U-rich Elements Correlates with Rapid mRNA Degradation," *J. Biol. Chem.*, vol. 271, no. 21, pp. 12179–12184, May 1996.

[113] B. Liao, Y. Hu, and G. Brewer, "Competitive binding of AUF1 and TIAR to MYC mRNA controls its translation," *Nat. Struct. Mol. Biol.*, vol. 14, no. 6, pp. 511–518, Jun. 2007.

[114] K. Mazan-Mamczarz, A. Lal, J. L. Martindale, T. Kawai, and M. Gorospe, "Translational Repression by RNA-Binding Protein TIAR," *Mol. Cell. Biol.*, vol. 26, no. 7, pp. 2716–2727, Apr. 2006.

[115] S. Yamamura, S. Saini, S. Majid, H. Hirata, K. Ueno, G. Deng, and R. Dahiya, "MicroRNA-34a modulates c-Myc transcriptional complexes to suppress malignancy in human prostate cancer cells," *PloS One*, vol. 7, no. 1, p. e29722, 2012.

[116] A. Lal, F. Navarro, C. A. Maher, L. E. Maliszewski, N. Yan, E. O'Day, D. Chowdhury, D. M. Dykxhoorn, P. Tsai, O. Hofmann, K. G. Becker, M. Gorospe, W. Hide, and J. Lieberman, "miR-24 Inhibits cell proliferation by targeting E2F2, MYC, and other cell-cycle genes via binding to 'seedless' 3'UTR microRNA recognition elements," *Mol. Cell*, vol. 35, no. 5, pp. 610–625, Sep. 2009.

[117] H. H. Kim, Y. Kuwano, S. Srikantan, E. K. Lee, J. L. Martindale, and M. Gorospe, "HuR recruits let-7/RISC to repress c-Myc expression," *Genes Dev.*, vol. 23, no. 15, pp. 1743–1748, Aug. 2009.

[118] Y.-C. Lu, S.-H. Chang, M. Hafner, X. Li, T. Tuschl, O. Elemento, and T. Hla, "ELAVL1 modulates transcriptome-wide miRNA binding in murine macrophages," *Cell Rep.*, vol. 9, no. 6, pp. 2330–2343, Dec. 2014.

[119] M. Kalkat and L. Z. Penn, "Regulation and Function of the MYC Oncogene," in *eLS*, John Wiley & Sons, Ltd, 2001.

[120] P. Jóźwiak, E. Forma, M. Bryś, and A. Krześlak, "O-GlcNAcylation and metabolic reprograming in cancer," *Mol. Struct. Endocrinol.*, vol. 5, p. 145, 2014.

[121] A. R. Wasylishen, M. Chan-Seng-Yue, C. Bros, D. Dingar, W. B. Tu, M. Kalkat, P.-K. Chan, P. J. Mullen, L. Huang, N. Meyer, B. Raught, P. C. Boutros, and L. Z. Penn, "MYC phosphorylation at novel regulatory regions suppresses transforming activity," *Cancer Res.*, vol. 73, no. 21, pp. 6504–6515, Nov. 2013.

[122] M. Yada, S. Hatakeyama, T. Kamura, M. Nishiyama, R. Tsunematsu, H. Imaki, N. Ishida, F. Okumura, K. Nakayama, and K. I. Nakayama, "Phosphorylation-dependent degradation of c-Myc is mediated by the F-box protein Fbw7," *EMBO J.*, vol. 23, no. 10, pp. 2116–2125, May 2004.

[123] P. P. Hsu, S. A. Kang, J. Rameseder, Y. Zhang, K. A. Ottina, D. Lim, T. R. Peterson, Y. Choi, N. S. Gray, M. B. Yaffe, J. A. Marto, and D. M. Sabatini, "The mTOR-regulated phosphoproteome reveals a mechanism of mTORC1-mediated inhibition of growth factor signaling," *Science*, vol. 332, no. 6035, pp. 1317–1322, Jun. 2011.

[124] H. R. Seo, J. Kim, S. Bae, J.-W. Soh, and Y.-S. Lee, "Cdk5-mediated phosphorylation of c-Myc on Ser-62 is essential in transcriptional activation of cyclin B1 by cyclin G1," *J. Biol. Chem.*, vol. 283, no. 23, pp. 15601–15610, Jun. 2008.

[125] E. Alvarez, I. C. Northwood, F. A. Gonzalez, D. A. Latour, A. Seth, C. Abate, T. Curran, and R. J. Davis, "Pro-Leu-Ser/Thr-Pro is a consensus primary sequence for substrate protein phosphorylation. Characterization of the phosphorylation of c-myc and c-jun proteins by an epidermal growth factor receptor threonine 669 protein kinase," *J. Biol. Chem.*, vol. 266, no. 23, pp. 15277–15285, Aug. 1991.

[126] K. Noguchi, C. Kitanaka, H. Yamana, A. Kokubu, T. Mochizuki, and Y. Kuchino, "Regulation of c-Myc through Phosphorylation at Ser-62 and Ser-71 by c-Jun N-Terminal Kinase," *J. Biol. Chem.*, vol. 274, no. 46, pp. 32580–32587, Nov. 1999.

[127] B. J. Pulverer, C. Fisher, K. Vousden, T. Littlewood, G. Evan, and J. R. Woodgett, "Site-specific modulation of c-Myc cotransformation by residues phosphorylated in vivo," *Oncogene*, vol. 9, no. 1, pp. 59–70, Jan. 1994.

[128] S. D. Conzen, K. Gottlob, E. S. Kandel, P. Khanduri, A. J. Wagner, M. O'Leary, and N. Hay, "Induction of cell cycle progression and acceleration of apoptosis are two separable functions of c-Myc: transrepression correlates with acceleration of apoptosis," *Mol. Cell. Biol.*, vol. 20, no. 16, pp. 6008–6018, Aug. 2000.

[129] F. Bahram, N. von der Lehr, C. Cetinkaya, and L.-G. Larsson, "c-Myc hot spot mutations in lymphomas result in inefficient ubiquitination and decreased proteasome-mediated turnover," *Blood*, vol. 95, no. 6, pp. 2104–2110, Mar. 2000.

[130] Z. Huang, J. A. Traugh, and J. M. Bishop, "Negative control of the Myc protein by the stress-responsive kinase Pak2," *Mol. Cell. Biol.*, vol. 24, no. 4, pp. 1582–1594, Feb. 2004.

[131] V. J. Sanchez-Arévalo Lobo, M. Doni, A. Verrecchia, S. Sanulli, G. Fagà, A. Piontini, M. Bianchi, M. Conacci-Sorrell, G. Mazzarol, V. Peg, J. H. Losa, P. Ronchi, M. Ponzoni, R. N. Eisenman, C. Doglioni, and B. Amati, "Dual regulation of Myc by Abl," *Oncogene*, vol. 32, no. 45, pp. 5261–5271, Nov. 2013.

[132] T. Y. Chou, C. V. Dang, and G. W. Hart, "Glycosylation of the c-Myc transactivation domain," *Proc. Natl. Acad. Sci. U. S. A.*, vol. 92, no. 10, pp. 4417–4421, May 1995.

[133] T. Y. Chou and G. W. Hart, "O-linked N-acetylglucosamine and cancer: messages from the glycosylation of c-Myc," *Adv. Exp. Med. Biol.*, vol. 491, pp. 413–418, 2001.

[134] Q. Zeidan and G. W. Hart, "The intersections between O-GlcNAcylation and phosphorylation: implications for multiple signaling pathways," *J Cell Sci*, vol. 123, no. 1, pp. 13–22, Jan. 2010.

[135] S. Adhikary, F. Marinoni, A. Hock, E. Hulleman, N. Popov, R. Beier, S. Bernard, M. Quarto, M. Capra, S. Goettig, U. Kogel, M. Scheffner, K. Helin, and M. Eilers, "The ubiquitin ligase HectH9 regulates transcriptional activation by Myc and is essential for tumor cell proliferation," *Cell*, vol. 123, no. 3, pp. 409–421, Nov. 2005.

[136] J. Vervoorts, J. Lüscher-Firzlaff, and B. Lüscher, "The ins and outs of MYC regulation by posttranslational mechanisms," *J. Biol. Chem.*, vol. 281, no. 46, pp. 34725–34729, Nov. 2006.

[137] R. González-Prieto, S. A. Cuijpers, R. Kumar, I. A. Hendriks, and A. C. Vertegaal, "c-Myc is targeted to the proteasome for degradation in a SUMOylation-dependent manner, regulated by PIAS1, SENP7 and RNF4," *Cell Cycle*, vol. 14, no. 12, pp. 1859–1872, Jun. 2015.

[138] A. S. Farrell and R. C. Sears, "MYC degradation," *Cold Spring Harb. Perspect. Med.*, vol. 4, no. 3, Mar. 2014.

[139] R. C. Sears, "The life cycle of C-myc: from synthesis to degradation," *Cell Cycle Georget. Tex*, vol. 3, no. 9, pp. 1133–1137, Sep. 2004.

[140] H. K. Arnold, X. Zhang, C. J. Daniel, D. Tibbitts, J. Escamilla-Powers, A. Farrell, S. Tokarz, C. Morgan, and R. C. Sears, "The Axin1 scaffold protein promotes formation of a degradation complex for c-Myc," *EMBO J.*, vol. 28, no. 5, pp. 500–512, Mar. 2009.

[141] X. Zhang, A. S. Farrell, C. J. Daniel, H. Arnold, C. Scanlan, B. J. Laraway, M. Janghorban, L. Lum, D. Chen, M. Troxell, and R. Sears, "Mechanistic insight into Myc stabilization in breast cancer involving aberrant Axin1 expression," *Proc. Natl. Acad. Sci. U. S. A.*, vol. 109, no. 8, pp. 2790–2795, Feb. 2012.

[142] S. Salahshor and J. R. Woodgett, "The links between axin and carcinogenesis," *J. Clin. Pathol.*, vol. 58, no. 3, pp. 225–236, Mar. 2005.

[143] M. Sato, R. Rodriguez-Barrueco, J. Yu, C. Do, J. M. Silva, and J. Gautier, "MYC is a critical target of FBXW7," *Oncotarget*, vol. 6, no. 5, pp. 3292–3305, Feb. 2015.

[144] X.-X. Sun, X. He, L. Yin, M. Komada, R. C. Sears, and M.-S. Dai, "The nucleolar ubiquitin-specific protease USP36 deubiquitinates and stabilizes c-Myc," *Proc. Natl. Acad. Sci. U. S. A.*, vol. 112, no. 12, pp. 3734–3739, Mar. 2015.

[145] N. Popov, S. Herold, M. Llamazares, C. Schuelein, and M. Eilers, "Fbw7 and Usp28 regulate Myc protein stability in response to DNA damage," *Cell Cycle*, vol. 6, no. 19, pp. 2327–2331, Oct. 2007.

[146] C. Schülein-Völk, E. Wolf, J. Zhu, W. Xu, L. Taranets, A. Hellmann, L. A. Jänicke, M. E. Diefenbacher, A. Behrens, M. Eilers, and N. Popov, "Dual regulation of Fbw7 function and oncogenic transformation by Usp28," *Cell Rep.*, vol. 9, no. 3, pp. 1099–1109, Nov. 2014.

[147] B.-Y. Kim, J.-S. Yang, S.-Y. Kwak, X. Zhang, and Y.-H. Han, "NEMO stabilizes c-Myc through direct interaction in the nucleus," *FEBS Lett.*, vol. 584, no. 22, pp. 4524–4530, Nov. 2010.

[148] L. Reavie, S. M. Buckley, E. Loizou, S. Takeishi, B. Aranda-Orgilles, D. Ndiaye-Lobry, O. Abdel-Wahab, S. Ibrahim, K. I. Nakayama, and I. Aifantis, "Regulation of c-Myc ubiquitination controls chronic myelogenous leukemia initiation and progression," *Cancer Cell*, vol. 23, no. 3, pp. 362–375, Mar. 2013.

[149] S. H. Choi, J. B. Wright, S. A. Gerber, and M. D. Cole, "Myc protein is stabilized by suppression of a novel E3 ligase complex in cancer cells," *Genes Dev.*, vol. 24, no. 12, pp. 1236–1241, Jun. 2010.

[150] L. 'a Bahnassawy, T. M. Perumal, L. Gonzalez-Cano, A.-L. Hillje, L. Taher, W. Makalowski, Y. Suzuki, G. Fuellen, A. del Sol, and J. C. Schwamborn, "TRIM32 modulates pluripotency entry and exit by directly regulating Oct4 stability," *Sci. Rep.*, vol. 5, p. 13456, 2015.

[151] J. C. Schwamborn, E. Berezikov, and J. A. Knoblich, "The TRIM-NHL Protein TRIM32 Activates MicroRNAs and Prevents Self-Renewal in Mouse Neural Progenitors," *Cell*, vol. 136, no. 5, pp. 913–925, Mar. 2009.

[152] H. B. Koch, R. Zhang, B. Verdoodt, A. Bailey, C.-D. Zhang, J. R. Yates, A. Menssen, and H. Hermeking, "Large-scale identification of c-MYC-associated proteins using a combined TAP/MudPIT approach," *Cell Cycle Georget. Tex*, vol. 6, no. 2, pp. 205–217, Jan. 2007.

[153] I. Paul, S. F. Ahmed, A. Bhowmik, S. Deb, and M. K. Ghosh, "The ubiquitin ligase CHIP regulates c-Myc stability and transcriptional activity," *Oncogene*, vol. 32, no. 10, pp. 1284–1295, Mar. 2013.

[154] N. Popov, C. Schülein, L. A. Jaenicke, and M. Eilers, "Ubiquitylation of the amino terminus of Myc by SCFβ-TrCP antagonizes SCFFbw7-mediated turnover," *Nat. Cell Biol.*, vol. 12, no. 10, pp. 973–981, Oct. 2010.

[155] D. Cepeda, H.-F. Ng, H. R. Sharifi, S. Mahmoudi, V. S. Cerrato, E. Fredlund, K. Magnusson, H. Nilsson, A. Malyukova, J. Rantala, D. Klevebring, F. Viñals, N. Bhaskaran, S. M. Zakaria, A. S. Rahmanto, S. Grotegut, M. L. Nielsen, C. A.-K. Szigyarto, D. Sun, M. Lerner, S. Navani, M. Widschwendter, M. Uhlén, K. Jirström, F. Pontén, J. Wohlschlegel, D. Grandér, C. Spruck, L.-G. Larsson, and O. Sangfelt, "CDK-mediated activation of the SCFFBXO28 ubiquitin ligase promotes MYC-driven transcription and tumourigenesis and predicts poor survival in breast cancer," *EMBO Mol. Med.*, vol. 5, no. 7, pp. 999–1018, Jul. 2013.

[156] S. Lee, W. Kim, C. Ko, and W.-S. Ryu, "Hepatitis B virus X protein enhances Myc stability by inhibiting SCFSkp2 ubiquitin E3 ligase-mediated Myc ubiquitination and contributes to oncogenesis," *Oncogene*, Jul. 2015.

[157] S. Y. Kim, A. Herbst, K. A. Tworkowski, S. E. Salghetti, and W. P. Tansey, "Skp2 regulates Myc protein stability and activity," *Mol. Cell*, vol. 11, no. 5, pp. 1177–1188, May 2003.

[158] N. von der Lehr, S. Johansson, S. Wu, F. Bahram, A. Castell, C. Cetinkaya, P. Hydbring, I. Weidung, K. Nakayama, K. I. Nakayama, O. Söderberg, T. K. Kerppola, and L.-G. Larsson, "The F-Box Protein Skp2 Participates in c-Myc Proteosomal Degradation and Acts as a Cofactor for c-Myc-Regulated Transcription," *Mol. Cell*, vol. 11, no. 5, pp. 1189–1200, May 2003.

[159] V. H. Cowling and M. D. Cole, "Mechanism of transcriptional activation by the Myc oncoproteins," *Semin. Cancer Biol.*, vol. 16, no. 4, pp. 242–252, Aug. 2006.

[160] C. V. Dang, "MYC on the Path to Cancer," *Cell*, vol. 149, no. 1, pp. 22–35, Mar. 2012.

[161] J. Seoane, C. Pouponnot, P. Staller, M. Schader, M. Eilers, and J. Massagué, "TGFbeta influences Myc, Miz-1 and Smad to control the CDK inhibitor p15INK4b," *Nat. Cell Biol.*, vol. 3, no. 4, pp. 400–408, Apr. 2001.

[162] K. E. Wiese, H. M. Haikala, B. von Eyss, E. Wolf, C. Esnault, A. Rosenwald, R. Treisman, J. Klefström, and M. Eilers, "Repression of SRF target genes is critical for Myc-dependent apoptosis of epithelial cells," *EMBO J.*, vol. 34, no. 11, pp. 1554–1571, Jun. 2015.

[163] C.-S. Yap, A. L. Peterson, G. Castellani, J. M. Sedivy, and N. Neretti, "Kinetic profiling of the c-Myc transcriptome and bioinformatic analysis of repressed gene promoters," *Cell Cycle Georget. Tex*, vol. 10, no. 13, pp. 2184–2196, Jul. 2011.

[164] M. Wanzel, A. C. Russ, D. Kleine-Kohlbrecher, E. Colombo, P.-G. Pelicci, and M. Eilers, "A ribosomal protein L23-nucleophosmin circuit coordinates Mizl function with cell growth," *Nat. Cell Biol.*, vol. 10, no. 9, pp. 1051–1061, Sep. 2008.

[165] S. K. Nair and S. K. Burley, "X-ray structures of Myc-Max and Mad-Max recognizing DNA. Molecular bases of regulation by proto-oncogenic transcription factors," *Cell*, vol. 112, no. 2, pp. 193–205, Jan. 2003.

[166] J. Guo, T. Li, J. Schipper, K. A. Nilson, F. K. Fordjour, J. J. Cooper, R. Gordân, and D. H. Price, "Sequence specificity incompletely defines the genome-wide occupancy of Myc," *Genome Biol.*, vol. 15, no. 10, p. 482, 2014.

[167] A. Sabò, T. R. Kress, M. Pelizzola, S. de Pretis, M. M. Gorski, A. Tesi, M. J. Morelli, P. Bora, M. Doni, A. Verrecchia, C. Tonelli, G. Fagà, V. Bianchi, A. Ronchi, D. Low, H. Müller, E. Guccione, S. Campaner, and B. Amati, "Selective transcriptional regulation by Myc in cellular growth control and lymphomagenesis," *Nature*, vol. 511, no. 7510, pp. 488–492, Jul. 2014.

[168] E. Guccione, F. Martinato, G. Finocchiaro, L. Luzi, L. Tizzoni, V. Dall' Olio, G. Zardo, C. Nervi, L. Bernard, and B. Amati, "Myc-binding-site recognition in the human genome is determined by chromatin context," *Nat. Cell Biol.*, vol. 8, no. 7, pp. 764–770, Jul. 2006.

[169] S. Walz, F. Lorenzin, J. Morton, K. E. Wiese, B. von Eyss, S. Herold, L. Rycak, H. Dumay-Odelot, S. Karim, M. Bartkuhn, F. Roels, T. Wüstefeld, M. Fischer, M. Teichmann, L. Zender, C.-L. Wei, O. Sansom, E. Wolf, and M. Eilers, "Activation and repression by oncogenic MYC shape tumour-specific gene expression profiles," *Nature*, vol. 511, no. 7510, pp. 483–487, Jul. 2014.

[170] B.-K. Lee, A. A. Bhinge, A. Battenhouse, R. M. McDaniell, Z. Liu, L. Song, Y. Ni, E. Birney, J. D. Lieb, T. S. Furey, G. E. Crawford, and V. R. Iyer, "Cell-type specific and combinatorial usage of diverse transcription factors revealed by genome-wide binding studies in multiple human cells," *Genome Res.*, vol. 22, no. 1, pp. 9–24, Jan. 2012.

[171] A. Orian, B. van Steensel, J. Delrow, H. J. Bussemaker, L. Li, T. Sawado, E. Williams, L. W. M. Loo, S. M. Cowley, C. Yost, S. Pierce, B. A. Edgar, S. M. Parkhurst, and R. N. Eisenman, "Genomic binding by the Drosophila Myc, Max, Mad/Mnt transcription factor network," *Genes Dev.*, vol. 17, no. 9, pp. 1101–1114, May 2003.

[172] K. I. Zeller, X. Zhao, C. W. H. Lee, K. P. Chiu, F. Yao, J. T. Yustein, H. S. Ooi, Y. L. Orlov, A. Shahab, H. C. Yong, Y. Fu, Z. Weng, V. A. Kuznetsov, W.-K. Sung, Y. Ruan, C. V. Dang, and C.-L. Wei, "Global mapping of c-Myc binding sites and target gene networks in human B cells," *Proc. Natl. Acad. Sci. U. S. A.*, vol. 103, no. 47, pp. 17834–17839, Nov. 2006.

[173] P. C. Fernandez, S. R. Frank, L. Wang, M. Schroeder, S. Liu, J. Greene, A. Cocito, and B. Amati, "Genomic targets of the human c-Myc protein," *Genes Dev.*, vol. 17, no. 9, pp. 1115–1129, May 2003.

[174] T. R. Kress, A. Sabò, and B. Amati, "MYC: connecting selective transcriptional control to global RNA production," *Nat. Rev. Cancer*, vol. 15, no. 10, pp. 593–607, Oct. 2015.

[175] A. C. Davis, M. Wims, G. D. Spotts, S. R. Hann, and A. Bradley, "A null c-myc mutation causes lethality before 10.5 days of gestation in homozygotes and reduced fertility in heterozygous female mice," *Genes Dev.*, vol. 7, no. 4, pp. 671–682, Apr. 1993.

[176] E. Baena, A. Gandarillas, M. Vallespinós, J. Zanet, O. Bachs, C. Redondo, I. Fabregat, C. Martinez-A, and I. M. de Alborán, "c-Myc regulates cell size and ploidy but is not essential for postnatal proliferation in liver," *Proc. Natl. Acad. Sci. U. S. A.*, vol. 102, no. 20, pp. 7286–7291, May 2005.

[177] N. V. Varlakhanova, R. F. Cotterman, W. N. deVries, J. Morgan, L. R. Donahue, S. Murray, B. B. Knowles, and P. S. Knoepfler, "myc maintains embryonic stem cell pluripotency and self-renewal," *Differ. Res. Biol. Divers.*, vol. 80, no. 1, pp. 9–19, Jul. 2010.

[178] C. Bouchard, P. Staller, and M. Eilers, "Control of cell proliferation by Myc," *Trends Cell Biol.*, vol. 8, no. 5, pp. 202–206, May 1998.

[179] B. Hoffman and D. A. Liebermann, "Apoptotic signaling by c-MYC," *Oncogene*, vol. 27, no. 50, pp. 6462–6472, 2008.

[180] D. J. Sussman, J. Chung, and P. Leder, "In vitro and in vivo analysis of the c-myc RNA polymerase III promoter.," *Nucleic Acids Res.*, vol. 19, no. 18, pp. 5045–5052, Sep. 1991.

[181] V. H. Cowling and M. D. Cole, "The Myc Transactivation Domain Promotes Global Phosphorylation of the RNA Polymerase II Carboxy-Terminal Domain Independently of Direct DNA Binding," *Mol. Cell. Biol.*, vol. 27, no. 6, pp. 2059–2073, Mar. 2007.

[182] M. D. Cole and V. H. Cowling, "Transcription-independent functions of MYC: regulation of translation and DNA replication," *Nat. Rev. Mol. Cell Biol.*, vol. 9, no. 10, Oct. 2008.

[183] D. Dominguez-Sola, C. Y. Ying, C. Grandori, L. Ruggiero, B. Chen, M. Li, D. A. Galloway, W. Gu, J. Gautier, and R. Dalla-Favera, "Non-transcriptional control of DNA replication by c-Myc," *Nature*, vol. 448, no. 7152, pp. 445–451, Jul. 2007.

[184] S. Campaner and B. Amati, "Two sides of the Myc-induced DNA damage response: from tumor suppression to tumor maintenance," *Cell Div.*, vol. 7, p. 6, 2012.

[185] R. Wang, C. P. Dillon, L. Z. Shi, S. Milasta, R. Carter, D. Finkelstein, L. L. McCormick, P. Fitzgerald, H. Chi, J. Munger, and D. R. Green, "The Transcription Factor Myc Controls Metabolic Reprogramming upon T Lymphocyte Activation," *Immunity*, vol. 35, no. 6, pp. 871–882, Dec. 2011.

[186] S. Adachi, A. J. Obaya, Z. Han, N. Ramos-Desimone, J. H. Wyche, and J. M. Sedivy, "c-Myc Is Necessary for DNA Damage-Induced Apoptosis in the G2 Phase of the Cell Cycle," *Mol. Cell. Biol.*, vol. 21, no. 15, pp. 4929–4937, Aug. 2001.

[187] R. Araki, Y. Hoki, M. Uda, M. Nakamura, Y. Jincho, C. Tamura, M. Sunayama, S. Ando, M. Sugiura, M. A. Yoshida, Y. Kasama, and M. Abe, "Crucial role of c-Myc in the generation of induced pluripotent stem cells," *Stem Cells Dayt. Ohio*, vol. 29, no. 9, pp. 1362–1370, Sep. 2011.

[188] M. Schuhmacher, M. S. Staege, A. Pajic, A. Polack, U. H. Weidle, G. W. Bornkamm, D. Eick, and F. Kohlhuber, "Control of cell growth by c-Myc in the absence of cell division," *Curr. Biol.*, vol. 9, no. 21, pp. 1255–1258, Nov. 1999.

[189] P. Juin, A.-O. Hueber, T. Littlewood, and G. Evan, "c-Myc-induced sensitization to apoptosis is mediated through cytochrome c release," *Genes Dev.*, vol. 13, no. 11, pp. 1367–1381, Jun. 1999.

[190] S. Campaner, M. Doni, P. Hydbring, A. Verrecchia, L. Bianchi, D. Sardella, T. Schleker, D. Perna, S. Tronnersjö, M. Murga, O. Fernandez-Capetillo, M. Barbacid, L.-G. Larsson, and B. Amati, "Cdk2 suppresses cellular senescence induced by the c-myc oncogene," *Nat. Cell Biol.*, vol. 12, no. 1, pp. 54–59, Jan. 2010.

[191] H. Hermeking and D. Eick, "Mediation of c-Myc-induced apoptosis by p53," *Science*, vol. 265, no. 5181, pp. 2091–2093, Sep. 1994.

[192] D. A. Spandidos, "The effect of exogenous human ras and myc oncogenes in morphological differentiation of the rat pheochromocytoma PC12 cells," *Int. J. Dev. Neurosci. Off. J. Int. Soc. Dev. Neurosci.*, vol. 7, no. 1, pp. 1–4, 1989.

[193] P. Cabochette, G. Vega-Lopez, J. Bitard, K. Parain, R. Chemouny, C. Masson, C. Borday, M. Hedderich, K. A. Henningfeld, M. Locker, O. Bronchain, and M. Perron, "YAP controls retinal stem cell DNA replication timing and genomic stability," *eLife*, vol. 4.

[194] G. Bretones, M. D. Delgado, and J. León, "Myc and cell cycle control," *Biochim. Biophys. Acta BBA - Gene Regul. Mech.*, vol. 1849, no. 5, pp. 506–516, May 2015.

[195] C. Hindley and A. Philpott, "The cell cycle and pluripotency," *Biochem. J.*, vol. 451, no. 2, pp. 135–143, Apr. 2013.

[196] M. K. Mateyak, A. J. Obaya, and J. M. Sedivy, "c-Myc Regulates Cyclin D-Cdk4 and -Cdk6 Activity but Affects Cell Cycle Progression at Multiple Independent Points," *Mol. Cell. Biol.*, vol. 19, no. 7, pp. 4672–4683, Jul. 1999.

[197] "Myc activation of cyclin E/Cdk2 kinase involves induction of cyclin E gene transcription and inhibition of p27Kip1 binding to newly formed complexes," *Publ. Online 21 May 1997 Doi101038sjonc1201197*, vol. 14, no. 20, May 1997.

[198] J. Y. Leung, G. L. Ehmann, P. H. Giangrande, and J. R. Nevins, "A role for Myc in facilitating transcription activation by E2F1," *Oncogene*, vol. 27, no. 30, pp. 4172–4179, Mar. 2008.

[199] G. Leone, J. DeGregori, R. Sears, L. Jakoi, and J. R. Nevins, "Myc and Ras collaborate in inducing accumulation of active cyclin E/Cdk2 and E2F," *Nature*, vol. 387, no. 6631, pp. 422–426, May 1997.

[200] M. Zörnig and G. I. Evan, "Cell cycle: On target with Myc," *Curr. Biol.*, vol. 6, no. 12, pp. 1553–1556, Dec. 1996.

[201] D. Barsyte-Lovejoy, S. K. Lau, P. C. Boutros, F. Khosravi, I. Jurisica, I. L. Andrulis, M. S. Tsao, and L. Z. Penn, "The c-Myc Oncogene Directly Induces the H19 Noncoding RNA by Allele-Specific Binding to Potentiate Tumorigenesis," *Cancer Res.*, vol. 66, no. 10, pp. 5330–5337, May 2006.

[202] M. Kitagawa, K. Kitagawa, Y. Kotake, H. Niida, and T. Ohhata, "Cell cycle regulation by long non-coding RNAs," *Cell. Mol. Life Sci.*, vol. 70, no. 24, pp. 4785–4794, Jul. 2013.

[203] R. E. Rhoads, *MiRNA Regulation of the Translational Machinery*. Springer, 2010.

[204] L. Lupini, C. Bassi, M. Ferracin, N. Bartonicek, L. D'Abundo, B. Zagatti, E. Callegari, G. Musa, F. Moshiri, L. Gramantieri, F. J. Corrales, A. J. Enright, S. Sabbioni, and M. Negrini, "miR-221 affects multiple cancer pathways by modulating the level of hundreds messenger RNAs," *Front. Genet.*, vol. 4, Apr. 2013.

[205] M. Gabay, Y. Li, and D. W. Felsher, "MYC activation is a hallmark of cancer initiation and maintenance," *Cold Spring Harb. Perspect. Med.*, vol. 4, no. 6, Jun. 2014.

[206] D. W. Felsher, "MYC Inactivation Elicits Oncogene Addiction through Both Tumor Cell-Intrinsic and Host-Dependent Mechanisms," *Genes Cancer*, vol. 1, no. 6, pp. 597–604, Jun. 2010.

[207] L. Zech, U. Haglund, K. Nilsson, and G. Klein, "Characteristic chromosomal abnormalities in biopsies and lymphoid-cell lines from patients with Burkitt and non-Burkitt lymphomas," *Int. J. Cancer J. Int. Cancer*, vol. 17, no. 1, pp. 47–56, Jan. 1976.

[208] P. A. Northcott, D. J. H. Shih, J. Peacock, L. Garzia, A. Sorana Morrissy, T. Zichner, A. M. Stütz, A. Korshunov, J. Reimand, S. E. Schumacher, R. Beroukhim, D. W. Ellison, C. R. Marshall, A. C. Lionel, S. Mack, A. Dubuc, Y. Yao, V. Ramaswamy, B. Luu, A. Rolider, F. M. G. Cavalli, X. Wang, M. Remke, X. Wu, R. Y. B. Chiu, A. Chu, E. Chuah, R. D. Corbett, G. R. Hoad, S. D. Jackman, Y. Li, A. Lo, K. L. Mungall, K. Ming Nip, J. Q. Qian, A. G. J. Raymond, N. Thiessen, R. J. Varhol, I. Birol, R. A. Moore, A. J. Mungall, R. Holt, D. Kawauchi, M. F. Roussel, M. Kool, D. T. W. Jones, H. Witt, A. Fernandez-L, A. M. Kenney, R. J. Wechsler-Reya, P. Dirks, T. Aviv, W. A. Grajkowska, M. Perek-Polnik, C. C. Haberler, O. Delattre, S. S. Reynaud, F. F. Doz, S. S. Pernet-Fattet, B.-K. Cho, S.-K. Kim, K.-C. Wang, W. Scheurlen, C. G. Eberhart, M. Fèvre-Montange, A. Jouvet, I. F. Pollack, X. Fan, K. M. Muraszko, G. Yancey Gillespie, C. Di Rocco, L. Massimi, E. M. C. Michiels, N. K. Kloosterhof, P. J. French, J. M. Kros, J. M. Olson, R. G. Ellenbogen, K. Zitterbart, L. Kren, R. C. Thompson, M. K. Cooper, B. Lach, R. E. McLendon, D. D. Bigner, A. Fontebasso, S. Albrecht, N. Jabado, J. C. Lindsey, S. Bailey, N. Gupta, W. A. Weiss, L. Bognár, A. Klekner, T. E. Van Meter, T. Kumabe, T. Tominaga, S. K. Elbabaa, J. R. Leonard, J. B. Rubin, L. M. Liau, E. G. Van Meir, M. Fouladi, H. Nakamura, G. Cinalli, M. Garami, P. Hauser, A. G. Saad, A. Iolascon, S. Jung, C. G. Carlotti, R. Vibhakar, Y. Shin Ra, S. Robinson, M. Zollo, C. C. Faria, J. A. Chan, M. L. Levy, P. H. B. Sorensen, M. Meyerson, S. L. Pomeroy, Y.-J. Cho, G. D. Bader, U. Tabori, C. E. Hawkins, E. Bouffet, S. W. Scherer, J. T. Rutka, D. Malkin, S. C. Clifford, S. J. M. Jones, J. O. Korbel, S. M. Pfister, M. A. Marra, and M. D. Taylor, "Subgroup-specific structural variation across 1,000 medulloblastoma genomes," *Nature*, vol. 488, no. 7409, pp. 49–56, Aug. 2012.

[209] T. C. G. A. Network, "Comprehensive molecular characterization of human colon and rectal cancer," *Nature*, vol. 487, no. 7407, pp. 330–337, Jul. 2012.

[210] M. L. Cher, G. S. Bova, D. H. Moore, E. J. Small, P. R. Carroll, S. S. Pin, J. I. Epstein, W. B. Isaacs, and R. H. Jensen, "Genetic Alterations in Untreated Metastases and Androgen-independent Prostate Cancer Detected by Comparative Genomic Hybridization and Allelotyping," *Cancer Res.*, vol. 56, no. 13, pp. 3091–3102, Jul. 1996.

[211] L. Thomas, J. Stamberg, I. Gojo, Y. Ning, and A. P. Rapoport, "Double minute chromosomes in monoblastic (M5) and myeloblastic (M2) acute myeloid leukemia: Two case reports and a review of literature," *Am. J. Hematol.*, vol. 77, no. 1, pp. 55–61, Sep. 2004.

[212] S. Tuupanen, M. Turunen, R. Lehtonen, O. Hallikas, S. Vanharanta, T. Kivioja, M. Björklund, G. Wei, J. Yan, I. Niittymäki, J.-P. Mecklin, H. Järvinen, A. Ristimäki, M. Di-Bernardo, P. East, L. Carvajal-Carmona, R. S. Houlston, I. Tomlinson, K. Palin, E. Ukkonen, A. Karhu, J. Taipale, and L. A. Aaltonen, "The common colorectal cancer predisposition SNP rs6983267 at chromosome 8q24 confers potential to enhanced Wnt signaling," *Nat. Genet.*, vol. 41, no. 8, pp. 885–890, Aug. 2009.

[213] S. Rennoll and G. Yochum, "Regulation of MYC gene expression by aberrant Wnt/β-catenin signaling in colorectal cancer," *World J. Biol. Chem.*, vol. 6, no. 4, pp. 290–300, Nov. 2015.

[214] R. Schmitz, M. Ceribelli, S. Pittaluga, G. Wright, and L. M. Staudt, "Oncogenic Mechanisms in Burkitt Lymphoma," *Cold Spring Harb. Perspect. Med.*, vol. 4, no. 2, p. a014282, Feb. 2014.

[215] L. Masramon, R. Arribas, S. Tórtola, M. Perucho, and M. A. Peinado, "Moderate amplifications of the c-myc gene correlate with molecular and clinicopathological parameters in colorectal cancer.," *Br. J. Cancer*, vol. 77, no. 12, pp. 2349–2356, Jun. 1998.

[216] H. Hermeking, "The MYC oncogene as a cancer drug target," *Curr. Cancer Drug Targets*, vol. 3, no. 3, pp. 163–175, Jun. 2003.

[217] N. E. Hynes and H. A. Lane, "Myc and mammary cancer: Myc is a downstream effector of the ErbB2 receptor tyrosine kinase," *J. Mammary Gland Biol. Neoplasia*, vol. 6, no. 1, pp. 141–150, Jan. 2001.

[218] J. Xu, Y. Chen, and O. I. Olopade, "MYC and Breast Cancer," *Genes Cancer*, vol. 1, no. 6, pp. 629–640, Jun. 2010.

[219] D. Hawksworth, L. Ravindranath, Y. Chen, B. Furusato, I. A. Sesterhenn, D. G. McLeod, S. Srivastava, and G. Petrovics, "Overexpression of C-MYC oncogene in prostate cancer predicts biochemical recurrence," *Prostate Cancer Prostatic Dis.*, vol. 13, no. 4, pp. 311–315, Dec. 2010.

[220] C. M. Koh, C. J. Bieberich, C. V. Dang, W. G. Nelson, S. Yegnasubramanian, and A. M. De Marzo, "MYC and Prostate Cancer," *Genes Cancer*, vol. 1, no. 6, pp. 617–628, Jun. 2010.

[221] K. Rosner, D. R. Mehregan, E. Kirou, J. Abrams, S. Kim, M. Campbell, J. Frieder, K. Lawrence, B. Haynes, M. P. V. Shekhar, K. Rosner, D. R. Mehregan, E. Kirou, J. Abrams, S. Kim, M. Campbell, J. Frieder, K. Lawrence, B. Haynes, and M. P. V. Shekhar, "Melanoma Development and Progression Are Associated with Rad6 Upregulation and β-Catenin Relocation to the Cell Membrane, Melanoma Development and Progression Are Associated with Rad6 Upregulation and β-Catenin Relocation to the Cell Membrane," *J. Skin Cancer J. Skin Cancer*, vol. 2014, 2014, p. e439205, May 2014.

[222] R. Grover, D. A. Ross, G. D. Wilson, and R. Sanders, "Measurement of c-myc oncoprotein provides an independent prognostic marker for regional metastatic melanoma," *Br. J. Plast. Surg.*, vol. 50, no. 7, pp. 478–482, Oct. 1997.

[223] P. Polakis, "Wnt signaling and cancer," *Genes Dev.*, vol. 14, no. 15, pp. 1837–1851, Aug. 2000.

[224] O. H. Ng, Y. Erbilgin, S. Firtina, T. Celkan, Z. Karakas, G. Aydogan, E. Turkkan, Y. Yildirmak, C. Timur, E. Zengin, J. J. M. van Dongen, F. J. T. Staal, U. Ozbek, and M. Sayitoglu, "Deregulated WNT signaling in childhood T-cell acute lymphoblastic leukemia," *Blood Cancer J.*, vol. 4, no. 3, p. e192, Mar. 2014.

[225] D. J. Stewart, "Wnt Signaling Pathway in Non–Small Cell Lung Cancer," *J. Natl. Cancer Inst.*, vol. 106, no. 1, p. djt356, Jan. 2014.

[226] S. P. Acebron, E. Karaulanov, B. S. Berger, Y.-L. Huang, and C. Niehrs, "Mitotic Wnt Signaling Promotes Protein Stabilization and Regulates Cell Size," *Mol. Cell*, vol. 54, no. 4, pp. 663–674, May 2014.

[227] Y. He, Z. Liu, C. Qiao, M. Xu, J. Yu, and G. Li, "Expression and significance of Wnt signaling components and their target genes in breast carcinoma," *Mol. Med. Rep.*, vol. 9, no. 1, pp. 137–143, Jan. 2014.

[228] V. Barbetti, A. Morandi, I. Tusa, G. Digiacomo, M. Riverso, I. Marzi, M. G. Cipolleschi, S. Bessi, A. Giannini, A. Di Leo, P. Dello Sbarba, and E. Rovida, "Chromatin-associated CSF-1R binds to the promoter of proliferation-related genes in breast cancer cells," *Oncogene*, vol. 33, no. 34, pp. 4359–4364, Aug. 2014.

[229] B. Culjkovic-Kraljacic, T. M. Fernando, R. Marullo, N. Calvo-Vidal, A. Verma, S. Yang, F. Tabbò, M. Gaudiano, H. Zahreddine, R. L. Goldstein, J. Patel, T. Taldone, G. Chiosis, M. Ladetto, P. Ghione, R. Machiorlatti, O. Elemento, G. Inghirami, A. Melnick, K. L. B. Borden, and L. Cerchietti, "Combinatorial targeting of nuclear export and translation of RNA inhibits aggressive B-cell lymphomas," *Blood*, vol. 127, no. 7, pp. 858–868, Feb. 2016.

[230] A. A. Chakraborty and W. P. Tansey, "Do changes in the c-MYC coding sequence contribute to tumorigenesis?," *Mol. Cell. Oncol.*, vol. 2, no. 2, p. e965631, Apr. 2015.

[231] X. Wang, M. Cunningham, X. Zhang, S. Tokarz, B. Laraway, M. Troxell, and R. C. Sears, "Phosphorylation Regulates c-Myc's Oncogenic Activity in the Mammary Gland," *Cancer Res.*, vol. 71, no. 3, pp. 925–936, Feb. 2011.

[232] A. A. Chakraborty, C. Scuoppo, S. Dey, L. R. Thomas, S. L. Lorey, S. W. Lowe, and W. P. Tansey, "A common functional consequence of tumor-derived mutations within c-MYC," *Oncogene*, vol. 34, no. 18, pp. 2406–2409, Apr. 2015.

[233] Q. Zhang, E. Spears, D. N. Boone, Z. Li, M. A. Gregory, and S. R. Hann, "Domain-specific c-Myc ubiquitylation controls c-Myc transcriptional and apoptotic activity," *Proc. Natl. Acad. Sci.*, vol. 110, no. 3, pp. 978–983, Jan. 2013.

[234] D. Perna, G. Fagà, A. Verrecchia, M. M. Gorski, I. Barozzi, V. Narang, J. Khng, K. C. Lim, W.-K. Sung, R. Sanges, E. Stupka, T. Oskarsson, A. Trumpp, C.-L. Wei, H. Müller, and B. Amati, "Genome-wide mapping of Myc binding and gene regulation in serum-stimulated fibroblasts," *Oncogene*, vol. 31, no. 13, pp. 1695–1709, Mar. 2012.

[235] R. Kanwal and S. Gupta, "Epigenetic modifications in cancer," *Clin. Genet.*, vol. 81, no. 4, pp. 303–311, Apr. 2012.

[236] K. Galaktionov, X. Chen, and D. Beach, "Cdc25 cell-cycle phosphatase as a target of c-myc," *Nature*, vol. 382, no. 6591, pp. 511–517, Aug. 1996.

[237] H. Hermeking, C. Rago, M. Schuhmacher, Q. Li, J. F. Barrett, A. J. Obaya, B. C. O'Connell, M. K. Mateyak, W. Tam, F. Kohlhuber, C. V. Dang, J. M. Sedivy, D. Eick, B. Vogelstein, and K. W. Kinzler, "Identification of CDK4 as a target of c-MYC," *Proc. Natl. Acad. Sci. U. S. A.*, vol. 97, no. 5, pp. 2229–2234, Feb. 2000.

[238] A. Cascón and M. Robledo, "MAX and MYC: a heritable breakup," *Cancer Res.*, vol. 72, no. 13, pp. 3119–3124, Jul. 2012.

[239] I. Comino-Méndez, F. J. Gracia-Aznárez, F. Schiavi, I. Landa, L. J. Leandro-García, R. Letón, E. Honrado, R. Ramos-Medina, D. Caronia, G. Pita, A. Gómez-Graña, A. A. de Cubas, L. Inglada-Pérez, A. Maliszewska, E. Taschin, S. Bobisse, G. Pica, P. Loli, R. Hernández-Lavado, J. A. Díaz, M. Gómez-Morales, A. González-Neira, G. Roncador, C. Rodríguez-Antona, J. Benítez, M. Mannelli, G. Opocher, M. Robledo, and A. Cascón, "Exome sequencing identifies MAX mutations as a cause of hereditary pheochromocytoma," *Nat. Genet.*, vol. 43, no. 7, pp. 663–667, Jul. 2011.

[240] A. R. Ferré-D'Amaré, G. C. Prendergast, E. B. Ziff, and S. K. Burley, "Recognition by Max of its cognate DNA through a dimeric b/HLH/Z domain," *Nature*, vol. 363, no. 6424, pp. 38–45, May 1993.

[241] A. Banerjee, J. Hu, and D. J. Goss, "Thermodynamics of Protein–Protein Interactions of cMyc, Max, and Mad: Effect of Polyions on Protein Dimerization," *Biochemistry (Mosc.)*, vol. 45, no. 7, pp. 2333–2338, Feb. 2006.

[242] J. M. O'Shea and D. E. Ayer, "Coordination of Nutrient Availability and Utilization by MAX- and MLX-Centered Transcription Networks," *Cold Spring Harb. Perspect. Med.*, vol. 3, no. 9, p. a014258, Sep. 2013.

[243] S. Rottmann and B. Lüscher, "The Mad Side of the Max Network: Antagonizing the Function of Myc and More," in *The Myc/Max/Mad Transcription Factor Network*, P. D. R. N. Eisenman, Ed. Springer Berlin Heidelberg, 2006, pp. 63–122.

[244] A. Sommer, S. Hilfenhaus, A. Menkel, E. Kremmer, C. Seiser, P. Loidl, and B. Lüscher, "Cell growth inhibition by the Mad/Max complex through recruitment of histone deacetylase activity," *Curr. Biol.*, vol. 7, no. 6, pp. 357–365, 1997.

[245] C. A. Hassig, T. C. Fleischer, A. N. Billin, S. L. Schreiber, and D. E. Ayer, "Histone deacetylase activity is required for full transcriptional repression by mSin3A," *Cell*, vol. 89, no. 3, pp. 341–347, 1997.

[246] Z. Ge, W. Li, N. Wang, C. Liu, Q. Zhu, M. Björkholm, A. Gruber, and D. Xu, "Chromatin remodeling: Recruitment of histone demethylase RBP2 by Mad1 for transcriptional repression of a Myc target gene, telomerase reverse transcriptase," *FASEB J.*, vol. 24, no. 2, pp. 579–586, 2010.

[247] A. Ullius, J. Lüscher-Firzlaff, I. G. Costa, G. Walsemann, A. H. Forst, E. G. Gusmao, K. Kapelle, H. Kleine, E. Kremmer, J. Vervoorts, and B. Lüscher, "The interaction of MYC with the trithorax protein ASH2L promotes gene transcription by regulating H3K27 modification," *Nucleic Acids Res.*, vol. 42, no. 11, pp. 6901–6920, Jul. 2014.

[248] B. Lüscher, "Function and regulation of the transcription factors of the Myc/Max/Mad network," *Gene*, vol. 277, no. 1–2, pp. 1–14, 2001.

[249] B. Lüscher, "MAD1 and its life as a MYC antagonist: an update," *Eur. J. Cell Biol.*, vol. 91, no. 6–7, pp. 506–514, Jul. 2012.

[250] D. Xu, N. Popov, M. Hou, Q. Wang, M. Björkholm, A. Gruber, A. R. Menkel, and M. Henriksson, "Switch from Myc/Max to Mad1/Max binding and decrease in histone acetylation at the telomerase reverse transcriptase promoter during differentiation of HL60 cells," *Proc. Natl. Acad. Sci. U. S. A.*, vol. 98, no. 7, pp. 3826–3831, 2001.

[251] C. Bouchard, O. Dittrich, A. Kiermaier, K. Dohmann, A. Menkel, M. Eilers, and B. Lüscher, "Regulation of cyclin D2 gene expression by the Myc/Max/Mad network: Myc-dependent TRRAP recruitment and histone acetylation at the cyclin D2 promoter," *Genes Dev.*, vol. 15, no. 16, pp. 2042–2047, 2001.

[252] K. M. Huynh, J.-W. Soh, R. Dash, D. Sarkar, P. B. Fisher, and D. Kang, "FOXM1 expression mediates growth suppression during terminal differentiation of HO-1 human metastatic melanoma cells," *J. Cell. Physiol.*, vol. 226, no. 1, pp. 194–204, 2011.

[253] C.-J. Lin, R. Cencic, J. R. Mills, F. Robert, and J. Pelletier, "c-Myc and eIF4F are components of a feedforward loop that links transcription and translation," *Cancer Res.*, vol. 68, no. 13, pp. 5326–5334, 2008.

[254] S. Rottmann, S. Speckgens, J. Lüscher-Firzlaff, and B. Lüscher, "Inhibition of apoptosis by MAD1 is mediated by repression of the PTEN tumor suppressor gene," *FASEB J.*, vol. 22, no. 4, pp. 1124–1134, 2008.

[255] C. M. Cultraro, T. Bino, and S. Segal, "Function of the c-Myc antagonist Mad1 during a molecular switch from proliferation to differentiation," *Mol. Cell. Biol.*, vol. 17, no. 5, pp. 2353–2359, 1997.

[256] J. C. Acosta, N. Ferrándiz, G. Bretones, V. Torrano, R. Blanco, C. Richard, B. O'Connell, J. Sedivy, M. D. Delgado, and J. León, "Myc inhibits p27-induced erythroid differentiation of leukemia cells by repressing erythroid master genes without reversing p27-mediated cell cycle arrest," *Mol. Cell. Biol.*, vol. 28, no. 24, pp. 7286–7295, 2008.

[257] K. Jiang, N. Hein, K. Eckert, J. Lüscher-Firzlaff, and B. Lüscher, "Regulation of the MAD1 promoter by G-CSF," *Nucleic Acids Res.*, vol. 36, no. 5, pp. 1517–1531, 2008.

[258] L.-G. Larsson, M. Pettersson, F. Öberg, K. Nilsson, and B. Lüscher, "Expression of mad, mxi1, max and c-myc during induced differentiation of hematopoietic cells: Opposite regulation of mad and c-myc," *Oncogene*, vol. 9, no. 4, pp. 1247–1252, 1994.

[259] A. Moustakas and C.-H. Heldin, "The regulation of TGFbeta signal transduction," *Dev. Camb. Engl.*, vol. 136, no. 22, pp. 3699–3714, Nov. 2009.

[260] L. Xu, J. Zhu, X. Hu, H. Zhu, H. T. Kim, J. LaBaer, A. Goldberg, and J. Yuan, "c-IAP1 Cooperates with Myc by Acting as a Ubiquitin Ligase for Mad1," *Mol. Cell*, vol. 28, no. 5, pp. 914–922, 2007.

[261] Z. Dai, W.-G. Zhu, C. D. Morrison, R. M. Brena, D. J. Smiraglia, A. Raval, Y.-Z. Wu, L. J. Rush, P. Ross, J. R. Molina, G. A. Otterson, and C. Plass, "A comprehensive search for DNA amplification in lung cancer identifies inhibitors of apoptosis cIAP1 and cIAP2 as candidate oncogenes," *Hum. Mol. Genet.*, vol. 12, no. 7, pp. 791–801, Apr. 2003.

[262] S.-A. Jung, Y.-M. Park, S.-W. Hong, J.-H. Moon, J.-S. Shin, H.-R. Lee, S.-H. Ha, D.-H. Lee, J. H. Kim, S.-M. Kim, J. E. Kim, K. Kim, Y. S. Hong, E. K. Choi, J. S. Lee, D.-H. Jin, and T. Kim, "Cellular Inhibitor of Apoptosis Protein 1 (cIAP1) Stability Contributes to YM155 Resistance in Human Gastric Cancer Cells," *J. Biol. Chem.*, vol. 290, no. 16, pp. 9974–9985, Apr. 2015.

[263] J. Zhu, J. Blenis, and J. Yuan, "Activation of PI3K/Akt and MAPK pathways regulates Myc-mediated transcription by phosphorylating and promoting the degradation of Mad1," *Proc. Natl. Acad. Sci. U. S. A.*, vol. 105, no. 18, pp. 6584–6589, 2008.

[264] Y. Kimura and K. Tanaka, "Regulatory mechanisms involved in the control of ubiquitin homeostasis," *J. Biochem. (Tokyo)*, vol. 147, no. 6, pp. 793–798, Jun. 2010.

[265] J. Gong and J. Huo, "New insights into the mechanism of F-box proteins in colorectal cancer (Review)," *Oncol. Rep.*, vol. 33, no. 5, pp. 2113–2120, May 2015.

[266] J. Jin, X. Li, S. P. Gygi, and J. W. Harper, "Dual E1 activation systems for ubiquitin differentially regulate E2 enzyme charging," *Nature*, vol. 447, no. 7148, pp. 1135–1138, Jun. 2007.

[267] Y.-H. Chiu, Q. Sun, and Z. J. Chen, "E1-L2 activates both ubiquitin and FAT10," *Mol. Cell*, vol. 27, no. 6, pp. 1014–1023, Sep. 2007.

[268] C. Pelzer, I. Kassner, K. Matentzoglu, R. K. Singh, H.-P. Wollscheid, M. Scheffner, G. Schmidtke, and M. Groettrup, "UBE1L2, a novel E1 enzyme specific for ubiquitin," *J. Biol. Chem.*, vol. 282, no. 32, pp. 23010–23014, Aug. 2007.

[269] S. Lorenz, A. J. Cantor, M. Rape, and J. Kuriyan, "Macromolecular juggling by ubiquitylation enzymes," *BMC Biol.*, vol. 11, p. 65, 2013.

[270] M. B. Metzger, J. N. Pruneda, R. E. Klevit, and A. M. Weissman, "RING-type E3 ligases: Master manipulators of E2 ubiquitin-conjugating enzymes and ubiquitination," *Biochim. Biophys. Acta BBA - Mol. Cell Res.*, vol. 1843, no. 1, pp. 47–60, Jan. 2014.

[271] J. M. Peters, W. W. Franke, and J. A. Kleinschmidt, "Distinct 19 S and 20 S subcomplexes of the 26 S proteasome and their distribution in the nucleus and the cytoplasm," *J. Biol. Chem.*, vol. 269, no. 10, pp. 7709–7718, Mar. 1994.

[272] N. D. Nassif, S. E. Cambray, and D. A. Kraut, "Slipping up: Partial substrate degradation by ATP-dependent proteases," *IUBMB Life*, vol. 66, no. 5, pp. 309–317, May 2014.

[273] M. Bianchi, E. Giacomini, R. Crinelli, L. Radici, E. Carloni, and M. Magnani, "Dynamic transcription of ubiquitin genes under basal and stressful conditions and new insights into the multiple UBC transcript variants," *Gene*, vol. 573, no. 1, pp. 100–109, Nov. 2015.

[274] C. P. Grou, M. P. Pinto, A. V. Mendes, P. Domingues, and J. E. Azevedo, "The de novo synthesis of ubiquitin: identification of deubiquitinases acting on ubiquitin precursors," *Sci. Rep.*, vol. 5, p. 12836, Aug. 2015.

[275] K. Rajalingam and I. Dikic, "SnapShot: Expanding the Ubiquitin Code," *Cell*, vol. 164, no. 5, p. 1074–1074.e1, Feb. 2016.

[276] F. Ohtake, Y. Saeki, K. Sakamoto, K. Ohtake, H. Nishikawa, H. Tsuchiya, T. Ohta, K. Tanaka, and J. Kanno, "Ubiquitin acetylation inhibits polyubiquitin chain elongation," *EMBO Rep.*, vol. 16, no. 2, pp. 192–201, Feb. 2015.

[277] S. Dantuluri, Y. Wu, N. L. Hepowit, H. Chen, S. Chen, and J. Maupin-Furlow, "Proteome targets of ubiquitin-like samp1ylation are associated with sulfur metabolism and oxidative stress in Haloferax volcanii," *Proteomics*, Feb. 2016.

[278] J. Herrmann, L. O. Lerman, and A. Lerman, "Ubiquitin and Ubiquitin-Like Proteins in Protein Regulation," *Circ. Res.*, vol. 100, no. 9, pp. 1276–1291, May 2007.

[279] Y. Gao, S. S. Theng, W.-C. Mah, and C. G. L. Lee, "Silibinin down-regulates FAT10 and modulate TNF-α/IFN-γ-induced chromosomal instability and apoptosis sensitivity," *Biol. Open*, vol. 4, no. 8, pp. 961–969, 2015.

[280] C. E. Berndsen and C. Wolberger, "New insights into ubiquitin E3 ligase mechanism," *Nat. Struct. Mol. Biol.*, vol. 21, no. 4, pp. 301–307, Apr. 2014.

[281] G. Zinzalla, "Paving the way to targeting HECT ubiquitin ligases," *Future Med. Chem.*, vol. 7, no. 16, pp. 2107–2111, Oct. 2015.

[282] M. B. Metzger, V. A. Hristova, and A. M. Weissman, "HECT and RING finger families of E3 ubiquitin ligases at a glance," *J Cell Sci*, vol. 125, no. 3, pp. 531–537, Feb. 2012.

[283] R. Budhidarmo, Y. Nakatani, and C. L. Day, "RINGs hold the key to ubiquitin transfer," *Trends Biochem. Sci.*, vol. 37, no. 2, pp. 58–65, Feb. 2012.

[284] D. M. Wenzel, K. E. Stoll, and R. E. Klevit, "E2s: structurally economical and functionally replete," *Biochem. J.*, vol. 433, no. 1, pp. 31–42, Jan. 2011.

[285] T. Cardozo and M. Pagano, "The SCF ubiquitin ligase: insights into a molecular machine," *Nat. Rev. Mol. Cell Biol.*, vol. 5, no. 9, pp. 739–751, Sep. 2004.

[286] Z. Chen, J. Sui, F. Zhang, and C. Zhang, "Cullin Family Proteins and Tumorigenesis: Genetic Association and Molecular Mechanisms," *J. Cancer*, vol. 6, no. 3, pp. 233–242, Jan. 2015.

[287] V. A. Hristova, D. K. Stringer, and A. M. Weissman, "Cullin RING Ligases: Glommed by Glomulin," *Mol. Cell*, vol. 47, no. 3, pp. 331–332, Aug. 2012.

[288] J. R. Skaar, J. K. Pagan, and M. Pagano, "Mechanisms and function of substrate recruitment by F-box proteins," *Nat. Rev. Mol. Cell Biol.*, vol. 14, no. 6, Jun. 2013.

[289] H. C. Ardley and P. A. Robinson, "E3 ubiquitin ligases," *Essays Biochem.*, vol. 41, pp. 15–30, 2005.

[290] A. W. Lau, Y. Liu, A. E. Tron, H. Inuzuka, and W. Wei, "The Role of FBXW Subfamily of F-box Proteins in Tumorigenesis," in *SCF and APC E3 Ubiquitin Ligases in Tumorigenesis*, Springer International Publishing, 2014, pp. 15–45.

[291] Y. Liu, S. Ren, A. Castellanos-Martin, J. Perez-Losada, Y.-W. Kwon, Y. Huang, Z. Wang, M. Abad, J. J. Cruz-Hernandez, C. A. Rodriguez, Y. Sun, and J.-H. Mao, "Multiple novel alternative splicing forms of FBXW7α have a translational modulatory function and show specific alteration in human cancer," *PloS One*, vol. 7, no. 11, p. e49453, 2012.

[292] J. E. Grim, S. E. Knoblaugh, K. A. Guthrie, A. Hagar, J. Swanger, J. Hespelt, J. J. Delrow, T. Small, W. M. Grady, K. I. Nakayama, and B. E. Clurman, "Fbw7 and p53 Cooperatively Suppress Advanced and Chromosomally Unstable Intestinal Cancer," *Mol. Cell. Biol.*, vol. 32, no. 11, pp. 2160–2167, Jun. 2012.

[293] M. Welcker and B. E. Clurman, "FBW7 ubiquitin ligase: a tumour suppressor at the crossroads of cell division, growth and differentiation," *Nat. Rev. Cancer*, vol. 8, no. 2, pp. 83–93, Feb. 2008.

[294] X. Tang, S. Orlicky, Z. Lin, A. Willems, D. Neculai, D. Ceccarelli, F. Mercurio, B. H. Shilton, F. Sicheri, and M. Tyers, "Suprafacial Orientation of the SCFCdc4 Dimer Accommodates Multiple Geometries for Substrate Ubiquitination," *Cell*, vol. 129, no. 6, pp. 1165–1176, Jun. 2007.

[295] D. Wu and W. Pan, "GSK3: a multifaceted kinase in Wnt signaling," *Trends Biochem. Sci.*, vol. 35, no. 3, pp. 161–168, Mar. 2010.

[296] R. S. Jope, C. J. Yuskaitis, and E. Beurel, "Glycogen Synthase Kinase-3 (GSK3): Inflammation, Diseases, and Therapeutics," *Neurochem. Res.*, vol. 32, no. 4–5, pp. 577–595, 2007.

[297] C. H. Spruck, H. Strohmaier, O. Sangfelt, H. M. Müller, M. Hubalek, E. Müller-Holzner, C. Marth, M. Widschwendter, and S. I. Reed, "hCDC4 gene mutations in endometrial cancer," *Cancer Res.*, vol. 62, no. 16, pp. 4535–4539, Aug. 2002.

[298] L. Wang, X. Ye, Y. Liu, W. Wei, and Z. Wang, "Aberrant regulation of FBW7 in cancer," *Oncotarget*, vol. 5, no. 8, pp. 2000–2015, Mar. 2014.

[299] J. Cao, M.-H. Ge, and Z.-Q. Ling, "Fbxw7 Tumor Suppressor: A Vital Regulator Contributes to Human Tumorigenesis," *Medicine (Baltimore)*, vol. 95, no. 7, p. e2496, Feb. 2016.

[300] S. Ji, Y. Qin, S. Shi, X. Liu, H. Hu, H. Zhou, J. Gao, B. Zhang, W. Xu, J. Liu, D. Liang, L. Liu, C. Liu, J. Long, H. Zhou, P. J. Chiao, J. Xu, Q. Ni, D. Gao, and X. Yu, "ERK kinase phosphorylates and destabilizes the tumor suppressor FBW7 in pancreatic cancer," *Cell Res.*, vol. 25, no. 5, pp. 561–573, May 2015.

[301] V. Kumar, R. Palermo, C. Talora, A. F. Campese, S. Checquolo, D. Bellavia, L. Tottone, G. Testa, E. Miele, S. Indraccolo, A. Amadori, E. Ferretti, A. Gulino, A. Vacca, and I. Screpanti, "Notch and NF-kB signaling pathways regulate miR-223/FBXW7 axis in T-cell acute lymphoblastic leukemia," *Leukemia*, vol. 28, no. 12, pp. 2324–2335, Dec. 2014.

[302] "Cell Defenses and the Sunshine Vitamin - vitamind-nov07.pdf." .

[303] J. H. White, "Vitamin D Signaling, Infectious Diseases, and Regulation of Innate Immunity," *Infect. Immun.*, vol. 76, no. 9, pp. 3837–3843, Sep. 2008.

[304] M. F. Holick, "Vitamin D Deficiency," *N. Engl. J. Med.*, vol. 357, no. 3, pp. 266–281, Jul. 2007.

[305] A. Arabi, R. El Rassi, and G. El-Hajj Fuleihan, "Hypovitaminosis D in developing countries-prevalence, risk factors and outcomes," *Nat. Rev. Endocrinol.*, vol. 6, no. 10, pp. 550–561, Oct. 2010.

[306] A. Gurlek, M. R. Pittelkow, and R. Kumar, "Modulation of growth factor/cytokine synthesis and signaling by 1alpha,25-dihydroxyvitamin D(3): implications in cell growth and differentiation," *Endocr. Rev.*, vol. 23, no. 6, pp. 763–786, Dec. 2002.

[307] R. Lin, Y. Nagai, R. Sladek, Y. Bastien, J. Ho, K. Petrecca, G. Sotiropoulou, E. P. Diamandis, T. J. Hudson, and J. H. White, "Expression profiling in squamous carcinoma cells reveals pleiotropic effects of vitamin D3 analog EB1089 signaling on cell proliferation, differentiation, and immune system regulation," *Mol. Endocrinol. Baltim. Md*, vol. 16, no. 6, pp. 1243–1256, Jun. 2002.

[308] E. Giovannucci, Y. Liu, E. B. Rimm, B. W. Hollis, C. S. Fuchs, M. J. Stampfer, and W. C. Willett, "Prospective study of predictors of vitamin D status and cancer incidence and mortality in men," *J. Natl. Cancer Inst.*, vol. 98, no. 7, pp. 451–459, Apr. 2006.

[309] Z. Liu, J. I. Calderon, Z. Zhang, E. M. Sturgis, M. R. Spitz, and Q. Wei, "Polymorphisms of vitamin D receptor gene protect against the risk of head and neck cancer," *Pharmacogenet. Genomics*, vol. 15, no. 3, pp. 159–165, Mar. 2005.

[310] J. E. Manson, S. T. Mayne, and S. K. Clinton, "Vitamin D and prevention of cancer--ready for prime time?," *N. Engl. J. Med.*, vol. 364, no. 15, pp. 1385–1387, Apr. 2011.

[311] J. Nicholas, "Vitamin D and Cancer: Uncertainty Persists; Research Continues," *J. Natl. Cancer Inst.*, May 2011.

[312] M. Hewison, F. Burke, K. N. Evans, D. A. Lammas, D. M. Sansom, P. Liu, R. L. Modlin, and J. S. Adams, "Extra-renal 25-hydroxyvitamin D3-1alpha-hydroxylase in human health and disease," *J. Steroid Biochem. Mol. Biol.*, vol. 103, no. 3–5, pp. 316–321, Mar. 2007.

[313] D. Zehnder, R. Bland, M. C. Williams, R. W. McNinch, A. J. Howie, P. M. Stewart, and M. Hewison, "Extrarenal expression of 25-hydroxyvitamin d(3)-1 alpha-hydroxylase," *J. Clin. Endocrinol. Metab.*, vol. 86, no. 2, pp. 888–894, Feb. 2001.

[314] S. Toropainen, S. Väisänen, S. Heikkinen, and C. Carlberg, "The down-regulation of the human MYC gene by the nuclear hormone 1alpha,25-dihydroxyvitamin D3 is associated with cycling of corepressors and histone deacetylases," *J. Mol. Biol.*, vol. 400, no. 3, pp. 284–294, Jul. 2010.

[315] J. N. P. Rohan and N. L. Weigel, "1Alpha,25-dihydroxyvitamin D3 reduces c-Myc expression, inhibiting proliferation and causing G1 accumulation in C4-2 prostate cancer cells," *Endocrinology*, vol. 150, no. 5, pp. 2046–2054, May 2009.

[316] M. Eilers and R. N. Eisenman, "Myc's broad reach," *Genes Dev.*, vol. 22, no. 20, pp. 2755–2766, Oct. 2008.

[317] F. Morrish, N. Isern, M. Sadilek, M. Jeffrey, and D. M. Hockenbery, "c-Myc activates multiple metabolic networks to generate substrates for cell-cycle entry," *Oncogene*, vol. 28, no. 27, pp. 2485–2491, Jul. 2009.

[318] R. Bouillon, G. Carmeliet, L. Verlinden, E. van Etten, A. Verstuyf, H. F. Luderer, L. Lieben, C. Mathieu, and M. Demay, "Vitamin D and human health: lessons from vitamin D receptor null mice," *Endocr. Rev.*, vol. 29, no. 6, pp. 726–776, Oct. 2008.

[319] L. Yang and R. Peng, "Unveiling hair follicle stem cells," *Stem Cell Rev.*, vol. 6, no. 4, pp. 658–664, Dec. 2010.

[320] S. Pelengaris, T. Littlewood, M. Khan, G. Elia, and G. Evan, "Reversible activation of c-Myc in skin: induction of a complex neoplastic phenotype by a single oncogenic lesion," *Mol. Cell*, vol. 3, no. 5, pp. 565–577, May 1999.

[321] S. Pelengaris, M. Khan, and G. Evan, "c-MYC: more than just a matter of life and death," *Nat. Rev. Cancer*, vol. 2, no. 10, pp. 764–776, Oct. 2002.

[322] K. M. Crusio, B. King, L. B. Reavie, and I. Aifantis, "The ubiquitous nature of cancer: the role of the SCF(Fbw7) complex in development and transformation," *Oncogene*, vol. 29, no. 35, pp. 4865–4873, Sep. 2010.

[323] I. Arnold and F. M. Watt, "c-Myc activation in transgenic mouse epidermis results in mobilization of stem cells and differentiation of their progeny," *Curr. Biol. CB*, vol. 11, no. 8, pp. 558–568, Apr. 2001.

[324] R. L. Waikel, Y. Kawachi, P. A. Waikel, X. J. Wang, and D. R. Roop, "Deregulated expression of c-Myc depletes epidermal stem cells," *Nat. Genet.*, vol. 28, no. 2, pp. 165–168, Jun. 2001.

[325] F. Santiago, E. Clark, S. Chong, C. Molina, F. Mozafari, R. Mahieux, M. Fujii, N. Azimi, and F. Kashanchi, "Transcriptional Up-Regulation of the Cyclin D2 Gene and Acquisition of New Cyclin-Dependent Kinase Partners in Human T-Cell Leukemia Virus Type 1-Infected Cells," *J. Virol.*, vol. 73, no. 12, pp. 9917–9927, Dec. 1999.

[326] H. Shima, M. Nakayasu, S. Aonuma, T. Sugimura, and M. Nagao, "Loss of the MYC gene amplified in human HL-60 cells after treatment with inhibitors of poly(ADP-ribose) polymerase or with dimethyl sulfoxide.," *Proc. Natl. Acad. Sci. U. S. A.*, vol. 86, no. 19, pp. 7442–7445, Oct. 1989.

[327] M. Welcker, A. Orian, J. A. Grim, R. N. Eisenman, and B. E. Clurman, "A Nucleolar Isoform of the Fbw7 Ubiquitin Ligase Regulates c-Myc and Cell Size," *Curr. Biol.*, vol. 14, no. 20, pp. 1852–1857, Oct. 2004.

[328] S. V. Ramagopalan, A. Heger, A. J. Berlanga, N. J. Maugeri, M. R. Lincoln, A. Burrell, L. Handunnetthi, A. E. Handel, G. Disanto, S.-M. Orton, C. T. Watson, J. M. Morahan, G. Giovannoni, C. P. Ponting, G. C. Ebers, and J. C. Knight, "A ChIP-seq defined genome-wide map of vitamin D receptor binding: Associations with disease and evolution," *Genome Res.*, vol. 20, no. 10, pp. 1352–1360, 2010.

[329] J. Rozowsky, A. Abyzov, J. Wang, P. Alves, D. Raha, A. Harmanci, J. Leng, R. Bjornson, Y. Kong, N. Kitabayashi, N. Bhardwaj, M. Rubin, M. Snyder, and M. Gerstein, "AlleleSeq: analysis of allele-specific expression and binding in a network framework," *Mol. Syst. Biol.*, vol. 7, p. 522, 2011.

[330] T. C. He, A. B. Sparks, C. Rago, H. Hermeking, L. Zawel, L. T. da Costa, P. J. Morin, B. Vogelstein, and K. W. Kinzler, "Identification of c-MYC as a target of the APC pathway," *Science*, vol. 281, no. 5382, pp. 1509–1512, Sep. 1998.

[331] M. E. Beildeck, E. P. Gelmann, and S. W. Byers, "Cross-regulation of signaling pathways: an example of nuclear hormone receptors and the canonical Wnt pathway," *Exp. Cell Res.*, vol. 316, no. 11, pp. 1763–1772, Jul. 2010.

[332] M. J. Larriba, P. Ordóñez-Morán, I. Chicote, G. Martín-Fernández, I. Puig, A. Muñoz, and H. G. Pálmer, "Vitamin D Receptor Deficiency Enhances Wnt/β-Catenin Signaling and Tumor Burden in Colon Cancer," *PLOS ONE*, vol. 6, no. 8, p. e23524, Aug. 2011.

[333] I. Driskell, H. Oda, S. Blanco, E. Nascimento, P. Humphreys, and M. Frye, "The histone methyltransferase Setd8 acts in concert with c-Myc and is required to maintain skin," *EMBO J.*, vol. 31, no. 3, pp. 616–629, Feb. 2012.

[334] C. R. Leemans, B. J. M. Braakhuis, and R. H. Brakenhoff, "The molecular biology of head and neck cancer," *Nat. Rev. Cancer*, vol. 11, no. 1, pp. 9–22, Jan. 2011.

[335] B.-S. An, L. E. Tavera-Mendoza, V. Dimitrov, X. Wang, M. R. Calderon, H.-J. Wang, and J. H. White, "Stimulation of Sirt1-regulated FoxO protein function by the ligand-bound vitamin D receptor," *Mol. Cell. Biol.*, vol. 30, no. 20, pp. 4890–4900, Oct. 2010.

[336] N. Akutsu, R. Lin, Y. Bastien, A. Bestawros, D. J. Enepekides, M. J. Black, and J. H. White, "Regulation of gene Expression by 1alpha,25-dihydroxyvitamin D3 and Its analog EB1089 under growth-inhibitory conditions in squamous carcinoma Cells," *Mol. Endocrinol. Baltim. Md*, vol. 15, no. 7, pp. 1127–1139, Jul. 2001.

[337] M. R. Hughes, P. J. Malloy, B. W. O'Malley, J. W. Pike, and D. Feldman, "Genetic defects of the 1,25-dihydroxyvitamin D3 receptor," *J. Recept. Res.*, vol. 11, no. 1–4, pp. 699–716, 1991.

[338] S. V. Ramagopalan, A. Heger, A. J. Berlanga, N. J. Maugeri, M. R. Lincoln, A. Burrell, L. Handunnetthi, A. E. Handel, G. Disanto, S.-M. Orton, C. T. Watson, J. M. Morahan, G. Giovannoni, C. P. Ponting, G. C. Ebers, and J. C. Knight, "A ChIP-seq defined genome-wide map of vitamin D receptor binding: Associations with disease and evolution," *Genome Res.*, vol. 20, no. 10, pp. 1352–1360, 2010.

[339] J. Rozowsky, A. Abyzov, J. Wang, P. Alves, D. Raha, A. Harmanci, J. Leng, R. Bjornson, Y. Kong, N. Kitabayashi, N. Bhardwaj, M. Rubin, M. Snyder, and M. Gerstein, "AlleleSeq: analysis of allele-specific expression and binding in a network framework," *Mol. Syst. Biol.*, vol. 7, p. 522, 2011.

[340] S. V. Ramagopalan, A. Heger, A. J. Berlanga, N. J. Maugeri, M. R. Lincoln, A. Burrell, L. Handunnetthi, A. E. Handel, G. Disanto, S.-M. Orton, C. T. Watson, J. M. Morahan, G. Giovannoni, C. P. Ponting, G. C. Ebers, and J. C. Knight, "A ChIP-seq defined genome-wide map of vitamin D receptor binding: associations with disease and evolution," *Genome Res.*, vol. 20, no. 10, pp. 1352–1360, Oct. 2010.

[341] Y. Zhang, T. Liu, C. A. Meyer, J. Eeckhoute, D. S. Johnson, B. E. Bernstein, C. Nusbaum, R. M. Myers, M. Brown, W. Li, and X. S. Liu, "Model-based Analysis of ChIP-Seq (MACS)," *Genome Biol.*, vol. 9, p. R137, 2008.

[342] T. Liu, J. A. Ortiz, L. Taing, C. A. Meyer, B. Lee, Y. Zhang, H. Shin, S. S. Wong, J. Ma, Y. Lei, U. J. Pape, M. Poidinger, Y. Chen, K. Yeung, M. Brown, Y. Turpaz, and X. S. Liu, "Cistrome: an integrative platform for transcriptional regulation studies," *Genome Biol.*, vol. 12, no. 8, p. R83, 2011.

[343] K. Colston, M. J. Colston, and D. Feldman, "1,25-dihydroxyvitamin D3 and malignant melanoma: the presence of receptors and inhibition of cell growth in culture," *Endocrinology*, vol. 108, no. 3, pp. 1083–1086, Mar. 1981.

[344] D. E. Ayer, L. Kretzner, and R. N. Eisenman, "Mad: A heterodimeric partner for Max that antagonizes Myc transcriptional activity," *Cell*, vol. 72, no. 2, pp. 211–222, 1993.

[345] S. Rottmann and B. Lüscher, "The Mad side of the Max network: Antagonizing the function of Myc and more," *Curr. Top. Microbiol. Immunol.*, vol. 302, pp. 63–122, 2006.

[346] J. Zimmermann, D. Erdmann, I. Lalande, R. Grossenbacher, M. Noorani, and P. Fürst, "Proteasome inhibitor induced gene expression profiles reveal overexpression of transcriptional regulators ATF3, GADD153 and MAD1," *Oncogene*, vol. 19, no. 25, pp. 2913–2920, 2000.

[347] C. W. Hooker and P. J. Hurlin, "Of Myc and Mnt," *J. Cell Sci.*, vol. 119, no. 2, pp. 208–216, Jan. 2006.

[348] F. Galli, M. Rossi, Y. D'Alessandra, M. De Simone, T. Lopardo, Y. Haupt, O. Alsheich-Bartok, S. Anzi, E. Shaulian, V. Calabrò, G. La Mantia, and L. Guerrini, "MDM2 and Fbw7 cooperate to induce p63 protein degradation following DNA damage and cell differentiation," *J. Cell Sci.*, vol. 123, no. Pt 14, pp. 2423–2433, Jul. 2010.

[349] Z. Wang, H. Inuzuka, J. Zhong, L. Wan, H. Fukushima, F. H. Sarkar, and W. Wei, "Tumor suppressor functions of FBW7 in cancer development and progression," *FEBS Lett.*, vol. 586, no. 10, pp. 1409–1418, May 2012.

[350] N. Liu, H. Li, S. Li, M. Shen, N. Xiao, Y. Chen, Y. Wang, W. Wang, R. Wang, Q. Wang, J. Sun, and P. Wang, "The Fbw7/human CDC4 tumor suppressor targets proproliferative factor KLF5 for ubiquitination and degradation through multiple phosphodegron motifs," *J. Biol. Chem.*, vol. 285, no. 24, pp. 18858–18867, Jun. 2010.

[351] H. Inuzuka, S. Shaik, I. Onoyama, D. Gao, A. Tseng, R. S. Maser, B. Zhai, L. Wan, A. Gutierrez, A. W. Lau, Y. Xiao, A. L. Christie, J. Aster, J. Settleman, S. P. Gygi, A. L. Kung, T. Look, K. I. Nakayama, R. A. DePinho, and W. Wei, "SCFFBW7 regulates cellular apoptosis by targeting MCL1 for ubiquitylation and destruction," *Nature*, vol. 471, no. 7336, pp. 104–109, Mar. 2011.

[352] J. A. Ubersax and J. E. Ferrell Jr, "Mechanisms of specificity in protein phosphorylation," *Nat. Rev. Mol. Cell Biol.*, vol. 8, no. 7, pp. 530–541, Jul. 2007.

[353] T. Ravid and M. Hochstrasser, "Degradation signal diversity in the ubiquitin-proteasome system," *Nat. Rev. Mol. Cell Biol.*, vol. 9, no. 9, pp. 679–690, Sep. 2008.

[354] L. Jia and Y. Sun, "SCF E3 Ubiquitin Ligases as Anticancer Targets," *Curr. Cancer Drug Targets*, vol. 11, no. 3, pp. 347–356, Mar. 2011.

[355] R. J. Davis, M. Welcker, and B. E. Clurman, "Tumor Suppression by the Fbw7 Ubiquitin Ligase: Mechanisms and Opportunities," *Cancer Cell*, vol. 26, no. 4, pp. 455–464, Oct. 2014.

[356] B. Pérez-Benavente, J. L. García, M. S. Rodríguez, A. Pineda-Lucena, M. Piechaczyk, J. Font de Mora, and R. Farràs, "GSK3-SCFFBXW7 targets JunB for degradation in G2 to preserve chromatid cohesion before anaphase," *Oncogene*, vol. 32, no. 17, pp. 2189–2199, Apr. 2013.

[357] X. Ye, G. Nalepa, M. Welcker, B. M. Kessler, E. Spooner, J. Qin, S. J. Elledge, B. E. Clurman, and J. W. Harper, "Recognition of Phosphodegron Motifs in Human Cyclin E by the SCFFbw7 Ubiquitin Ligase," *J. Biol. Chem.*, vol. 279, no. 48, pp. 50110–50119, Nov. 2004.

[358] Z. Zhou, C. He, and J. Wang, "Regulation mechanism of Fbxw7-related signaling pathways (Review)," *Oncol. Rep.*, vol. 34, no. 5, pp. 2215–2224, Nov. 2015.

[359] H. C. Hwang and B. E. Clurman, "Cyclin E in normal and neoplastic cell cycles," *Oncogene*, vol. 24, no. 17, pp. 2776–2786, Apr. 2005.

[360] K. Lee, A. Lee, B. J. Song, and C. S. Kang, "Expression of AIB1 protein as a prognostic factor in breast cancer," *World J. Surg. Oncol.*, vol. 9, p. 139, Oct. 2011.

[361] L. Blau, R. Knirsh, I. Ben-Dror, S. Oren, S. Kuphal, P. Hau, M. Proescholdt, A.-K. Bosserhoff, and L. Vardimon, "Aberrant expression of c-Jun in glioblastoma by internal ribosome entry site (IRES)-mediated translational activation," *Proc. Natl. Acad. Sci. U. S. A.*, vol. 109, no. 42, pp. E2875-2884, Oct. 2012.

[362] M. Conacci-Sorrell, L. McFerrin, and R. N. Eisenman, "An overview of MYC and its interactome," *Cold Spring Harb. Perspect. Med.*, vol. 4, no. 1, p. a014357, Jan. 2014.

[363] R. Salehi-Tabar, L. Nguyen-Yamamoto, L. E. Tavera-Mendoza, T. Quail, V. Dimitrov, B.-S. An, L. Glass, D. Goltzman, and J. H. White, "Vitamin D receptor as a master regulator of the c-MYC/MXD1 network," *Proc. Natl. Acad. Sci. U. S. A.*, vol. 109, no. 46, pp. 18827–18832, Nov. 2012.

[364] X.-Y. Li, M. Boudjelal, J.-H. Xiao, Z.-H. Peng, A. Asuru, S. Kang, G. J. Fisher, and J. J. Voorhees, "1,25-Dihydroxyvitamin D3 Increases Nuclear Vitamin D3 Receptors by Blocking Ubiquitin/Proteasome-Mediated Degradation in Human Skin," *Mol. Endocrinol.*, vol. 13, no. 10, pp. 1686–1694, Oct. 1999.

[365] M. Kongsbak, M. R. von Essen, L. Boding, T. B. Levring, P. Schjerling, J. P. H. Lauritsen, A. Woetmann, N. Ødum, C. M. Bonefeld, and C. Geisler, "Vitamin D Up-Regulates the Vitamin D Receptor by Protecting It from Proteasomal Degradation in Human CD4 + T Cells," *PLOS ONE*, vol. 9, no. 5, p. e96695, May 2014.

[366] I. E. Wertz, S. Kusam, C. Lam, T. Okamoto, W. Sandoval, D. J. Anderson, E. Helgason, J. A. Ernst, M. Eby, J. Liu, L. D. Belmont, J. S. Kaminker, K. M. O'Rourke, K. Pujara, P. B. Kohli, A. R. Johnson, M. L. Chiu, J. R. Lill, P. K. Jackson, W. J. Fairbrother, S. Seshagiri, M. J. C. Ludlam, K. G. Leong, E. C. Dueber, H. Maecker, D. C. S. Huang, and V. M. Dixit, "Sensitivity to

antitubulin chemotherapeutics is regulated by MCL1 and FBW7," *Nature*, vol. 471, no. 7336, pp. 110–114, Mar. 2011.

[367] M. A. Nikiforov, N. Popov, I. Kotenko, M. Henriksson, and M. D. Cole, "The Mad and Myc basic domains are functionally equivalent," *J. Biol. Chem.*, vol. 278, no. 13, pp. 11094–11099, 2003.

[368] "Search Database for Sequence Pattern." [Online]. Available: http://scansite.mit.edu/dbsequence_one.html. [Accessed: 05-Apr-2016].

[369] M. A. Gregory and S. R. Hann, "c-Myc Proteolysis by the Ubiquitin-Proteasome Pathway: Stabilization of c-Myc in Burkitt's Lymphoma Cells," *Mol. Cell. Biol.*, vol. 20, no. 7, pp. 2423–2435, Apr. 2000.

[370] S. Heikkinen, S. Väisänen, P. Pehkonen, S. Seuter, V. Benes, and C. Carlberg, "Nuclear hormone 1α,25-dihydroxyvitamin D3 elicits a genome-wide shift in the locations of VDR chromatin occupancy," *Nucleic Acids Res.*, vol. 39, no. 21, pp. 9181–9193, 2011.

[371] M. B. Meyer, P. D. Goetsch, and J. W. Pike, "VDR/RXR and TCF4/β-catenin cistromes in colonic cells of colorectal tumor origin: Impact on c-FOS and c-MYC gene expression," *Mol. Endocrinol.*, vol. 26, no. 1, pp. 37–51, 2012.

[372] M. B. Meyer, P. D. Goetsch, and J. W. Pike, "Genome-wide analysis of the VDR/RXR cistrome in osteoblast cells provides new mechanistic insight into the actions of the vitamin D hormone," *J. Steroid Biochem. Mol. Biol.*, vol. 121, no. 1–2, pp. 136–141, 2010.

[373] S. H. Zhuang and K. L. Burnstein, "Antiproliferative effect of 1alpha,25-dihydroxyvitamin D3 in human prostate cancer cell line LNCaP involves reduction of cyclin-dependent kinase 2 activity and persistent G1 accumulation," *Endocrinology*, vol. 139, no. 3, pp. 1197–1207, Mar. 1998.

[374] Y.-J. Li, Z.-M. Wei, Y.-X. Meng, and X.-R. Ji, "Beta-catenin up-regulates the expression of cyclinD1, c-myc and MMP-7 in human pancreatic cancer: relationships with carcinogenesis and metastasis," *World J. Gastroenterol.*, vol. 11, no. 14, pp. 2117–2123, Apr. 2005.

[375] S. Zhang, Y. Li, Y. Wu, K. Shi, L. Bing, and J. Hao, "Wnt/β-catenin signaling pathway upregulates c-Myc expression to promote cell proliferation of P19 teratocarcinoma cells," *Anat. Rec. Hoboken NJ 2007*, vol. 295, no. 12, pp. 2104–2113, Dec. 2012.

[376] M. J. Larriba, J. M. González-Sancho, A. Barbáchano, N. Niell, G. Ferrer-Mayorga, and A. Muñoz, "Vitamin D Is a Multilevel Repressor of Wnt/β-Catenin Signaling in Cancer Cells," *Cancers*, vol. 5, no. 4, pp. 1242–1260, Oct. 2013.

[377] S. Shah, M. N. Islam, S. Dakshanamurthy, I. Rizvi, M. Rao, R. Herrell, G. Zinser, M. Valrance, A. Aranda, D. Moras, A. Norman, J. Welsh, and S. W. Byers, "The Molecular Basis of Vitamin D Receptor and β-Catenin Crossregulation," *Mol. Cell*, vol. 21, no. 6, pp. 799–809, Mar. 2006.

[378] L. Hu, D. D. Bikle, and Y. Oda, "Reciprocal role of vitamin D receptor on β-catenin regulated keratinocyte proliferation and differentiation," *J. Steroid Biochem. Mol. Biol.*, vol. 144, Part A, pp. 237–241, Oct. 2014.

[379] P. J. Malloy and D. Feldman, "Genetic Disorders and Defects in Vitamin D Action," *Endocrinol. Metab. Clin. North Am.*, vol. 39, no. 2, pp. 333–346, Jun. 2010.

[380] D. D. Bikle, Y. Oda, and A. Teichert, "The Vitamin D Receptor: A Tumor Suppressor in Skin," *Discov. Med.*, vol. 11, no. 56, pp. 7–17, Jan. 2011.

[381] Q. Wu, Z. Yang, Y. An, H. Hu, J. Yin, P. Zhang, Y. Nie, K. Wu, Y. Shi, and D. Fan, "MiR-19a/b modulate the metastasis of gastric cancer cells by targeting the tumour suppressor MXD1," *Cell Death Dis.*, vol. 5, p. e1144, 2014.

[382] R. Wang, Y. Wang, N. Liu, C. Ren, C. Jiang, K. Zhang, S. Yu, Y. Chen, H. Tang, Q. Deng, C. Fu, Y. Wang, R. Li, M. Liu, W. Pan, and P. Wang, "FBW7 regulates endothelial functions by targeting KLF2 for ubiquitination and degradation," *Cell Res.*, vol. 23, no. 6, pp. 803–819, Jun. 2013.

[383] Y. Luan and P. Wang, "FBW7-mediated ubiquitination and degradation of KLF5," *World J. Biol. Chem.*, vol. 5, no. 2, pp. 216–223, May 2014.

[384] S. Rottmann, A. R. Menkel, C. Bouchard, J. Mertsching, P. Loidl, E. Kremmer, M. Eilers, J. Lüscher-Firzlaff, R. Lilischkis, and B. Lüscher, "Mad1 function in cell proliferation and

transcriptional repression is antagonized by cyclin E/CDK2," *J. Biol. Chem.*, vol. 280, no. 16, pp. 15489–15492, 2005.

[385] K. P. Foley, G. A. McArthur, C. Quéva, P. J. Hurlin, P. Soriano, and R. N. Eisenman, "Targeted disruption of the MYC antagonist MAD1 inhibits cell cycle exit during granulocyte differentiation," *EMBO J.*, vol. 17, no. 3, pp. 774–785, Feb. 1998.

[386] L. Busino, S. E. Millman, L. Scotto, C. A. Kyratsous, V. Basrur, O. O'Connor, A. Hoffmann, K. S. Elenitoba-Johnson, and M. Pagano, "Fbxw7α- and GSK3-mediated degradation of p100 is a pro-survival mechanism in multiple myeloma," *Nat. Cell Biol.*, vol. 14, no. 4, pp. 375–385, Apr. 2012.

[387] A. Hergovich, J. Lisztwan, C. R. Thoma, C. Wirbelauer, R. E. Barry, and W. Krek, "Priming-Dependent Phosphorylation and Regulation of the Tumor Suppressor pVHL by Glycogen Synthase Kinase 3," *Mol. Cell. Biol.*, vol. 26, no. 15, pp. 5784–5796, Aug. 2006.

[388] X. D. Zhang, S. K. Gillespie, and P. Hersey, "Staurosporine induces apoptosis of melanoma by both caspase-dependent and -independent apoptotic pathways," *Mol. Cancer Ther.*, vol. 3, no. 2, pp. 187–197, Feb. 2004.

[389] "Staurosporine induces apoptosis through both caspase-dependent and caspase-independent mechanisms," *Publ. Online 08 June 2001 Doi101038sjonc1204436*, vol. 20, no. 26, Jun. 2001.

[390] K. W. Colston, S. Y. James, E. A. Ofori-Kuragu, L. Binderup, and A. G. Grant, "Vitamin D receptors and anti-proliferative effects of vitamin D derivatives in human pancreatic carcinoma cells in vivo and in vitro.," *Br. J. Cancer*, vol. 76, no. 8, pp. 1017–1020, 1997.

[391] J. Chen, D. Bruce, and M. T. Cantorna, "Vitamin D receptor expression controls proliferation of naïve CD8+ T cells and development of CD8 mediated gastrointestinal inflammation," *BMC Immunol.*, vol. 15, p. 6, 2014.

[392] D. M. Peehl, R. J. Skowronski, G. K. Leung, S. T. Wong, T. A. Stamey, and D. Feldman, "Antiproliferative Effects of 1,25-Dihydroxyvitamin D3 on Primary Cultures of Human Prostatic Cells," *Cancer Res.*, vol. 54, no. 3, pp. 805–810, Feb. 1994.

[393] N. T. Hill, J. Zhang, M. K. Leonard, M. Lee, H. N. Shamma, and M. Kadakia, "1α, 25-Dihydroxyvitamin D3 and the vitamin D receptor regulates ΔNp63α levels and keratinocyte proliferation," *Cell Death Dis.*, vol. 6, no. 6, p. e1781, Jun. 2015.

[394] W. Ip, Y.-T. A. Chiang, and T. Jin, "The involvement of the wnt signaling pathway and TCF7L2 in diabetes mellitus: The current understanding, dispute, and perspective," *Cell Biosci.*, vol. 2, no. 1, p. 28, 2012.

[395] Y. Zhou, S.-Y. Park, J. Su, K. Bailey, E. Ottosson-Laakso, L. Shcherbina, N. Oskolkov, E. Zhang, T. Thevenin, J. Fadista, H. Bennet, P. Vikman, N. Wierup, M. Fex, J. Rung, C. Wollheim, M. Nobrega, E. Renström, L. Groop, and O. Hansson, "TCF7L2 is a master regulator of insulin production and processing," *Hum. Mol. Genet.*, vol. 23, no. 24, pp. 6419–6431, Dec. 2014.

[396] L. Wu, C. Timmers, B. Maiti, H. I. Saavedra, L. Sang, G. T. Chong, F. Nuckolls, P. Giangrande, F. A. Wright, S. J. Field, M. E. Greenberg, S. Orkin, J. R. Nevins, M. L. Robinson, and G. Leone, "The E2F1–3 transcription factors are essential for cellular proliferation," *Nature*, vol. 414, no. 6862, pp. 457–462, Nov. 2001.

[397] N. Rochel, G. Tocchini-Valentini, P. F. Egea, K. Juntunen, J. M. Garnier, P. Vihko, and D. Moras, "Functional and structural characterization of the insertion region in the ligand binding domain of the vitamin D nuclear receptor," *Eur. J. Biochem. FEBS*, vol. 268, no. 4, pp. 971–979, Feb. 2001.

[398] M. Welcker and B. E. Clurman, "Fbw7/hCDC4 dimerization regulates its substrate interactions," *Cell Div.*, vol. 2, p. 7, 2007.

[399] D. Feldman, J. W. Pike, and J. S. Adams, *Vitamin D: Two-Volume Set*. Academic Press, 2011.

Appendix

Table S4.1: List of proteins that contain canonical phosphodegron motif.

1B37	41	ACOX2	CSMD1	DYH11	IFT74	5-Sep	3-Sep	SNMP1_PEDHC	1B53
1B38	1B07	C11B2	CSMD2	FEM1A	IFT80	9-Sep	OPHN1	SP9	ADNP
1B39	1B08	CFAH	CSMD3	HXD1	IG2R	12-Sep	OPN4	SPA11	AGO61
1B41	1B14	CSKP	CSN1	IF	IGDC4	IQCK	OPTN	SPAG5	AKIB1
1B44	1B18	CSN2	CSPG2	IGDC3	IGF2	OPALI	OR1E2	SPAG8	ANLN
1B47	1B27	CSPG5	CSPG4	IGFL2	IGHA1	OPLA	OR2D2	SPAT4	ANR17
1B51	1B35	CSR2B	CSRN2	IGFN1	IGHG1	OPN3	OR2M4	SPAT6	ANR33
1B54	1B40	CSRN3	CSTF1	IGFR1	IGHG3	OPRM	OR2M7	SPATL	APBP2
1B55	1B42	CSTFT	CSTF2	IGHE	IGHG4	OPRX	OR2S1	SPB3	ARC1B
1B59	1B45	CSTN1	CSTN2	IGHG2	IGS23	OPT	OR3A4	SPB7	ARHG7
1B78	1B48	CSTN3	CT004	IGHM	IGSF2	OR1I1	OR4Q2	SPD2A	ARI4B
1C02	1B49	CT026	CT007	IGJ	IGSF3	OR2F1	OR4X2	SPD2B	ARMC5
1C03	1B50	CT085	CT011	IGLL1	IGSF5	OR2M2	OR5K3	SPDE2	ARSD
1C04	1B52	CT111	CT072	IGS10	IHH	OR2M3	OR5M1	SPDE4	ATAD2
1C06	1B56	CT112	CT078	IGSF1	IKBB	OR2M5	OR5MA	SPDE8	ATM
1C08	1B58	CT165	CT094	IKBZ	IKBD	OR4S2	OR5MB	SPDYC	BAP1
1C12	1B67	CT166	CT118	IKKB	IKKA	OR6K6	OR6K2	SPEF2	BCAS1
1C14	1B73	CT177	CT123	IKZF1	IKZF3	ORC2	OR7G2	SPEG	C560
1C15	1B81	CT18	CT151	IKZF2	IKZF4	ORML1	ORAI3	SPEM1	CA185
1C17	1B82	CT194	CT173	IL16	IL1R1	ORML3	ORC1	SPG16	CAC1A
1C18	1C01	CTDP1	CT202	IL17	IL23A	OS9	ORML2	SPG17	CALL5
3BHS7	1C05	CTF18	CT2NL	IL1AP	IL23R	OSBL3	OSB10	SPHK2	CAN6
3BP1	1C07	CTL4	CTBP1	IL1R2	IL27B	OSBL7	OSB11	SPI2A	CAND2
3BP5	1C16	CTL5	CTGF	IL21R	IL3	OTP	OSBL1	SPI2B	CC14A
3BP5L	2A5B	CTLA4	CTL1	IL2RA	IL34	OTU1	OSBL5	SPIR2	CDCP1
4EBP3	2A5D	CTNA2	CTLFB	IL2RB	IL5RA	OTU7A	OSBL8	SPKAP	CELR2
4ET	3BHS1	CTR2	CTNB1	IL32	IL6	OTUD1	OSBL9	SPN90	CMTA1
5HT1B	3BHS2	CTR3	CTND2	IL33	IL9R	OTUD3	OSBP2	SPNS2	CO4A2
5HT1E	3BP2	CTR4	CTR3L	IL3RB	ILDR1	OTUD4	OSGEP	SPNS3	CQ059
5HT2B	3MG	CTSL2	CTR9	IL4RA	ILFT1	OTUD5	OSGI1	SPOC1	CRTC3
5HT3D	4EBP1	CTSR1	CTRO	IL6RA	IMA2L	OTX1	OSPT	SPON2	CSRN1
5NT1A	4EBP2	CTSR3	CTSRG	IL6RB	IMDH1	OVGP1	OST48	SPOP	CTIF
5NT1B	4F2	CTSR4	CTTB2	ILDR2	IMPG1	OX1R	OTOF	SPOT1	DDX59
5NTC	5HT3C	CU084	CU024	ILRL1	INAR1	OXA1L	OTOG	SPRE1	DPTOR
A16L1	5HT5A	CU086	CU025	IMA1	INAR2	P12L2	OTOGL	SPT13	DRA
A1AG2	5HT7R	CU104	CU030	IMA2	INE1	P1L12	OTOP1	SPT4H	DUS16
A1BG	5NTD	CU129	CU032	IMA5	INGR1	P20L1	OTOP2	SPT6H	EDN2
A4GCT	8ODP	CU136	CU037	IMA7	INHA	P2RX2	OTOP3	SPTA1	EHD3
AAAS	A16A1	CUL2	CU054	IMDH2	INHBE	P2RY2	OTU7B	SPTA3	ELMD1

AAAT	A16L2	CUL9	CU056	IMMT	INP4B	P2RY4	OTX2	SPTB2	ERH
AACT	A1AG1	CUX1	CU067	IMP5	INP5E	P2Y11	OVCH2	SPTC2	ESRP2
AADAT	A2AP	CV034	CU082	IMPCT	INPP	P3C2A	OVOS1	SPTC3	EXD1
AAK1	A2MG	CV045	CUBN	IMPG2	INSM1	P3C2B	OXDA	SPXN1	EXOS7
AAKG1	A2ML1	CX022	CUL4B	IN80D	INSM2	P3C2G	OXDD	SPXN2	FARP1
AAKG2	A4	CXB3	CUX2	IN80E	INSR	P3H2	OXER1	SPXN3	FAT2
AAPK2	AAKG3	CXD2	CUZD1	INADL	INT1	P4R3A	OXR1	SPXN5	FCHO2
AASD1	AAMP	CXD4	CV024	INCE	INT9	P4R3B	P121A	SQRD	FGF5
AASS	AAPK1	CXE1	CV029	INF2	INVS	P53	P121B	SQSTM	FLII
AATC	AARD	CXG2	CV031	INHBA	IP3KB	P5CR1	P20D2	SRBD1	FRMD8
AATF	ABC3A	CXXC1	CV046	INHBB	IP3KC	P5CR3	P210L	SRBP1	GALT3
ABC3B	ABC3D	CXXC5	CWC22	INMT	IP6K1	P5CS	P2RX1	SRBS1	GFI1
ABC3F	ABC3G	CY017	CWC25	INO1	IP6K3	P66A	P2RX6	SRBS2	GG6LA
ABCA4	ABC3H	CYGB	CX023	INO80	IPIL2	PA24A	P4K2A	SRC8	GGT1
ABCA7	ABCA1	CYLC1	CX030	INP4A	IPMK	PA24D	P4K2B	SRCA	GNA1
ABCA8	ABCA2	CYR61	CX049	INT12	IPO11	PA24E	P52K	SREK1	GNL3
ABCAB	ABCA6	CYTN	CX057	INT2	IPO4	PA24F	P5CR2	SRF	GPR75
ABCAD	ABCA9	CYTSB	CX064	INT3	IPP2	PA2GX	P5F1B	SRGP1	GRD2I
ABCBB	ABCAA	CYTT	CX067	INT4	IPYR2	PABP1	P5I13	SRGP2	HAUS8
ABCCB	ABCAC	D11L8	CXA10	INT6	IQCE	PABP4	P63	SRMS	HBP1
ABCD2	ABCC8	D19L4	CXA3	INT7	IQCH	PACE1	P66B	SRP72	HPS6
ABCG5	ABCCD	D42E1	CXCL9	INT8	IQEC1	PACS1	P85B	SRPX	HS3SA
ABCG8	ABCD1	DAAF1	CXL16	INVO	IQEC2	PADI4	PA21B	SRPX2	I12R1
ABEC1	ABCE1	DAB1	CXX1	IP3KA	IQGA1	PADI6	PA24B	SRRM1	IL31R
ABHD1	ABEC4	DACT1	CXXC4	IPO9	IRAK2	PAEP	PA2G4	SRRM2	IPRI
ABHDB	ABHD5	DACT3	CY24B	IPP	IRF8	PAF	PA2G6	SRRM4	IRK14
ABHEA	ABHDD	DAG1	CYB	IPP2L	IRG1	PAF1	PA2GC	SRRM5	K0913
ABI2	ABHEB	DAPL1	CYHR1	IPP4	IRK10	PAI1	PA2GF	SRRT	KCNU1
ABL1	ABI1	DAPLE	CYLD	IPPK	IRK11	PAK2	PABP3	SRS10	KCRS
ABP1	ABL2	DAZ3	CYTIP	IQCB1	IRK13	PAK4	PACS2	SRS11	KDM3A
ABRA	ABLM1	DAZL	CYTSA	IQCC	IRK15	PALB2	PADI1	SRS12	KDM4C
ABTB2	ABLM2	DB123	D10OS	IQCG	IRK2	PALLD	PADI2	SRSF1	KLKB1
ACACA	ABLM3	DBF4B	D19L1	IQEC3	IRK5	PALMD	PADI3	SRSF2	KS6A3
ACACB	ABR	DBND1	D19P1	IQGA3	IRK9	PAN2	PAFA	SRSF7	LAR4B
ACADS	ACAD8	DBNL	D2HDH	IRAK1	IRS2	PAN3	PAG1	SRSF8	LCE2D
ACBD6	ACAP2	DBPA	DAB2	IRAK4	IRX2	PAOX	PAIRB	SSBP2	LIPB2
ACD10	ACAP3	DBR1	DAB2P	IREB2	IRX3	PAPD7	PAK1	SSBP3	LPIN2
ACE	ACATN	DC1I1	DACH1	IRF1	ISL2	PAPP1	PAK3	SSFA2	LRIT3
ACHA2	ACBG1	DC1L1	DACH2	IRF2	ISLR	PAQR6	PAK6	SSH2	LZTS1
ACHA9	ACCN3	DCA10	DAF	IRF4	ISM1	PAR14	PAK7	SSH3	M4A4A
ACHB2	ACCN4	DCA11	DAPK1	IRF6	ISM2	PARD3	PALM	SSPO	MBD5
ACHB4	ACD	DCA15	DAPK2	IRF7	ITA10	PARG	PALM3	SSR3	MEG11
ACINU	ACHA4	DCAF6	DAXX	IRGM	ITA11	PARM1	PANK2	SSRP1	MKRN1
ACK1	ACHA6	DCAM	DAZ1	IRGQ	ITA2B	PARP1	PAPD5	ST18	MPP7

ACM1	ACHB3	DCD2C	DAZ2	IRK1	ITA4	PARP4	PAPOA	ST2A1	MSX2
ACM3	ACL6B	DCDC5	DAZ4	IRK12	ITAL	PARP8	PAPOG	ST38L	MYOC
ACM5	ACLY	DCE1	DB125	IRK18	ITAM	PARPT	PAPP2	ST5	MYOM1
ACO11	ACM2	DCLK1	DB129	IRK3	ITAX	PASD1	PAR10	STA13	MZF1
ACOXL	ACOD	DCLK2	DBF4A	IRK4	ITB4	PATL1	PAR15	STAB1	N62CL
ACPL2	ACON	DCLK3	DBND2	IRK6	ITB7	PATL2	PAR3L	STAC3	NALP8
ACRO	ACOT9	DCMC	DBP	IRK8	ITFG3	PATZ1	PAR4	STAG3	NCOA6
ACSA	ACOX1	DCNP1	DBX1	IRS1	ITGBL	PAX1	PAR6A	STAP2	NDUV1
ACSL5	ACOX3	DCP1A	DBX2	IRS4	ITIH1	PAX2	PARF	STAR3	NECA3
ACSM3	ACPH	DCR1A	DC1L2	IRX4	ITIH4	PAX5	PARN	STAR6	NEK11
ACSM5	ACRBP	DCST1	DCA16	IRX6	ITPR1	PAX7	PARP6	STAT2	NELFE
ACTBL	ACS2L	DCTN2	DCAF4	ISK2	ITPR3	PAXI1	PARP9	STAU1	NOX1
ACTL9	ACSF3	DCX	DCAF5	ISK4	ITSN1	PB1	PARVA	STB5L	NPC2
ACTT2	ACSF4	DD19A	DCAF8	ISK5	ITSN2	PBIP1	PASK	STBD1	OSMR
ADA2B	ACSL4	DD19B	DCBD1	ISL1	JADE3	PBLD	PAX3	STK16	OSTA
ADA2C	ACSM1	DDHD1	DCBD2	ISOC1	JAG2	PBMU1	PAX4	STK24	OVOS2
ADAD1	ACSM6	DDI1	DCC	ITA2	JAK3	PBMU2	PAX6	STK25	P121C
ADAL	ACTL8	DDIT3	DCD2B	ITA5	JAM1	PBOV1	PAX8	STK40	PA1
ADAM8	ACTN2	DDX11	DCDC1	ITA7	JARD2	PC11Y	PAX9	STMN2	PA2G3
ADAT3	ACTT1	DDX12	DCHS	ITA8	JAZF1	PCBP4	PBX2	STMN3	PCTL
ADCK1	ACVR1	DDX18	DCP1B	ITAD	JERKY	PCCA	PC11X	STON2	PDZD6
ADCK3	ACY3	DDX23	DCR1B	ITAV	JIP1	PCCB	PCAT1	STOX1	PHF19
ADCK4	ADA10	DDX25	DCR1C	ITB5	JIP2	PCD12	PCBP3	STOX2	PLA2R
ADCY4	ADA15	DDX4	DCST2	ITB8	JKIP1	PCD16	PCD10	STPAP	PLCL1
ADCY5	ADA18	DDX46	DCTN1	ITCH	JKIP3	PCD17	PCD15	STRA6	PLPL5
ADCY6	ADA19	DDX53	DCTN4	ITF2	JPH1	PCD19	PCD18	STRAA	POC5
ADCY7	ADA22	DDX54	DCTN6	ITFG2	JPH2	PCDA1	PCD20	STRAB	POLH
ADCY8	ADA28	DDX55	DCTP1	ITH5L	JPH4	PCDA6	PCD23	STRC	PRA14
ADCY9	ADA29	DDX6	DDC	ITIH2	JUN	PCDA8	PCDA2	STRCL	PRAM
ADDB	ADA30	DDX60	DDHD2	ITIH3	JUNB	PCDAA	PCDA3	STRN3	PRCA1
ADH1B	ADAD2	DEAF1	DDX10	ITIH5	JUND	PCDAB	PCDA4	STRN4	PRR7
ADH1G	ADAM7	DEMA	DDX20	ITM2C	K0100	PCDAD	PCDA5	STT3A	PTCD1
ADH7	ADAM9	DEN1A	DDX24	ITPR2	K0146	PCDB2	PCDA7	STT3B	PTGIS
ADM2	ADAS1	DEN2A	DDX31	JADE1	K0232	PCDB4	PCDA9	STX16	RENT2
ADM5	ADCYA	DEN4C	DDX42	JADE2	K0240	PCDB5	PCDAC	STX4	RGPA1
ADML	ADDA	DEP1A	DDX43	JAG1	K0415	PCDB6	PCDB1	STX7	RHAG
ADPRM	ADDG	DEPD5	DDX47	JAK2	K0494	PCDB7	PCDB3	STXB2	RNF25
AEBP1	ADEC1	DET1	DDX49	JAM2	K0586	PCDBC	PCDB8	STXB5	RPKL1
AEBP2	ADH1A	DGKH	DDX51	JDP2	K0614	PCDBD	PCDB9	SUGP1	RT29
AEN	ADH4	DGKI	DDX52	JHD2C	K0895	PCDBI	PCDBA	SUGP2	RUNX2
AF10	ADH6	DGKK	DDX6L	JIP3	K0930	PCDG1	PCDBB	SUN5	RYR2
AF1L1	ADIP	DGKZ	DECR2	JIP4	K1109	PCDG2	PCDBE	SUPT3	S12A2
AF9	ADNP2	DHB14	DELE	JKIP2	K1199	PCDG3	PCDBF	SURF6	S22A6
AFAP1	ADRB1	DHB2	DEN1C	JMY	K1210	PCDG4	PCDBG	SUSD5	SC31A

AFG32	ADRM1	DHI1L	DEN2C	JPH3	K1239	PCDG5	PCDC1	SVEP1	SCAPE
AGA11	ADSV	DHR13	DEN2D	JUB	K1310	PCDG7	PCDC2	SVIP	SOCS6
AGAP1	ADXL	DHRS4	DEN4B	K0195	K1324	PCDGB	PCDG6	SYAC	SP7
AGAP8	AEGP	DHRS9	DEN5A	K0284	K132L	PCDGD	PCDG8	SYAP1	SP8
AGFG2	AER61	DHRSX	DEND	K0319	K1370	PCDGE	PCDG9	SYC2L	SPA2L
AGGF1	AF17	DHTK1	DENR	K0355	K1407	PCDGF	PCDGA	SYCP2	SPAC7
AGRIN	AF1L2	DHX29	DESM	K0408	K1430	PCDGG	PCDGC	SYDE1	SPAG4
AHI1	AFAD	DHX30	DESP	K0513	K1486	PCDGI	PCDGH	SYDE2	SPAG6
AHR	AFF1	DHX34	DG2L7	K0528	K1522	PCDGJ	PCDGL	SYEM	SPAT1
AHRR	AFF2	DHX57	DGAT1	K0556	K1539	PCDGK	PCDH8	SYFM	SPAT2
AIM1	AFF3	DHX9	DGC14	K0564	K1549	PCDGM	PCF11	SYHC	SPAT7
AIM2	AFF4	DI3L1	DGKB	K0649	K1609	PCDH1	PCGF2	SYLC	SPB11
AIPL1	AFTIN	DI3L2	DGKQ	K0753	K1671	PCDH7	PCIF1	SYLM	SPDE3
AK17A	AGA10	DIAP1	DGLB	K0754	K1683	PCDH9	PCKGC	SYN1	SPDE6
AK1A1	AGAP2	DIM1	DHCR7	K0825	K1826	PCLO	PCMD2	SYN2	SPDEF
AK1BA	AGAP3	DIP2B	DHI2	K0889	K1875	PCM1	PCNA	SYN3	SPDL1
AK1BF	AGAP4	DISC1	DHR12	K0907	K1920	PCSK4	PCNT	SYNC	SPDLY
AK1D1	AGAP5	DISP1	DHRS2	K0947	K1C12	PCX1	PCOC1	SYNCI	SPE2L
AKAP3	AGAP6	DISP2	DHX15	K1045	K1C23	PCX3	PCP	SYNEM	SPERI
AKIP	AGAP7	DJB12	DHX32	K1107	K1C28	PD1L2	PCP2	SYNJ1	SPERT
AKIR1	AGAP9	DJB13	DHX33	K1191	K1C39	PDC6I	PCSK5	SYNPO	SPESP
AL1A1	AGFG1	DJC10	DHX36	K1211	K1C40	PDD2L	PCSK6	SYNPR	SPG20
AL2S8	AGT2	DJC13	DHX58	K1257	K1H2	PDE12	PCSK7	SYNRG	SPG7
AL2SA	AHDC1	DJC18	DHYS	K1267	K2C7	PDE1A	PCX2	SYP2L	SPI1
AL3A2	AHNK	DJC22	DIAP2	K1328	K2C73	PDE1B	PCY1A	SYPL1	SPIB
ALG2	AHNK2	DJC30	DIAP3	K1377	K6PP	PDE3A	PCY1B	SYRC	SPICE
ALG8	AIDA	DLEC1	DICER	K1383	KALRN	PDE4A	PDE11	SYT11	SPIN1
ALKB5	AIM1L	DLG1	DIDO1	K1462	KANK1	PDE4B	PDE1C	SYT14	SPIN3
ALMS1	AIMP2	DLG2	DIP2A	K1467	KANK3	PDE4D	PDE3B	SYT3	SPIR1
ALPK2	AIRE	DLG3	DIP2C	K1468	KAP1	PDIA2	PDE4C	SYT7	SPIT1
ALPK3	AK1C3	DLGP2	DIRA2	K1586	KAT3	PDIA4	PDE6C	SYTC	SPN1
ALS2	AKA10	DLGP3	DIXC1	K1614	KAT5	PDIP2	PDE8B	SYTL2	SPNS1
ALX3	AKA11	DLGP4	DJC12	K1654	KAT6A	PDLI2	PDGFB	SYTL3	SPON1
ALX4	AKA12	DLGP5	DJC15	K1660	KAZRN	PDLI3	PDGFD	SYVC	SPRE3
AMACR	AKAP1	DLL3	DKK4	K1731	KBTB2	PDLI4	PDILT	SYVM	SPS1
AMD	AKAP2	DLL4	DKKL1	K1737	KBTB7	PDLI5	PDK1	SYVN1	SPS2L
AMER1	AKAP4	DLX2	DLG4	K1755	KBTBB	PDPK1	PDK2	T11L1	SPT16
AMFR2	AKAP5	DLX3	DLG5	K1797	KC1G1	PDPN	PDLI1	T132A	SPT21
AMGO1	AKAP6	DMAP1	DLGP1	K1841	KC1G2	PDPR	PDLI7	T132B	SPT5H
AMGO2	AKAP8	DMB	DLK1	K1908	KCC1G	PDRG1	PDXD2	T161A	SPTA2
AMHR2	AKAP9	DMBT1	DLN1	K1958	KCC2B	PDS5A	PDZD2	T176B	SPTB1
AMPB	AKIR2	DMD	DLX1	K1967	KCD12	PDS5B	PDZD4	T179A	SPTN4
AMPL	AKNA	DMKN	DLX4	K1C13	KCMA1	PDX1	PDZD7	T179B	SPTN5
AMPQ	AKND1	DMPK	DLX5	K2012	KCMB3	PDXD1	PDZD8	T184B	SPXN

AMRA1	AKP13	DMRT2	DMA	K2013	KCNA3	PDXK	PE2R2	T191B	SPXN4
AMYP	AKP8L	DMRT3	DMBTL	K2018	KCNB1	PDXL2	PEAK1	T191C	SPY3
AN13C	AKT2	DMRTA	DMP1	K2022	KCNC1	PDZ1P	PEAR1	T194A	SR140
AN30A	AKTIP	DMTA2	DMRT1	K2026	KCNC2	PECA1	PEBB	T200B	SR1IP
AN34A	AKTS1	DMTF1	DMRTB	K226L	KCNC4	PEF1	PECR	T22D2	SRAC1
AN34B	AL1A2	DMWD	DMRTD	K2C5	KCND2	PEG3	PEDF	T22D4	SRBP2
AN34C	AL2CL	DMXL2	DMXL1	K2C8	KCNE4	PELI1	PEG10	T2EB	SRCAP
ANC2	AL3B1	DNJB2	DNAI2	K2C80	KCNG4	PELO	PELI2	T2FA	SRCH
ANGE1	AL4A1	DNJB9	DND1	K319L	KCNH1	PEO1	PELI3	T4S20	SRCN1
ANGE2	ALDR	DNLI1	DNER	K6PL	KCNH2	PEPC	PELP1	T53I1	SRCRL
ANGP1	ALEX	DNLI3	DNHD1	K895L	KCNK5	PER1	PENK	T73AS	SREC
ANGP2	ALG1	DNLI4	DNJA4	KAAG1	KCNKF	PER2	PEPL1	TA2R4	SREC2
ANK3	ALG13	DNM1L	DNJB4	KAD2	KCNN3	PERI	PER3	TA6P	SRGEF
ANKAR	ALG14	DNMBP	DNJB8	KAD4	KCNQ2	PERL	PERF	TAF1	SRPK1
ANKF1	ALK	DNMT1	DNJC1	KAISO	KCNQ4	PERM	PERQ1	TAF1D	SRPK2
ANKL1	ALKB1	DOC10	DNJC2	KALM	KCNQ5	PERPL	PERQ2	TAF2	SRPK3
ANKR6	ALKB2	DOC11	DNJC4	KANK2	KCNRG	PEX3	PERT	TAF4	SRR
ANKS3	ALLC	DOC2B	DNJC9	KANK4	KCNV1	PEX5	PESC	TAF4B	SRRM3
ANKZ1	ALO17	DOCK2	DNLZ	KAP2	KCP	PF21B	PEX1	TAF6	SRSF4
ANM10	ALPK1	DOCK5	DNM3B	KAT2A	KCT2	PG2IP	PEX14	TAF7L	SRSF5
ANM7	ALR	DOCK6	DNPEP	KAT6B	KCTD4	PGBM	PEX19	TANC1	SRSF9
ANO1	AMBN	DOCK7	DNSL3	KAT7	KCTD9	PGH1	PEX5R	TANC2	SRTD4
ANO5	AMGO3	DOCK8	DOCK3	KAT8	KD4DL	PGM1	PEX6	TAOK3	SSBP4
ANO8	AMOL1	DOK1	DOCK4	KAZD1	KDEL1	PGM2L	PF21A	TARA	SSH1
ANR24	AMOL2	DOK2	DOCK9	KBP	KDM1B	PGM5	PF2R	TARB1	SSR1
ANR26	AMOT	DOM3Z	DOK3	KBTBC	KDM2B	PGRP2	PG12B	TARM1	ST17A
ANR28	AMPD2	DONS	DOK7	KBTBD	KDM4D	PHAR2	PGAM4	TAZ	ST20
ANR31	AMPD3	DP13B	DOP1	KCAB1	KDM7	PHAR4	PGBD1	TBB2B	ST2B1
ANR35	AMPH	DPCA2	DOP2	KCAB2	KDM8	PHC1	PGCA	TBB2C	ST32B
ANR45	AMPN	DPCR1	DOS	KCC2G	KDSR	PHF10	PGCB	TBB3	ST65G
ANR49	AMPO	DPEP1	DOT1L	KCD11	KELL	PHF13	PGFRB	TBB4	ST7L
ANR53	AMRP	DPEP3	DP13A	KCD16	KHDR3	PHF3	PGRC2	TBB4Q	STA5B
ANR56	AMTN	DPH1	DPEP2	KCD18	KI13B	PHF7	PGS1	TBB6	STAB2
ANR57	AMY1	DPH2	DPM1	KCD19	KI18B	PHF8	PHAR3	TBB8	STAC
ANRA2	AMY2B	DPOA2	DPOD3	KCNB2	KI26A	PHIPL	PHAX	TBC16	STAC2
ANT3	AMZ1	DPOE1	DPOE3	KCNC3	KI26B	PHLB1	PHB2	TBC19	STAG1
ANTRL	AMZ2	DPOE4	DPOG2	KCND1	KI2L4	PHLB2	PHC2	TBC23	STAG2
ANXA1	AN13B	DPOG1	DPOLA	KCND3	KI3L1	PHLB3	PHC3	TBC24	STALP
AOC2	AN13D	DPOLN	DPOLM	KCNE1	KI3P1	PHOP1	PHF1	TBC30	STAR
AP180	AN30B	DPOLQ	DPP2	KCNG1	KI3X1	PHTF2	PHF12	TBC8B	STAR8
AP1AR	ANDR	DPOLZ	DPP3	KCNH3	KIF15	PHX2A	PHF14	TBC9B	STAR9
AP1B1	ANF	DPP10	DPP6	KCNH4	KIF1A	PHYIP	PHF2	TBCC1	STAT6
AP2A1	ANFB	DPP4	DPPA2	KCNH5	KIF1C	PI3R4	PHF20	TBCD7	STAU2
AP2A2	ANFC	DPP8	DPPA3	KCNH7	KIF22	PI3R5	PHF6	TBCD8	STC1

AP2B	ANFY1	DPP9	DPRX	KCNH8	KIF24	PI3R6	PHIP	TBCD9	STIL
AP2B1	ANGL1	DPYD	DR4L2	KCNK2	KIF27	PI42A	PHLD	TBCK	STIM2
AP2D	ANGL7	DPYL1	DRAXI	KCNK9	KIF4B	PI51C	PHLP1	TBD2A	STK19
AP2E	ANGT	DPYL2	DRD4	KCNKA	KIF6	PI5PA	PHLP2	TBD2B	STK36
AP2M1	ANK1	DPYL3	DREB	KCNQ3	KIF7	PIAS3	PHRF1	TBE	STK38
APBB1	ANK2	DQB1	DRGX	KCNT2	KIFC3	PIBF1	PHTNS	TBG2	STON1
APBB2	ANKH	DQB2	DRP2	KCNV2	KIME	PIGB	PI16	TBK1	STP2
APC	ANKH1	DQX1	DSCAM	KCP3	KLC1	PIGP	PI42B	TBKB1	STRAP
APC2	ANKL2	DRAM1	DSCR8	KCRU	KLDC2	PIGQ	PI4KA	TBL1X	STRUM
APEX2	ANKR5	DRD1	DSEL	KCTD3	KLDC9	PILRA	PI4P2	TBL3	STS
APLF	ANKS6	DRD5	DSG3	KCTD5	KLF11	PININ	PI51A	TBX1	SUH
AQP2	ANKY1	DSC3	DTD1	KCTD7	KLF12	PIPSL	PI5L1	TBX15	SUIS
AQR	ANO6	DSCL1	DTL	KCTD8	KLF17	PITC1	PIAS2	TBX2	SUMF1
AR13B	ANPRB	DSCR4	DTNA	KDEL2	KLF2	PITM3	PICAL	TBX21	SUN1
AR6P4	ANPRC	DSE	DTX2	KDIS	KLF4	PITX3	PIEZ1	TBX3	SUN2
ARAF	ANR11	DSG1	DU4L4	KDM1A	KLF6	PK1L2	PIEZ2	TBX4	SUV92
ARAP2	ANR12	DSG4	DU4L5	KDM2A	KLH13	PK1L3	PIFO	TBX5	SUZ12
ARBK1	ANR16	DSRAD	DUS10	KDM3B	KLH17	PK2L1	PIGG	TC1D3	SVIL
AREG	ANR27	DTHD1	DUS26	KDM4A	KLH20	PK3C3	PIGN	TCAL6	SWT1
ARFG2	ANR32	DTNB	DUS3L	KDM4B	KLH23	PKCB1	PIGO	TCF20	SYBU
ARFG3	ANR40	DTX3L	DUS4	KDM5A	KLH24	PKD1	PIGT	TCF7	SYCP1
ARG35	ANR43	DTX4	DUS4L	KDM5B	KLHL4	PKDCC	PIGU	TCO1	SYG
ARGI1	ANR50	DU4L2	DUS5	KDM5C	KLHL8	PKH4B	PIGZ	TCOF	SYGP1
ARGI2	ANR62	DU4L3	DUS7	KDM5D	KLK13	PKHA3	PIM1	TCP1L	SYHM
ARH37	ANR63	DU4L6	DUT	KDM6A	KLK14	PKHA6	PISD	TCPB	SYIC
ARHG2	ANS1A	DU4L7	DUX1	KDM6B	KLK7	PKHA7	PITM1	TCPQL	SYMC
ARHG5	ANS1B	DUFFY	DUX2	KGP1	KLRF1	PKHA9	PITM2	TCPQM	SYMPK
ARHG6	ANTR1	DUOX1	DUX4	KHDR2	KNTC1	PKHB1	PITX1	TCPR2	SYNE1
ARHG8	ANTR2	DUOX2	DUX5	KHNYN	KPB1	PKHF2	PITX2	TCRG1	SYNE2
ARHGB	ANUB1	DUPD1	DYH1	KI13A	KPB2	PKHG2	PIWL2	TCRGL	SYNJ2
ARHGF	AP1G1	DUS1	DYH12	KI20A	KPCD3	PKHG6	PIWL4	TCTA	SYNM
ARHGJ	AP2A	DUS2	DYH5	KI21A	KPCE	PKHH3	PJA1	TCTE1	SYNP2
ARHGQ	AP2C	DUS27	DYH9	KI21B	KPCG	PKHM1	PK1IP	TDR12	SYPM
ARHL1	AP3B1	DUS8	DYHC2	KI3S1	KPCT	PKHM2	PK1L1	TDRD3	SYSM
ARI1A	AP3B2	DUX3	DYM	KI67	KPCZ	PKHM3	PK3CA	TDRD6	SYT16
ARI1B	AP3D1	DUX4C	DYN1	KIAS3	KPYM	PKHO1	PK3CD	TDT	SYT5
ARI3A	APAF	DVL1	DYR1A	KIBRA	KR101	PKHO2	PK3CG	TEAD1	SYTL5
ARI5B	APBA1	DVL3	DYSF	KIF11	KR104	PKN2	PKD2	TEANC	SZT2
ARK72	APBA2	DX26B	DZIP1	KIF14	KR105	PKN3	PKDRE	TECTA	T11L2
ARK73	APC1	DYH10	DZIP3	KIF19	KR10C	PKNX2	PKHA4	TEF	T126B
ARLY	APC10	DYH14	E2AK1	KIF1B	KR10D	PKP1	PKHA5	TEFM	T131L
ARMC1	APC4	DYH17	E2F1	KIF23	KR131	PKP2	PKHA8	TELO2	T132C
ARMC2	APCD1	DYH2	E2F2	KIF25	KR133	PKP3	PKHD1	TEN2	T132E
ARMC3	APLP1	DYH3	E2F3	KIF2B	KR271	PKP4	PKHG1	TENA	T151B

ARMC7	APLP2	DYH6	E2F4	KIF2C	KRA21	PLAC1	PKHG3	TENC1	T176A
ARMC8	APOA	DYH7	E2F8	KIF4A	KRA24	PLAC2	PKHG5	TENX	T184C
ARMX2	APOA1	DYH8	E400N	KIF5A	KRA2X	PLAC4	PKHH1	TEP1	T185A
ARMX6	APOB	DYHC1	E41L1	KIF9	KRA32	PLACL	PKHH2	TERF2	T191A
ARNT	APOBR	DYN3	EA3L2	KIFC1	KRBA1	PLAG1	PKHL1	TESK1	T200C
ARP21	APOC1	DYR1B	EAA3	KIFC2	KRIP1	PLAL1	PKHN1	TET1	T22D1
ARP5	APOE	DYRK3	EAA5	KIRR3	KRR1	PLAL2	PKN1	TET3	T23O
ARP5L	APOL5	DYRK4	EAF1	KISS1	KRT36	PLCB2	PKNX1	TEX15	T49L1
ARRB2	APRV1	DYST	EBLN1	KITH	KRT82	PLCB3	PKRI1	TEX2	T53G3
ARSB	AQP5	DYTN	ECE2	KIZ	KS6A2	PLCD3	PL8L1	TEX28	TAB1
ARSE	ARAP1	DZI1L	ECHB	KKCC2	KS6A5	PLCE	PLAK	TF2AY	TAB2
ARX	ARAP3	E2AK3	ECSCR	KLC2	KS6C1	PLCE1	PLAP	TF2H3	TAB3
ASA2C	ARC1A	E2AK4	EDAD	KLC4	KTI12	PLCH1	PLB1	TF2LX	TAC2N
ASAH2	ARFP1	E2F5	EDC3	KLDC3	KTN1	PLCH2	PLBL1	TF2LY	TACC1
ASB12	ARG33	E2F7	EDC4	KLDC4	KTNB1	PLD2	PLCB1	TF3C1	TACC2
ASB13	ARGAL	E41L3	EDNRB	KLF10	KTU	PLD5	PLCB4	TFE3	TACC3
ASB15	ARGFX	E41L5	EDRF1	KLF13	L1CAM	PLDN	PLCC	TFEC	TACT
ASB16	ARH38	E41LA	EED	KLF14	L2GL1	PLET1	PLCD1	TFP11	TAD2B
ASB9	ARH40	E41LB	EF1G	KLF15	LACB2	PLGF	PLCL2	TFPI2	TAF10
ASCC2	ARHG1	E4F1	EF2K	KLF16	LACE1	PLK3	PLCX2	TFR1	TAF1C
ASCL3	ARHGA	EA3L1	EFC1	KLF3	LACRT	PLK4	PLCX3	TGFB3	TAF1L
ASCL5	ARHGC	EAF2	EFCB6	KLF5	LAIR1	PLP2	PLD4	TGFI1	TAF3
ASF1B	ARHGG	EBLN2	EFCB8	KLF7	LAIR2	PLPL1	PLEC	TGIF2	TAF5
ASH1L	ARHGH	EBP2	EFHC1	KLF9	LAMA1	PLPL6	PLEK2	TGM1	TAF5L
ASH2L	ARHGI	ECE1	EFNA3	KLH11	LAMA2	PLPL8	PLIN4	TGM4	TAF6L
ASM	ARHGP	ECI2	EFNA4	KLH12	LAMA3	PLXB2	PLK2	TGON2	TAF7
ASPH	ARHL2	ECM1	EFNB2	KLH14	LAMA4	PM2P2	PLK5	THA	TAGAP
ASPH1	ARI3B	ECM29	EFNB3	KLH22	LAMA5	PM2P5	PLMN	THA11	TAL1
ASPM	ARI4A	ECT2	EFRD1	KLH33	LAMB2	PMEL	PLOD1	THADA	TAL2
ASPP1	ARI5A	EDA	EGFL6	KLH34	LAMB3	PML	PLPL2	THAP4	TALAN
ASPP2	ARID2	EDEM2	EGLN	KLH35	LAMC1	PMS1	PLPL7	THAP8	TANK
ASSY	ARIP4	EDN3	EGLN2	KLHL1	LAMC2	PNISR	PLXA1	THAP9	TAOK1
ASTN1	ARL17	EEA1	EGR2	KLHL5	LANC1	PNKP	PLXA2	THB	TAOK2
ASXL1	ARMC4	EFC2	EGR3	KLHL7	LAP2A	PNMA1	PLXA3	THBG	TAP2
ASXL2	ARMC6	EFC4A	EH1L1	KLHL9	LAP2B	PNOC	PLXA4	THIL	TARSH
AT10B	ARMC9	EFCB3	EHBP1	KLK5	LAR1B	PNPT1	PLXB1	THIM	TATD2
AT10D	ARMS2	EFCB5	EHD1	KLOTB	LARP1	PO3F2	PLXC1	THIOM	TAU
AT11A	ARNT2	EFCB7	EHD4	KLRG2	LAS1L	PO4F3	PLXD1	THMS1	TAXB1
AT11B	ARRB1	EFHA2	EHMT1	KNG1	LATS1	PO5F1	PM2P1	THMS2	TB10B
AT133	ARRD1	EFHB	EI2BE	KPCD1	LAX1	PODN	PM2PB	THOC2	TB182
AT134	ARRD3	EFR3A	ELF3	KPCL	LAYN	PODO	PMGT1	THOC3	TBB1
AT1A1	ARRD5	EFR3B	ELFN1	KR103	LBR	PODXL	PMM1	THRB	TBB2A
AT1A3	ARSA	EFS	ELK1	KR106	LCAT	POF1B	PMYT1	THY1	TBB5
AT1A4	ARSF	EFTU	ELK3	KR107	LCE1D	POGK	PNKD	THYG	TBB8B

AT1B2	ARSH	EGFEM	ELK4	KR108	LCHN	POGZ	PNMA5	TIAF1	TBC12
AT2A1	ARSI	EGFR	ELL2	KR109	LCK	POK10	PNML2	TIAM2	TBC15
AT2B1	ARSJ	EGR1	ELOA1	KR132	LCMT2	POK12	PNO1	TIGD4	TBC17
AT2C1	ARSK	EHD2	ELOA2	KR151	LDB2	POK17	PO210	TIM	TBC21
AT2C2	ARY2	EHMT2	ELOV4	KR241	LDHD	POK20	PO2F1	TIM22	TBC25
AT2L1	ASA2B	EI24	ELP2	KRA22	LDOCL	POK4	PO2F2	TIMP1	TBCC
AT2L2	ASAP1	EI2BD	EMAL3	KRA23	LEAP2	POK7	PO2F3	TIMP4	TBCD1
AT5G1	ASAP3	EIF2A	EMAL5	KRA31	LEG12	PON1	PO3F1	TIRAP	TBCD4
AT7L1	ASB11	EIF3A	EMAL6	KRA33	LEMD2	POPD1	PO4F2	TITIN	TBCD5
AT7L3	ASB18	EIF3B	EMB	KRBA2	LENG9	PP12C	PO6F1	TJAP1	TBCEL
AT8B3	ASB3	EIF3E	EMD	KREM2	LEPR	PP13	POK2	TKT	TBG1
ATCAY	ASB4	EIF3G	EMR3	KRT35	LFA3	PP13G	POK3	TLCD2	TBP
ATD2B	ASB5	EIF3L	ENC1	KS6A1	LHX3	PP14C	POK5	TLE3	TBPL2
ATD3C	ASCL1	ELAV2	ENC2	KS6A4	LHX8	PP16A	POK6	TLK1	TBR1
ATE1	ASCL4	ELAV4	ENH1	KS6A6	LHX9	PP2BA	POLI	TLN1	TBRG1
ATF2	ASHWN	ELF1	ENHO	KS6B1	LICH	PP2BB	POLS2	TLXNB	TBRG4
ATF6A	ASM3A	ELF2	ENK8	KS6B2	LIFR	PP2BC	PONL1	TM100	TBX10
ATG13	ASM3B	ELF4	ENR1	KSR1	LIME1	PP2D1	POP1	TM102	TBX18
ATG9A	ASNA	ELL	ENTD1	KSR2	LIMK2	PP4R4	POPD2	TM104	TBX19
ATG9B	ASPC1	ELL3	ENTK	KV311	LIN52	PP4RL	PORIM	TM108	TBX20
ATL2	ASPH2	ELMO1	ENTP4	L2HDH	LIN54	PP6R2	POTE1	TM119	TBX22
ATL3	ASTE1	ELMO3	EOMES	L37A1	LIPA1	PPAC	POZP3	TM11E	TCA
ATL4	ASTL	ELOA3	EP300	L37A2	LIPA2	PPAC2	PP14D	TM11F	TCAL1
ATP7A	ASTN2	ELP1	EP3B	L37A3	LIPA3	PPAL	PP16B	TM127	TCAL3
ATP9B	ASXL3	ELP4	EP400	L9056	LIPA4	PPAP	PP1B	TM129	TCAL5
ATPO	AT10A	ELYS	EPAB2	LAC6	LIPB1	PPARA	PP1RA	TM130	TCAM1
ATRX	AT11C	EMAL4	EPAS1	LACTB	LIPG	PPB1	PP4R1	TM131	TCEA2
ATS1	AT131	EME1	EPB42	LAD1	LIPI	PPBI	PP4R2	TM134	TCF25
ATS10	AT132	EME2	EPC2	LAG3	LIPL	PPCE	PP6R1	TM143	TCFL5
ATS13	AT135	EMIL2	EPDR1	LAMB1	LIPR1	PPE2	PPA6	TM144	TCHL1
ATS15	AT1A2	EMIL3	EPG5	LAMC3	LIPS	PPIG	PPARG	TM163	TCP10
ATS5	AT2A3	EMR2	EPHA2	LAMP1	LIPT	PPIL4	PPBN	TM171	TCPD
ATS7	AT2B2	EMSY	EPHA3	LAMP2	LIRA1	PPM1A	PPE1	TM180	TCPR1
ATX2	AT2B3	ENAH	EPHA4	LAMP3	LIRA4	PPM1B	PPHLN	TM196	TDIF2
ATX2L	AT2B4	ENAM	EPHA7	LAP2	LIRA5	PPM1D	PPIP1	TM1L2	TDRD1
ATX3L	AT7L2	ENASE	EPHAA	LARGE	LIRA6	PPM1F	PPL13	TM211	TDRD5
AUTS2	ATAD5	ENDD1	EPHB2	LARP4	LIRB4	PPM1H	PPM1E	TM214	TDRD7
AXIN2	ATD3A	ENDOU	EPHB3	LARP6	LIRB5	PPM1M	PPM1G	TM236	TDRKH
AZI1	ATD3B	ENH3	EPIPL	LAT	LITFL	PPME1	PPM1J	TM55A	TEAD2
AZI2	ATF1	ENL	EPN1	LAT1	LKAP	PPR1B	PPN	TM55B	TEAD3
B2L10	ATF3	ENOX2	EPN3	LATS2	LKHA4	PPR3B	PPOX	TMC6	TEAD4
B2L13	ATF4	ENPL	EPOR	LBN	LLR1	PPR3F	PPR3A	TMC7	TECT1
B3A2	ATF6B	ENPP2	EPS15	LCA5	LMAN2	PR14L	PPR3C	TMCO3	TECT3
B3A3	ATF7	ENTP6	EPS8	LCE2B	LMBL2	PR15A	PPR3D	TMCO7	TEKT2

B3AT	ATG12	ENTP8	EPT1	LCMT1	LMBL3	PR15B	PPRC1	TMM31	TEN1
B3GA2	ATG2A	ENW1	ERAP1	LCN12	LMNB1	PR20A	PPT2	TMM52	TEN3
B3GLT	ATG2B	EP15R	ERBB2	LCOR	LMNB2	PR20C	PQLC2	TMM61	TEN4
B3GN6	ATG4C	EP3A	ERBB4	LCORL	LMOD1	PR20D	PR20B	TMM62	TENR
B3GN8	ATHL1	EPC1	ERCC6	LCP2	LMOD2	PR20E	PR23A	TMM71	TENS1
B4GN2	ATL1	EPGN	ERCC8	LCTL	LMTK2	PR23A	PR23B	TMM74	TENS3
B4GN3	ATL5	EPHA1	ERF1	LDB1	LMX1A	PR23C	PR285	TMM79	TENS4
B4GN4	ATLA1	EPHA5	ERG1	LDB3	LMX1B	PR38A	PR38B	TMM91	TENXA
B4GT2	ATOH1	EPHB1	ERI2	LDH6B	LNX2	PRA16	PR40A	TMPPE	TERF1
B4GT3	ATP4A	EPHB4	ERIC1	LDLR	LONF2	PRA25	PR40B	TMPS2	TERT
B7H6	ATP4B	EPM2A	ERMAP	LEF1	LONF3	PRAM1	PRA13	TMTC1	TET2
B9D1	ATP7B	EPMIP	ERMP1	LEG2	LOX12	PRAM2	PRA17	TMTC3	TEX12
BACD1	ATP9A	EPN2	ERN1	LENG8	LOXH1	PRAM3	PRA18	TMUB2	TEX14
BACE1	ATPB	EPN4	ERN2	LETM1	LOXL2	PRAM8	PRA19	TMX3	TF
BACE2	ATPF2	ERC2	ERO1A	LETM2	LOXL3	PRAML	PRA22	TNAP3	TF2H1
BACH1	ATR	ERC6L	ERP44	LEU7	LOXL4	PRC2B	PRA24	TNF13	TF2L1
BACH2	ATRIP	ERCC5	ERR1	LEUK	LPAR3	PRC2C	PRAM7	TNI3K	TF3B
BAG1	ATS12	ERF	ERR2	LEUTX	LPH	PRCC	PRAME	TNIP1	TF3C2
BAG3	ATS14	ERF3A	ERR3	LFNG	LPHN1	PRCM	PRAX	TNK1	TF7L1
BAG6	ATS16	ERI1	ERVV2	LG3BP	LPHN2	PRD10	PRC1	TNKS2	TF7L2
BAGE5	ATS17	ERI3	ESAM	LGMN	LPIN1	PRD13	PRC2A	TNPO1	TFCP2
BAHC1	ATS18	ERMIN	ESCO1	LHX1	LPIN3	PRDM1	PRD14	TNR11	TFDP3
BAI1	ATS2	ERP27	ESIP1	LHX2	LPPR2	PRDM7	PRD15	TNR12	TFE2
BAI2	ATS20	ERRFI	ESPL1	LHX5	LPXN	PRDM9	PRD16	TNR14	TFEB
BAI3	ATS3	ERVV1	ESPNL	LHX6	LR16A	PRDX2	PRDM2	TNR16	TFG
BANK1	ATS4	ES8L1	ESR2	LIMA1	LR37B	PRDX5	PRDM4	TNR17	TFPI1
BARH1	ATS6	ES8L2	ESRP1	LIMC1	LRBA	PREP	PRDM6	TNR19	TFR2
BASI	ATS9	ES8L3	ESYT3	LIMD1	LRC14	PRGC2	PRDM8	TNR1B	TGBR3
BASP1	ATX1	ESCO2	ETS1	LIMK1	LRC17	PRGR	PRDX3	TNR21	TGFB2
BAZ1A	ATX1L	ESF1	ETV1	LIN37	LRC25	PRIC2	PRDX6	TNR25	TGIF1
BAZ2B	ATX7	ESPN	ETV2	LIN9	LRC26	PRIC4	PREX1	TNR27	TGM3L
BBC3	AUP1	EST1A	ETV3L	LINES	LRC32	PRKDC	PREX2	TNR3	TGM7
BBS1	AUXI	EST2	ETV5	LIPC	LRC36	PRLHR	PRG2	TNR6A	TGS1
BBS10	AVEN	EST3	EVC	LIPE	LRC46	PROP	PRG4	TNR6B	TGT
BBS12	AVL9	EST4A	EVI1	LIPT2	LRC4C	PROP1	PRGC1	TNR9	THAS
BBS2	AXDN1	EST5A	EVI2B	LIRA2	LRC53	PRP16	PRI2	TNT	THS7A
BBX	AXIN1	ESYT1	EVI5	LIRA3	LRC56	PRP17	PRIC3	TOE1	THS7B
BCAM	B2L12	ETAA1	EVI5L	LIRB1	LRC63	PRP39	PRLR	TOM1	THSD1
BCAP	B3GA1	ETFD	EVL	LIRB2	LRC66	PRP4B	PRM3	TONSL	THSD4
BCCIP	B3GA3	ETHE1	EX3L1	LIRB3	LRC67	PRPF3	PROL1	TOP1	THTPA
BCDO1	B3GL2	ETV3	EXO1	LITD1	LRC68	PRR14	PROX1	TOP2B	THUM2
BCL2	B3GN4	ETV6	EXOC1	LMA2L	LRC6X	PRR17	PROZ	TOP3B	TIA1
BCL7A	B3GN7	ETV7	EXOC7	LMAN1	LRC8B	PRR24	PRP19	TOPB1	TIAM1
BCL9L	B4GT7	EVG1	EXPH5	LMBD2	LRCH4	PRR5L	PRP4	TOR3A	TIAR

BCLF1	BABA1	EVPL	EYA2	LMBL1	LRFN3	PRRC1	PRP8	TOX	TICRR
BCS1	BAG4	EVX1	EYA3	LMF2	LRIF1	PRRX1	PRR11	TOX2	TIE1
BEST2	BAGE1	EVX2	EYS	LMNA	LRIG2	PRS35	PRR12	TOX3	TIF1A
BEST4	BAGE2	EX3L4	F100A	LMO7	LRIT2	PRS41	PRR15	TOX4	TIF1B
BGLR	BAGE3	EXC6B	F100B	LMTK1	LRMP	PRS53	PRR18	TPA	TIG3
BHA15	BAGE4	EXOC5	F101A	LMTK3	LRP11	PRS54	PRR19	TPC1	TIGD1
BHE41	BAHD1	EXOC8	F101B	LNP	LRP1B	PRS55	PRR5	TPC11	TIGD3
BI2L1	BAIP2	EXT1	F102A	LNX1	LRP2	PRS56	PRRT1	TPC2A	TIGD5
BI2L2	BAIP3	EXT2	F102B	LONF1	LRP5	PSD1	PRRT2	TPC3L	TIGIT
BIG2	BAKOR	EXTL1	F108B	LOXL1	LRRC9	PSD2	PRRT4	TPD52	TIM9B
BIN1	BANP	EYA1	F110A	LP35A	LRRF1	PSD4	PRRX2	TPD54	TIMD4
BIN2	BARD1	EYA4	F110B	LPAR4	LRRK2	PSF2	PRS23	TPGS2	TINAL
BINCA	BARH2	F105B	F110C	LPCT4	LRRN1	PSG1	PRS27	TPOR	TINF2
BIRC1	BAZ1B	F108C	F111B	LPHN3	LRRN4	PSG11	PRS29	TPP1	TISB
BIRC6	BAZ2A	F1142	F116B	LPP	LRRT2	PSG3	PRS42	TPP2	TISD
BIRC8	BBS4	F116A	F117B	LPPR1	LRRT4	PSG6	PRSR1	TPPC3	TKTL1
BLK	BC11A	F117A	F124B	LPPR3	LRWD1	PSL1	PRSS8	TPPP	TKTL2
BLM	BC11B	F118B	F126B	LPPR4	LS14A	PSMD2	PRTG	TPRA1	TLE1
BMI1	BCAR1	F120A	F127C	LR14B	LS14B	PSN1	PRUN2	TPRX1	TLE2
BMP10	BCAR3	F122A	F134A	LR16B	LSR	PSRC1	PRUNE	TPSN	TLE4
BMP2K	BCAS3	F122B	F135A	LR16C	LST2	PTBP2	PSA	TPTE2	TLK2
BMP5	BCL10	F123A	F135B	LRAD2	LST8	PTC2	PSA1	TPX2	TLL2
BMP8B	BCL3	F123B	F13B	LRC18	LTBP1	PTF1A	PSA5	TR10A	TLN2
BMPR2	BCL6	F123C	F149A	LRC23	LTBP2	PTHD2	PSAL	TR10C	TLR10
BMS1	BCL6B	F124A	F149B	LRC27	LTK	PTK7	PSB11	TR10D	TLR9
BNC1	BCL7B	F125B	F150A	LRC43	LTN1	PTN14	PSB2	TR13B	TM105
BNC2	BCL7C	F131A	F153B	LRC45	LV001	PTN18	PSB6	TR13C	TM115
BNI3L	BCL9	F131C	F161B	LRC4B	LV201	PTN20	PSB9	TR150	TM139
BNIPL	BCOR	F134C	F163A	LRC58	LV202	PTN23	PSD3	TR3N	TM155
BOC	BCORL	F150B	F166A	LRC71	LV203	PTN3	PSG2	TRA2A	TM173
BOLL	BCR	F151A	F167A	LRC8A	LV204	PTN4	PSG4	TRAD1	TM189
BORA	BDP1	F161A	F16A1	LRC8C	LV207	PTN5	PSG7	TRAF2	TM1L1
BOREA	BEAN1	F168A	F16A2	LRC8D	LV209	PTN9	PSG8	TRAF7	TM201
BORG5	BEGIN	F168B	F16B1	LRC8E	LV211	PTPC1	PSL2	TRAK2	TM208
BPTF	BEND2	F169A	F16P2	LRCH1	LV401	PTPRC	PSMD1	TRAP1	TM209
BRAC	BEND4	F16B2	F171B	LRCH2	LV402	PTPRJ	PSMD8	TREM1	TM215
BRAT1	BEND5	F170A	F175A	LRCH3	LV403	PTPRQ	PSME4	TREX1	TM217
BRCA1	BEND7	F170B	F179A	LRFN6	LV404	PTPRS	PSMF1	TRFR	TM221
BRCA2	BEST3	F1711	F179B	LRIG1	LV405	PTTG1	PSN2	TRGC1	TM232
BRD1	BFAR	F1712	F181B	LRIG3	LV601	PTTG2	PSPB	TRGC2	TM38B
BRD3	BFSP1	F173B	F186A	LRP1	LV603	PUF60	PSPC1	TRHY	TM39A
BRIT2	BFSP2	F176B	F187A	LRP10	LV605	PUR6	PTC1	TRI11	TM40L
BROMI	BICC1	F178A	F188A	LRP3	LX15B	PUR8	PTCRA	TRI14	TM63A
BRPF1	BICD1	F181A	F188B	LRP4	LXN	PURG	PTEN	TRI18	TM63C

BRPF3	BICD2	F184A	F1892	LRP6	LY65C	PUSL1	PTGDS	TRI26	TM87A
BRSK2	BICR2	F184B	F189B	LRP8	LY6D	PWP2	PTGR1	TRI33	TMC2
BRWD1	BIG1	F186B	F18A1	LRR70	LYAG	PYGO1	PTGR2	TRI35	TMC3
BRWD3	BIG3	F1882	F190A	LRRC4	LYAM3	PYRD1	PTH1R	TRI37	TMC4
BRX1	BIRC2	F1891	F190B	LRRC7	LYSM2	PZP	PTHB1	TRI39	TMC5
BSDC1	BIRC3	F195B	F193A	LRRD1	LYSM4	PZRN3	PTHD3	TRI42	TMCO2
BSH	BIRC7	F196A	F193B	LRRF2	LYST	QKI	PTN12	TRI45	TMED8
BT1A1	BIVM	F199X	F194A	LRRK1	M10L1	QORL1	PTN13	TRI52	TMF1
BTAF1	BLACE	F200A	F194B	LRRN2	M18BP	QRFPR	PTN21	TRI58	TMG2
BTBD1	BLCAP	F203B	F195A	LSG1	M3K12	QRIC1	PTN22	TRI59	TMG3
BTBD7	BLNK	F208B	F196B	LSM11	M3K14	QRIC2	PTOV1	TRI61	TMIG2
BTBDA	BM2KL	F27D1	F198A	LSP1	M3K2	R10B1	PTPR2	TRI66	TMM26
BTBDH	BMAL1	F27E1	F203A	LTBP3	M3K4	R113B	PTPRA	TRI67	TMM35
BTC	BMP6	F71E1	F205A	LTBP4	M3K7	R3GEF	PTPRB	TRI74	TMM44
BTD	BMP8A	F71E2	F205B	LTC4S	M4A10	R3HD1	PTPRD	TRIL	TMM51
BUB1	BMPER	F71F2	F262	LUZP1	M89BB	R3HD2	PTPRF	TRIM7	TMM78
BUB1B	BNIP3	F75A7	F263	LV205	MA13P	R51A1	PTPRG	TRIPB	TMM95
BUB3	BOD1L	F86A1	F27E2	LV210	MA2B1	R7BP	PTPRK	TRIPC	TMPS9
BUD13	BORG1	F86B1	F27E3	LV602	MA2B2	RAB10	PTPRN	TRM11	TMPSD
BY55	BPIB2	F86B3	F75A1	LV604	MABP1	RAB26	PTPRO	TRM13	TMUB1
C102A	BPIB3	F90A1	F75A2	LY10	MACC1	RAB37	PTPRT	TRM2	TNC18
C163A	BPIFC	F90AA	F75A3	LY65B	MACF1	RAB3I	PTPRU	TRM2A	TNFB
C163B	BPL1	F90AC	F75A4	LY66D	MADL2	RAB44	PTPRZ	TRML3	TNFL6
C19L1	BRAF	F90AG	F75A5	LY75	MAEL	RAB6C	PTSS1	TRML4	TNFL9
C19L2	BRAP	F90AI	F75A6	LY9	MAF	RAB8A	PTSS2	TRMT5	TNIK
C1QR1	BRD2	F90AL	F75D1	LYAM1	MAF1	RABE1	PUM1	TRNK1	TNIP2
C1TC	BRD4	F91A1	F86A3	LYAM2	MAFIP	RAD52	PUM2	TRPA1	TNKS1
C1TM	BRD7	FA12	F86B2	LYG1	MAG	RAD54	PUR1	TRPC3	TNNC2
C2C4A	BRD8	FA13B	F90A2	LYN	MAGA2	RADIL	PUR4	TRPC5	TNR18
C2C4C	BRDT	FA156	F90A5	LYNX1	MAGA5	RAE2	PUR9	TRPC6	TNR1A
C2CD3	BRE	FA20A	F90A7	LYSM1	MAGA9	RAF1	PVRL2	TRPM1	TNR4
C2D1A	BRE1B	FA21A	F90A8	LYVE1	MAGAB	RAG1	PVRL4	TRPM2	TNR6C
C56D1	BRS3	FA21C	F90A9	LZTS2	MAGB5	RAG2	PWP1	TRPM3	TNR8
C8AP2	BRSK1	FA22A	F90AD	M21D1	MAGBH	RAI1	PWP2A	TRPM6	TOB2
CA043	BSN	FA22B	F90AE	M2GD	MAGC2	RAI14	PWP2B	TRPS1	TOIP1
CA051	BSND	FA22E	F90AJ	M3K1	MAGC3	RAMP2	PXDC1	TRPT1	TOIP2
CA063	BSPRY	FA22F	F90AK	M3K10	MAGD1	RANB3	PXDC2	TRPV1	TOP2A
CA086	BT2A3	FA22G	F90AM	M3K11	MAGD2	RANG	PXDNL	TRRAP	TOPRS
CA101	BT3A3	FA26D	F90AN	M3K13	MAGE1	RARA	PXK	TRXR1	TP4AP
CA106	BTBD2	FA35A	F90AO	M3K15	MAGI1	RASA3	PYC	TS101	TP53B
CA111	BTBDG	FA40A	F91A2	M3K3	MAGI2	RASEF	PYR1	TS1R1	TPBG
CA127	BTBDI	FA46B	FA13A	M3K5	MAGI3	RASFA	PYRD2	TS1R3	TPC10
CA133	BTK	FA47A	FA13C	M3K6	MAMC2	RASL3	PYRG1	TSAP1	TPC12
CA141	BTNL2	FA47B	FA21B	M3K9	MAMD1	RB3GP	PZRN4	TSH1	TPC2

CA144	BUP1	FA47D	FA22D	M3KL4	MAML1	RBBP6	QCR1	TSN10	TPC2B
CA157	C144B	FA53C	FA27L	M4A12	MANS4	RBBP7	QPCT	TSN16	TPO
CA170	C170L	FA57A	FA47C	M4A14	MAON	RBCC1	QPCTL	TSNA1	TPPC8
CA172	C1AS1	FA59A	FA48A	M4A15	MAP1A	RBG1L	QSER1	TSP1	TPR
CA173	C1S	FA60A	FA5	M4A6A	MAP1S	RBL2	QSOX1	TSP3	TPRN
CA182	C2C2L	FA63A	FA53A	M4K1	MAP2	RBL2A	R10B2	TSP4	TPRXL
CA186	C2C4B	FA65C	FA53B	M4K2	MAP4	RBL2B	R51A2	TSR1	TPSNR
CA191	C2D1B	FA66E	FA54A	M4K4	MAP7	RBM10	RAB12	TSR3	TPTE
CA200	C2D4D	FA7	FA54B	MA2A1	MAP9	RBM15	RAB36	TSSC1	TR10B
CA212	C2G1L	FA70A	FA55A	MA2A2	MAPK2	RBM19	RAB7B	TSY26	TR19L
CA229	C56D2	FA70B	FA55B	MA6D1	MAPK3	RBM20	RABE2	TSYL2	TR61B
CA2D1	CA031	FA71B	FA55D	MA7D1	MARCS	RBM25	RABEK	TSYL4	TRA2B
CA2D2	CA050	FA71C	FA59B	MA7D2	MARE2	RBM26	RABX5	TT39A	TRAF3
CAB39	CA056	FA71D	FA63B	MA7D3	MARH3	RBM27	RAD18	TT39C	TRAK1
CABP1	CA065	FA81B	FA64A	MAAI	MARH4	RBM39	RAD50	TTC12	TRBM
CABS1	CA087	FA83B	FA65A	MACF4	MARHA	RBM40	RAE1L	TTC14	TRBP2
CAC1E	CA094	FA83H	FA65B	MACOI	MARK1	RBM44	RANB9	TTC17	TRDN
CAC1I	CA096	FA84A	FA76B	MADCA	MARK2	RBM47	RAPH1	TTC18	TREF1
CAC1S	CA114	FA89A	FA8	MADD	MASP2	RBM4B	RARB	TTC28	TRFL
CAD10	CA124	FA8A1	FA83C	MAFA	MAST1	RBM5	RARG	TTDN1	TRHDE
CAD12	CA131	FA98A	FA83D	MAFB	MASTR	RBM7	RAS4B	TTF2	TRI16
CAD16	CA135	FA98B	FA86A	MAFF	MATN1	RBMS1	RASA1	TTHY	TRI17
CAD20	CA140	FAAH2	FA92B	MAGA4	MATN3	RBMS2	RASA2	TTK	TRI32
CAD26	CA167	FACE1	FAAH1	MAGA8	MATN4	RBMS3	RASD1	TTL13	TRI36
CADH6	CA168	FAD1	FACD2	MAGAC	MBD1	RBMXL	RASF1	TTLL2	TRI38
CADH7	CA194	FAD2L	FAK1	MAGB1	MBD4	RBP1	RASF5	TTLL3	TRI46
CAF1B	CA211	FAF1	FAM27	MAGB4	MBD6	RBP2	RASF7	TTLL5	TRI50
CAGE1	CA222	FAK2	FAM3D	MAGB6	MBIP1	RBPMS	RASL2	TTLL7	TRI55
CAH11	CA2D4	FAKD1	FAN	MAGBG	MBNL3	RBY1A	RAVR1	TTMP	TRI56
CAH14	CA5BL	FAKD3	FANCJ	MAGC1	MBOA5	RBY1B	RB	TTP	TRI62
CAH3	CABIN	FAKD5	FANK1	MAGD4	MCAF1	RBY1E	RB12B	TTYH3	TRI68
CAH6	CABL2	FAM3A	FARP2	MAGIX	MCAR1	RCAN1	RB15B	TULP1	TRI73
CALD1	CABP2	FAM3B	FAT1	MAGL2	MCAR2	RCAN3	RB40C	TULP4	TRIB1
CALR3	CABYR	FAM7A	FAT4	MAK	MCLN1	RCBT1	RB6I2	TUT7	TRIB2
CALU	CAC1B	FAN1	FBAS1	MALD2	MCLN3	RCL	RBBP4	TUTLB	TRIM1
CALX	CAC1C	FANCA	FBF1	MALT1	MCM10	RCN1	RBFA	TVB1	TRIM2
CAMKV	CAC1D	FANCB	FBLN2	MAML2	MCM3A	RCOR1	RBGP1	TWF1	TRIM3
CAMP2	CAC1F	FANCC	FBN1	MAML3	MCM4	RD23A	RBGPR	TWF2	TRIM4
CAN12	CAC1G	FANCE	FBN2	MAN1	MCM5	RDH1	RBL1	TXIP1	TRIM9
CAN7L	CAC1H	FANCG	FBN3	MANBA	MCMBP	RDH8	RBM12	TXLNA	TRIML
CAPON	CACB1	FANCI	FBP1L	MANEL	MCP	REBL1	RBM14	TXN4B	TRIO
CAPS1	CACB2	FANCL	FBSL	MANS1	MCSP	REC8	RBM23	TXND3	TRIX3
CAPS2	CACB3	FANCM	FBX10	MAP1B	MD12L	RECQ4	RBM28	TXND5	TRM1
CAR14	CACB4	FAS	FBX22	MAP6	MD13L	RED2	RBM33	TYDP1	TRM1L

CARD8	CACO1	FAT3	FBX30	MAPK5	MDHC	REEP5	RBM38	TYRO3	TRM44
CARD9	CAD13	FBLI1	FBX31	MARCO	MDN1	REG3G	RBM4	TYRP1	TRM61
CASC1	CAD19	FBLN4	FBX34	MARE3	MDR1	RELB	RBM41	TYW2	TRNP1
CASC3	CAD22	FBW10	FBX40	MARH1	ME3L1	RELN	RBM45	U17L1	TROAP
CASD1	CAD23	FBW12	FBX42	MARH2	MED12	RENBP	RBM46	U17L3	TROP
CASL	CAD24	FBW1A	FBX43	MARH6	MED15	RENI	RBMX2	U2AF2	TRPC1
CASP2	CADH1	FBW1B	FBX47	MARH7	MED16	REPS1	RBNS5	U2AFL	TRPC4
CASS4	CADH3	FBX15	FBX9	MARH8	MED19	REST	RBP10	U2QL1	TRPC7
CATB	CADM2	FBX16	FBXL6	MARK3	MED23	RET	RBPJL	U5S1	TRPM4
CATC	CADM3	FBX24	FBXL7	MARK4	MED24	RET3	RBPS2	U632A	TRPV2
CB027	CAF17	FBX25	FBXW4	MASP1	MED27	REXO1	RBSK	U638B	TRPV4
CB053	CAF1A	FBX38	FBXW8	MAST2	MEF2A	REXON	RBX1	U639	TRPV5
CB068	CAH5A	FBX41	FBXW9	MAST3	MEG10	RF1ML	RBY1D	UAP1	TRPV6
CB069	CAH5B	FBX5	FCER2	MAST4	MEGF6	RFL3S	RBY1F	UB2D1	TRUB1
CB073	CAH7	FBX6	FCG2B	MATN2	MEGF8	RFNG	RC3H1	UB2D2	TRUB2
CB081	CAH9	FBXW5	FCHO1	MAVS	MEGF9	RFPL1	RC3H2	UB2D4	TRXR2
CB39L	CAHD1	FBXW7	FCRL3	MBB1A	MEI1	RFPL3	RCAN2	UB2E2	TRXR3
CBL	CALI	FCAMR	FCRL4	MBLC1	MEIS1	RFPLA	RCBT2	UB2G2	TRYG1
CBPA5	CALR	FCG2A	FCRL5	MBNL2	MEIS2	RFPLB	RCC1	UB6L2	TS1R2
CBPB2	CALRL	FCG2C	FCRL6	MBOA4	MELK	RFT	RCN3	UBA3	TSC1
CBPC5	CAMP1	FCGBP	FCSD1	MBP	MENTO	RFT1	RCOR3	UBA7	TSC2
CBS	CAMP3	FCGR1	FCSD2	MBRL	MEP1B	RFT3	RD23B	UBAP1	TSCOT
CBY1	CAN10	FCGRN	FDXA1	MBTP1	MEPCE	RFTN1	RD3	UBAP2	TSEAR
CC017	CAN11	FCRL2	FEAS1	MCAF2	MEPE	RFX1	RDH14	UBE2A	TSG10
CC018	CAN15	FCRLA	FEM1C	MCAR6	MERL	RFX4	RECK	UBE2C	TSH2
CC019	CAND1	FCRLB	FERM1	MCCA	MERTK	RFX5	RECQ5	UBE2O	TSH3
CC021	CAP2	FDSCP	FEZ1	MCCB	MESP2	RFX6	RELL1	UBE2Z	TSHR
CC022	CAPR1	FES	FEZ2	MCE1	MET	RFX8	REM2	UBE3A	TSP2
CC025	CAPR2	FETUA	FEZF2	MCF2	MET22	RFXK	REN3A	UBE3C	TSSC4
CC026	CAR10	FEZF1	FFR	MCF2L	METH	RG9D3	REN3B	UBE4A	TSYL1
CC037	CAR11	FGD3	FGD1	MCHR1	MEX3B	RGAG4	REPS2	UBE4B	TTBK1
CC056	CARD6	FGD5	FGD2	MCL1	MEX3D	RGAP1	REQU	UBIP1	TTBK2
CC062	CARF	FGF19	FGD6	MCM2	MF2L2	RGC32	RERE	UBL3	TTC13
CC063	CASC5	FGF4	FGF1	MCM8	MFRN2	RGDSR	RETST	UBL7	TTC16
CC067	CASK	FGFR1	FGF10	MCM9	MFS2B	RGF1B	REV1	UBN2	TTC24
CC071	CASP9	FHAD1	FGF11	MCPH1	MFS6L	RGF1C	RFA1	UBP1	TTC27
CC072	CASR	FHDC1	FGF13	MCR	MFSD7	RGL1	RFA2	UBP10	TTC3
CC079	CASZ1	FHOD1	FGF14	MCTP1	MGA	RGL2	RFC1	UBP13	TTC31
CC106	CAYP2	FICD	FGF22	MD1L1	MGAL1	RGNEF	RFIP1	UBP15	TTC37
CC107	CAZA2	FIL1L	FGF23	MD2BP	MGAT3	RGP1	RFIP3	UBP19	TTC38
CC108	CB016	FILA	FGF6	MDC1	MGLL	RGPD4	RFIP4	UBP20	TTC5
CC111	CB029	FIP1	FGFR2	MDGA1	MGST2	RGPD8	RFIP5	UBP21	TTC9B
CC116	CB044	FITM2	FGFR3	MDGA2	MGT4A	RGPS1	RFOX1	UBP24	TTC9C
CC120	CB046	FKB11	FGRL1	MDH1B	MIA3	RGS19	RFOX3	UBP25	TTI1

CC132	CB048	FKBP5	FHOD3	MDHM	MIB1	RGS22	RFPL2	UBP27	TTL10
CC138	CB055	FKS43	FHR1	MDM1	MICA1	RGS7	RFT2	UBP2L	TTL11
CC142	CB057	FLNA	FHR2	MDS1	MICA2	RGS9	RFTN2	UBP30	TTL12
CC14C	CB067	FLT3	FHR3	MDSP	MICA3	RHBD2	RFWD2	UBP33	TTLL1
CC154	CB071	FMN1	FHR4	ME3L2	MICLK	RHBG	RFWD3	UBP34	TTLL4
CC162	CB078	FMNL	FHR5	MECP2	MIER1	RHBT1	RFX2	UBP37	TTLL6
CC165	CB082	FMNL3	FIBG	MED1	MIER2	RHBT2	RFX7	UBP38	TTLL9
CC166	CB083	FNBP1	FIGLA	MED13	MILK1	RHCG	RG9D2	UBP42	TTY13
CC168	CB084	FND3A	FIGN	MED14	MILK2	RHDF2	RGAG1	UBP43	TTYH2
CC50A	CBLB	FND3B	FILA2	MED22	MINK1	RHES	RGL3	UBP48	TULP2
CC74A	CBP	FNDC5	FINC	MED26	MIO	RHG01	RGMA	UBP54	TUT4
CC74B	CBPA2	FNDC7	FKB15	MEF2B	MIS12	RHG05	RGMC	UBP6	TUTLA
CC85A	CBPC1	FNIP1	FL2D	MEF2C	MISSL	RHG06	RGN	UBP7	TVA2
CC85C	CBPC2	FOH1B	FLCN	MEF2D	MITF	RHG08	RGPA2	UBP8	TWSG1
CCAR1	CBR4	FOLH1	FLIP1	MEIS3	MK03	RHG17	RGPD1	UBQL2	TWST2
CCBE1	CBX2	FOLR3	FLNB	MELT	MK06	RHG28	RGPD3	UBR2	TX13A
CCD13	CBX4	FOS	FLNC	MEN1	MK07	RHG33	RGPD5	UBR3	TX13B
CCD15	CBX6	FOXA1	FLRT1	MEOX1	MK08	RHG35	RGRF1	UBR4	TX264
CCD27	CBX8	FOXA2	FLRT2	MEOX2	MK10	RHG39	RGRF2	UBR5	TXD11
CCD30	CBY3	FOXB1	FLT3L	MEP1A	MK11	RHG42	RGS12	UBS3B	TXD16
CCD33	CC020	FOXC1	FLVC1	MESD	MK12	RHGBA	RGS14	UBX2A	TXLNB
CCD39	CC024	FOXC2	FLVC2	MESP1	MK13	RIC8B	RGS17	UBX2B	TXND2
CCD41	CC053	FOXD1	FMN2	MEST	MK14	RIF1	RGS20	UBXN1	TY3H
CCD48	CC070	FOXD4	FMO1	MET16	MK67I	RILP	RGS21	UBXN4	TYOBP
CCD57	CC077	FOXG1	FNBP2	METL9	MKNK1	RIMB2	RGS3	UCK1	TYPH
CCD62	CC115	FOXI1	FNBP4	MEX3A	MKNK2	RIN1	RGSL	UCN2	TYRP2
CCD66	CC117	FOXI2	FNDC1	MEX3C	MKS1	RIN2	RHBD1	UD2A1	TYW1
CCD73	CC129	FOXI3	FNDC4	MFAP2	MLC1	RIN3	RHBD3	UD2B7	TYW1B
CCD82	CC130	FOXJ3	FNIP2	MFF	MLF2	RIPK3	RHBT3	UDB10	U17L2
CCD92	CC134	FOXK1	FNTB	MFHA1	MLH3	RIPL1	RHDF1	UDB28	U17L4
CCD94	CC135	FOXL1	FOG1	MFNG	MLL1	RIPL2	RHG04	UFO	U17L7
CCDB1	CC140	FOXM1	FOG2	MFRP	MLL4	RISC	RHG07	UHMK1	U17L8
CCDC7	CC151	FOXN2	FOSB	MFSD5	MLP3B	RL1D1	RHG10	UHRF1	U2AFM
CCDC9	CC153	FOXO1	FOSL1	MFSD6	MLTK	RL3L	RHG12	UIMC1	U3IP2
CCG1	CC155	FOXO3	FOSL2	MGAL2	MLX	RL3R1	RHG18	ULK1	UAP1L
CCG2	CC159	FOXO4	FOXA3	MGAP	MLXPL	RLF	RHG19	UN13B	UB2D3
CCG4	CC160	FOXO6	FOXB2	MGRN1	MMP13	RM01	RHG20	UNC5A	UB2E1
CCL19	CC88B	FOXP1	FOXF2	MGT5A	MMP14	RM24	RHG21	UNC80	UB2E3
CCNB1	CCD14	FOXP3	FOXJ1	MGT5B	MMP17	RM46	RHG22	UNG	UB2Q1
CCNB2	CCD17	FPRP	FOXJ2	MIB2	MMP20	RM47	RHG23	UPK2	UB2Q2
CCNE2	CCD24	FR1L4	FOXK2	MIC1	MMP23	RM50	RHG24	UR2R	UBA1
CCNJ	CCD40	FR1L5	FOXN1	MID49	MMP25	RM52	RHG25	URGCP	UBA1L
CCNJL	CCD51	FR1OP	FOXN3	MIDA	MMP7	RN111	RHG26	USF2	UBE2B
CCNK	CCD60	FREM2	FOXP2	MIDN	MMP8	RN115	RHG27	USH2A	UBE2K

CCNL2	CCD61	FRITZ	FOXP4	MIEAP	MNDA	RN128	RHG29	USP9Y	UBE2W
CCNO	CCD67	FRMD1	FOXS1	MIER3	MO2R2	RN133	RHG30	UT14A	UBE3B
CCNT2	CCD71	FRMD3	FP100	MIIP	MO4L1	RN146	RHG31	UTP15	UBN1
CCPG1	CCD77	FRMD5	FPR1	MILR1	MOGS	RN168	RHG32	UTRO	UBP11
CCR4	CCD79	FRMD7	FPR2	MINA	MON1B	RN182	RHG40	UTY	UBP12
CCYL1	CCD80	FRPD2	FPR3	MINT	MON2	RN19B	RHG44	V1BR	UBP14
CCYL3	CCD89	FRRS1	FR1L6	MIXL1	MORC3	RN212	RHINO	VAPA	UBP16
CD014	CCD91	FRS2	FRAS1	MK01	MOS	RN213	RHN2L	VASH1	UBP2
CD019	CCD97	FRS3	FREM3	MK09	MOT11	RN214	RHPN1	VASP	UBP22
CD021	CCDC6	FRY	FRM4A	MKL1	MOT13	RN220	RHPN2	VATB1	UBP28
CD038	CCG6	FSBP	FRM4B	MKL2	MOT4	RN222	RIC1	VAX2	UBP31
CD040	CCKAR	FSD1L	FRP2L	MKRN3	MOT8	RN224	RIC3	VCIP1	UBP32
CD042	CCL27	FSTL1	FRPD1	MKRN4	MOV10	RN5A	RICTR	VCX2	UBP35
CD046	CCL4	FSTL3	FRPD3	MKX	MP2K7	RNAS1	RIG	VDR	UBP36
CD049	CCL5	FTO	FRPD4	MLF1	MPDZ	RNC	RIM3A	VEGFD	UBP4
CD109	CCM2	FUCM	FRYL	MLIP	MPIP2	RNF12	RIM3B	VEZA	UBP44
CD11A	CCNB3	FURIN	FSCB	MLL2	MPP6	RNF38	RIM3C	VGF	UBP47
CD11B	CCNE1	FUT1	FSD1	MLL3	MPP8	RNFT1	RIMB1	VGFR2	UBP5
CD123	CCNF	FUT11	FSD2	MLL5	MPP9	RNT2	RIMS1	VGFR3	UBQL4
CD20	CCNL1	FUT6	FSIP1	MLXIP	MPPA	RNZ2	RIMS2	VILL	UBR1
CD22	CCR1	FUT7	FSIP2	MMAB	MPPD1	ROBO1	RIMS3	VINEX	UBR7
CD226	CCZ1	FUT9	FSTL4	MMAC	MPPE1	ROBO3	RINL	VIPAR	UBX11
CD248	CCZ1L	FX4L1	FSTL5	MMP19	MPRIP	RON	RIP	VIPR2	UBXN6
CD2AP	CD037	FX4L5	FTM	MMP21	MPTX	ROR2	RIPK2	VIR	UCN3
CD2B2	CD044	FX4L6	FUCO	MMP26	MPZL1	RORA	RITA	VKIND	UD11
CD33	CD051	FXL14	FUCT1	MMP9	MRC2	ROS1	RL11	VLDLR	UD14
CD48	CD14	FXL17	FUT10	MMRN2	MRCKA	RP3A	RLGPB	VMAT2	UD19
CD5	CD158	FXL19	FUT4	MMS22	MRCKB	RPA34	RM10	VMP1	UDB11
CD52	CD166	FZD1	FUZZY	MN1	MRCKG	RPA43	RM14	VNN1	UFSP2
CD5L	CD177	FZD10	FX4L2	MNT	MRGX3	RPA49	RM23	VOPP1	UGDH
CD68	CD180	FZD2	FX4L3	MNX1	MRM1	RPAB2	RM35	VP13C	UGGG1
CD69	CD19	FZD6	FX4L4	MO2R1	MRP	RPAC1	RM39	VP13D	UH1BL
CD7	CD20B	FZD7	FXL20	MO4L2	MRP3	RPB1	RMD1	VP37A	ULK2
CD83	CD276	FZR	FXR1	MOBP	MRP4	RPB11	RMP	VP37C	ULK3
CD8A	CD302	G2E3	FXYD4	MON1A	MRP6	RPB1C	RN112	VPK1	ULK4
CDC16	CD320	G6PC2	FXYD5	MORC1	MRP7	RPB2	RN126	VPS35	UN13A
CDC23	CD34	G6PE	FXYD7	MORC2	MRRP3	RPC2	RN138	VPS39	UN13C
CDC27	CD36	GA2L1	FYB	MOST1	MRT4	RPESP	RN149	VPS53	UN45A
CDC5L	CD4	GA2L2	FYCO1	MOT12	MRVI1	RPF2	RN151	VPS72	UN5CL
CDCA4	CD44	GA2L3	FYV1	MOT7	MS18B	RPGF3	RN157	VRTN	UN93A
CDCA5	CD5R2	GAB1	G3PT	MOT9	MS3L2	RPGF6	RN165	VS10L	UNC4
CDHR1	CD79B	GAB3	G3ST4	MP2K2	MSH4	RPGP2	RN167	VSIG4	UNC5B
CDHR3	CD80	GABR1	G6PC	MP2K3	MSI1H	RPN1	RN180	VTM2B	UNC5C
CDHR4	CD8B	GABR2	G7C	MP2K5	MSPD3	RPTOR	RN185	VTM2L	UNC5D

CDHR5	CD8BL	GABT	GAB2	MP3B2	MSRB3	RRAGC	RN207	VW5B2	UNC79
CDK10	CD97	GADL1	GAB4	MPCP	MSX1	RRAS2	RN216	VWA3B	UNK
CDK17	CDA7L	GAGB1	GAGC1	MPI	MTA2	RREB1	RN217	VWC2	UNKL
CDK18	CDAN1	GAGE1	GAK	MPIP1	MTA70	RRN3	RN219	VWCE	UPK3A
CDK5	CDC20	GAH6	GALM	MPIP3	MTBP	RRNAD	RN223	VWDE	UPK3B
CDK7	CDC7	GALA	GALNS	MPND	MTCH2	RRP12	RND1	WAC	UPP
CDKA2	CDCA2	GALR1	GALT	MPP10	MTF2	RRP44	RNF10	WAHS7	URB2
CDO1	CDCA3	GALT1	GALT5	MPP2	MTG16	RRP5	RNF11	WAP53	URFB1
CDON	CDHR2	GALT6	GAPD1	MPP3	MTG8	RRP7A	RNF14	WASF3	UROK
CDR2L	CDK1	GAMT	GARL3	MPPB	MTHR	RRP8	RNF34	WASP	UROL1
CDS2	CDK12	GANAB	GAS2	MPRD	MTHSD	RRS1	RNF39	WBP1	UROM
CDSN	CDK13	GAPR1	GAS6	MPRI	MTL2B	RS2	RNF4	WBP2	US6NL
CDY1	CDK16	GAS1	GASP2	MRC1	MTMR1	RS20	RNF44	WBP2L	USBP1
CDY2	CDK20	GASP1	GATA3	MRF	MTMR3	RS27	RNH1	WBP4	USF1
CDYL1	CDK3	GATA1	GATD1	MRGBP	MTMR4	RS3	RNPS1	WBS23	USH1C
CE004	CDKA1	GATA2	GATL3	MRGRD	MTMR6	RS8	RNZ1	WDFY4	USH1G
CE042	CDKAL	GATA4	GATM	MRGRG	MTMR8	RSBN1	ROAA	WDR1	USP9X
CE056	CDKL5	GATA6	GBA2	MRGX2	MTMRA	RSH4A	ROBO2	WDR11	USPL1
CE104	CDN1B	GBB5	GBA3	MRI	MTMRC	RSH6A	ROBO4	WDR12	UST
CE112	CDN1C	GBF1	GBG3	MRP1	MTMRE	RSPH3	ROCK2	WDR13	UT14C
CE120	CDR2	GBP1	GBLP	MRP2	MTO1	RT17	ROP1L	WDR17	UT2
CE152	CDS1	GBRA4	GBP3	MRP5	MTPN	RT18A	ROR1	WDR20	UTF1
CE170	CDT1	GBRG2	GBP7	MRP9	MTRR	RT31	RORB	WDR26	UTP18
CE290	CDX2	GBRR1	GBRA1	MRRP1	MTSSL	RT34	RP1	WDR31	UVRAG
CE350	CDX4	GCC2	GBRA3	MS3L1	MTUS1	RTEL1	RP1L1	WDR35	V1AR
CEA16	CDYL2	GCET2	GBRA5	MS4A3	MUC15	RTN1	RPA1	WDR37	VAPB
CEAM3	CE025	GCNT6	GBRG3	MSGN1	MUC19	RTN3	RPA2	WDR43	VASN
CEAM5	CE027	GCP2	GBRT	MSH6	MUC2	RTN4	RPAP1	WDR48	VAT1
CEAM7	CE034	GCP3	GBX2	MSL1	MUC20	RTN4R	RPB1B	WDR59	VATB2
CEBPB	CE041	GCP6	GCC1	MSL2	MUC24	RTP1	RPC1	WDR5B	VAV2
CECR1	CE045	GCP60	GCFC1	MSPD2	MUC3A	RUBIC	RPC4	WDR6	VCAM1
CECR6	CE047	GCR	GCM2	MSRB2	MUC4	RUN3B	RPGF1	WDR62	VGFR1
CECR9	CE060	GCSP	GCN1L	MSTO1	MUC6	RUNX3	RPGF2	WDR63	VGLL2
CELF1	CE065	GCYA2	GCNT1	MT1X	MUC7	RUSC1	RPGF4	WDR66	VGLL3
CELF3	CE128	GCYB1	GCNT7	MT21D	MUCEN	RUSC2	RPGFL	WDR67	VGLL4
CELF5	CE164	GDF8	GCOM1	MTA3	MUDEN	RUSD2	RPGP1	WDR73	VIP1
CELR1	CE192	GDIR1	GCP5	MTF1	MUT7B	RUVB1	RPN2	WDR82	VIP2
CELR3	CEA18	GDIR3	GCYA3	MTG8R	MXRA5	RUVB2	RPOM	WDR85	VKGC
CEMP1	CEA19	GDS1	GDE	MTLR	MY15B	RX	RPP29	WDR86	VMA5A
CENP1	CEAM1	GELS	GDF1	MTMR2	MY18A	RXRB	RPP40	WDR96	VMAT1
CENPA	CEAM4	GEMI4	GDF15	MTMR5	MY18B	RXRG	RPRD2	WEE1	VN1R1
CENPC	CEAM8	GEMI5	GDF5O	MTMR7	MYBA	RYBP	RPTN	WEE2	VN1R4
CENPE	CEBPA	GEN	GDF9	MTMRB	MYBPH	RYR1	RRAGD	WFKN2	VNRL4
CENPF	CEBPD	GEPH	GDIA	MTOR	MYCD	S12A5	RRP1	WFS1	VP13A

CENPI	CECR2	GFI1B	GDIB	MTR1	MYCL1	S12A8	RRP1B	WIBG	VP13B
CENPJ	CELF2	GFRA1	GDIR2	MTR1A	MYCL2	S13A1	RS14	WIPF1	VP33A
CENPR	CELF6	GFRA2	GEMC1	MTSS1	MYCN	S13A2	RSAD1	WIPF2	VP33B
CEP44	CEND	GG6L1	GFPT1	MTU1	MYCT	S13A3	RSBNL	WISP1	VP37D
CEP63	CENPL	GG6L3	GFRA3	MTUS2	MYCT1	S14L1	RSF1	WISP2	VPRBP
CEP68	CENPN	GG6L5	GG6L2	MTX1	MYF5	S14L5	RSRC2	WIZ	VPS11
CEP76	CENPV	GG6L7	GG6L4	MTX3	MYH14	S15A2	RT11	WNK2	VPS16
CEP78	CEP41	GG6L9	GG6L6	MUC1	MYL10	S17A4	RT22	WNK3	VPS4B
CEP85	CEP57	GG6LB	GGA1	MUC12	MYL3	S17A5	RT35	WNK4	VPS54
CEP89	CEP95	GG8L2	GGA3	MUC13	MYL4	S19A3	RT4I1	WNT6	VPS8
CEP97	CEPT1	GGA2	GGH	MUC16	MYLIP	S20A1	RTBDN	WNT9B	VRK3
CERK1	CER1	GGCT	GGN	MUC17	MYO1E	S22A2	RTL1	WSB2	VSX1
CERKL	CETN2	GGED1	GGNB2	MUC18	MYO1H	S22A3	RTN2	WSDU1	VW5B1
CERS5	CF015	GGT3	GGT6	MUC3B	MYO3A	S22AG	RTTN	WT1	VWA2
CERU	CF052	GGT7	GGTL2	MUC5A	MYO3B	S22AK	RUAS1	WWC2	VWA3A
CF064	CF097	GHITM	GHR	MUC5B	MYO5A	S23A3	RUFY3	X3CL1	VWF
CF070	CF146	GI24	GHRHR	MUM1	MYO5B	S23IP	RUN3A	XDH	WASF2
CF106	CF176	GIMA4	GHSR	MUML1	MYO7B	S2535	RUND1	XIRP2	WASL
CF122	CF204	GL1AD	GIMA6	MUS81	MYO9A	S2610	RUNX1	XK	WBS27
CF132	CF226	GL6D1	GIPC3	MUSK	MYOF	S26A2	RXRA	XKRY	WDFY2
CF138	CG025	GLCI1	GIT1	MUT7	MYOM3	S26A3	RYK	XKRY2	WDFY3
CF174	CG040	GLCM	GLBL2	MUTYH	MYOZ2	S26A6	RYR3	XP32	WDR24
CF186	CG042	GLE1	GLBL3	MYBB	MYOZ3	S26A8	S10AB	XPF	WDR3
CF195	CG051	GLI1	GLD2	MYBPP	MYPC3	S26A9	S11IP	XPO4	WDR38
CF222	CG052	GLI2	GLDN	MYC	MYPT1	S27A3	S12A4	XPO6	WDR41
CFTR	CG055	GLI3	GLHA	MYCB2	MYPT2	S28A3	S12A6	XPO7	WDR44
CG013	CG058	GLIS2	GLI4	MYCPP	MYRIP	S352B	S12A9	XPP2	WDR47
CG029	CG060	GLP3L	GLIS1	MYEOV	MYT1	S35A5	S14L6	XPP3	WDR5
CG043	CG061	GLT10	GLIS3	MYLK	N4BP2	S35E1	S18L2	XRN2	WDR52
CG047	CG065	GLT14	GLO2	MYLK2	N4BP3	S35F5	S19A1	XRRA1	WDR60
CG057	CG074	GLTD2	GLOD4	MYLK3	N6MT2	S35G1	S1PBP	XYLB	WDR65
CG072	CGNL1	GLTL2	GLPC	MYNN	NAA15	S36A1	S20A2	XYLK	WDR7
CH012	CGT	GLTL3	GLR	MYO10	NAB2	S36A2	S22A1	XYLT1	WDR70
CH014	CH039	GLTP	GLSK	MYO15	NAC2	S36A3	S22A5	YA043	WDR76
CH033	CH045	GLYC	GLTL5	MYO16	NACC1	S38A3	S22AF	YB002	WDR78
CH034	CH048	GLYG2	GLU2B	MYO19	NADE	S38A6	S22AN	YB035	WDR81
CH058	CH049	GLYL3	GLYG	MYO1C	NAL10	S38A9	S23A1	YB047	WDR87
CH077	CH60	GNAS1	GMEB2	MYO1D	NAL14	S39A1	S2546	YB052	WDR90
CH078	CHD1	GNAS3	GMIP	MYO5C	NALDL	S39AA	S2548	YC005	WDR91
CH086	CHD7	GNL1	GNAO	MYO7A	NALP1	S3TC1	S26A7	YC006	WDTC1
CHAC1	CHD9	GNL3L	GNDS	MYO9B	NALP5	S45A4	S29A4	YC018	WFDC8
CHCH3	CHIP	GNN	GNMT	MYOM2	NALP6	S4A5	S2A4R	YD002	WHRN
CHD2	CHK1	GNPTA	GNRR2	MYOME	NANO1	S4A7	S35B2	YD023	WIPF3
CHD3	CHMP7	GOG6B	GNS	MYOTI	NAP1	S61A1	S35C2	YE027	WIPI4

CHD4	CHPF2	GOG6C	GNT2C	MYPC1	NAT10	S6A14	S35E2	YES	WLS
CHD6	CHRC1	GOG8A	GOG6A	MYPC2	NAT6	S6A18	S35E4	YETS2	WN10A
CHD8	CHST2	GOG8B	GOG6D	MYPN	NAV2	S6A20	S35F2	YF005	WNK1
CHERP	CHST3	GOG8C	GOG8J	MYPOP	NB5R2	S6OS1	S35F3	YF006	WRN
CHFR	CHSTB	GOG8H	GOGA1	MYSM1	NB5R4	SACS	S35G4	YF013	WSB1
CHIC1	CI004	GOG8I	GOGA2	MYT1L	NBAS	SAFB2	S39A4	YG006	WTIP
CHID1	CI005	GOGA4	GOGB1	N4BP1	NCAM2	SAGE1	S39A6	YG008	WWC3
CHIT1	CI030	GOLI	GOLM1	NAA10	NCAN	SAHH2	S39A7	YG024	WWP1
CHODL	CI062	GOLI4	GORS2	NAA25	NCF1	SALL1	S39AC	YG045	XCR1
CHPT1	CI079	GON2	GP101	NAA40	NCF1B	SALL2	S39AD	YG046	XG
CHRD	CI084	GON4L	GP111	NAB1	NCF1C	SALL3	S3TC2	YG055	XIAP
CHSP1	CI106	GORS1	GP113	NAC1	NCF4	SALL4	S41A1	YH007	XIRP1
CHST5	CI129	GP112	GP116	NAC3	NCK5L	SAM11	S47A2	YI007	XKR5
CHST6	CI130	GP124	GP123	NACAD	NCKP5	SAM14	S4A10	YI014	XKR7
CI024	CI131	GP128	GP126	NACC2	NCOA1	SAM15	S4A11	YI020	XPO1
CI031	CI150	GP132	GP143	NADK	NCOA3	SAM9L	S4A4	YI035	XPO5
CI038	CI152	GP133	GP144	NAGS	NCOR2	SAMD3	S4A8	YI039	XPOT
CI091	CI172	GP139	GP155	NAGT1	NCRP1	SAMD8	S61A2	YIPF1	XPP1
CI092	CIC	GP142	GP156	NALCN	NDC1	SAMH1	S6A11	YJ004	XRCC1
CI102	CIDEB	GP152	GP157	NALP7	NDE1	SAP25	S6A12	YJ005	XRN1
CI128	CIKS	GP153	GP161	NANO3	NDF1	SARDH	S6A13	YJ015	XYLT2
CI135	CILP1	GP162	GP1BA	NANOG	NDF4	SARG	S6A15	YJ017	YA001
CI139	CILP2	GP171	GPA33	NANP8	NDF6	SAS10	S6A16	YK026	YA011
CI141	CING	GP176	GPAN1	NARF	NDRG3	SASH1	S6A17	YK045	YA028
CI142	CIP4	GP179	GPAT4	NARG2	NDST3	SATB2	S6A19	YLPM1	YA033
CI173	CIR1A	GP180	GPBAR	NARR	NDUB3	SBNO1	S7A14	YM009	YA037
CI174	CISD3	GPAA1	GPC5	NASP	NDUB4	SBNO2	S9A10	YM012	YAF2
CIP1	CISH	GPAT1	GPC5C	NAV1	NDUB9	SBP2L	SAAL1	YN001	YAP1
CIP2A	CITE1	GPAT3	GPR19	NAV3	NDUS6	SBSN	SAC2	YO001	YB028
CITE2	CJ011	GPBL1	GPR27	NB5R1	NEB2	SC16A	SACA1	YO027	YB043
CIZ1	CJ012	GPBP1	GPR34	NB5R3	NEBL	SC22C	SACA3	YP002	YD020
CJ071	CJ047	GPC3	GPR4	NBEA	NEBU	SC24C	SAHH3	YP009	YD021
CJ082	CJ068	GPCP1	GPR56	NBEL1	NEC1	SC24D	SAM10	YP029	YF009
CJ093	CJ076	GPKOW	GPR61	NBEL2	NEC2	SC31B	SAMD9	YQ015	YF010
CJ099	CJ085	GPR22	GPR64	NBL1	NECP1	SC5A1	SAMN1	YQ024	YG053
CJ112	CJ090	GPR37	GPR83	NBN	NEDD1	SC5A3	SASH3	YQ050	YH010
CJ113	CJ095	GPR55	GPSM1	NBPF3	NEGR1	SC5AB	SAST	YR010	YI016
CJ136	CJ105	GPR98	GPTC3	NBR1	NEIL1	SC6A4	SATB1	YS001	YI025
CK016	CJ108	GPTC8	GPVI	NCAM1	NEIL3	SC6A5	SATT	YS003	YI029
CK024	CJ114	GPV	GRAM	NCDN	NEK1	SC6A6	SC16B	YS045	YJ012
CK035	CJ115	GPX5	GRAM3	NCK2	NEK10	SC6A8	SC23A	YSK4	YJ018
CK039	CJ118	GRAM4	GRASP	NCKP1	NEK3	SC6A9	SC23B	YTDC1	YK038
CK041	CJ128	GRAP1	GRB10	NCKPL	NEK4	SCAF8	SC24A	YTDC2	YL016
CK045	CJ131	GRB14	GRB7	NCKX1	NEK5	SCAFB	SC24B	YV008	YL023

CK048	CK049	GRB1L	GRDN	NCKX3	NELFB	SCAP	SC5A7	YV009	YLAT1
CK063	CK053	GRCR2	GREB1	NCKX5	NELL1	SCEL	SC5A9	YV023	YMEL1
CK066	CK061	GRHPR	GRHL1	NCOA2	NELL2	SCFD1	SC5D	YX004	YN009
CK068	CK065	GRIA3	GRHL2	NCOA4	NEMF	SCHI1	SC61B	Z280B	YO010
CK070	CK073	GRIA4	GRHL3	NCOA5	NEO1	SCMH1	SC6A2	Z280C	YO011
CK072	CK080	GRIK2	GRIA1	NCOA7	NEST	SCML2	SC6A3	Z280D	YP008
CK074	CK084	GRIK3	GRIA2	NCOAT	NET1	SCML4	SC6A7	Z324A	YP034
CK089	CK087	GRIP1	GRID1	NCOR1	NET3	SCN1A	SCAM5	Z385B	YQ048
CK091	CK096	GRIP2	GRID2	NCTR1	NEU1	SCN2A	SCAR3	Z385C	YR005
CK093	CKLF6	GRL1A	GRIK1	NCUG1	NEU1A	SCN3A	SCC4	Z512B	YS027
CK5P2	CKP2L	GRL1B	GRIK4	NDF2	NEU2	SCN4A	SCGBL	Z518A	YS038
CKAP2	CL012	GRM1A	GRIN1	NDNF	NEUFC	SCNAA	SCN5A	Z585A	YS039
CKAP5	CL042	GRP1	GRIN2	NDRG2	NEUL4	SCND2	SCN7A	Z804B	YS049
CL004	CL053	GRP4	GRIN3	NDST1	NEUM	SCND3	SCN8A	ZACN	YS059
CL026	CL054	GRPP1	GRM1	NDST4	NEUR1	SCNNG	SCN9A	ZADH2	YT009
CL035	CL055	GRWD1	GRM1B	NDUA8	NEUT	SCRB1	SCNBA	ZBED4	YU004
CL040	CL056	GSCR1	GRM1C	NDUB5	NF2L2	SCRB2	SCNNA	ZBED6	YV020
CL041	CL066	GSDMA	GRM5	NDUBB	NFAC1	SCRIB	SCOT1	ZBP1	YV021
CL045	CL074	GSDMC	GRM6	NDUS3	NFAC3	SCRN1	SCOT2	ZBT11	YV028
CL047	CL16A	GSHR	GRN	NDUS7	NFAC4	SCRN3	SCRN2	ZBT16	YYAP1
CL050	CL18A	GSKIP	GRP2	NEAS1	NFH	SCYL2	SCRT1	ZBT22	Z280A
CL060	CLAP1	GST2	GRP78	NEB1	NFIB	SDC1	SCRT2	ZBT24	Z324B
CL063	CLASR	GSTT2	GRPL2	NECA1	NFIC	SDC4	SCTM1	ZBT25	Z354B
CL071	CLAT	GTF2I	GSC2	NECD	NFIL3	SDCG3	SCUB1	ZBT32	Z385D
CLAP2	CLC1A	GTPB1	GSE1	NED4L	NFKB1	SDCG8	SCUB2	ZBT34	Z3H7A
CLC11	CLCA1	GTPB2	GSH0	NEDD4	NFU1	SDHF2	SCUB3	ZBT37	Z3H7B
CLC14	CLCA2	GTSFL	GSH1	NEIL2	NFYC	SDHL	SCX	ZBT38	Z518B
CLC1B	CLCA4	GUAD	GSK3A	NEK2	NGN1	SDK1	SDC2	ZBT40	Z585B
CLC4A	CLCKA	GUC1A	GSK3B	NEK9	NGN2	SDK2	SDC3	ZBT41	Z780A
CLC4C	CLCKB	GUC2D	GSTM4	NELF	NGN3	SDS3	SDPR	ZBT44	Z804A
CLCA	CLCN2	GUC2F	GSX1	NEMO	NGRN	SE1L1	SDSL	ZBT49	ZAN
CLCB	CLCN7	H12	GT251	NET5	NHS	SE6L1	SE1L3	ZBT7B	ZBT20
CLCC1	CLD10	H14	GT252	NETR	NHSL2	SE6L2	SELB	ZBTB1	ZBT42
CLCN1	CLD14	H1BP3	GT2D1	NEU1B	NIBAN	SEBOX	SELV	ZBTB3	ZBT43
CLCN4	CLDN1	H1FOO	GTD2A	NEUL3	NIBL1	SEBP2	SEM3C	ZBTB9	ZBT45
CLIC6	CLIC1	H2AW	GTD2B	NEUR3	NIBL2	SEC62	SEM4A	ZC3H1	ZBT46
CLIP2	CLIC5	H2B2C	GTPB3	NEUR4	NICA	SELN	SEM4B	ZC3H6	ZBT47
CLIP4	CLIP1	H2B2D	GTPB6	NF1	NID2	SELPL	SEM4D	ZC3H8	ZBT48
CLM4	CLIP3	H2BFM	GTR2	NF2IP	NIF3L	SELS	SEM4G	ZCCHL	ZBT7A
CLM6	CLM1	H6ST1	GTR6	NF2L1	NIPA	SELW	SEM5A	ZCH18	ZBT7C
CLM7	CLM2	HABP4	GTR7	NFAC2	NIPA1	SEM3A	SEM6D	ZCH24	ZBTB2
CLM8	CLM9	HAGHL	GTSE1	NFASC	NIT1	SEM3D	SEN15	ZCHC5	ZBTB4
CLMN	CLOCK	HARB1	GUAA	NFAT5	NIT2	SEM3E	SEN54	ZCHC8	ZBTB5
CLN3	CMC2	HAUS6	GUC2C	NFIA	NK2R	SEM3F	SENP1	ZDBF2	ZBTB6

CLP1L	CMIP	HAVR2	GVIN1	NFIX	NKAP	SEM3G	SENP3	ZDH14	ZC11A
CLPB	CMTA2	HBEGF	GWL	NFKB2	NKD2	SEM4F	SENP5	ZDH15	ZC12A
CLPT1	CN050	HCD2	GYS1	NFM	NKPD1	SEM5B	SENP6	ZDH16	ZC12B
CLSPN	CN082	HCN1	GYS2	NFRKB	NKRF	SEM6A	SENP7	ZDH18	ZC12C
CLYBL	CN093	HCN2	GZF1	NFS1	NKTR	SEM6B	SERA	ZDH20	ZC12D
CM033	CN102	HCN3	H13	NFX1	NKX12	SEM6C	SERC5	ZDHC1	ZC3H3
CM044	CN105	HCN4	H6ST3	NFXL1	NKX21	SENP8	SESN2	ZDHC3	ZC3H4
CMC1	CN118	HD	HACL1	NGAP	NKX22	SEPR	SET1A	ZDHC5	ZC3HA
CML1	CN16B	HDA10	HAIR	NGEF	NKX23	SERC2	SET1B	ZDHC6	ZC3HD
CMPK2	CN183	HDA11	HAKAI	NHRF2	NKX24	SERC4	SETB1	ZDHC9	ZC3HE
CMYA5	CND1	HDAC5	HAOX2	NHRF3	NKX25	SESQ2	SETB2	ZEB1	ZCC18
CN021	CND2	HDAC9	HAP1	NHRF4	NKX32	SETBP	SETD2	ZEB2	ZCH12
CN037	CND3	HDX	HASP	NHSL1	NKX61	SETD6	SETD5	ZEP1	ZCH14
CN043	CNDD3	HEAT3	HAUS5	NICN1	NLE1	SEZ6	SETD8	ZEP2	ZCHC2
CN159	CNDG2	HEAT4	HAVR1	NID1	NLGN1	SF3B1	SETX	ZF106	ZCPW1
CN164	CNNM1	HEAT6	HBAT	NIN	NLGN3	SFR15	SF01	ZF112	ZCPW2
CN182	CNNM2	HEAT8	HCDH	NINJ1	NLRC3	SFR19	SF3B2	ZF161	ZDH22
CN37	CNNM3	HECA2	HCFC1	NINL	NLRC5	SFSWA	SF3B3	ZFAN3	ZDHC7
CNDH2	CNNM4	HECD1	HCFC2	NIPA4	NLRX1	SFXN3	SFPQ	ZFAT	ZDHC8
CNGB1	CNOT1	HECW1	HCK	NIPBL	NMD3B	SFXN4	SFR1	ZFHX4	ZEP3
CNGB3	CNOT2	HECW2	HCLS1	NISCH	NMDE1	SG223	SFT2C	ZFP1	ZFAN5
CNKR1	CNOT3	HEG1	HCST	NJMU	NMDE4	SGCD	SG110	ZFP3	ZFAN6
CNKR2	CNR1	HELZ	HDAC4	NK1R	NMNA2	SGCE	SG196	ZFP37	ZFHX2
CNKR3	CNRP1	HEM0	HDAC6	NK3R	NMT1	SGCG	SGCA	ZFP41	ZFHX3
CNOT4	CNTFR	HEM1	HDAC7	NKD1	NNTM	SGCZ	SGE1L	ZFY26	ZFN2B
CNPY3	CNTN1	HEM2	HDC	NKX11	NO66	SGSM1	SGIP1	ZHX1	ZFPL1
CNST	CNTN2	HEM6	HDGR2	NKX26	NOB1	SGSM2	SGK1	ZHX3	ZFR
CNT3B	CNTN3	HENMT	HDGR3	NKX28	NOBOX	SGSM3	SGK2	ZIC2	ZFR2
CNTD2	CNTN5	HEP2	HEAT1	NLGNY	NOC2L	SGTB	SGOL1	ZIC3	ZFY16
CNTLN	CNTN6	HERC1	HEAT2	NLK	NOCT	SH2B1	SGOL2	ZIC4	ZFY27
CNTP2	CNTP1	HERC2	HECAM	NMB	NOD1	SH2B3	SGT1	ZIC5	ZFYV1
CNTP3	CNTP5	HERC5	HECD2	NMD3A	NODAL	SH319	SGTA	ZIM2	ZFYV9
CNTP4	CNTRB	HERC6	HECD3	NMDE2	NOL4	SH321	SH22A	ZMAT1	ZHANG
CNTRL	CO027	HEXA	HELB	NMDE3	NOL6	SH3B4	SH23A	ZMAT2	ZIC1
CO002	CO032	HEXI1	HELQ	NMDZ1	NOMO1	SH3G1	SH2B2	ZMAT3	ZKSC3
CO033	CO037	HEXI2	HELT	NMI	NOS1	SH3K1	SH2D3	ZMAT4	ZKSC4
CO043	CO038	HEYL	HEMGN	NMNA1	NOTC1	SH3R2	SH2D7	ZMIZ2	ZKSC5
CO044	CO039	HFE	HEMK2	NMU	NOTC3	SH3R3	SH3G2	ZMYM2	ZMIZ1
CO056	CO052	HGS	HERP1	NNMT	NOTC4	SHAN2	SH3R1	ZN114	ZMY15
CO1A2	CO054	HHLA1	HERP2	NOD2	NOV	SHAN3	SHAN1	ZN148	ZMYM1
CO2	CO059	HHLA2	HES6	NOG2	NOVA1	SHB	SHC1	ZN174	ZMYM3
CO3	CO062	HIAL1	HEXB	NOL3	NOX3	SHF	SHC4	ZN185	ZMYM6
CO3A1	CO1A1	HIAL2	HEY1	NOL8	NOX4	SHIP1	SHD	ZN189	ZN133
CO4A6	CO2A1	HIC1	HEY2	NOL9	NOX5	SHIP2	SHE	ZN195	ZN135

CO4B	CO4A	HIF1A	HFM1	NOLC1	NP311	SHKB1	SHRM1	ZN197	ZN138
CO5A1	CO4A1	HIP1	HGFA	NOMO2	NPAS1	SHLB1	SHRM2	ZN200	ZN142
CO5A2	CO4A3	HIP1R	HGNAT	NOMO3	NPAS4	SHLB2	SHRM3	ZN202	ZN160
CO5A3	CO4A4	HIPL1	HHEX	NONO	NPAT	SHOX2	SHRM4	ZN227	ZN165
CO6	CO5	HIRA	HHIP	NOP14	NPCR1	SHPK	SHSA6	ZN235	ZN167
CO6A3	CO6A2	HIRP3	HIBCH	NOP2	NPDC1	SHPRH	SHSA7	ZN238	ZN184
CO6A5	CO6A6	HKR1	HIDE1	NOP56	NPFF2	SHPS1	SHSA8	ZN251	ZN192
CO9A1	CO7	HLAF	HIF3A	NOS2	NPHN	SHQ1	SI1L1	ZN256	ZN207
COBA1	CO7A1	HLTF	HIG2	NOS3	NPL	SI1L2	SIA4B	ZN276	ZN212
COCA1	CO8A2	HLX	HIPK1	NOSIP	NPNT	SI1L3	SIA8E	ZN277	ZN217
COE1	CO8G	HMBX1	HIPK2	NOTC2	NPRL2	SIA7A	SIAE	ZN281	ZN219
COE2	CO9	HMCN1	HIPK3	NOVA2	NPSR1	SIA8F	SIDT1	ZN283	ZN221
COE3	CO9A2	HMCN2	HIPL2	NOXIN	NPTX1	SIDT2	SIGL5	ZN285	ZN232
COE4	COAA1	HME1	HJURP	NOXO1	NPTX2	SIG10	SIK1	ZN287	ZN263
COEA1	COASY	HMGN3	HLAH	NPA1P	NPY2R	SIG11	SIK3	ZN295	ZN264
COFA1	COBA2	HMGX3	HMDH	NPAS2	NR1H4	SIG12	SIM1	ZN302	ZN273
COG1	COBL	HMGX4	HMMR	NPAS3	NR2C2	SIG14	SIN1	ZN316	ZN292
COG2	COBL1	HMHA1	HMX1	NPC1	NR5A2	SIG15	SIN3A	ZN319	ZN296
COG3	COG5	HMN5	HMX2	NPCL1	NR6A1	SIG16	SIN3B	ZN335	ZN317
COG6	COGA1	HNF1A	HMX3	NPHP1	NRAM2	SIGL8	SIPA1	ZN347	ZN318
COG7	COHA1	HNF4A	HN1L	NPHP3	NRBF2	SIK2	SIRPG	ZN358	ZN326
COKA1	COIL	HNF4G	HNF1B	NPHP4	NRBP	SIM2	SIRT1	ZN362	ZN331
COLI	COL11	HNF6	HNRDL	NPM2	NRBP2	SIRB1	SIRT6	ZN367	ZN363
COLQ	COL12	HNRPD	HNRL1	NPRL3	NRCAM	SIRB2	SIX2	ZN384	ZN382
COM1	COMA1	HOME2	HNRL2	NPT2A	NRDC	SIRBL	SIX5	ZN394	ZN395
COPB	COMP	HOMEZ	HNRLL	NPTN	NRF1	SIRT2	SIX6	ZN398	ZN416
COPG2	COOA1	HOOK2	HNRPC	NPY4R	NRG1	SIX1	SKI	ZN414	ZN428
COQ6	COPB2	HORM1	HNRPK	NR1D1	NRP1	SIX3	SKOR2	ZN423	ZN430
COQ9	COR2A	HP1B3	HOGA1	NR1D2	NRP2	SKA3	SKT	ZN434	ZN431
COR1B	COSA1	HPBP1	HOME1	NR1H2	NRSN2	SKOR1	SL9A1	ZN438	ZN446
COR2B	COT2	HPIP	HOME3	NR2C1	NRX3B	SL9A3	SLAF7	ZN444	ZN451
CORA1	COX2	HPLN3	HOOK1	NR2E3	NS1BP	SL9A4	SLAF8	ZN445	ZN454
CORIN	CP045	HPS4	HORN	NR2F6	NSA2	SL9A7	SLAI1	ZN449	ZN461
CORO6	CP054	HPS5	HOT	NR4A1	NSD1	SL9A8	SLAP2	ZN462	ZN467
CORO7	CP058	HRC23	HPDL	NR4A2	NSE4A	SL9A9	SLIK2	ZN474	ZN469
COT1	CP079	HRES1	HPS1	NR4A3	NSG1	SLAF5	SLMAP	ZN487	ZN473
COX10	CP086	HRH1	HPS3	NRAP	NSN5B	SLAI2	SLMO1	ZN488	ZN483
CP003	CP088	HRH3	HRSL2	NRG2	NSN5C	SLAP1	SLN11	ZN500	ZN490
CP007	CP093	HRSL5	HS105	NRG3	NSRP1	SLIK1	SLN13	ZN503	ZN496
CP011	CP110	HS12A	HS12B	NRIP1	NSUN5	SLIK5	SLTM	ZN521	ZN497
CP046	CP17A	HS3SB	HS74L	NRIP2	NT5D4	SLIK6	SLX4	ZN530	ZN507
CP048	CP19A	HSF2	HSF1	NRK	NTAN1	SLIT3	SMA5O	ZN551	ZN510
CP070	CP20A	HSF4	HSFY1	NRL	NTHL1	SLNL1	SMAD9	ZN567	ZN516
CP071	CP250	HSF5	HSH2D	NRX3A	NTR2	SLPI	SMAG1	ZN571	ZN526

CP081	CP2F1	HSP74	HSP77	NSD2	NTRK1	SLUR1	SMAGP	ZN581	ZN532
CP087	CP2J2	HSPB3	HSPB1	NSD3	NTRK3	SMAD1	SMAL1	ZN583	ZN536
CP096	CP2U1	HTR5A	HSPB8	NSDHL	NU107	SMAD3	SMAP2	ZN584	ZN541
CP135	CP4F8	HTR5B	HTF4	NSF	NU133	SMAD5	SMBP2	ZN597	ZN554
CP27B	CPEB1	HUTU	HTRA2	NSF1C	NU153	SMAD6	SMC5	ZN598	ZN579
CP2W1	CPEB2	HUWE1	HTRA3	NSL1	NU155	SMAG2	SMCA2	ZN608	ZN582
CP343	CPEB3	HXA1	HTRB1	NSMA2	NU160	SMAP	SMCA4	ZN618	ZN592
CP3A4	CPNE1	HXA11	HTRB2	NSMA3	NU188	SMBT1	SMG1L	ZN621	ZN600
CP3A5	CPNE3	HXA3	HTSF1	NSUN2	NU214	SMBT2	SMG5	ZN628	ZN609
CP3A7	CPNE4	HXA4	HUG1	NT5C	NU2M	SMC4	SMG7	ZN629	ZN623
CP4F2	CPNE5	HXB1	HUNK	NT5M	NU4M	SMCA1	SMG8	ZN645	ZN624
CP4FB	CPPED	HXB13	HUTH	NTAL	NUAK1	SMCA5	SMHD1	ZN648	ZN638
CP4FC	CPSF1	HXC10	HV207	NTCP4	NUDT6	SMCR8	SMN	ZN653	ZN641
CP4X1	CPT1C	HXC6	HV319	NTCP7	NUFP2	SMEK3	SMPX	ZN654	ZN644
CPEB4	CPXM1	HXD10	HXA10	NTKL	NUMBL	SMG1	SMRCD	ZN662	ZN646
CPMD8	CPXM2	HXD12	HXA2	NTRK2	NUP43	SMG9	SMTL1	ZN673	ZN652
CPNE6	CQ028	HXD8	HXA6	NU205	NUP53	SMO	SMU1	ZN674	ZN669
CPNE7	CQ047	HXK2	HXA7	NU5M	NUP62	SMOC1	SMUG1	ZN683	ZN687
CPNE8	CQ054	HXK3	HXB2	NUAK2	NUP93	SMR3A	SN	ZN691	ZN699
CPSF6	CQ057	HYAL1	HXB3	NUB1	NUPL1	SMR3B	SN12L	ZN692	ZN704
CPSF7	CQ064	HYDIN	HXB4	NUBP1	NUPL2	SMRC1	SNCAP	ZN703	ZN708
CPT2	CQ067	HYLS1	HXB8	NUBP2	NUT	SMRC2	SNED1	ZN738	ZN710
CPVL	CQ069	HYOU1	HXB9	NUCB1	NXF1	SMRD2	SNG3	ZN746	ZN711
CPZIP	CQ072	I10R2	HXC4	NUCKS	NXF2	SMS1	SNG4	ZN767	ZN713
CQ046	CQ074	I17RA	HXD11	NUFP1	NXF3	SMTL2	SNIP1	ZN768	ZN717
CQ051	CQ082	I17RE	HXD13	NUP37	NXPH2	SMTN	SNP47	ZN775	ZN750
CQ053	CQ097	I18RA	HXD3	NUP50	NXPH3	SMUF1	SNPC2	ZN776	ZN770
CQ055	CQ099	I22R2	HXD9	NUP54	NXT1	SMYD4	SNTB1	ZN784	ZN772
CQ056	CQ100	I27L1	HXK1	NUP85	NYNRI	SNAI1	SNTG2	ZN791	ZN777
CQ063	CQ104	I27L2	HXK4	NUP88	O10H4	SND1	SNUT1	ZN792	ZN778
CQ080	CR023	I27RA	HYCCI	NUP98	O10H5	SNPC4	SNX1	ZN800	ZN782
CQ085	CR032	I28RA	HYEP	NUSAP	O10V1	SNPH	SNX13	ZN827	ZN783
CQ096	CR034	IAH1	HYES	NVL	O10X1	SNR27	SNX16	ZN828	ZN787
CR025	CR054	IAPP	I12R2	NWD1	O11H7	SNR40	SNX17	ZN830	ZN805
CR026	CR2	IASPP	I15RA	NXP20	O4A15	SNTA1	SNX2	ZN839	ZN806
CR1	CR3L3	IBP3	I17EL	NXT2	O4C45	SNTB2	SNX21	ZNAS2	ZN829
CR1L	CRAC1	IBPL1	I18BP	NYX	O52B2	SNX11	SNX22	ZNF16	ZN831
CR3L1	CRBG3	IBTK	I20L2	O10H1	O52P1	SNX14	SNX29	ZNF20	ZN835
CR3L2	CRCM	ICA1L	I22R1	O10H2	O56A5	SNX15	SNX9	ZNF23	ZN837
CR3L4	CREB3	ICAL	I2BP1	O10H3	O5AU1	SNX19	SO1B1	ZNF3	ZN852
CRBB1	CREM	ICAM4	I2BP2	O10J4	O7E24	SNX30	SO1B3	ZNF8	ZN862
CRDL2	CRKL	ICAM5	I2BPL	O11G2	OAS2	SNX33	SO2B1	ZNHI2	ZNF2
CREB5	CRLF1	ICK	I4E1B	O51G2	OBP2B	SNX5	SO5A1	ZNT1	ZNF24
CRF	CRNL1	ID2	I5P1	O51V1	OC90	SNX8	SOCS3	ZNT5	ZNF41

CRIP3	CRNN	IDHC	I5P2	O56A1	OCTC	SO1A2	SOCS7	ZO1	ZNF48
CRIS2	CRTC1	IDHP	IBP1	OAS1	OD3L1	SO1C1	SON	ZO2	ZNFX1
CRLD2	CRTC2	IDI2	ICA69	OAS3	OD3L2	SO4A1	SORC1	ZO3	ZNRF3
CRLF2	CRUM1	IDUA	ICAM1	OBF1	ODBA	SO4C1	SORL	ZRAN1	ZNT10
CRML	CRY1	IER2	ICAM3	OBSCN	ODFP2	SO6A1	SORT	ZSA5C	ZNT6
CROCC	CRY2	IER5L	ICEF1	OCAD1	ODO2	SOBP	SOS1	ZSC10	ZNT9
CRPAK	CS029	IF172	ICOSL	OCLN	OFCC1	SOCS4	SOS2	ZSC21	ZP1
CRX	CS047	IF2B2	ID2B	ODAM	OGFR	SOCS5	SOSB1	ZSC29	ZP2
CS021	CS051	IF2M	IDD	ODB2	OGRL1	SOLH2	SOX12	ZSCA1	ZP3
CS035	CS054	IF2P	IER5	ODBB	OGT1	SORC3	SOX17	ZSCA4	ZPLD1
CS044	CS055	IF3M	IEX1	ODC	OLFL1	SOSD1	SOX3	ZSWM1	ZRAB2
CS045	CS067	IF4G1	IF122	ODO1	OLFM4	SOX10	SOX30	ZSWM2	ZRAB3
CS050	CS073	IFFO2	IF140	ODP2	OLM2A	SOX11	SOX5	ZSWM4	ZSA5A
CS057	CS081	IFIH1	IF16	ODPB	OMD	SOX13	SOX7	ZSWM5	ZSA5B
CS071	CS14L	IFIT3	IF2B3	ODPX	OMGP	SOX18	SOX8	ZSWM6	ZSC12
CS29O	CSDC2	IFIT5	IF44L	ODR4	OMP	SOX2	SOX9	ZWILC	ZSC18
CSDE1	CSF1	IFM3	IF4B	OFD1	ONCM	SOX4	SP100	ZXDA	ZSC20
CSF2	CSF1R	IFNW1	IF4G3	OGDHL	ONEC2	SOX6	SP110	ZY11B	ZSCA2
CSF3R	CSK2B	IFRD2	IFFO1	OGFD2	OOEP	SP1	SP130	ZYX	ZXDB
CSK21	CSKI1	IFT46	IFIX	OIT3	OPA1	SP3	SP2	ZZEF1	ZXDC
	CSKI2	IFT52	IFM2	OLM2B	OPA1L	SP4	SP5	ZZZ3	ZY11A

Table S4.2: List of proto-oncogenes that contain canonical phosphodegron motif.

ABL1	CSK23	GAS7	FYN	MYCN	RASH	TPM3
AF10	DCNL1	CYTSB	GFI1B	MYEOV	RASK	TOP1
AF17	DDIT3	DCNL1	GLI1	MYH11	RASN	TPR
AF1Q	DDX6	DDIT3	GNAS2	NCOA1	RBM15	TRI27
AFAD	DEK	DDX6	GUAA	NCOA4	RBP56	TRI37
AF9	DMBT1	DEK	HCK	NFKB2	RBTN1	UBP4
AFF1	DOCK4	DMBT1	HLF	NPM	RBTN2	UBP6
AFF4	ELF4	DOCK4	HMGA2	NR4A3	RB	UFO
AGR2	ELL	ELF4	HOP	NSD1	REL	VAV
AKIP1	ENL	ELL	HXA9	NSD2	RET	WDR11
AKP13	ENTP5	ENL	IL2	NSD3	RHG26	WISP1
AKT2	EPS15	ENTP5	JAK2	NTRK1	RHOA	WNT1
AKT1	ERG	EPS15	JAZF1	NU214	RN213	WNT3
ALK	ETS1	ERG	JUN	OBF1	RNZ2	WWTR1
ANCHR	ETS2	ETS1	KAT6A	OLIG2	ROS1	YAP1
ARAF	ETV1	ETS2	KDSR	PATZ1	RRAS2	YES
ARHG5	ETV6	ETV1	KIT	PAX3	RUNX1	ZBT16
ARHG8	EVI2A	ETV6	KMT2A	PAX5	SC31A	ZN320
ARHGC	EVI2B	EVI2A	KPCA	PAX7	SET	ZN521
ASPC1	EVI1	EVI2B	KPCI	PBX1	SH3G1	
AURKA	EWS	EVI1	LCK	PCM1	SKI	
BCAS3	FA83B	EWS	LHX4	PDGFD	SPI1	
BCAS4	FA83A	FA83B	LITAF	PDGFB	SPN90	
BCL6	FA83D	FA83A	LTMD1	PEBB	SRC	
BCL2	FCG2B	FA83D	LYL1	PGFRA	SSX1	
BCL3	FER	FCG2B	LYN	PGFRB	SSX2	
BCL9	FES	FER	M3K8	PHB	SSXT	
BCR	FGF3	FES	MAFA	PICAL	STIL	
BMI1	FGF5	FGF3	MAFB	PIM1	STYK1	
BRAF	FGF6	FGF5	MAF	PIM2	SUZ12	
BRCC3	FGF4	FGF6	MAS	PIM3	SYCC	
BRI3B	FGFR2	FGF4	MCF2L	PK3CA	TAL1	
BTG1	FGR	FGFR2	MCF2	PLAG1	TAL2	
CBL	FLI1	FGR	MDM2	PML	TBC3A	
CCDC6	FLT3	FLI1	MDS2	PRCC	TCL1A	
CCND1	FOS	FLT3	MERTK	PTTG1	TCL1B	
CCNL1	FOXO1	FOS	MET	PTTG3	TCTA	
CDN1B	FOXO4	FOXO1	MKL1	PTTG2	TFE2	
CDT1	FOXO3	FOXO4	MOS	RAB8A	TFE3	
CMC4	FRAT1	FOXO3	MTCP1	RAF1	TFG	
CR3L2	FSTL3	FRAT1	MTG8	RARA	TFPT	
CRK	FUS	FSTL3	MXI1	RARB	TLX1	
CSF1R	FYN	FUS	MYB	RASA1	TNR17	

Table S4.3: List of Tumor supressors that contain canonical phosphodegron motif.

AGAP2	CDKA1	DPH1	IRF1	MFHA1	PALB2	RASF5	TBRG1
AIM2	CDN1C	E41L3	KANK1	MN1	PB1	RBCC1	TCP1L
APC	CJ090	EGFR	KCD11	MTSS1	PHLP1	RBL1	TET2
ARI3B	CRCM	EPHB2	KS6A2	MTUS1	PININ	RBL2	TIF1A
ATM	CYLD	ERRFI	LATS1	MUC1	PKHG2	RECK	TM127
AXIN1	DAB2	EXT1	LATS2	MUTYH	PKHO1	RHG07	TSC1
BANP	DAB2P	EXT2	LIMD1	NAT6	PLK2	RHG20	TSC2
BCL10	DCC	F120A	LIN9	NBL1	PML	RHG35	VMA5A
BIN1	DEMA	FES	LZTS1	NDRG2	PMS1	SASH1	WT1
BRCA1	DI3L2	FLCN	MAFA	NF1	PRR5	SIK1	XRN1
BRCA2	DLEC1	HIC1	MAFB	NPRL2	PTC1	ST20	ZBT7C
BRD7	DMBT1	HIF3A	MAPK5	P53	PTEN	STA13	
BUB1B	DMTF1	IFIX	MERL	PAF1	RASF1	T53I1	